

POLITECNICO DI TORINO
Master of Science in Biomedical Engineering

Master's degree Thesis

**Biomechanical Analysis of Judo-Related
Head Injuries: A Pilot Study over Ages and
Experience Levels**



Supervisors:

Prof.ssa Laura Gastaldi

Prof. Stefano Paolo Pastorelli

Candidate:

Luca Vacca

Academic Year 2017/2018

Table of Contents

ABSTRACT	III
LIST OF FIGURES.....	V
LIST OF TABLES	IX
1 INTRODUCTION.....	- 1 -
2 MOTION ANALYSIS IN SPORT ACTIVITIES.....	- 3 -
2.1 INTRODUCTION	- 3 -
2.1.1 <i>Correlation of Acceleration Magnitude and Duration</i>	- 5 -
2.1.2 <i>Cumulative Head Impacts Effects</i>	- 8 -
2.2 MOTION ANALYSIS APPLIED TO JUDO	- 8 -
2.2.1 <i>Performance Analysis and Improvement</i>	- 8 -
2.2.2 <i>Injuries Analysis for Prevention</i>	- 17 -
2.2.3 <i>Technologies Used in Experimentation</i>	- 30 -
2.2.3.1 <i>Anthropometric Test Devices (ATD)</i>	- 30 -
2.3 TRAUMATIC BRAIN INJURIES (TBI)	- 32 -
2.3.1 <i>Acute TBIs</i>	- 33 -
2.3.2 <i>Chronic TBIs</i>	- 35 -
3 INERTIAL MEASUREMENT UNIT (IMU).....	- 37 -
3.1 ACCELEROMETER.....	- 37 -
3.2 GYROSCOPE	- 38 -
3.3 MAGNETOMETER.....	- 39 -
3.4 TECHNICAL SPECIFICATIONS OF EXPLOITED SENSORS	- 39 -
4 PRELIMINARY TESTS.....	- 41 -
4.1 LINEAR TESTS	- 41 -
4.2 ROTATIONAL TESTS	- 43 -
4.3 INITIAL TESTS ON JUDO MAT	- 47 -
4.4 IMU MARKET ANALYSIS.....	- 49 -
5 BREAKFALL TECHNIQUES ANALYSIS.....	- 53 -
5.1 PRELIMINARY TEST	- 53 -
5.2 ANALYSIS OF THE TECHNICAL GESTURE.....	- 54 -
5.3 REPEATABILITY MEASURES.....	- 61 -
5.4 DIFFERENCES BETWEEN BREAKFALLS TECHNIQUES	- 70 -
6 HEAD INJURY RISK ASSESSMENT.....	- 75 -
6.1 PRELIMINARY ANALYSIS.....	- 75 -
6.1.1 <i>Sensors Calibration and Comparison</i>	- 77 -
6.2 METHODS	- 81 -
6.2.1 <i>Subjects</i>	- 81 -
6.2.2 <i>Protocol</i>	- 83 -
6.3 RESULTS AND DISCUSSION.....	- 84 -
6.3.1 <i>Techniques Analysis</i>	- 86 -
6.3.2 <i>Not-Agonists</i>	- 89 -

6.3.3	<i>Agonists</i>	- 93 -
7	CONCLUSIONS AND FUTURE DEVELOPMENTS.....	- 97 -
	REFERENCES.....	- 101 -
	APPENDIX A: JUDO BREAKFALLS AND TECHNIQUES	- 105 -
	APPENDIX B: TESTING 3-SPACE™ SENSORS.....	- 111 -
	APPENDIX C: MATLAB SCRIPTS.....	- 117 -
	ACKNOWLEDGEMENTS.....	- 165 -
	RINGRAZIAMENTI.....	- 166 -

Abstract

Negli ultimi anni, l'analisi del movimento ha trovato vaste applicazioni nell'area della scienza dello sport grazie allo sviluppo di nuove tecnologie adatte alla variabilità delle situazioni presenti in ciascuna disciplina sportiva. In particolare, l'applicazione dell'analisi del movimento allo sport può avere due obiettivi principali: il miglioramento delle prestazioni di un atleta e la prevenzione di traumi e rischi legati alla pratica dell'attività fisica.

Questo studio si propone di studiare e di analizzare nel dettaglio, tramite l'ausilio di sensori inerziali (IMU), il rischio di traumi alla testa e al collo associato alla pratica del Judo e le strategie insegnate agli atleti per evitare tali danni.

Inizialmente, è esaminata la tipica caduta all'indietro deputata alla prevenzione di traumi alla nuca (ushiro ukemi): essa è analizzata nel dettaglio suddividendo le curve in fasi per elucidare il meccanismo di base. Inoltre, l'esecuzione standard è paragonata ad uno svolgimento senza l'ausilio delle braccia e delle mani, come può accadere in combattimento. I risultati sono interpretati in termini di accelerazione lineare e angolare della testa e del tronco e angolo di flessione-estensione del collo.

In secondo luogo, è presentato uno studio sul rischio di traumi cerebrali (TBI) quando proiettati con tecniche del Judo. Quattro tecniche (o-soto-gari, o-uchi-gari, ippon-seoi-nage and tai-otoshi) sono state testate su un campione di 40 soggetti, divisi in Agonisti e Pre-Agonisti sulla base dell'età e ulteriormente suddivisi in base all'esperienza nella pratica del Judo. Le misure ottenute sono state poi analizzate per trovare valori del Gadd Severity Index (GSI) sopra soglia e differenze significative nelle variabili considerate tra i gruppi dei Non-Esperti e degli Esperti. Inoltre, sono state valutate anche differenze statisticamente rilevanti tra le quattro tecniche esaminate per verificare quali possono essere considerate più soggette a rischio di traumi cerebrali.



List of Figures

Figure 2.1: Linear and rotational acceleration of principal impacts related to their duration [5].....	5 -
Figure 2.2: The Wayne State Tolerance Curve gained from experimentation.....	6 -
Figure 2.3: Threshold curves for linear and rotational acceleration versus duration of the impact [5]. TBI = Traumatic Brain Injury, PCS = Post Concussive Syndrome, mTBI= mild TBI, MMA = Mixed Martial Arts.	7 -
Figure 2.4: Epidemiology of head (A,C) and neck (B,D) injuries in Judo in 2003-2010 by Kamitani and al. [29]. A,B) Age category distribution: ES = elementary school; JH = junior high school; SH = senior high school; US = university student. C,D) Distribution of experience years. Adapted from [29].	18 -
Figure 2.5: Outcomes of Judo-related head and neck injuries detected by Kamitani et al. [29].	18 -
Figure 2.6: Diving movement. While throwing especially with uchi-mata technique, many athletes tries to use their head as an additional support (phase B): in this way, neck is hyper-flexed provoking dangerous traumas to the cervical spine. This movement is now prohibited and punished with the immediate exclusion from the competition.....	19 -
Figure 2.7: Catastrophic head injuries in Japanese scholars (7–18 years) described by the Japan Sports Council during the period from 1998 to 2011. As can be seen, Judo was the primary cause of death or severe disease: among 88 athletes with catastrophic sports head injuries, 40 joined in Judo [30].... -	19 -
Figure 3.1: Strain-gage based accelerometer [51].	37 -
Figure 3.2: Accelerometer based on the piezoelectric effect [51].	38 -
Figure 3.3: Schematic representation of a MEMS capacitance accelerometer. A) Overall vision of the device. Highlighted portion is presented in part B. B) Particular of the device functioning principle. Adapted from [52].	38 -
Figure 3.4: Functioning of MEMS gyroscope. A) No angular motion is provided, thus the mass moves only on the driving direction. B) Angular rate takes place, inducing a movement in the sensing direction which is detected by electrodes.....	39 -
Figure 4.1: Measures obtained in different axes configurations.....	41 -
Figure 4.2: Acceleration module during the first linear test.....	42 -
Figure 4.3: Linear acceleration preliminary test.....	42 -
Figure 4.4: Experimental setup for angular tests. A) X-axis rotation, B) Y-axis rotation, C) Z-axis rotation. ...	43 -
Figure 4.5: Rotational test, angular velocity in the X direction.....	44 -
Figure 4.6: Rotational test, angular velocity in the Y direction.....	44 -
Figure 4.7: Rotational test, angular velocity in the Z direction.....	44 -
Figure 4.8: Anatomical planes and axes considered in the test.	45 -
Figure 4.9: Angular velocities obtained in studying the range of motion of a human neck. “Sensor15” was placed onto forehead, while “Sensor13” on the sternum.....	46 -
Figure 4.10: Angles gained from integration of the angular velocities presented in Figure 4.9. “Sensor15” was placed onto forehead, while “Sensor13” on the sternum.....	46 -
Figure 4.11: Angle between the two IMUs used in the test. Angle in the X direction represents head rotation movements, in the Y direction flexion/extension and in the Z direction lateral flexion.....	47 -
Figure 4.12: First measurement of linear acceleration during backward breakfalls.....	47 -
Figure 4.13: Linear acceleration obtained by o-soto-gari technique.....	48 -
Figure 4.14: Particular of the second o-soto-gari throw.	48 -
Figure 4.15: Linear acceleration measured while being thrown with tai-otoshi technique.....	49 -
Figure 4.16: Particular of the second tai-otoshi projection. Both sensors saturated, as in the case of the first throw.	49 -

Figure 5.1: Triangular path followed for verifying trajectory reconstruction.	- 53 -
Figure 5.2: Comparison between Kinovea and IMU trajectory reconstruction. Data are normalized to the maximum of their module, because even if IMU data are in standard units of measurement, Kinovea data are exported in pixels and no comparison could be easily made. IMU data are resampled to match the lower video sampling rate.	- 54 -
Figure 5.3: Analysis of standard backward breakfall. Positive angle values mean neck extension while negatives flexion.	- 55 -
Figure 5.4: Analysis of "no-hands" backward breakfall. Positive angle values mean neck extension while negatives flexion.	- 56 -
Figure 5.5: Head acceleration during backward breakfalls.	- 57 -
Figure 5.6: Trunk acceleration during backward breakfalls.	- 57 -
Figure 5.7: Head angular velocity during backward breakfalls.	- 58 -
Figure 5.8: Trunk angular velocity during backward breakfalls.	- 58 -
Figure 5.9: Head angular acceleration during backward breakfalls.	- 59 -
Figure 5.10: Trunk angular acceleration during backward breakfalls.	- 59 -
Figure 5.11: Angle between head and trunk during backward breakfalls. Neck flex-extension angle is represented by Y-angle: positive values mean neck extension, while negative denotes flexions. ...	- 60 -
Figure 5.12: Virtual markers placement for coordinates extraction in Kinovea. Here are reported some frames used for points tracking.	- 61 -
Figure 5.13: Comparison between the angle obtained by IMU and the one gained from Kinovea video analysis.	- 61 -
Figure 5.14: Correlation mean values of principal variables involved in breakfalls movement.	- 69 -
Figure 5.15: ICC values for main variables cited in the ukemi analysis. Negative values are not presented because of the lack of physical meaning.	- 70 -
Figure 5.16: Wilcoxon signed rank test results. P-values < 0.05 are presented for main variables used in the comparison between standard and "no-hands" backward breakfall.	- 72 -
Figure 5.17: Comparison of neck angle gained by IMU. Values of the four phases statistically analysed are here evidenced. The time instant for each phase is respectively selected from the X-acceleration curve of the head for each type of breakfall. As previous figures, means and standard deviations were computed from all 30 breakfalls for the two breakfalls types. Values obtained in phases C and D demonstrate statistical differences with $p < 0.05$ and $p < 0.01$ respectively.	- 73 -
Figure 6.1: Mean values and standard deviations for each repetition among the three days of test. Means are interpolated with a linear regression.	- 76 -
Figure 6.2: Peak values for every repetition. Best fit lines for each day are calculated on peak values gained in each daily repetition.	- 76 -
Figure 6.3: Mean values and standard deviations calculated among all eight repetitions for each day.	- 76 -
Figure 6.4: Acquisitions while performing the static test before calibration.	- 77 -
Figure 6.5: Linear acceleration gained in the static test after sensors calibration.	- 78 -
Figure 6.6: Filtered acceleration values obtained after calibration.	- 78 -
Figure 6.7: Angular velocity gained in the static test before calibration.	- 79 -
Figure 6.8: Comparison of data gained simultaneously by the two sensors placed on subject's head.	- 79 -
Figure 6.9: Comparison of data gained by the two sensors placed on subject's trunk.	- 80 -
Figure 6.10: Comparison of the acceleration module calculated from data acquired by the sensors placed on subject's head and trunk.	- 80 -
Figure 6.11: Experiment setup used in the protocol. Two collaborators were exploited to avoid stresses on the cables.	- 83 -
Figure 6.12: Values experimentally gained through the tested protocol. Values on the head are here displayed for the two groups analysed.	- 85 -
Figure 6.13: Mean values and standard deviation of variables considered for finding significant differences among the four tested techniques. Values divided for the two group are here presented. Head angular acceleration is represented divided per 100 and duration divided per 10 to increase images readability.	- 87 -
Figure 6.14: Comparison of variables among the four techniques for the Agonists group: T1 = o-soto-gari, T2 = o-uchi-gari, T3 = ippon-seoi-nage, T4 = tai-otoshi. All significant p-values obtained with the	

Friedman and post hoc tests are highlighted, one star means $p < 0.05$, two stars $p < 0.01$ and three stars $p < 0.001$.	- 89 -
Figure 6.15: Accelerations values grouped for repetitions. Fatigue or adaption may be visible by particular trends in all techniques.	- 89 -
Figure 6.16: Results of the Mann-Whitney test for main variables involved in the study. The lowest value obtained is 0.055.	- 90 -
Figure 6.17: Results of the Mann-Whitney test conducted between Not-Agonists with one or two years of experience in practicing Judo.	- 90 -
Figure 6.18: Mean values and standard deviation of linear and rotational accelerations for the Not-Agonists category. Values are compared between Expert and Not-expert groups.	- 91 -
Figure 6.19: Mean values and standard deviation of neck extension and flexion angles for the Not-Agonists category. Values are compared between Expert and Not-expert groups.	- 92 -
Figure 6.20: Mean values and standard deviation of impact duration for the Not-Agonists category. Values are compared between Expert and Not-expert groups.	- 92 -
Figure 6.21: Mean values and standard deviations of the neck angle at the acceleration peak time. Positive values mean neck extension, negative correspond to flexion. Results for the significance test are proposed below.	- 93 -
Figure 6.22: Accelerations values grouped for the three repetition among subjects.	- 93 -
Figure 6.23: Mann-Whitney test results for the main variables involved in the study for Agonists category. P-values lower than 0.1 are presented.	- 94 -
Figure 6.24: Mean values and standard deviation of linear and rotational accelerations for the Agonists category. Values are compared between Expert and Not-expert groups. Statistical differences are highlighted by star sign, one meaning $p < 0.05$.	- 94 -
Figure 6.25: Mean values and standard deviation of neck extension and flexion angles for the Agonists category. Values are compared between Expert and Not-expert groups.	- 95 -
Figure 6.26: Mean values and standard deviations of the neck angle at the acceleration peak time. Positive values mean neck extension, negative correspond to flexion. Results of the significance test are proposed below.	- 95 -
Figure 6.27: Mean values and standard deviation of impact duration for the Agonists category. Values are compared between Expert and Not-expert groups. P-value < 0.05 is highlighted with star sign....	- 96 -
Figure 7.1: Ura-nage technique.	- 99 -
Figure A.1: Ushiro ukemi execution.	- 105 -
Figure A.2: Yoko ukemi.	- 106 -
Figure A.3: Zempo kaiten ukemi.	- 106 -
Figure A.4: O-soto-gari.	- 108 -
Figure A.5: O-uchi-gari.	- 108 -
Figure A.6: Ippon-seoi-nage.	- 109 -
Figure A.7: Tai-otoshi.	- 109 -
Figure B.1: Initial windows of the 3-Space Suite by Yost Labs. A) Mac version. B) Windows version...	- 111 -
Figure B.2: Comparison between ATR-Promotions and 3-SpaceTM sensors, with a sample rate of respectively 1000 Hz and about 50 Hz, while doing three consecutive breakfalls (the last is here reported). The positive peaks in X-acceleration and Y-angular velocity were missed by Yost Labs sensor due to the low sample rate.	- 113 -



List of Tables

Table 2.1: Values of linear and angular acceleration and duration of head impacts reproduced by Hoshizaki et al. [5].....	- 7 -
Table 2.2: Articles examined in the research on performances in Judo.	- 11 -
Table 2.3: Articles found in literature on the application of accelerometers to Judo athletes.	- 20 -
Table 2.4: Papers regarding studies on the path of neck flexion/extension angle during typical Judo movements.	- 21 -
Table 2.5: Articles regarding head and neck injuries found in literature.	- 24 -
Table 2.6: Articles inherent to biomechanical analysis of Judo techniques with dummies technology....	- 31 -
Table 2.7: Return to play (RTP) protocol after head injuries [30]. Every step must require at least 24 hours, therefore minimum interval between impact and RTP is about a week.....	- 34 -
Table 3.1: Technical specifications of ATR-Promotions TSND121. * = values obtained through the equation resolution = range / 2^{NBIT} , where NBIT = 12 bit from datasheet information.....	- 40 -
Table 4.1: IMUs on the market appropriated for the research purpose. * = Reference accelerometer used in studies found in literature, N.D. = Not Declared in available documentation.	- 51 -
Table 4.2: Technical specifications of Yost Labs 3-Space™ Bluetooth sensors Ultra High-G. * = values obtained through the equation resolution = range / 2^{NBIT} , where NBIT = 12 bit for accelerometer and magnetometer, 16 bit for gyroscope (data from datasheet information).	- 52 -
Table 5.1: Values of ICC and correlation gained from SPSS software. Highlighted cells reflect thresholding by Koo et al. [53] for ICC and by Evans [54] for correlation: dark green means excellent reliability or very strong correlation, light green means good reliability or strong correlation, yellow means moderate reliability or moderate correlation.	- 63 -
Table 5.2: P-values obtained with the Wilcoxon signed rank test. Highlighted cells reflect significance level: light green means $p < 0.05$, dark green means $p < 0.01$. No values with $p < 0.001$ were found.....	- 71 -
Table 6.1: Age and experience years of the subjects involved in the study. Groups: Aex = Expert Agonists, An = Not-expert Agonists, NAex = Expert Not-agonists, NAn = Not-expert Not-Agonists. Belts order is the following: white, yellow, orange, green, blue, brown and black (I dan, II dan, III dan and so on).	- 81 -
Table 6.2: Mean values and standard deviations (std) of height and weight of the different groups involved in the study. Groups: Aex = Expert Agonists, An = Not-expert Agonists, NAex = Expert Not-agonists, NAn = Not-expert Not-Agonists.....	- 82 -
Table 6.3: Physical and Judo-related characteristics of selected throwers.....	- 82 -
Table 6.4: Techniques order used in the tests. for both categories. 1 = T1 (o-soto-gari), 2 = T2 (o-uchi-gari), 3 = T3 (ippon-seoi-nage), 4 = T4 (tai-otoshi).	- 84 -
Table 6.5: Results of the post hoc test. All values are reported even if Friedman’s test found differences just in accelerations and angles for the Agonist category. Cells are evidenced in colours corresponding to the p-value found: very light green means $p < 0.05$, light green $p < 0.01$ and dark green $p < 0.001$.-	- 87 -
Table B.1: Pros and cons of proposed solutions.	- 116 -

1 Introduction

Since the development of technology has taken place, new ways for opening the wisdom doors about how the human body works have been found. New technologies have been exploited in many fields such as Medicine, from Surgery to Imaging, Engineering, from Mechanics to Electronics, and other areas in which their application has improved the knowledge of phenomena or the manipulation of such phenomena in order to get advantage of them.

In particular, new technologies have become a fundamental part of experimentation on the human body for increasing the understanding of its functions. The innovation has met also a field in which the only instruments to define, analyse and improve subject's capabilities were the human eye and other subjects' opinion: the sport. Indeed, the introduction of high-speed video cameras, computers with higher performances and several types of sensors brought innovations in this field, in particular from the point of view of performances improvement.

In recent years, the interest has moved to another aspect of the sport science which involves athletes' safety and traumas avoidance. Injuries prevention has become a primary aspect for sport association in countries, but also for National, International and Olympic committees. Moreover, this aspect is related to many sports, in particular to sports in which the contact between athletes often occurs due to the agonism or to the sport regulation itself, such as happens in collision sports (American Football, Rugby, Soccer, Hockey) and contact sports (Wrestling, Judo, Mixed Martial Arts).

American Football and Hockey have been studied for years in the United States of America because of the presence of violent impacts, leading to variations on rules about mandatory gears and helmets.

In Japan, the interest has shifted to Judo, a martial art used as a moral, spiritual and physical form of education in schools. Due to the great number of Japanese people doing Judo every day, the number of injured people has increased in last years. Even if the main typology of injuries comprises hands and fingers, when head and neck are involved the outcome is often serious and many cases of death and permanent diseases have been reported.

In addition to the interest about injury prevention, a new technology, principally developed for aviation and other areas involving position estimation tasks, has started to approach sport science: the new technology here cited is inertial sensors. These devices are probably the best solution for studying Judo, because occlusion problems related to video analysis are excluded and the same information can be acquired wirelessly through very small devices. Furthermore, other problems related to optoelectronic systems such as the limited sample rate can be overcome achieving frequencies above 1 kHz needed for impacts assessment.

The study here reported is aimed to analyse and figure out the mechanism related to head and neck injuries in Judo and the strategies adopted by judokas to avoid them. Moreover, an analysis on the risks of head injuries due to over-threshold values of linear and angular acceleration is carried out on athletes of different ages and levels of experience.

Firstly, the Inertial Measurement Unit (IMU) technology used in the tests is briefly described, then a preliminary analysis on how one of the fundamental Judo breakfall (ushiro ukemi) works for reducing linear and angular acceleration on the head during falls is presented. Phases of the movement are highlighted and an analysis on the differences about two types of breakfall, the standard one and a variation of it which may happen during fights, is built up. Head and trunk linear acceleration, rotational acceleration and the angle of flexion/extension of the neck are monitored to study their variations in time in terms of physiological values.

After that, an in-depth analysis on the potential risk of Traumatic Brain Injuries (TBI) while doing Judo is conducted. Four techniques (o-soto-gari, o-uchi-gari, ippon-seoi-nage and tai-otoshi) are tested on a group of 40 athletes of various ages and years of experience in practicing Judo: results are thus discussed in terms of linear and angular accelerations of the head and of the trunk, values of neck flexion and extension angles, neck angle at impact time and impact duration, verifying the level to which subjects are exposed and searching for differences between groups and techniques. Moreover, a measure of the severity of the impact is used for determining if acceleration levels here acquired could be considered safe or dangerous for humans: the Gadd Severity Index (GSI) is considered for taking into account the whole impact.

2 Motion Analysis in Sport Activities

A literature review was conducted to understand which approaches had been applied for studying Judo in quantitative manner until today. The research was carried out on PubMed, PICO and on the web looking for articles and documents comprising words as "Judo", "sport biomechanics", "combat sports", "acceleration", "injuries", "head", "traumas", "motion analysis", "IMU", "concussion", "acute subdural hematoma", "TBI" and their combinations.

At first, an introduction about motion analysis applied to sport science is given, then it is contextualized to the main topic of the research, Judo, considering its application for performances and injuries prevention. Specific cases of head and neck injuries are thus presented focusing on the physiopathology of traumatic brain injuries typical of collision and contact sports.

2.1 Introduction

The existing motion analysis systems allow to obtain detailed information for qualitative or quantitative investigation of movements performed by athletes. Exploiting this information allows coaches and athletes to revise skills and eliminate errors, as well as reduce principal causes of injury: it will lead surely to an improvement of the efficiency and the effectiveness of training method.

Motion analysis systems are currently used in various areas of modern life. Nowadays, many studies concerning capture human motion and then extract information have been conducted by researcher and coaches [1]. Indeed, motion analysis systems are a major tool for athletes, coaches and engineers in a wide-ranging field of applications in sports, such as technical research, athletic performance analysis, evaluation of physical condition, injuries prevention and investigation, rehabilitation. This type of systems is currently used for scientific research or for training athletes in individual and team sports, for example Tennis, Swimming, Golf, Gymnastics, Baseball, Basketball, Volleyball, Football, Rugby, combat sports and Martial Arts.

Martial Arts and combat sports require complex abilities and strategic excellence. In these sports, movements executed by athletes are precise stances and dynamic actions, performed individually (punches, kicks, strikes) or in contact with the competitor (throws, blocks, articular levers or chokes). Moreover, actions are performed on an aerial trajectory or laying on the ground, in standing, kneeling or lying situations and movements are described by high dynamics and short time duration, making fairly impossible to catch all the details of the movement even through an expert eye. The use of technology in these sports will surely help coaches and athletes to improve their performances giving essential information and data regarding complex movements.

The key point of the training progression in combat sports and Martial Arts, but also in many other sports, is to reach excellence in the execution of techniques and strategic conducts together with the development of physical condition allowing for challenging with other contestants without the possibility of incurring in damages.

The analysis of athlete's movements during trainings and competitions is an important element for his growth. Motion analysis of these activities provides information about the correctness and the effectiveness of the specific technique and supports errors identification. This information will then serve for coaches and athletes to improve the training phase and to eliminate errors. In the end, thanks to information gained by motion analysis systems, they would improve movements efficiency and reach then projected progresses and competitive results.

Data acquired through motion analysis may be used for many dedications, but main goal is refining the technical performance of movements distinctive for every kind of sport activity. Polak et al. [1] identified the particular objectives of the usage of motion analysis systems on athletes:

- gain detailed comprehension of qualitative features of the motion;
- understand the exactness of the specific techniques;
- recognise errors in the technical execution;
- define risks and reasons of body damages;
- obtain a graphical feedback for coaches and athletes.

These points can be achieved if trainers and players complete the motion analysis by their own, or they may take advantage of the material written by scientists of motion analysis in sports or other research areas. Information, in association with qualified knowledge of human biomechanics, would so be helpful in quotidian preparation program for reaching sought results. This kind of cooperation will certainly lead to benefits to both sport activity and research studies.

Another principal aspect in dealing with sport is undoubtedly the possibility of receiving and causing body traumas: deepening knowledge on prevention of injuries must be a dominant field in sport research field. Unfortunately, injuries occur in every sport activity, from the ones which could be considered safer to the more dangerous ones, such as combat sports. Injuries comprehend traumas related to every human body segment, but the most reviewed are head and neck injuries which may lead to severe consequences or even decease.

Most analysed sports for the prevention of traumas are the ones in which great impacts often occur, i.e. collision sports (American Football, Rugby, Soccer, Hockey) and contact sports (Wrestling, Judo, Mixed Martial Arts).

As stated by O'Connor et al. [2], in 2012, among the 23.6 million US youth athletes, 19% joined collision sports and 57% participated in contact sports. Considering that these athletes are more exposed to risk for traumas, an estimated 1.6 million to 3.8 million sport-related traumatic brain injuries befall in the USA every year. Moreover, analysing in detail the traumas, head concussive injuries contribute for 8.9% of all high school and 5.8% of all collegiate sport injuries.

Since rules differ in each combat sport, injury profile is different between styles agreeing with fight rules (e.g. allowed targets and techniques). Indeed, injuries location and severity are a consequence of which portions of the human figure are mostly attacked in fights: primary sites of injuries are actually main targets and the parts of the body used for attacking. In fact, as it can be supposed, lower limb injuries are infrequent in Boxing, while they are usual in Taekwondo (51%), Karate (45%) and Judo (47%), since the foot is employed to kick the opponent's trunk or head, or it is used as a tool to brake opponent's balance. However, blows to enemy's head are extremely rare in Judo in which punches, kicks, elbow and knee strikes to the head are illegal, but they are remarkably usual in Boxing (84%), Karate (74%), Mixed Martial Arts (64%), and Kickboxing (55%) in which striking the opponent's head is permitted. Hurts to the upper limbs are mostly involved in Taekwondo (40%) and Aikido (43%). Moreover, spine injuries are infrequent in all combat sports (2–10%), thanks to the prevention rules for severe outcomes [3].

Because they are the main target in several combat sports, head and neck are regularly injured, but being thrown to the ground and knockouts are counted at superior probability of head injuries. Cerebral concussions for example, bringing to dizziness, headaches, nausea, and problems to balance, concentration and memory, are always viewed as severe damages compelling a stop from all activities. This fact together with the high proportion of cases must be a cause for concern and study, especially if it is considered that recurring head traumas, also mild head traumas, may cause brain degeneration, disabilities and loss of cerebral functions [4].

Thinking of the proportion of cases in which head injuries occur due to impact and the severity of damages that they may lead to, an investigation on impact biomechanics during sport activities must be carried out to couple the injury mechanism to the clinical effect. In this way, by realizing insult mechanism, sports

medicine experts can decide, with a more accurate vision of the issue, on equipment improvements and rule changes in order to reduce injuries rate, especially concerning concussions and head impacts. Indeed, biomechanical data gained by experimentation have successfully enhanced players' security through the development of protecting apparatus and rule variations. This fact has been demonstrated in youth Ice Hockey and American Football in which rule changes have remarkably reduced head traumas incidence. More research is needed to determine if the incidence of traumatic injuries could be reduced for all sports at all levels and ages. Thus, sport impacts have to be scientifically examined in order to elucidate the insult mechanism and provide efficient solutions for avoiding traumas.

2.1.1 Correlation of Acceleration Magnitude and Duration

Many researches have been conducted in analysing the correlation between acceleration peaks and duration of the impact. These studies involve actions and accidents that unfortunately may happen every day, not only while doing sport activities. Moreover, data from sport activities have been included in such investigations (Figure 2.1). Lots of studies have been conducted involving the analysis of head impacts deriving from everyday life and sport activities in order to provide information on a threshold curve comprehending different environments and situations.

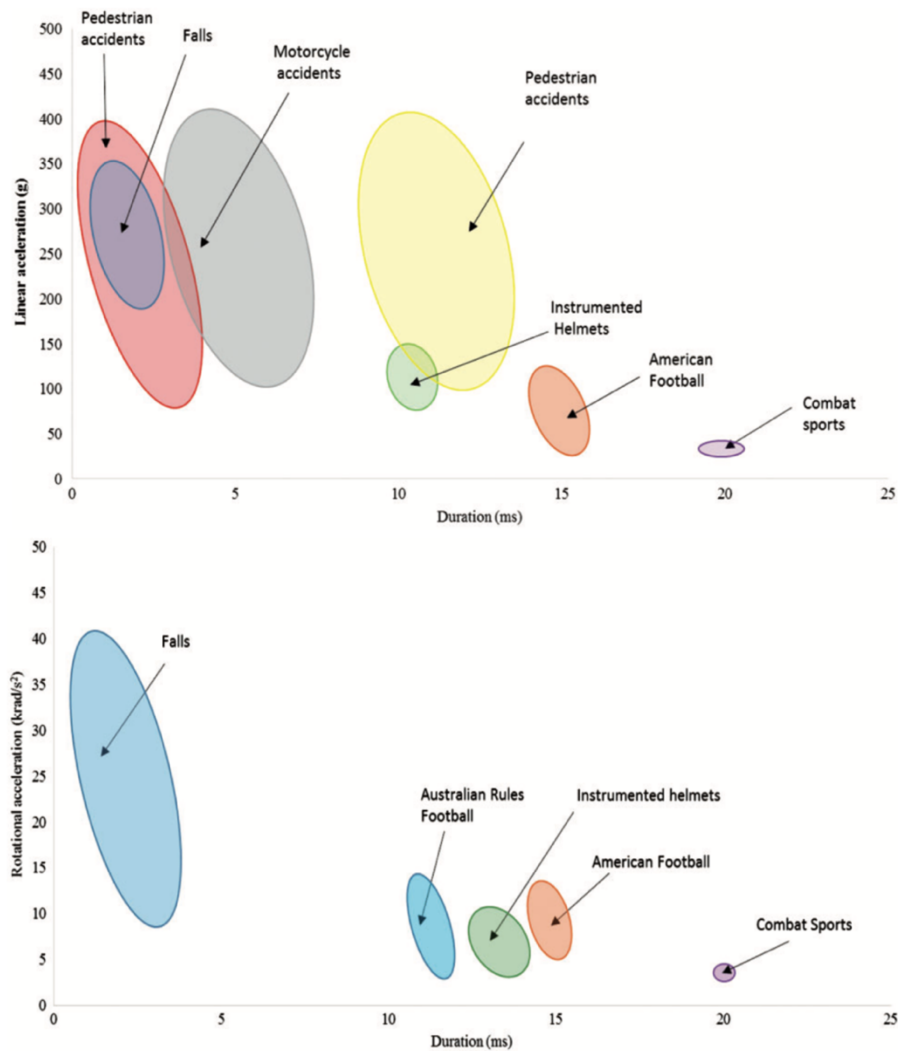


Figure 2.1: Linear and rotational acceleration of principal impacts related to their duration [5].

In addition to the simple acceleration module, other parameters can be used in estimating human tolerance. The first threshold curve was established working on car impacts to develop materials for lessening skull fracture risk during accidents: these studies brought to the Wayne State Tolerance Curve (WSTC), the first graph in which injury are linked to impact features. This curve was obtained from frontal head impacts to animals and corpses considering skull fracture as the boundary because highly correlated with brain injury. Even if this assumption may not be always true, a tolerance curve containing impact conditions was firstly provided (Figure 2.2). As can be seen from data plotted in the graph obtained from experimentation, high accelerations can be tolerated just for short duration while longer impacts can be withstood if acceleration magnitude becomes lower.

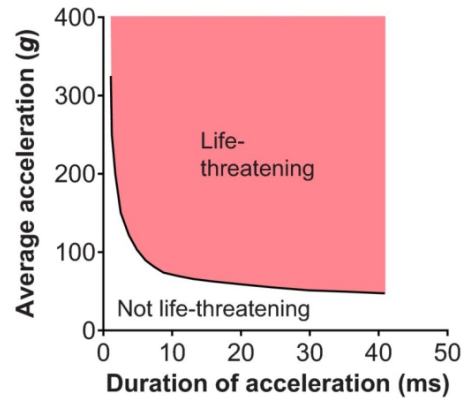


Figure 2.2: The Wayne State Tolerance Curve gained from experimentation.

In the '50s, academics of the Wayne State University scientifically proved that duration as well as magnitude of intracranial pressure conveyed by blowing air on animals' bare dura was of paramount importance in establishing injury level. They found that high pressures can be tolerated without injuries if exposition was very short. Many years after, thanks to new ways of measuring accelerations (cadavers' head acceleration), which is linked to occiput intracranial pressure, would be used to study impacts to automotive panels, windshields and other surfaces. In this way, the preliminary WSTC was developed, predicting head injury manifestation through values of duration and mean acceleration during the impact. The curve obtained confirmed the results in term of intracranial pressure gained years before and was thus refined by further testing and experimenting on cadavers and human beings.

The WSTC can be considered as the first quantitative human brain injury criterion basing on linear acceleration; angular acceleration was lately introduced as the basis for curve threshold and generally it is not already used as a standard in automotive or sport safety.

The curve has become the foundation for many others injury metrics currently exploited, such as the Gadd Severity Index (GSI) and the Head Injury Criterion (HIC). In particular, the GSI takes in account the entire traumatic event by calculating the value of the integral during the time impact of the acceleration to the 2.5: this power value was obtained through a logarithmic analysis of the WSTC and represent its gradient. Values greater than 1000 may cause severe complication in the 50% of cases [6].

HIC instead evaluates the integral of a portion of the mean acceleration curve, to the 2.5 and multiplied for the interval of time considered, representing its maximum value.

Recently, Hoshizaki et al. [5] compared the WSTC curve and the one suggested by Van Lierde in 2005: simulating bicyclist to car and bicyclist to concrete impacts, he developed a threshold curve pondering on angular acceleration of the head, named Brain Injury Curve Leuven (BICLE). Data from BICLE and WSTC were plotted together with data gained from reconstructions of head injuries event coming from literature (Table 2.1) utilising the Hybrid III anthropometric test device (Figure 2.3).

Table 2.1: Values of linear and angular acceleration and duration of head impacts reproduced by Hoshizaki et al. [5].

Event type	Injury type	Peak resultant linear acceleration (g)	Peak resultant rotational acceleration (krad/s ²)	Duration (ms)
Falls	TBI/skull fracture	300–400	30 or more	3–5
Bicycle fall	TBI	400	18	n/a
Australian rules football	Concussion	60–182	3.5–16.5	n/a
Instrumented helmets – football	Concussion	64–134	2.8–6.7	n/a
American football collisions	Concussion	32–102	4.0–12.8	15
Judo	Subdural hematoma	41	3.3	20
American football, motorcycle, pedestrian collision	Concussion and TBI	100–400	n/a	4–14

TBI: traumatic brain injury.

As can be seen from linear acceleration graphs, for short time accidents the WSTC is lower than the best fit line so it is meant to be conservative, thus the same degree of acceleration may be tolerated for more time. Otherwise, for longer impacts there is an inversion of the two curves and so the WSTC overestimates the acceleration threshold. Furthermore, considering rotational acceleration, the BICLE seems to approximate injury values reconstructed in laboratory by Hoshizaki, demonstrating its reliability as angular acceleration threshold.

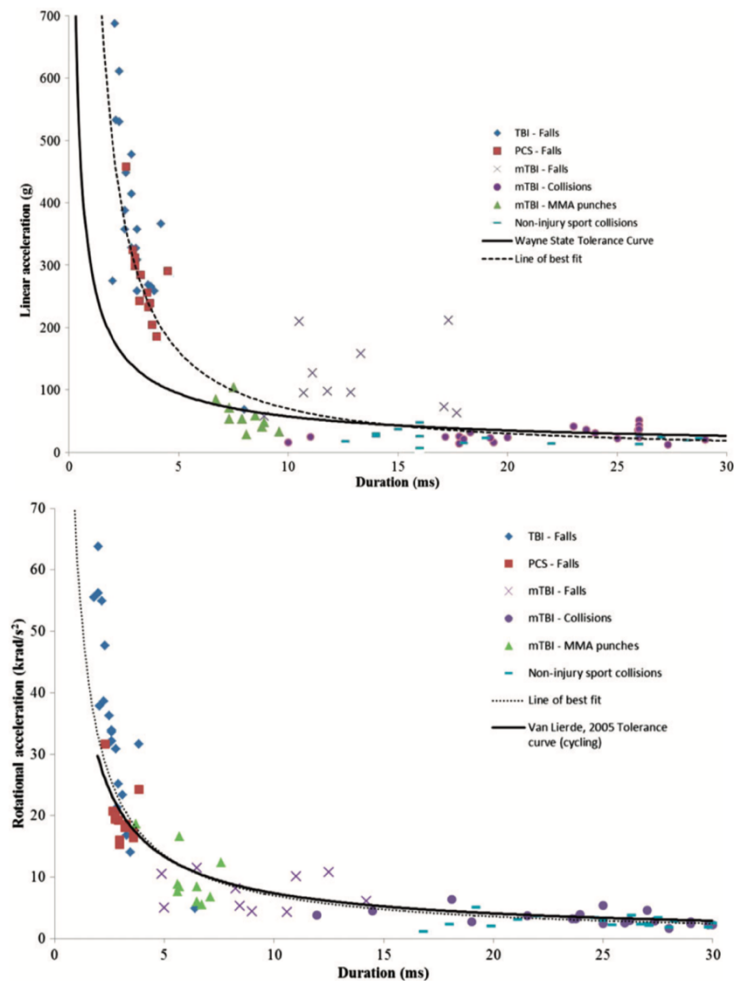


Figure 2.3: Threshold curves for linear and rotational acceleration versus duration of the impact [5]. TBI = Traumatic Brain Injury, PCS = Post Concussive Syndrome, mTBI= mild TBI, MMA = Mixed Martial Arts.

2.1.2 Cumulative Head Impacts Effects

Head traumas can develop not only from high values of acceleration localized in time, but also after many repeated events in which acceleration did not exceed the threshold.

Recently, an increasing interest has developed in determining and analysing neuropathological effects of repetitive head impacts and multiple concussions in athletes. Considering the rate of sport head impacts, repercussion of these traumas on public health should be noteworthy [7].

As previously stated, brain injuries can develop even through repetitive sub-threshold impacts. This fact has been demonstrated by many animal studies, for example the one conducted by Gao et al. [8] who, modelling TBIs to identify neurobehavioral variations in rats, concluded that repetitive mTBI may result in severe neurobehavioral damages and the accumulation of impacts could be linked to augmented brain inflammation.

The argumentation has been carried out by researchers examining Soccer, Ice Hockey, Boxing and American Football [7]: however, the most analysed sport was American Football [9] [10] [11] [12] [13] [14] [15] [16].

Accelerometers were used in this field of application to measure and calculate parameters like linear and rotational acceleration, number of impacts above a threshold, cumulative accelerations and traumas index, as for example Head Injury Criterion (HIC), Gadd Severity Index (GSI or SI). The predictive power of these indexes was investigated by Greenwald et al. [11]: using the Principal Component Analysis they hypothesized a new index to be the more reliable in detecting concussions.

Other studies were conducted in measuring quantities related to acceleration during a whole season, considering both training sessions and matches [9] [10] [12] [13] [16]. Furthermore, they studied also differences in parameters measured onto players in distinct roles gaining as expected different results. After having measured cumulative impacts characteristics, researchers could not compare their results to a determined threshold because no data in this field have been published in medical literature [13] [16]. Moreover, no correlation between multiple head injuries and lowering of concussion threshold have been demonstrated yet [14].

In conclusion, O'Connor et al. [15] stated that results obtained from their research encourage the hypothesis that concussion probability is not influenced by cumulative acceleration magnitude of sustained traumas. Indeed, magnitude summation is a rudimentary method to quantify the overall exposition to traumatic accelerations over a certain period of time, assuming athlete's brain as static and incapable of self-repairing. Future studies may then reflect on the influence of physiological tissue re-healing among impacts on TBIs probability.

2.2 Motion Analysis Applied to Judo

As in other sport activities, the introduction of motion analysis has developed also in Martial Arts, remarkably in Judo. As stated in previous sections, the main purpose of this application is to analyse and improve the execution of all techniques during the training phase, but also during simulated matches. Another strategy of using sensors on an athlete deals with injuries prevention: moreover, this is a crucial aspect in Judo because of the ability which is required to competitors not to fall incorrectly avoiding serious traumas. While the first purpose is mainly related to elite judokas, the latter comprehends children and novice judokas for which learning the correct breakfall technique is of paramount importance.

2.2.1 Performance Analysis and Improvement

Since last twenty years, the interest in improving performances of elite athletes or in comparing them with novice judokas has been growing determining a great expansion in this literature field (Table 2.2, presented at the end of Section 2.2.1). In these studies, many systems were used to quantify linear and angular acceleration and velocities, such as optoelectronic systems and accelerometers. Furthermore, other types of transducers were adopted to quantify physical quantities, for example force sensors, force platforms and ergometers.

These analyses brought important results in determining the optimal technique and movements essential for the most efficient throw: the outcome derives also from the comparison between experienced judokas and not-elite athletes, and from the comparison of different Judo throws.

Judo is a situational sport: the development of the fight phases is directed by the mutable environmental situation. Actions of attack and defence are generally subjected to opponent's movements and reactions. It is a sport centred on the changeability of the situation, because the opponent seeks, through false and misleading actions, not to reveal his future action (see Appendix A for further information about Judo).

In this type of sport, performances are complicated to be scientifically investigated due to the interaction with the opponent and to the variability of possible situations in a competition. Furthermore, a large amount of aspects correlated to performance are involved: for example, the extreme irregularity of circumstances and the high dynamism make it hard to accurately outline the psychomotor features required to players to be efficient and successful in a Judo competition.

Considering the hard background, the capability in evaluating required capacity and motor skills will guarantee a superior methodology useful in training, leading to an effectiveness improvement. Following this approach many studies were conducted considering parameters derived from Judo techniques as a performance measure.

Imamura et al. [17] hypothesized the thrower's COM velocity as the leading parameter in determining the level of performance. Studying harai-goshi technique in different situations, i.e. competitive and non-competitive conditions, they found lower velocity in the throwing movements when the opponent dynamically resist to this action while, in this situation, faller's (in Japanese uke) velocity was the largest measured thanks to the great pulling force exerted by the thrower (in Japanese tori).

The comparison between competitive and non-competitive conditions was largely studied in literature: for example, Exton et al. [18] gained similar results measuring velocities during tomoe-nage throw. Tori's COM moves faster under non-competitive conditions because of standing of uke, while in competitive situation the same movement results slower due to opposing forces and movements employed by the opponent.

Another interesting research area is the one regarding the comparison between elite and collegiate athletes to obtain skill indexes useful in determining athlete's skill level and then training more successfully in order to increase his motor abilities. Many studies were conducted on this aspect: Ishii et al. [19] [20] measured the velocity of the two classes of athletes while performing seoi-nage Judo technique. They discovered that elite players drove themselves to the opponent more rapidly in the turning stage, suggesting that the quicker movement allows them to complete the technique before the opponent could respond in a defensive manner, avoiding any potential countermovement. In this way velocity gained by motion analysis systems could be used as a parameter to establish the skill level of the athlete.

Frassinelli et al. [21] [22] evaluated motor skills and abilities required for generate an efficient performance in Judo analysing elite athlete and created a useful tool to collect specific data to measure athletic performance during workout and simulation of Judo competitions. Combining aspects of sport science and direct engineering acquisitions of lower limbs accelerations, they developed a method to assess the level of performances and skills owned by an individual athlete, highlighting the possibility of comparing and linking technical and physical skills apparently uncorrelated.

Moreover, in research programs, other kinds of sensors were used to overcome restriction in optoelectronic and inertial systems. In particular, force was considered as the primary parameter in determining athletes' level of performance. Many analyses were managed in this field using force sensors [23] [24], tensometric sensors [25], force platforms [26] and strain-measurement platforms [27].

Blais et al. [23] monitored pulling force of athletes in time while training with a Judo-specific machine, determining that it can be used as a monitoring parameter to evaluate their performances. Similarly, Hassmann et al. [24] linked parameters gained from force sensors, such as maximal force, maximal force variation and maximal velocity, to athletes' performances and abilities related to Judo throws. Lech et al. [25] tried to correlate mechanical torque developed by muscles to the level of sport performance: it emerged

that highest values of muscle torque did not correlate significantly with sport performance level in elite Judo competitors.

Another aspect of this research area is studying the force path involved in Judo techniques and also defining how and when a counterattack may be successful during a match. Blais et al. [26] indeed examined the distribution of forces and energy expenditure in time during morote-seoi-nage technique. In a similar means, Dimitrova [27] analysed uki-goshi technique to establish a countermovement to block and overcome this base technique. She approached the problem using dynamographic records of the force vector, but the multidimensionality of the attack considered and of the defence movements proved the untenability of using the classic strain sensors for this scope.

2 Motion Analysis in Sport Activities

Table 2.2: Articles examined in the research on performances in Judo.

Title	Authors	Journal	Date of Publication	Purpose	Methods	Results
<i>A Kinematic Comparison of the Judo Throw Harai-Goshi During Competitive and Non-Competitive Conditions</i>	Rodney T. Imamura, Misaki Iteya, Alan Hreljac and Rafael F. Escamilla	Journal of Sports Science and Medicine	October 2007	Compare the kinematics (COM peak velocity, peak angular velocity) of the harai-goshi technique in competitive and non-competitive environments	<ul style="list-style-type: none"> - Two video cameras (JVC 60 Hz) - Three-dimensional motion analysis system (Vicon-Peak Performance Technologies) - Collection of data at a local judo tournament and at a local facility - No markers, manual digitization of 18 body points 	Under competition, thrower's COM was discovered to be mostly slower due to faller's defensive effort. Furthermore, faller's peak velocity was found to be greater demonstrating the major pulling force used by the thrower in fight circumstances.
<i>The Centre of Mass Kinematics for Elite Women Judo Athletes in Seoi-Nage</i>	Takanori Ishii, Michiyoshi Ae, Sentaro Koshida and Norihisa Fujii	34th International Conference on Biomechanics in Sport, Tsukuba, Japan	July 2016	Investigate kinematics of the COM in the seoi-nage technique executed by elite and collegiate women Judo competitors	<ul style="list-style-type: none"> - 18 cameras using a VICON-MX system (250 Hz) - 47 markers for each person 	Relative forward velocity of the COM would be an index to evaluate the skill level of seoi-nage for women Judo athletes.
<i>Validation of a Specific Machine to the Strength Training of Judokas</i>	Laurent Blais, Francis Trilles and Patrick Lacouture	Journal of Strength and Conditioning Research	2007	Measure the maximal pulling forces of a judoka while using a Judo-specific machine and a colleague for certifying the machine in strength training of judokas' grips and power	<ul style="list-style-type: none"> - Judo-specific machine with 4 different masses (15, 20, 25, and 30 kg) - Force sensors employed were gauge pressure sensors of the type ENTRAN ELPm (1 kHz) - Sensors attached to the masses of the machine - Sensors fixed on partner's judogi (sleeve and collar) with strong mountaineering ropes 	Significant differences were found between the peak pulling force utilizing the Judo-specific machine and a mate: it could be so used to assess and compare the performances of athletes.

2 Motion Analysis in Sport Activities

<i>Wearable Inertial Sensors for Human Motion Analysis: A review</i> <i>Biomechanics of Judo Backward Breakfall for Different Throwing Techniques in Novice Judokas</i>	Irvin Hussein López-Nava, Angélica Muñoz-Meléndez Sentaro Koshida, Takanori Ishii, Tadimitsu Matsuda and Toshihiko Hashimoto	IEEE Sensors Journal European Journal of Sport Science	2016 February 2017	Review on articles about sensors, algorithms and performances of systems for motion analysis Investigate the kinematics and possible risk factors of judo-related head injury when being thrown by comparing the breakfall motion for osoto-gari with that for ouchi-gari in novice judokas	- 41 reflective markers placed on participants landmarks and secured with adhesive tape - Participants also wore tight-fitting spandex shorts and judogi designed to augment markers prominence, as well as headgear for safety - A 20-camera Mac3D motion analysis system (200 Hz)	The significant differences with large effect size in the peak neck extension momentum and the head position with greater neck extension angle between the two techniques suggest that from both epidemiological and biomechanical points of view, being thrown with osoto-gari probably increases the risk head injury to a greater degree than does being thrown with ouchi-gari in novice judokas.
<i>Fight without Sight: The Contribution of Vision to Judo Performance</i>	Kai J. Krabben, John van der Kamp, David L. Mann	Psychology of Sport and Exercise	2017	Examine if vision is linked to performance while doing a contact sport	Data from two Vision Impaired (VI) Judo competitions and data from sighted judokas while competing sighted and blindfolded were analysed.	The level of vision deficiency influences performance, so blind athletes could not compete against moderately sighted opponents in VI Judo. The deficiency of visual intelligence decreases performances significantly.
<i>Impulsive Force on the Head During Performance of Typical Ukemi Techniques</i>	Toshihiko Hashimoto, Takanori Ishii, Naoyuki Okada and Masahiro Itoh	Journal of Sports Sciences	January 2015	Quantify kinematically the breakfall movement getting kinematic data about head	- Judo uniforms with a collar and sleeves - Three high-speed digital cameras CASIO EXILIM EX-F1 (300 fps)	Increasing the contact surface and time spent for diminishing vertical component of head velocity helps in reducing

2 Motion Analysis in Sport Activities

<i>Following Different Judo Throws</i>								the impact on the head.
<i>Kinematic Comparison of the Sei-Nage Judo Technique Between Elite and College Athletes</i>	Takanori Ishii, Michiyoshi Ae, Yuta Suzuki and Yasuto Kobayashi	Sports Biomechanics	February 2017	Investigate sei-nage by matching elite and college Judo athletes to attain ideas for improving the execution	- 25 body parts analysed - VICON-MX system with 18 cameras (250 Hz) - 47 markers per athlete - Specially designed judo gear	Elite athletes turn to uke more quickly, advising that the faster forward movement permits elite athletes to end the technique before rival might react in a defensive manner.		
<i>Kinematics of Judo Breakfall for Osoto-Gari: Considerations for Head Injury Prevention</i>	Sentarō Koshida, Takanori Ishii, Tadimitsu Matsuda and Toshihiko Hashimoto	Journal of Sports Sciences	July 2016	Study the kinematics of the breakfall for o-soto-gari to recognise possibility of head traumas by associating experienced and novice judokas	- 41 reflective markers - Tight-fitting spandex shorts, judo clothes and headgear - A 20-camera Mac3D motion analysis system (200 Hz)	Kinematic parameters (peak angular momentum of neck extension, movement patterns of trunk, hip and knee) can discriminate great from lacking breakfall skills concomitant with o-soto-gari technique.		
<i>Muscle Torque and Its Relation to Technique, Tactics, Sports Level and Age Group in Judo Contestants</i>	Grzegorz Lech, Wiesław Chwała, Tadeusz Ambroży, Stanisław Sterkiewicz	Journal of Human Kinetics	March 2015	Link maximal muscle torques at distinct phases of the athlete's improvement to the level of sport performance	- Hottinger tensometric sensor to measure force during isometric contraction	No significant correlation was found.		
<i>Rotational Acceleration during Head Impact Resulting from Different Judo Throwing Techniques</i>	Haruo Murayama, Masahito Hitosugi, Yasuki Motozawa, Masahiro Ogino and Katsuhiko Koyama	Neurologia Medico-Chirurgica (Tokyo)	May 2014	Measure translational and rotational head acceleration in Judo major throwing techniques which are responsible for head injuries	- An anthropomorphic test device (ATD), a POLAR dummy (h=175 cm, w=75 kg), and high bio-fidelity - Tri-axial accelerometer on the COG at dummy head, sampled at 20 kHz - Three DOF rotational accelerometers - High speed digital video camera (1 kHz)	The fast and vigorous movement produces a rotational force sufficient to cause injury, even with an under-mat.		

2 Motion Analysis in Sport Activities

<i>Three-Dimensional Joint Dynamics and Energy Expenditure During the Execution of a Judo Throwing Technique (Morote Seoi-Nage)</i>	Laurent Blais, Francis Trilles and Patrick Lacouture	Journal of Sports Sciences	July 2007	Validating a method for calculating joint moments while executing a Judo technique and analysing dispersal of energy outflow from the subjects	<ul style="list-style-type: none"> - Mayeur ergometer for judo training loaded with 20 kg and equipped with two Entran mono-axial force sensors - Five synchronized video cameras - Two Kistler force platforms (50 Hz) - SAGA 3 RT system, with six infrared cameras (50 Hz) - 33 external reflective markers 	The authenticity of the situation was reduced, but the study permitted to make the needed calculations while a precise technique was executed.
<i>Magnitude and Duration of the Impact Generated on the Athletes' Body During Training in Ippon Seoi-nage</i>	T. Piuco, S.G. Santos	Motricidade	2010	Analyse magnitude and duration of impacts in different regions of the human body when thrown by ippon seoi-nage	<ul style="list-style-type: none"> - Tri-axial accelerometer (Type 4321 da Brüel & Kjaer) fasten on uke's fist, hip and ankle 	Magnitude of the impacts: <ul style="list-style-type: none"> - 350g fist - 15g hip - 240g ankle
<i>A Three-dimensional Analysis of the Center of Mass for Three Different Judo Throwing Techniques</i>	Rodney T. Imamura, Alan Hreljac, Rafael F. Escamilla and W. Brent Edwards	Journal of Sport Science and Medicine	July 2006	Average linear momentum in the three axes and their resultant impulse of faller's COM were examined when falling from three different Judo techniques	<ul style="list-style-type: none"> - Two video cameras (JVC 60 Hz) synchronized by LED - Manual digitization of 18 body points 	The hip (harai-goshi) and leg throw (o-soto-gari) produced great impacts onto uke's body. Instead, the shoulder throw (seoi-nage) generated smaller collisions underlining the prominence of skill rather than power.
<i>Biodynamic Analysis of the Uki-Goshi Technique in Judo</i>	Nikolina Dimitrova	The Exercise and Quality of Life (EQOL) Journal	2009	Construction of controlled active experiment for quantitative biodynamic evaluation of the compensative possibilities for opponent's force reactions overcoming	<ul style="list-style-type: none"> - Three-dimensional strain-measurement platform - Dummy 	Untenability of sport-technical master ship evaluation based on classic (or simple) dynamographic record of the tori force vector.
<i>Motion Analysis of Performance Tests</i>	Michaela Hassmann,	8th Conference of the International Sports	2010	Measuring parameters related to judo throws	<ul style="list-style-type: none"> - Pulling Force Device (PFD) 	PFD has demonstrated to be a suitable and effective

2 Motion Analysis in Sport Activities

<i>Using a Pulling Force Device (PFD) Simulating a Judo Throw</i>	Michael Buegger, Klaus-Peter Stollberg, Alexander Sever, Anton Sabo	Engineering Association (ISEA)			<ul style="list-style-type: none"> - A force and a velocity sensor (1 kHz) - Four digital video cameras (50 fps) - Markers 	system for defining the parameters F_{max} , dF_{max} , $t(F_{max})$ and v_{max} .
<i>Event-Based Measurement of Power in Sport Activities by Means of Distributed Wireless Sensors</i>	Stefano Frassinelli, Alessandro Nicolai, Tullio Marzi, Mohammadreza Aghaei, Marco Mussetta, Riccardo Zich	International Conference on Event-based Control, Communication, and Signal Processing (EBCCSP)	June 2015	Evaluate motor skills and abilities required for creating efficient performance in Judo	<ul style="list-style-type: none"> - Wearable Arduino-based microcontroller (LilyPad Arduino) - Data collected saved on a drive 	An event-based analysis cannot be considered as the best explanation for in estimate of Judo performances.
<i>Reliability of a Portable Accelerometer for Measuring Workload During Mixed Martial Arts</i>	Howard Thomas Hurst, Stephen Atkins and Christopher Kirk	Journal of Athletic Enhancement	September 2014	Define the consistency of a movable accelerometer for measuring outer load in Mixed Martial Arts	<ul style="list-style-type: none"> - Standard MMA competition shorts, a groin protector, gum shield, t-shirt or rash guard, and competition standard 5-ounce MMA gloves - Minimax X3 tri-axial accelerometers (100 Hz) - Each unit was placed in a neoprene harness worn on the participant's torso, ensuring the accelerometer was positioned at the T3-T4 vertebrae 	The Minimax X3 can provide a useful tool for following and examining workloads in training and competition circumstances. Results also suggest that the Minimax X3 could also be used to determine the efficiency and variability in skills amongst MMA competitors of differing ability levels and could be used to determine benchmark values for workloads in different weight categories in the future.
<i>A Biomechanical Study on Tomoe-Nage of Judo Techniques</i>	Matthew Exton, Yoshihiko Iura	Research Journal of Budo	2012	Tomoe-nage technique was examined associating standard and competitive execution with different masses fallers	<ul style="list-style-type: none"> - Camera (64 fps) - Three accelerometers (wiring ran along the body, 	In competitive conditions with the middle-weight uke, a larger variation of angular acceleration and

2 Motion Analysis in Sport Activities

<i>A Review of Instrumented Equipment to Investigate Head Impacts in Sport</i>	Declan A. Patton	Applied Bionics and Biomechanics	2016	Review on instrumented helmets, headgear, mouthguards, skin patches, skullcaps, headbands, earplugs, gloves, shirts	an operator followed tori for avoiding wires twisting) - Swimming shorts with white tape on six joints for video-analysis	reduction in period spent in throwing uke were measured.
<i>Motion Analysis Systems as Optimization Training Tools in Combat Sports and Martial Arts</i>	Ewa Polak, Jerzy Kulasa, António Vencesbrito, Maria António Castro and Orlando Fernandes	Revista de Artes Marciales Asiáticas	January 2016	Review on motion analysis systems (optical, electromechanical, acoustic, inertial) applied to combat and martial sports	-	-
<i>Inquiry of the Discomfort Offered for Different Tatamis Used in the Practical of the Judo</i>	Saray Giovana dos Santos, Carlos Rodrigo de Melo Roesler, Sebastião Iberes Lopes Melo	Revista Brasileira de Cineantropometria & Desempenho Humano	2007	Investigate the discomfort existing on different tatamis exploited in the practice of Judo (Ippon-seoi-nage and Zempo-kaiten-ukemi)	- Tatamis - Tri-axial piezoelectric accelerometer (model 4321, Brüel e Kjaer) with a maximum 1000 g (40 kHz), fist and hip	Magnitude of the worst impacts: - 305g fist - 12g hip

2.2.2 Injuries Analysis for Prevention

As mentioned above, injuries are one of the primary stimuli for the application of sensors to athletes while performing sport activities. Many studies have been conducted to analyse how head traumas develop during movements related to uke's falling technique (Table 2.5, presented at the end of Section 2.2.2).

Most analysed injuries are head and neck traumas: many results have been discovered since the first application of sensors to Judo and many regulations have been modified to precisely lower the occurrence of these kind of injuries (e.g. prohibition of diving movement in throws, i.e. using additionally the head as a foothold in throwing movements, as subsequently presented in Figure 2.6). Outcomes have also been used specially in Japan to instruct more efficiently Judo trainers: a new approach in teaching ukemi techniques emerging from these studies will help novice judokas to understand the importance of a correct body shape, during Judo training but also in real life, to quickly and safely manage falling situations.

As emerged from many studies analysed in the literature, investigation on Judo injuries will be crucial in detecting risk factors and proposing preventive approaches.

To safeguard its athletes' health, for example, the International Olympic Committee settled and started the injury and illness surveillance system throughout the 2008 Beijing and 2012 London Olympic Games [28]. Cataloguing injuries, most frequent and severe wounds in Judo matches can be recognised to enrich knowledge on trends over time, to create foundations for additional examination on risk factors and mechanisms of trauma, and to develop or advance injury prevention programs.

During Judo fights injuries typically hurt body extremities, principally knee (up to 28%), shoulder (up to 22%) and hand/fingers (up to 30%). Depending on the classification, fingers are occasionally specified as the principal injury location in competition as a result of grip fighting, which lasts for almost all match. Nevertheless, fingers injuries are typically not considered and categorised as "soft". Instead, many findings identified knees and shoulders as the principal injury locations as the outcome of throwing or being thrown [28].

About 85% of Judo injuries happened while fighting in a standing position compared with ground fighting, probably due to the more time spent in standing position rather than on the ground.

The most recurrent situation which leads to injuries in Judo appears to be being thrown, indeed it covers 70% of cases, comprehending also severe or catastrophic injuries. Moreover, the lack of falling abilities is related to acute as well as chronic diseases [28].

Catastrophic injuries in Judo occurs mainly in brain and cervical spine. From 2003 to 2010, accidents while doing Judo in Japan were conveyed to the All Japan Judo Federation, comprising 30 cases (26 male, 4 female) of head injury and 19 cases (18 male, 1 female) of neck injury. The 49 cases were revised by Kamitani et al. [29] considering injury mechanism, age when the injury occurs, length of Judo practise, clinical diagnosis, medical treatment and final outcome. Considering all data gained by the Federation, the incidence of head injury was about 2.44 per 100,000 players per year in 2003 and 1.09 in 2010, while the frequency of neck injury was 1.47 per 100,000 per year in 2003 and none in 2010.

They found more injury cases in athletes with less than 20 years of age: head traumas befell athletes which had been doing Judo for less than 3 years, while neck injuries happened in athletes with more than 3 years of experience due to the more complex movement and the more force control needed for developing the situation in which injury can occurs.

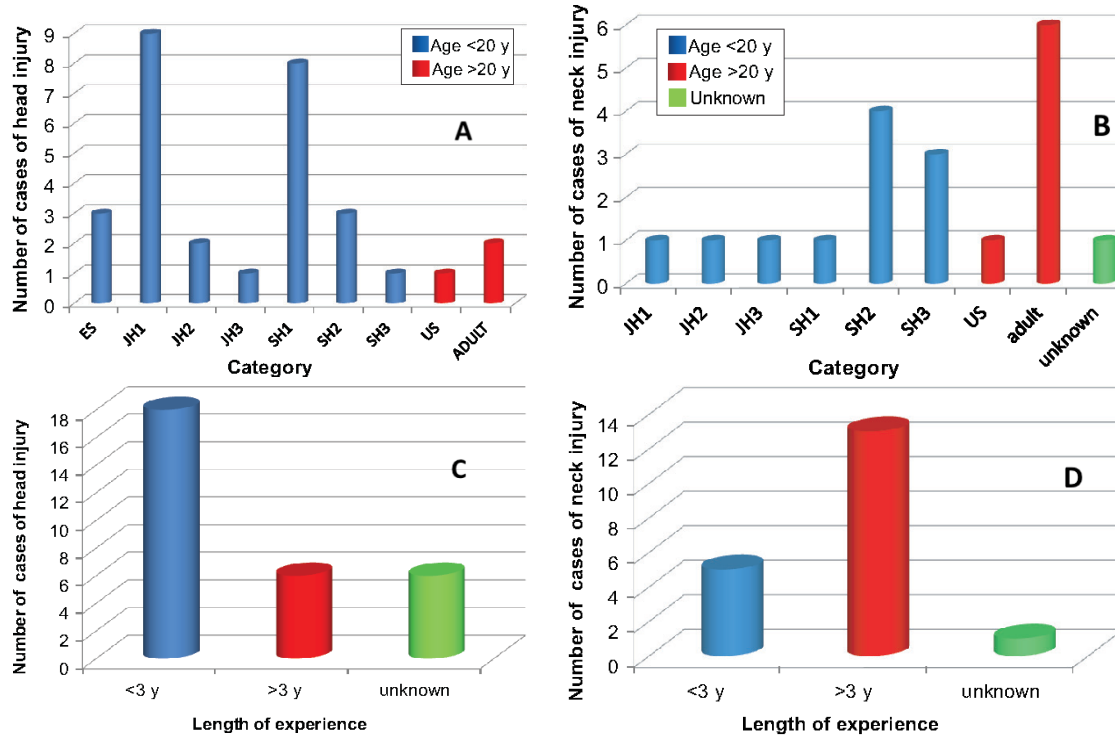


Figure 2.4: Epidemiology of head (A,C) and neck (B,D) injuries in Judo in 2003-2010 by Kamitani and al. [29]. A,B) Age category distribution: ES = elementary school; JH = junior high school; SH = senior high school; US = university student. C,D) Distribution of experience years. Adapted from [29].

Considering reported head injury cases, the diagnosis was acute subdural hematoma in 28 cases (94%) while cerebral contusion and sub-arachnoid haemorrhage in 1 case respectively. Craniotomy to eliminate the hematoma or decompression craniotomy was required in 26 (88%) of the 28 cases. Surgery could not be executed in 4 patients, 3 of whom died before or while incoming to the hospital; in these cases, acute subdural hematoma was detected through autopsy or computed tomography. Operative treatments were not required for remaining players. Otherwise, among neck injury events, 18 cervical spine injuries were identified, 11 of whom associated with fracture/dislocation of the cervical vertebra, 1 case of atlantoaxial subluxation was found.

The consequences of the 30 head injury cases considered were the following: 15 (50%) players died; 5 (17%) continued to live in a persistent vegetative state; 6 (20%) suffered from severe residual disability, hemiplegia, or aphasia; 4 (13%) fully recovered. Considering neck injury events, instead, results were complete paralysis in 7 cases (37%), incomplete paralysis in 7 (37%), and full recovery in 5 (26%) (Figure 2.5).

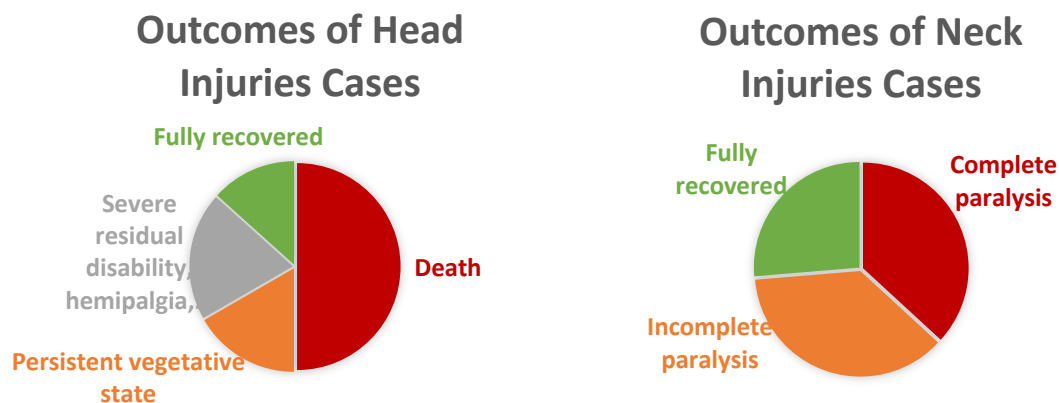


Figure 2.5: Outcomes of Judo-related head and neck injuries detected by Kamitani et al. [29].

Most head injuries studied happened while being thrown on the mat on the back, but it has to be considered that it is the main purpose of Judo fight: o-soto-gari technique was the principal reason (41%) of head injury. O-soto-gari is an attacking technique to throw the adversary on his back. If a correct breakfall would not be performed by the faller, rotational acceleration will not be properly dispersed, and the backside of the skull may then strike the underlying mat. The brain will so keep moving in the skull thanks to the moment of inertia, and a separation may originate between brain and the dura mater. Rupture of bridging veins could then occur, causing acute subdural hematoma.

Instead, considering neck injury situations, 60% happened when an athlete tried to throw the opponent, while 40% befell in being thrown. It is commonly supposed that the most dangerous situation is being thrown due to the impact to the mat, but in fact many neck injuries befell players while attacking. The classic movement that caused neck injury in the considered cases was hyper-flexion of the cervical spine, which happened when an athlete struggled for throwing the opponent, failed falling directly to the mat and striking his cranium (Figure 2.6).

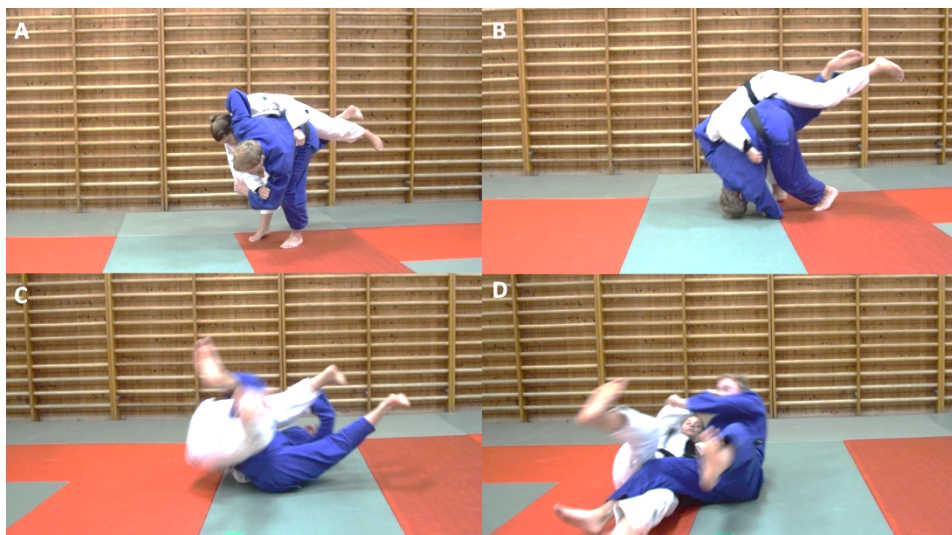


Figure 2.6: Diving movement. While throwing especially with uchi-mata technique, many athletes tries to use their head as an additional support (phase B): in this way, neck is hyper-flexed provoking dangerous traumas to the cervical spine. This movement is now prohibited and punished with the immediate exclusion from the competition.

Conclusions of this research were that the main reason of head injury was the poor skills of novice judokas in falling techniques and then lot of practice in breakfalls is crucial in beginning Judo [29].

In a complementary way Nagahiro et al. [30] found 40 cases of catastrophic head injuries in Judo athletes in Japan in the period from 1998 to 2011, on a total number of cases of 88 (Figure 2.7).

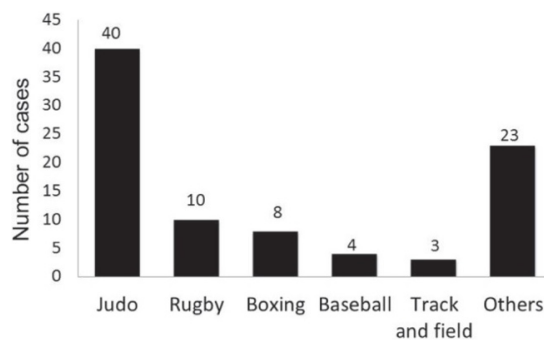


Figure 2.7: Catastrophic head injuries in Japanese scholars (7–18 years) described by the Japan Sports Council during the period from 1998 to 2011. As can be seen, Judo was the primary cause of death or severe disease: among 88 athletes with catastrophic sports head injuries, 40 joined in Judo [30].

Nishimura et al. [31], was the first in reporting four cases of acute sub-dural haematoma, not considered in the previously cited studies, which occurred between 1967 and 1983: the outcomes of the four cases were two in vegetative states, one dead and one completely recovered. Yokota et al. [32] described the case of a 16-years-old Judo competitor with recurrent head traumas which led to convulsion and loss of consciousness.

Instructors, athletes and parents of children who enrolled competitive sport activities have to be aware of the scientific evidences and of the correct clinical management of sports-related head injuries. Because there is a high rate of head traumas as well during in schools as in quotidian sports activities, coaches must be competent in recognising supposed concussion and accurately managing that situation. Consequently, instructors must be trained about possible head injuries and the managing of them. Evidences of risk and proper managing of head injuries in persons joining many activities should be extensively distributed in educational institutes and through public relations crusades organized by sportive associations. Energies should thus be spent on instructing not just sport staff involved in athletes’ caring, but also sportive community [30].

Between 1988 and 2011, Judo was the sporting top cause of terrible head injury among all-ages institutes in Japan. Thus, applied strategies for Judo-related head injuries prevention appear inadequate. In 2011 the All Japan Judo Federation released “The Safety Instruction of Judo” which declares that suitable carefulness and attention to concussion are essential, that athletes with signs of concussion must be inspected by neurosurgical specialist, and that coaches must reflect on the diagnosis in order to decide if the player should further play or not [33].

Looking forward to determining a correct procedure to avoid or safely manage traumas in Judo players, many studies have been carried out to assess the level of acceleration or angular velocity to which the faller’s body undergoes when projected with Judo throws (Table 2.3).

Table 2.3: Articles found in literature on the application of accelerometers to Judo athletes.

Citation, year	Sample characteristics	Test protocol	Type of Sensor	Results
Piucco et al., 2010	Two black belted Judo athletes, one thrower and one faller	Ten falls executed for each of the three articulations considered	Tri-axial accelerometer 4321 da Brüel & Kjaer (1000 g)	Fist: 140 g (x), 76 g (y), 352 g (z) Hip: 9 g (x), 5 g (y), 15 g (z) Ankle: 76 g (x), 102 g (y), 243 g (z) Technique: Ippon-seoi-nage
Dos Santos et al., 2007	At least two years of experience	Firstly, two athletes were studied, then 63 judokas fall ones on each mat tested for each segment investigated	Tri-axial accelerometer 4321 da Brüel & Kjaer (1000 g)	Fist: 1500-3000 m/s ² Hip: 30-120 m/s ² Technique: Ippon-seoi-nage
Florentin et al., 2017	14 judokas, brown or black belt	Five set of six different techniques and five set of six falls each, in a random and repeated design	Tri-axial accelerometer	Tai-otoshi: 27.94 g, 2.8 krad/s ² Deashi-barai: 20.58 g, 1.59 krad/s ² Uchi-mata: 28.16 ± 4.92 g, 3.94 ± 1.83 krad/s ²
Murayama et al., 2017	Two male Judo experts, one thrower and one faller	Four falls, two techniques	3-axis angular rate sensor	Osoto-gari: 740.7 ± 139.2 rad/s ² Ouchi-gari: 581.5 ± 69.5 rad/s ²

Piucco et al. [34], studying the ippon-seoi-nage technique with tri-axial accelerometers, observed that the greatest magnitudes of the acceleration were found in the vertical axis (z axis), in all the body regions analysed while the hip presented the smallest magnitudes of impacts in all axes. They concluded that it is

of great importance to carry out further investigations on the subject, since the characteristics of the mechanical impacts (magnitudes and time duration) obtained in the study can generate deleterious effects on the body of judokas over years of practice. They also pointed out to teachers and judokas the importance of correct and constant practice of breakfalls, both for beginner and experienced judokas. It is necessary to develop methodologies of practice that always emphasize the correct execution of each type of breakfall specific to each type of projection. With such measures it is possible to minimize the fatigue process and the overload to which the organism is subjected constantly during the training [34].

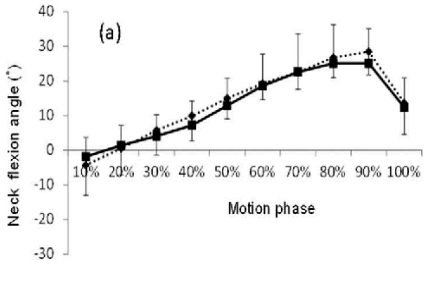
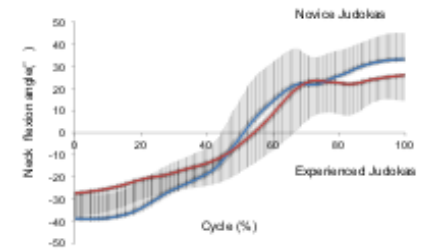
Analysing the same technique, Dos Santos et al. [35] investigated the discomfort offered by different mats, evidenced according to the subjective judgment of the athletes and associated with a scalar measurement obtained through the treatment of the experimental data collected through accelerometers. Similar values of linear acceleration were obtained, comparable to the ones gained by Piuccio et al. [34] and Dos Santos et al. [35] considering each body segment examined.

Florentin et al. [36] quantified and compared linear and angular acceleration experimented by uke's head while being thrown with different techniques: throws considered in the tests were tomoe-nage, tai-otoshi, harai-tsuru-komi-ashi, seoi-nage, deashi-barai and uchi-mata. Uchi-mata and the subsequent breakfall technique had the highest rate of sub-concussive head accelerations in the range 20-40 g. However, none of the tested techniques and related breakfalls rose in impacts too close to concussion (approximately 80 g, which lead to a GSI of about 1000 for an impact of 15-20 ms, as stated previously about Judo) [36]. In this study athletes were at least brown belted 19-years-old; expert athletes were considered also by Murayama et al. [37] and results were compared to the ones obtained previously with an anthropometric test device (ATD) [38]. Thanks to the falling experience, angular head acceleration was always inferior to the one measured with ATD for both o-uchi-gari and o-soto-gari techniques. These results proposed that the possession of sufficient skills in performing breakfalls may considerably lower the rotational head acceleration during impacts and the probability of catastrophic head injuries while doing Judo. Limitations on the use of ATDs are further discussed in Section 2.2.3.1.

Prevention of neck injuries covers another area of research in traumas related to Judo [29]. As stated before, neck injuries occur principally when throwing, especially with uchi-mata technique. Many articles written by Koshida et al. [39] [40] [41] deal with neck flexion/extension angle to elucidate how and in which situations injuries may happen (Table 2.4).

Table 2.4: Papers regarding studies on the path of neck flexion/extension angle during typical Judo movements.

Citation, year	Sample characteristics	Test protocol	Type of Sensor	Results
Koshida et al., 2017	12 novice male judokas with no experience in competitive or recreational Judo and a III dan expert thrower	Three sets of successful breakfalls to techniques (o-soto-gari, o-uchi-gari)	20-camera Mac3D motion analysis system	<p>The graph shows the neck flexion angle in degrees over the motion phase of a throw. The angle starts at approximately 15 degrees at the 10% phase and increases steadily to a peak of about 35 degrees at the 90% phase, before decreasing to 15 degrees at the 100% phase. Error bars are included for each data point, and significance markers (***) are present for most points, indicating statistical significance.</p>

Koshida et al., 2016	10 experienced judokas with at least 7 years of experience, 12 novice male judokas with no experience in competitive or recreational Judo (only a 90-minutes course) and a III dan expert thrower	Three sets of successful breakfalls to the technique (o-soto-gari)	20-camera Mac3D motion analysis system	
Koshida et al., 2012	6 experienced judokas with 7-12 years of experience, 4 novice male judokas with 10 sessions of Judo classes	Five sets of backward breakfall (ushiro ukemi)	<ul style="list-style-type: none"> - 8-camera Mac3D motion analysis system - 8-channel Tele MyoG2 system (EMG) 	

In their first study, the group investigated neck and trunk angle waveforms and electromyographic activity (EMG) of principal muscles involved (sternocleidomastoid, external oblique and rectus abdominis) during backward breakfalls and compared these variables between novice and experienced judokas [41]. No noteworthy variances were discovered in the biomechanical pattern of neck and trunk between the novice and experienced judokas. Both groups used not only neck, but also trunk flexion to prevent their head from hitting the floor during a backward breakfall. On the basis of visual observations of the angle curves, the neck flexion angle augmented from the beginning of the motion to approximately 60% of the phase, whereas the trunk flexion angle started at a slight flexion position and then further increased from 40–60%. The neck and trunk flexion angles remained stable during the last phase of motion. In addition, the EMG data revealed that the muscle activation profiles were similar between the two groups. In both groups, the external oblique muscle appeared to be more activated during the earlier phase, whereas the sternocleidomastoid muscle showed to be more activated during the later phase of the breakfall. It has to be noted that the force applied to the head during the breakfall task would likely be much lower than that applied when being thrown in Judo practice or a Judo match. Therefore, they were not able to conclude that in real Judo situation novice judokas would benefit from the backward breakfall skill and subsequent prevention of head injury. Further investigation of neck and trunk biomechanics were needed in more challenging situations requiring breakfalls.

To overcome the limitations discovered in that research, a second study was carried out by Koshida et al. [40]: they considered kinematic parameters related to the breakfall subsequent o-soto-gari throw in order to detect the possibility of injuries through the comparison between expert and novice judokas. Experienced judokas demonstrated a considerably lower peak angular momentum of the neck than novice, suggesting that these parameters can discriminate between high and low breakfall abilities related to techniques. Thus, the capability of Judo breakfall in decreasing neck extension momentum can have a central role in decreasing trauma possibility: improved breakfall aptitude for o-soto-gari implies that neck reinforcement has a crucial role in diminishing the probability of head and neck injuries.

Koshida et al. then analysed how biomechanics of Judo backward breakfalls changes comparing o-soto-gari and o-uchi-gari technique in novice judokas [39]. The significant differences with large effect size in the peak neck extension momentum and the head position with greater neck extension angle between the two techniques suggested that from both epidemiological and biomechanical points of view, being thrown with o-soto-gari probably increases the risk of Judo-related head injury to a greater degree than does being thrown with o-uchi-gari in novice judokas. Previous studies have consistently reported that direct and hard

contact of the occipital area with the Judo mat is the predominant mechanism of head injury in Judo [30] [31]. Therefore, the greater rotational force applied to the cervical region in the antero-posterior direction for the lower head position during the breakfall for o-soto-gari may be related to the greater number of Judo-related injuries. Considering these results together, being thrown with o-soto-gari technique may be a more challenging task than being thrown with o-uchi-gari, and this needs to be taken into consideration when coaches and teachers develop teaching plans for breakfall motions for novice judokas.

The neck strength of novice judokas should be assessed prior to instruction for breakfall motions so as to prevent injury. In case of Judo, neck strength may play a major role in reducing the angular momentum produced in the neck, and the neck strength training may be beneficial in lowering the risk of direct contact between the occipital area of the head and the Judo mat; nevertheless, the hypothetical connection between neck and trunk muscles role and the chance of head injury while doing Judo merits meticulous attention and consideration [39].

2 Motion Analysis in Sport Activities

Table 2.5: Articles regarding head and neck injuries found in literature.

Title	Authors	Journal	Date of Publication	Purpose	Methods	Results
<i>A Review of Sport-Related Head Injuries</i>	Yoshifumi Mizobuchi, Shinji Nagahiro	Korean J Neurotrauma	2016	Review on acute subdural hematoma (ASDH), traumatic cerebrovascular disease, concussion, chronic traumatic encephalopathy (CTE) deriving from sport activities	-	-
<i>Acute Subdural Hematoma in a Judo Player with Repeated Head Injuries</i>	Hiroshi Yokota and Yuki Ida	World Neurosurgery	July 2016	Case of ASDH developed and enlarged in a Judo contestant with recurring cranium traumas; surgical evacuation was required	-	Coaches have to be conscious of the probability that minor ASDH could bring to successive lethal ASDH after a further collision.
<i>Biomechanical Analysis of Acute Subdural Hematoma Resulting from Judo</i>	Masahito Hitosugi, Haruo Murayama, Yasuki Motozawa, Kanto Ishii, Masahiro Ogino, and Katsuhiko Koyama	Biomedical Research (Tokyo)	2014	Investigate the biomechanical mechanism of ASDH produced by Judo throws and search precautionary methods to decrease injury rate	<ul style="list-style-type: none"> - POLAR anthropomorphic test device (ATD) - Tri-axial accelerometer placed on the centre of gravity of the ATD's head - Three degrees of freedom rotational accelerometers - High-speed data acquisition system (up to 20 kHz) - High-speed digital video camera (1000 Hz) 	<p>Severe contact of the occipital part of the head to the mat and high values for linear and angular accelerations could lead to the occurrence of ASDH. Therefore, to reduce severe head injuries in judo, youth participants should master Ukemi.</p> <p>Osoto-gari: $a = 41 \text{ g}$ (ant-post dir.) $\alpha = 3315 \text{ rad/s}^2$ (sagit. plane) Ouchi-gari: $a = 86.5 \text{ g}$ (ant-post dir.) $\alpha = 1328 \text{ rad/s}^2$ (sagit. plane)</p>

2 Motion Analysis in Sport Activities

<i>Can Ideas from United States Youth Sports Reduce Judo-Related Head Injuries in Japan?</i>	Eddie E. Zusman, Peter Zoptfi, Joshua Kuluva, Scott Zuckerman	World Neurosurgery	January 2017	Annotation on: <i>Acute Subdural Hematoma in a Judo Player with Repeated Head Injuries</i>	-	Japanese sports associations may acquire the familiarity of American Football when focusing on head injury avoidance in Judo.
<i>Catastrophic Head and Neck Injuries in Judo Players in Japan from 2003 to 2010</i>	Takeshi Kamitani, Yuji Nimura, Shinji Nagahiro, Seiji Miyazaki and Taisuke Tomatsu	The American Journal of Sports Medicine	2013	Define catastrophic head and neck injury in Judo athletes in Japan between 2003 and 2010 by examining the traumatic events testified by the "All Japan Judo Federation's System for Compensation for Loss or Damage"	Descriptive epidemiological report	The principal reason of head traumas was being thrown. The contusion area was occipital, caused by osoto-gari technique. The principal trigger of neck traumas was throwing with uchi-mata technique.
<i>Acute Subdural Hematoma in Judo Practitioners - Report of Four Cases</i>	Kenichi Nishimura, Kiyotaka Fujii, Ryutaro Maeyama, Iwao Saiki, Shuji Sakata and Katsutoshi Kitamura	Neurologia Medico- Chirurgica (Tokyo)	1988	Description and discussion about four injuries cases while doing Judo	-	Judo was the cause of all considered ASDH. The form of occipital shock sustained in Judo leads the brain to rotate, stretching parasagittal veins and producing hematomas.
<i>Combat Sport Injuries Profile: A Review</i>	N. Hammamia, S. Hattabia, A. Salhia, T. Rezguib, M. Oueslatia, A. Bouassidaa	Science & Sport	2017	Detail information about injuries among contestants in dissimilar combat sports	-	-
<i>Current Topics in Sports-related Head Injuries: A Review</i>	Shinji Nagahiro and Yoshifumi Mizobuchi	Neurologia Medico- Chirurgica (Tokyo)	2014	Review on sports-related head injuries considering Judo and American Football	-	-

2 Motion Analysis in Sport Activities

<i>Dysautoregulation/Second- Impact Syndrome with Recurrent Athletic Head Injury</i>	Robert C. Cantu	World Neurosurgery	November 2016	Annotation on: <i>Acute Subdural Hematoma in a Judo Player with Repeated Head Injuries</i>	-	Concussion needs greater forces to be produced than SDH. The acceleration forces moreover can lead to increase of intracranial pressure and brain herniation.
<i>Head Accelerations Associated with Six Standard Judo Throws and Break Falls</i>	Tyler K. Florentin, Casey Snodgrass, Shawn O. Henry	International Journal of Exercise Science: Conference Proceedings	May 2017	Measure and compare head accelerations related with six standard Judo techniques	- Headband-mounted tri- axial accelerometer	Uchi-mata technique gained the main frequency of sub- concussive head accelerations in the range 20-40 g. Judo techniques tested did not result in high risk for concussion (< 80 g). Tai-otoshi: a = 27.9 g α = 2.8 krad/s ² Deashi-barai: a = 20.6 g α = 1.6 krad/s ² Uchi-mata: a = 28.2 g α = 3.9 krad/s ²
<i>Head Injuries in Sport</i>	Robert C. Cantu	British Journal of Sports Medicine	1996	Review on pathophysiology of concussion, intracranial haemorrhage, second impact syndrome, Post-traumatic seizure, malignant brain oedema syndrome, deriving from American football	-	-

2 Motion Analysis in Sport Activities

<i>Injuries in Judo: A Systematic Literature Review Including Suggestions for Prevention</i>	Elena Pocecco, Gerhard Ruedl, Nemanja Stankovic, Stanislaw Sterkowicz, Fabricio Boscolo Del Vecchio, Carlos Gutiérrez-García, Romain Rousseau, Mirjam Wolf, Martin Kopp, Bianca Miarka, Verena Menz, Philipp Krüsmann, Michel Calmet, Nikolaos Malliaropoulos, Martin Burtcher	British Journal of Sports Medicine	2013	Review on the incidence and features of injuries in Judo considering Olympic Games in 2008 and 2012	-	-
<i>Kinematics of Judo Breakfall for Osoto-gari: Considerations for Head Injury Prevention</i>	Sentaro Koshida, Takatori Ishii, Tadimitsu Matsuda, and Toshihiko Hashimoto	Journal of Sports Sciences	July 2016	Study the kinematic parameters for o-soto-gari breakfall for recognising the chance of head traumas by relating skilled and beginner athletes	- 41 reflective markers - Tight-fitting spandex shorts, parts of judogi and a headgear - 20-camera Mac3D motion analysis system (200 Hz)	Novice judokas exhibited a greater angular momentum of neck extension and a significantly greater flexed position of trunk and lower limbs while falling. As the impact interval increases, the magnitude of acceleration necessary to get harmful strains will decrease.
<i>Peak Linear and Rotational Acceleration Magnitude and Duration Effects on Maximum Principal Strain in the Corpus Callosum for Sport Impacts</i>	Andrew Post, T. Blaine Hoshizaki, Michael D. Gilchrist, Michael D. Cusimano	Journal of Biomechanics	2017	Study the interaction between linear and rotational acceleration and duration in typical of sport situations	- University College Dublin Brain Trauma Model (FEM) - Sinusoidal acceleration pulses with resultant magnitudes and durations gained from sports	

2 Motion Analysis in Sport Activities

<i>The Development of a Threshold Curve for the Understanding of Concussion in Sport</i>	T Blaine Hoshizaki, Andrew Post, Marshall Kendall, Janie Courmoyer, Philippe Rousseau, Michael D Gilchrist, Susan Brien, Michael Cusimano, and Shawn Marshall	Trauma	November 2016	Develop the knowledge of injury levels by comparing threshold curves as the WSTC and the BICLE	<ul style="list-style-type: none"> - Data collected in patient interviews and video analysis of sport impacts - Hybrid III head-form and linear impactor system, linear and rotational acceleration and time duration were measured 	Data gained prove a trend line for concussion with an offset in comparison to the WSTC.
<i>Rotational Head Acceleration of Thrown Person with Break-fall skills by Judo Throwing Techniques</i>	Haruo Murayama, Masahito Hitosugi, Yasuki Motozawa, Masahiro Ogino, Katsuhiko Koyama	Medicine & Science in Sports & Exercise	May 2017	Evaluate rotational head acceleration (RHA) on a human and relate it with values acquired with an ATD (from: <i>Biomechanical analysis of acute subdural hematoma resulting from judo</i>)	<ul style="list-style-type: none"> - Tri-axial angular rate sensor - Digital video cameras for kinematic data 	The resultant RHA of faller (o-soto-gari, 741 rad/s ² , o-uchi-gari, 582 rad/s ²) was considerably inferior than those detected with the Anthropometric Test Device.
<i>Simple Strategy to Prevent Severe Head Trauma in Judo</i>	Haruo Murayama, Masahito Hitosugi, Yasuki Motozawa, Masahiro Ogino, and Katsuhiko Koyama	Neurologia Medico-Chirurgica (Tokyo)	September 2013	Determine if the use of an under-mat may diminish impact to the head when being thrown.	<ul style="list-style-type: none"> - POLAR anthropomorphic test device (ATD) - Tri-axial accelerometer onto ATD head's - High-speed acquisition system (20 kHz) - High-speed digital video camera for kinematics (1000 fps) 	Without an under-mat, ax oscillated from 51.6 to 79.9 g (o-soto-gari) and 124.9 to 143.2 g (o-uchi-gari). With the under-mat mounted, duration of the acceleration was extended, and values were reduced. Peak ax fluctuated from 36.1 to 45.7 g (o-soto-gari) and 73.7 to 92.4 g (o-uchi-gari). The HIC values calculated without an

2 Motion Analysis in Sport Activities

<i>Sports-Related Head Injuries</i>	Allan White	Journal of Emergency Nursing	September 2012	Determine how nurses and medical staff have to deal with head trauma as bleedings and concussions	under-mat forecast a risk of head traumas (HIC > 250). Concussion must not be underestimated: if there is any doubt, it is suggested complete rest and relaxation until the patient can be further evaluated by a neurologist.
<i>Subconcussive Head Impacts in Sport: A Systematic Review of the Evidence</i>	Lynda Mainwaring, Kaleigh M. Ferdinand Pennock, Sandhya Mylabathula, Benjamin Z. Alavie	International Journal of Psychophysiology	2018	Review on the determination of how sub-concussion is characterized in the current literature and on the identification of directions for future research	-
<i>Neck and Trunk Kinematics and Electromyographic Activity During Judo Backward Breakfalls</i>	Sentaro Koshida and Tadimitsu Matsuda	30th Annual Conference of Biomechanics in Sports (Melbourne)	2012	Demonstrate the neck and trunk angle time curves as well as electromyographic (EMG) activities during a judo backward breakfall in both experienced and novice judokas	Even short-term judo practice may improve backward breakfall skill in novice judokas. In this study, no dissimilarities occurred in neck and trunk kinematic between the novice and experienced judokas.

2.2.3 Technologies Used in Experimentation

Since last tens of years, the quick evolution of technology has allowed the development and the improvement of the principal solutions to capture and analyse human movement. They exploit several types of sensors, markers or transmitters, and can be divided into video-based, optical, electromechanical, electromagnetic, acoustic, inertial and depth-sensing.

Considering collision and contact sports, many of the previously cited technologies cannot be used in studying and analysing movements related to these activities. Most exploited in this field are video-based technology or optoelectronic systems and inertial sensors, due to their versatility, accuracy and low-encumbrance [1]. Main advantages of each technology are here briefly exposed.

Video-based systems are transportable, not expensive and can be used indoor as outdoor. Furthermore, they may assist existing camcorders. The systems can read parameters acquired directly from motion video recording without exploiting any kind of markers. Additional benefit is the possibility to capture movements executed by two or more athletes who fight against each other. In this way, they can be advantageous for time-based and qualitative investigation in combat sports, such as Judo and Wrestling. Drawbacks of the technology are small recorded motion area, restricted to camera field of view, as well as faults in video recording or improper identification of the particular objects on the images. This kind of systems are frequently used for scientific dedications in studying combat sports: research areas are the investigation of time structure of sports competitions, such as in Muai-Thai and Kick-Boxing, Judo, Karate or Taekwondo, and the spatiotemporal features of different techniques, such as Capoeira kick, Karate punches and kicks, Taekwondo turning kick and Judo throw.

Instead, main benefit of using optical systems is the opportunity to exploit indefinite quantity of markers, the high precision, accuracy and spatio-temporal resolution. The range of capture speed is 50 to 10000 Hz, so very fast movements can be accurately analysed. These advantages make them suitable for capturing and investigating quick and dynamic actions, which are emblematic of combat sports and Martial Arts.

Paradigms of the novel technologies are small-scale inertial sensors. These sensors comprise accelerometers, gyroscope and magnetometers. The small scale lets them to be positioned on subject's body through flexible bands or particular suit, providing great freedom of movements. The direct measurement of acceleration and angular velocity facilitates to obtain mechanical variables, such as positions, velocities, forces and torques. Furthermore, they allow to catch motion of athletes fighting each other in an individual manner, even if they interact to each other. The consequences of their application in many sports (e.g. Rowing, Archery, Golf, Baseball, Tennis, Swimming and athletics) activate researchers to discover fascinating uses in combat sports and Martial Arts, which have been always considered too problematic to scientifically approach.

2.2.3.1 Anthropometric Test Devices (ATD)

Other types of technology used for the analysis of combat sport movements and techniques are dummies. Deriving from car crash tests, the application of high-biofidelity mechanical model of human body spreads in a large variety of research areas. This kind of technology have been used so far in tests where humans could suffer from the procedure examined.

Great potential is related to their application in the analysis of sports traumas, such as the biomechanics of head injuries related to Judo breakfalls and techniques. Dummies, or anthropometric test devices (ATDs), have been exploited in this field in many research programs, as can be seen in Table 2.6.

Table 2.6: Articles inherent to biomechanical analysis of Judo techniques with dummies technology.

Citation, year	Test protocol	Sensors in Dummy	Results
Murayama et al., 2014	One male Judo expert (V dan) repetitively threw an ATD with two techniques	- Tri-axial accelerometer - 3-DOF rotational accelerometer Both sensors were on ATD COG head	O-uchi-gari: 88 ± 3.8 g, 2.18 ± 0.83 krad/s ² O-soto-gari: 46.5 ± 3.8 g, 4.57 ± 0.36 krad/s ²
Hitosugi et al., 2014	One male Judo expert (V dan) threw four times an ATD with two techniques each	- Tri-axial accelerometer - 3-DOF rotational accelerometer Both sensors were on ATD COG head	O-uchi-gari: • 86.5 ± 4.3 g (x), 14.5 ± 8.2 g (y), 15.1 ± 2.7 g (z) • 1109 ± 413 rad/s ² (x), 1328 ± 201 rad/s ² (y), 651 ± 652 rad/s ² (z) O-soto-gari: • 41.0 ± 2.6 g (x), 19.2 ± 3.2 g (y), 18.7 ± 0.7 g (z) • 1760 ± 227 rad/s ² (x), 3315 ± 168 rad/s ² (y), 2225 ± 104 rad/s ² (z)
Murayama et al., 2013	One male Judo expert (V dan) threw four times an ATD with two techniques each	Tri-axial accelerometer on ATD's COG head	O-uchi-gari: 90 g O-soto-gari: 50 g

In the literature reviewed, dummies were always thrown by expert judoka with o-soto-gari and o-uchi-gari, then linear and rotational acceleration gained from experimentation were analysed to detect possible stages of head traumas and to search preventive measures to reduce injuries.

Hitosugi et al. [38] reconstructed the mechanism causing severe head injuries, especially acute sub-dural haematoma, in Judo. They confirmed that when the occipital area of the head struck the mat, high linear acceleration values are obtained, and the rapid forceful movement generates a sagittal plane rotational force on the brain. Such movement produces stretching and ruptures to parasagittal bridging veins and causes acute sub-dural haematoma. Death may also result from the massive increase in intracranial pressure and the resultant decrease in cerebral perfusion. Severe head injury can occur when Judo participants fail to perform a falling technique in a manner that minimizes contact of the head with the mat. In real-world accidents, a high magnitude of angular acceleration requires head contact to occur. In this kind of studies, high values for both linear and angular accelerations were obtained with head contact.

Murayama et al. [42] [43] concluded as Hitosugi et al. [38]: even if the initial purpose of the two studies were different, i.e. to assess the utility of an under-mat with the tatami [42] and to examine acceleration to elucidate the mechanism of head injuries [43], obtained linear and rotational acceleration were almost the same indicating an excessive risk of head injuries. They established that novice or inexperienced person may experience severe head injury if the falling technique is not properly performed. Hence, as a crucial measure to prevent injuries, athletes and especially youths must firstly master ukemi (Japanese typical word standing for breakfall). Additionally, as severe head injuries may happen if faller's head contacts the mat, throwing techniques may be limited to players exhibiting satisfactory ukemi skills.

Since the dummy model exploited in all studies here considered does not reflect differences in head shape, structure and densities among people, outcomes cannot be related to authentic injuries studies in Judo. However, results provide informative recommendation that other devices, techniques, and/or carefulness will be necessary to lower head accelerations.

Moreover, the peaks of linear and rotational acceleration observed in tests with dummies are greater than the ones obtained with human beings: values acquired in the first way approach tightly the limits for head traumas presented in literature. This fact is a limitation of the technology, indeed maximum values acquired occurred when ATD's head reached the mat. It is not realistic because also novice judokas, which have been

doing Judo for a few hours, tries to activate neck and trunk muscles to avoid contacting the floor and so a minimum reaction force is exerted [39] [40]. Furthermore, no muscle activity of neck, trunk, hip, inferior and superior limbs can be considered employing dummies, while for example hands reaction to the ground could play an important role [39].

Concluding, ATDs are a useful technology to study the worst situation to which a Judo technique (or other combat sport movements) can lead the human body, but they cannot be used to learn how to improve the movement required to fall without damages because of the lack of human behaviour during falls.

2.3 Traumatic Brain Injuries (TBI)

Benefits of regular physical activities and sports participation on cardiovascular system and brain health are unquestionable. Indeed, physical exercise lowers the danger of cardiovascular diseases, type 2 diabetes, hypertension, obesity, and stroke, and leads positive effects on cholesterol levels, antioxidant systems, inflammation, and vascular function. Training similarly improves psychological health, diminishes age-related loss of brain volume, increases cognition, decreases the risk of developing dementia, and delays neurodegeneration. However, playing sports, almost all sports comprehending agonism, is linked with dangers, involving a risk for mild or severe Traumatic Brain Injuries (TBI) and, rarely, catastrophic traumatic injuries and death. Furthermore, an increasing awareness is growing, considering that repetitive mild TBIs, e.g. sub-concussion, could lead to persistent cognitive, behavioural and psychiatric complications and could also produce neurodegeneration [44].

Sports related to an increased probability of TBI comprise, as stated before, those concerning contact and/or collisions, such as Boxing, American Football, Ice Hockey, Soccer, Rugby and in general Martial Arts, together with high-velocity sports such as Cycling, Motor Racing, equestrian sports, Skiing and Roller Skating. Even if most sport-related TBIs happens while involved in contact, collision or high-velocity sports, involvement in any sport activities brings a risk of suffering from head injuries.

Acceleration of the skull can generate three distinct types of stress to the brain: compressive, tensile, and shearing force. Neural tissue relatively well accepts uniform compressive and tensile forces, while shearing forces are particularly badly tolerated. The cerebrospinal fluid (CSF), which contours the brain, behaves as a defensive shock absorber by transforming focal external stress to compressive stress: because the liquid surrounds the sulci and gyri of the brain, it spreads the applied force in a uniform manner. However, the CSF does not completely avoid the transmission of shearing forces to the brain, in particular when rotational forces affect head. Shearing forces are highest where rotational sliding is impeded into the brain, such as at the brain-dura mater interface which contacts the brain and the skull. In comprehending how forces due to body acceleration are transmitted to the brain, it is essential to consider Newton's second law stating that force is equal to mass multiplied for acceleration, or in other words, force divided by mass equals acceleration. Consequently, athlete's head can tolerate larger stresses without injury risk if neck muscles are tensed: indeed, in this state, the mass of the head can be approximated to the whole-body mass, lowering the value of acceleration to be borne. In a relaxed state, instead, the mass of the head is lower, basically its own, and therefore similar levels of force applied can produce far larger accelerations [4].

TBI can be divided into acute and chronic. Acute TBI are injuries which arise instantly at the time of the impact, with consequent signs and symptoms, whereas chronic TBI denotes long-term concerns of single or repeated head traumas. Although brain injuries fortunately are not the leading category of sport-related injury, they have been far analysed because TBI can be related also with morbidity and, potentially, mortality. Due to not adequate formation of coaches on this topic, traumas such as concussions are frequently unrecognized and consequently not reported. Following this way, the number of cases reported is much lower than the one of the actuals, giving less attention to this phenomenon which may be considered as a primary consequence of sport-related traumas. Accordingly, identification of concussion in ordinary sport through education and medical observation must be of paramount prominence. Failure to effectively

administer concussion can lead to persistent and chronic disorders. Catastrophic head and neck injuries, due to contact among athletes or between athlete and sports equipment, produce fatal, non-fatal permanent, or non-fatal non-permanent injuries, including for example skull fracture, subdural and epidural hematoma, rupture of vertebral artery with subarachnoid haemorrhage, second-impact syndrome [44] [45].

2.3.1 Acute TBIs

Acute TBIs are injuries in which consequences of the blow follow subsequently the impact. Typical sport-related acute TBIs are [45]:

- Diffuse brain injury
 - Cerebral concussion
 - Diffuse axonal injury
 - Diffuse cerebral swelling (DCS)
- Focal brain injury
 - Epidural haematoma
 - Subdural haematoma (ASDH)
 - Cerebral contusion
 - Intracerebral haemorrhage
 - Subarachnoid haemorrhage
 - Intraventricular haemorrhage
 - Subdural hygroma
- Skull fracture
- Penetrating brain injury

Most common acute brain injuries due to sport activities are concussion and DCS, while other listed injuries, such as skull fracture, penetrating brain injuries, axonal injuries, are particularly unusual in sports but can however happen. The firsts are further described below.

For tens of years, head-impacts biomechanics has been examined to investigate the kinematic of concussion: if it will be clarified, clinicians and coaches could be able to quickly recognise concussed player to save his life or the quality of his future life and recommend improvements of the sports equipment or rule variations to reduce concussion risk [5].

From a mechanic standpoint, head collisions cause linear and rotational acceleration of the cranium. The combined accelerations result in transitory pressure gradients and strain fields, which affect brain soft tissues: if they exceed the tolerable brain physiological limits, injury takes place. Brain tissue response cannot be measured directly in vivo, instead pressure and strain responses can be easily related to skull acceleration which can be simply measured through sensors [5]. In this way, common sports gestures can be classified from extremely dangerous for athletes to safe movements, in order to improve athletes' safety.

Concussion is clinically described as "a complex pathophysiological process that affects the brain and is induced by traumatic biomechanical forces" [45]. It generally arises after the diffusion of impulsive forces to the head producing momentary neurological impairments and can be clinically recognized by the presence of cognitive, physical and behavioural signs and symptoms, such as headache, dizziness and memory deficiency.

As stated by many clinicians and researchers, concussion must be considered as a possible cause for individuals affected by one or more of the following indicators [45] [30]:

1. Subjective symptoms: somatic (e.g. headache), cognitive (e.g. disorientation, confusion)
2. Physical signs (e.g. loss of consciousness, amnesia, vertigo, loss of balance, convulsion)
3. Behavioural changes (e.g. irritability, fatigue, psychomotor retardation)
4. Cognitive impairment (e.g. slowed reaction time)
5. Sleep disturbance (e.g. insomnia)

Considering adults, concussions spontaneously resolve in one or two weeks of rest, while in children and teenagers the recovery phase may be longer. Even if conventional structural neuroimaging can detect the presence of concussion, clinical symptoms following head impact generally suggest a functional disorder. Concussions occur principally through quick acceleration and deceleration of the brain, caused by angular or linear acceleration and impact deceleration. When forces cause head rotation, rotational accelerations take place: it provokes axons stretching and tearing, producing concussion and potentially traumatic axonal injury. Forces that cause the head to move along one direction result in linear accelerations: if it happens in the antero-posterior direction, acceleration is able of causing gliding contusions in the parasagittal regions of the cerebral cortex and axonal injuries of the brainstem. Impact deceleration happens when the head quickly stops, usually when it strikes the playing field or other subjects: it can lead to double injury, an injury on the side of the head where the collision happened, and countercoup injury of the cerebral cortex in the opposite area.

While accelerations, decelerations and rotational forces occur, brain stretches and deforms, elongating neurons, glial cells and blood vessels, changing the membrane permeability: these traumatic stretch damages disturb neuronal cell bodies, axons, dendrites, blood vessels and glial cells. Axons are particularly susceptible because of the long-covered distance in the nervous system and damages can also occur without neuronal cell body death [44].

The transmission of forces to the brain triggers multiple neuro-pathophysiological cascades [45]. The primary neuro-metabolic cascade includes neuronal depolarization, release of excitatory neurotransmitters, ionic shifts, variations in glucose metabolism and cerebral blood flow, and weakened axonal function. Moreover, further processes can develop, such as apoptosis, mitochondrial dysfunction, free radical formation, neuro-inflammation, growth factors alterations and inflammatory processes. Additionally, an amyloid cascade, with or without appropriate clearance of amyloid components (which can be hypothesized as one of Alzheimer's diseases causes), may begin.

Suitable concussion management necessitates the direct exclusion of the athlete from competitions and training, and an evaluation by health-care experts: a consequent period of cognitive and physical rest until symptoms disappear is mandatory. Once the athlete can be considered asymptomatic and medications to handle or alter concussion symptoms are no longer used, a measured stepwise return to activity may be employed (Table 2.7). Finally, once asymptomatic at rest and on effort, return to full activity can be prescribed. If an athlete does not improve his condition after, for example, one month, a low-level, sub-symptom limit convalescence should benefit in eluding post-concussion syndrome (PCS). Indeed, the mishandling of concussions may theoretically lead to assiduous PCS and/or second-impact syndrome, so an adequate rehabilitation protocol must be followed with the support of specialized clinicians [4] [45] [30] [46] [28] [47] [48] [49].

Table 2.7: Return to play (RTP) protocol after head injuries [30]. Every step must require at least 24 hours, therefore minimum interval between impact and RTP is about a week.

Rehabilitation at age	Functional exercise at each stage of rehabilitation	Objective(s) of each stage
1. No activity	Symptom-limited physical and cognitive rest	Recovery
2. Light aerobic exercise	Walking, swimming, or stationary cycling, keeping intensity 70% of maximum permitted heart rate; no resistance training	Increase heart rate
3. Sport specific exercise	Skating drills in ice hockey, running drills in soccer; No head-impact nor head-rotation activities	Add movement
4. Noncontact training drills	Progression to more complex training drills, e.g., passing drills in football and ice hockey; may start progressive resistance training	Exercise, coordination, and cognitive
5. Full-contact practice	After medical clearance, participation in normal training activities	Restore confidence and assessment of functional skills by coaching staff
6. RTP	Normal game play	

If an athlete, while still symptomatic from an earlier concussion, sustains a second impact, likely if the first concussion has not been recognized, another fatal injury could happen [45]: the second-hit shock brings to

Diffuse Cerebral Swelling (DCS), cerebral oedema or brain herniation. Second-impact syndrome causes loss of autoregulation of the cerebral blood flow, which brings to vascular engorgement, consequent augmented intracranial pressure and eventually herniation.

Another injury that often occurs in sports is Acute Sub-Dural Haematoma (ASDH): severe head injuries are prevalent in collision and contact sports such as American Football, Rugby, Boxing, Judo, Ice Hockey, Skiing and Snowboarding. Sports-related ASDH is one of the primary reasons of death and severe disease in widespread sports like American Football and Japanese Judo. In the United States, severe head injuries in sports are most commonly associated with American football, moreover 90% of reported cases involve ASDHs [30] [46].

Considering pathology development, a major blow to the occipital region of athlete's head while falling to the ground causes rotational acceleration of the brain in the antero-posterior direction that can provoke the separation of the brain and the dura mater, with the rupture of the bridging veins [30] [46]. Rotational it is more dangerous than linear acceleration because it creates greater tension on bridging veins and brain. Animals trials indeed demonstrated that angular acceleration in the sagittal plane tends to generate ASDH because of the rupture of parasagittal bridging veins. These veins are delicate, and they can be broken more likely by rotational than translational acceleration since relative brain-skull movements are vaster during rotation than in merely linear actions [30].

Primary symptoms of ASDH are loss of consciousness, headache, vomiting, dizziness, and convulsive seizures. Assiduous headaches following mild head traumas in contact sports players shows with high probability the manifestation of thin or small subdural hematoma [30]. Most patients with consciousness deterioration necessitate surgery, involving decompression craniotomies and, in many situations, subdural hematoma exclusion.

2.3.2 Chronic TBIs

Chronic TBI embraces a variety of disorders related with long-term effects of brain trauma. The typical disorder of chronic TBI is Chronic Traumatic Encephalopathy (CTE), a syndrome which comes from durable neurological damages due to repeated mild TBIs [45]. Pugilistic dementia is the Boxing expression of CTE, a severe type of dementia developed after a prolonged Boxing career. Post-traumatic Parkinsonism designates a Parkinsonian syndrome developed next to a first TBI. It involves for example pugilistic Parkinsonism, a form of pugilistic dementia in which limbs rigor and tremor prevail. Many evidences indicate that involvement in contact sports may increase the risk of some neurodegenerative syndromes in athletes, as mild cognitive impairment, Alzheimer disease (AD), motor neuron disease (MND) or Parkinson disease. The relationship denotes a further public health alarm to the problem of sport-related CTE which should be considered by sports clinicians.

As reported by Jordan [45], an investigation on retired professional American Football players presented a relationship among repeated concussions, clinically diagnosed minor cognitive deficiency and memory difficulties. Another survey in an analogous group of retired athletes showed a substantial, direct connection between the amount of self-reported concussion and occurrences of memory fluctuations, confusion, speech troubles, difficulties in remembering brief lists and recollecting fresh happenings. Furthermore, a high incidence of headache, paraesthesia and vestibular problems was observed, and higher AD-associated and MND-associated mortality percentages have been found in retired professional American Football athletes than in all US population.

CTE is the durable neurological outcome of recurring mild TBIs [45]. It clinically leads to behavioural, cognitive and/or motor-related complications. Behavioural disorders are frequently the earliest symptoms of CTE: depression, mood swings, apathy, impulsivity, aggression and suicidality are the most common. Considering cognitive disturbances, players can present diminished attention and/or concentration, memory troubles, executive dysfunction and, with disease progression, dementia. The motor expressions of CTE, which include spasticity, tremor, ataxia, dysarthria and coordination problems, reveal damages to the pyramidal tracts, the extrapyramidal system and the cerebellum. Pathological signs of CTE comprise diffuse

brain atrophy, ventricular dilatation, cavum septum pellucidum with or without fenestrations, cerebellar scarring, depigmentation and degeneration of the substantia nigra. With the disease development, evident atrophy of medial temporal lobe, thalamus, hypothalamus and mammillary bodies manifests.

The term Chronic Post-Concussion Syndrome (CPCS) refers instead to an infrequent clinical phenomenon involving the non-resolution of post-concussive symptoms leading so the athlete to retire from sport activities [45]. In the general non-sporting population, 10–15% of persons persist in a symptomatic condition one year after concussion: usual indicators of CPCS comprise headache, dizziness, reduced attention, leakage of memory, executive dysfunction, irritability and depression. Moreover, it is negatively influenced by age, pre-morbid anxiety and depression, and the gravity of primary post-concussive symptoms. Motor system dysfunctions among concussed players embrace postponed and mitigated evoked potentials on acoustic stimulus, extended cortical silence period (an evaluation of motor cortex excitability measured through transcranial magnetic stimulation), and bradykinesia. Unlike CTE, CPCS has an important beginning associated with a specific concussive episode, and it does not have a period of latency which is a distinctive feature of CTE.

3 Inertial Measurement Unit (IMU)

Probably the most common sensors involved in everyday life, IMUs technology comprises smartphones, tablets, videogame controllers, cars and planes. Regarding biomedical uses, this kind of sensor has been successfully used in falls detection, remote surveillance of old people, rehabilitation, gait analysis, ergonomics and sport science [50].

Generally referred as a sensor, this technology is instead an example of sensors fusion, in which returned data come from the elaboration of single information deriving from each sensor. IMUs indeed are sensing units composed of accelerometer, gyroscope and magnetometer: components of linear acceleration, angular velocity and magnetic field are so returned along their sensitive axes. All these sensors can have up to three sensing axes, leading to a 9 degree-of-freedom (DOF) unit.

In the following sections, sensors composing an IMU are distinctly analysed.

3.1 Accelerometer

Accelerometers are devices which measure the proper acceleration of a body along a definite direction.

Basing on a spring-mass system, the proper acceleration of the proof mass is equal to its acceleration plus the Earth gravitational acceleration vector. Indeed, if an accelerometer is left on a static surface with its sensitive axis upward, the instruments will return a positive value equal to the gravitational acceleration, 9.81 m/s^2 (which corresponds to the acceleration due to the reaction force of the surface), while if dropped along its sensitive axis, it will return an acceleration equal to zero. In this elementary accelerometer, the acceleration value is calculated from the spring elongation respective to the rest condition, knowing its elastic constant and the proof mass. If the primitive system is replicated on the three direction, a tri-axial accelerometer able of measuring three components of acceleration can be easily obtained. Actual accelerometers types are based on strain-gage sensors, piezoelectric effect or electrical capacitance.

Strain-gage accelerometers (Figure 3.1) use the deflection of a mass positioned at the end of a cantilever beam. The deflection sensed by a Wheatstone bridge with four gages, positioned two on the top surface and two on the bottom surface of cantilever in order to maximize the sensitivity. In this way, frequencies from zero to a few hundred of Hertz can be measured [51].

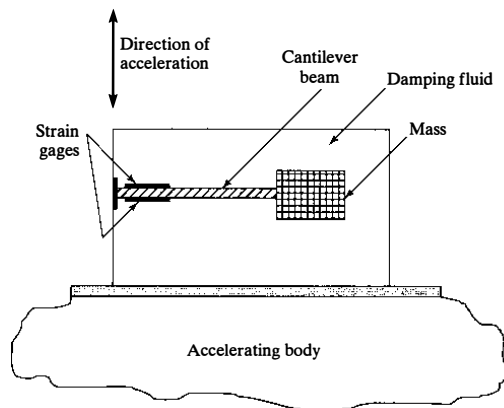


Figure 3.1: Strain-gage based accelerometer [51].

A second strategy for measuring the rate of change of velocity is by piezoelectric crystals: a proof mass is positioned on the crystal and produces a force on it (Figure 3.2). Piezoelectric material undergoes to a force, which induces electrons to move inside the crystal and thus a net charge is created. Charge is then measured by a charge amplifier which gives a voltage value read by electronics. A preloading spring sleeve can be used to for the mass on the crystal, in order to avoid the detachment of the mass from the crystal surface. Due the presence of charge, which decays in time, piezoelectric accelerometer cannot measure constant acceleration. On the other hand, they can reach upper frequencies of tens of kHz.

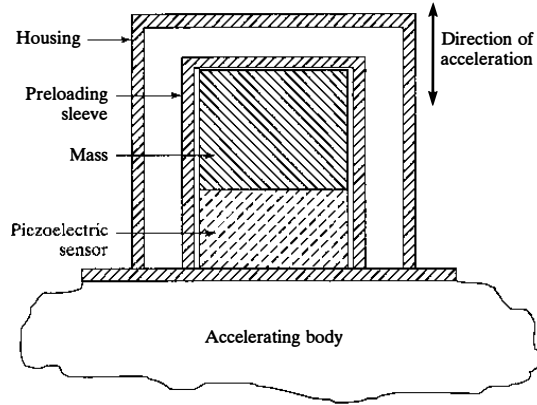


Figure 3.2: Accelerometer based on the piezoelectric effect [51].

In recent years, thanks to the development of micro-machining technology, capacitive accelerometers begin to diffuse. A typical Micro-Electro Mechanical System (MEMS) accelerometer is constituted of a movable proof mass which is attached by a mechanical suspension system to a reference frame (Figure 3.3). The mass has some elongations which develop from it to the space between two fixed outer plates. This configuration with movable plates and fixed outer plates represents a capacitor. Accelerations cause the mass to move along suspensions axis, so the distance between mass elongations and fixed plates varies. This fact can be detected through capacitance change, and then the distance between electrodes can be calculated in order to gain the actual acceleration value [52].

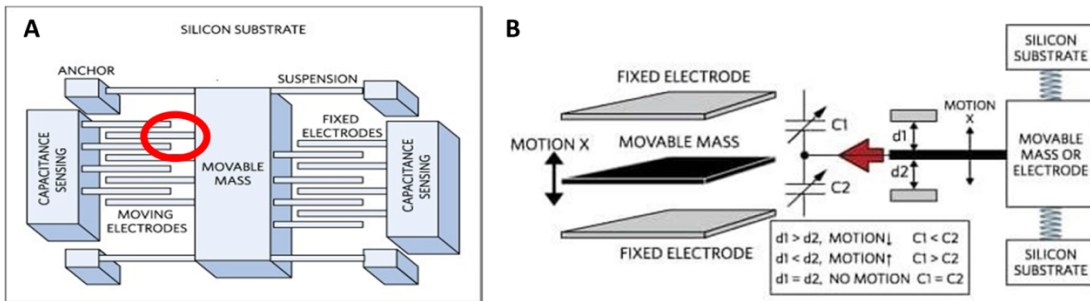


Figure 3.3: Schematic representation of a MEMS capacitance accelerometer. A) Overall vision of the device. Highlighted portion is presented in part B. B) Particular of the device functioning principle. Adapted from [52].

3.2 Gyroscope

Micro-machined gyroscopes are based on the measure of Coriolis force, an apparent force experienced by a mass while moving with a linear velocity in a rotating reference frame. Supposing an object moving along

a straight line in a spinning frame of reference: an outside observer will see a curved trajectory, thus there might be a force in the rotating frame that maintains object's path straight.

The physical principle exploited in gyroscopes is the following: a moving mass, oscillating along a direction with a defined speed, will experience the Coriolis force if a rotation with a certain angular velocity takes place. By measuring the deflection of the mass along an axis perpendicular to linear velocity and angular velocity, for example through a spring, the Coriolis force can be directly measured and used for calculating the unknown angular speed.

Simple devices consist of a proof mass which is induced to vibrate along a direction by an oscillating current and of circuitry to detect oscillations along an orthogonal axis due to rotations (Figure 3.4). In MEMS sensors, a change in electrical capacitance is detected and linked to a specific angular rate.

As for accelerometers, tri-axial devices are a replication of this simple system along three directions.

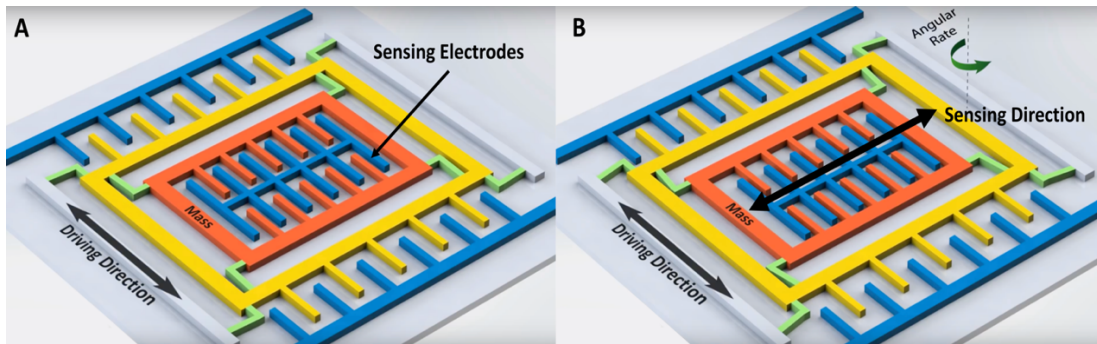


Figure 3.4: Functioning of MEMS gyroscope. A) No angular motion is provided, thus the mass moves only on the driving direction. B) Angular rate takes place, inducing a movement in the sensing direction which is detected by electrodes.

3.3 Magnetometer

Magnetometer are sensors used to gain the strength and the direction of the magnetic field. Earth magnetic field can be measured by magnetometer: it has to be carefully considered that magnetic objects near to the sensor modify that vector, so values obtained do not represent its actual value.

Two types of measuring principles are exploited in this technology: the Hall effect and the magneto-resistive effect.

Hall effect is the development of a voltage difference inside a current carrying conductor while a magnetic field is applied. Indeed, the presence of a magnetic field deflects electrons pathway inside the conductor, creating a voltage in a direction perpendicular to the magnetic field and the current flow.

Magneto-resistive effect is instead the change in electrical resistance of a material inside a magnetic field. It is due to the reorientation of the magnetic domains inside the material caused by the magnetic field, which provokes changing in electrons pathway responsible of increasing or decreasing in resistance values.

As for other mentioned sensors, the replication of one measure system along three perpendicular direction led to a 3 DOF magnetometer, able to obtain the values of the three components of the local magnetic field.

3.4 Technical Specifications of Exploited Sensors

IMU sensor where selected for the specific application because of their high sample rate, useful for identifying the impact phases and the actual peak value, the easy experimental setup required for their use and the reduced dimensions, making them suitable for a dynamic sport such as Judo.

The selected sensor was the TSND121 of the ATR-Promotions. It features high sample rate, good accuracy and resolution and ranges up to 16 g of linear acceleration and 2000 dps of angular velocity.

Moreover, it works with a Bluetooth connection, thus making it extremely suitable and appropriated for studying Judo techniques which involve complex movements, also of the body extremities of both contestants, not easily predictable.

Main characteristics of the selected sensors are listed in Table 3.1.

Table 3.1: Technical specifications of ATR-Promotions TSND121. * = values obtained through the equation $\text{resolution} = \text{range} / 2^{\text{NBIT}}$, where NBIT = 12 bit from datasheet information.

Physical specifications	
Dimensions (mm)	37 x 46 x 12
Weight (g)	22
Data transmission/collection methods	
Radio transmission	Bluetooth 2.0 + EDR, USB
Memory storage (Mbyte)	512
Wired connection	USB serial communication
Mounted sensors	
Accelerometer and gyroscope	<p>InvenSense MPU-6050 Sampling: 1 to 255 ms cycle (1000 to approximately 4 Hz)</p> <p>Acceleration range: $\pm 2 \text{ g}$, $\pm 4 \text{ g}$, $\pm 8 \text{ g}$, $\pm 16 \text{ g}$ Acceleration accuracy: 0.06 mg, 0.12 mg, 0.24 mg, 0.48 mg Acceleration resolution: 0.001 g, 0.002 g, 0.004 g, 0.008 g *</p> <p>Angular velocity range: $\pm 250 \text{ dps}$, $\pm 500 \text{ dps}$, $\pm 1000 \text{ dps}$, $\pm 2000 \text{ dps}$ Angular velocity accuracy: 0.008 dps, 0.015 dps, 0.030 dps, 0.061 dps Angular velocity resolution: 0.122 dps, 0.244 dps, 0.488 dps, 0.977 dps *</p>
Geomagnetic sensor	<p>Aichi Steel AMI 306 Sampling: 10 to 255 ms cycle (100 to approximately 4 Hz) Detection range: $\pm 1200 \mu\text{T}$ Accuracy: 0.3 μT Resolution: 0.586 μT *</p>

4 Preliminary Tests

Tests conducted in this Section were performed using ATR-Promotions compact sensors TSND121. Two sensors were considered in the experimental setup, "Sensor13" and "Sensor15", and to verify that both sensors would measure the same quantities they were fastened together so they were affected by same movements.

Inertial sensors directly measure linear acceleration and angular velocity in the three directions X, Y and Z. Moreover, information about the magnetic field in the three directions is gained by the magnetometer, but these data were not considered at first stage. To verify that accelerometers really measured these quantities for each axis and to detect if data were consistent with the measurand, two types of tests were developed, one for linear quantities and one for rotational variables.

Data gained from accelerometers were post-processed using MATLAB scripts reported in Appendix C.

4.1 Linear Tests

Accelerations in the three directions were first proved. In particular, sensors were left on a stable surface to measure the value of gravitational acceleration on their three axes. The sequence of axes sense followed in the test was:

- X-axis upward;
- Z-axis upward;
- X-axis downward;
- Z-axis downward;
- Y-axis upward;
- Y-axis downward.

Sensors were maintained in each position for about 5 seconds.

As can be seen from the first column of Figure 4.1, accelerations were measured on the right direction; moreover the value, which represent gravitational acceleration or gravitational acceleration on the opposite direction, is near to 1 g with a maximum difference of about 0.1 g. The second column represents raw data filtered with a passband filter in order to remove gravitational acceleration and reveal accelerations due to external forces: these signals will be used later to be integrated over time avoiding drift problems. Acceleration due to external forces can be easily detected in Figure 4.2 where a value greater or lower than gravitational acceleration module is depicted.

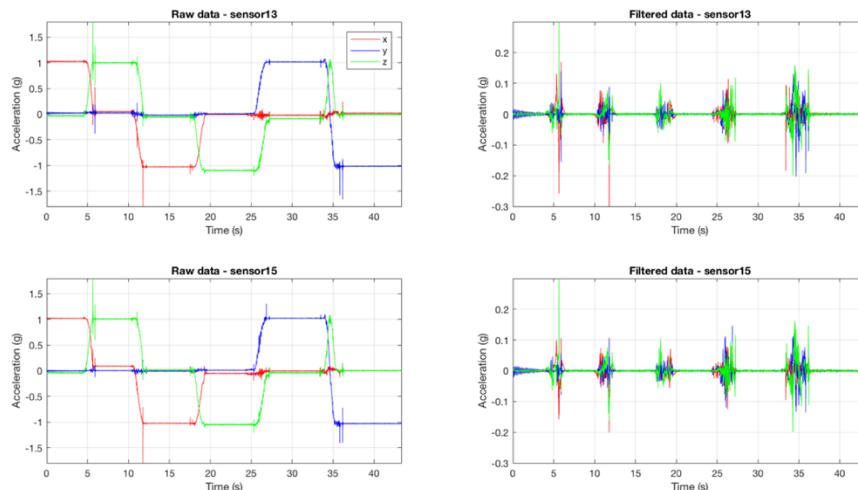


Figure 4.1: Measures obtained in different axes configurations.

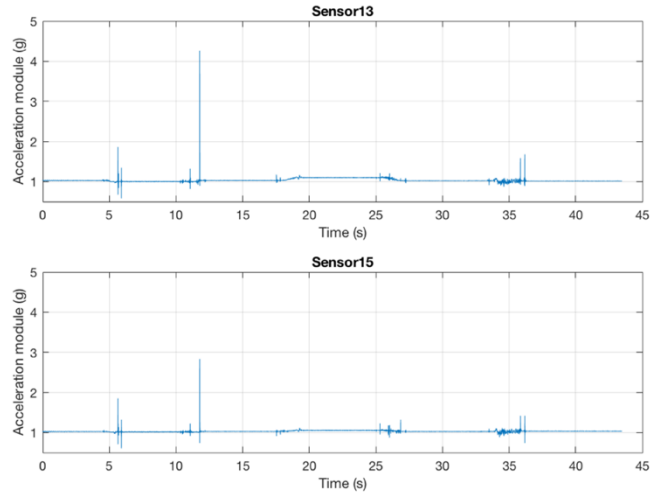


Figure 4.2: Acceleration module during the first linear test.

After having tested sensors in a static condition, a dynamic acquisition with manual oscillations in the three directions was performed.

The protocol respected in the test was the following:

- rest
- 5 seconds of oscillation in the X-direction;
- 3 seconds of rest;
- 5 seconds of oscillation in the Y-direction;
- 3 seconds of rest;
- 5 seconds of oscillation in the Z-direction.
- rest

In rest condition no external forces were applied on sensors. Results are reported in Figure 4.3. As can be seen, the greatest amplitudes were obtained in the actual axis, while other oscillations are due to the manual execution of the test in which completely excluding movements in other directions was not feasible. No important differences were found between the two sensors.

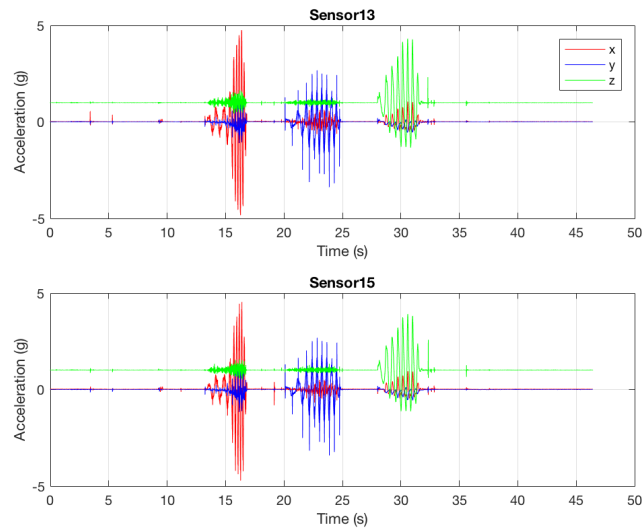


Figure 4.3: Linear acceleration preliminary test.

4.2 Rotational Tests

Tests conducted in this Section were aimed to ensure a proper reconstruction of the angle path followed by the two sensors by numerical integration of the measured angular velocity.

To create a similar and well-determined time-angle diagram, a specific tool was designed to guarantee proper angle values and a chronometer was used during the test to obtain the right temporal sequence (Figure 4.4).

The test for each of the three directions was performed as follows:

- rest at 0° ;
- 5 seconds of angle increasing from 0° to 45° with a constant angular velocity;
- 5 seconds of rest at 45° ;
- 5 seconds of angle increasing from 45° to 90° with a constant angular velocity;
- 3 seconds of rest at 90° ;
- 5 seconds of angle increasing from 90° to 135° with a constant angular velocity;
- 5 second of rest at 135° ;
- 5 second of angle decreasing from 135° to 0° with a constant angular velocity;
- rest at 0° .

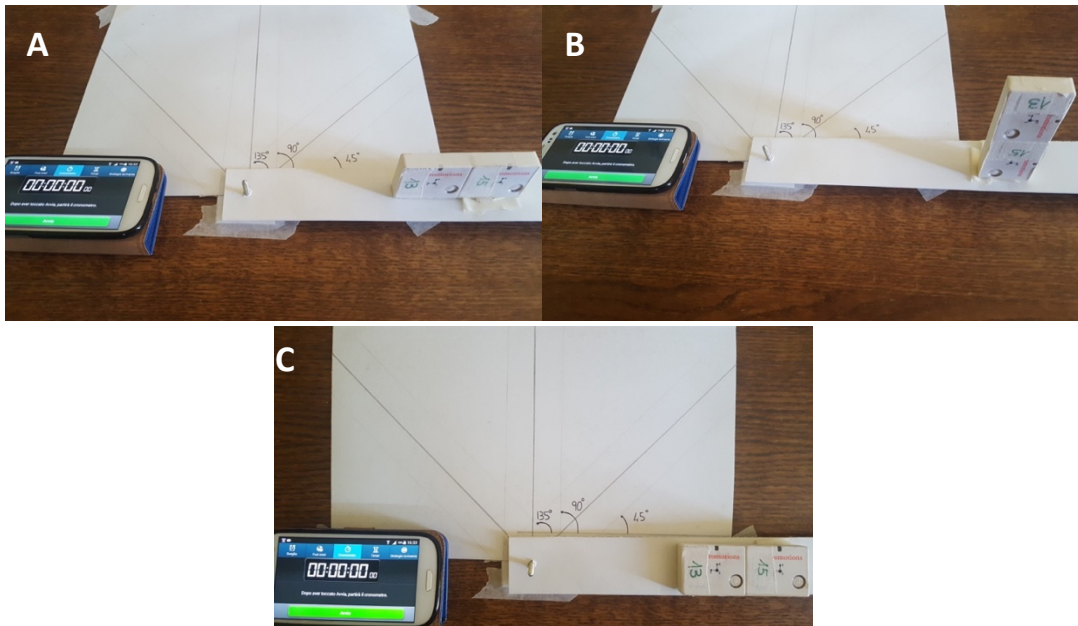


Figure 4.4: Experimental setup for angular tests. A) X-axis rotation, B) Y-axis rotation, C) Z-axis rotation.

Diagrams gained by integration of angular velocity present how the angle varies in time during the test: in each of the three tests, the angle which varies is the one in the direction of the angular velocity as expected, while others remain about 0° because of the complete exclusion of these directions from the experiment thanks to the on-a-plane movement. Furthermore, as for the linear test, no substantial differences were found between the two sensors (Figure 4.5, Figure 4.6, Figure 4.7).

Angles were obtained by integration of the angular velocity through the MATLAB function `cumtrapz()`: drift was excluded by filtering the angular velocity before numerical integrating data. A pass-band filter was employed for this task, in particular a 4th order Butterworth filter with cut-off frequencies of 1 Hz and 50 Hz was used.

4 Preliminary Tests

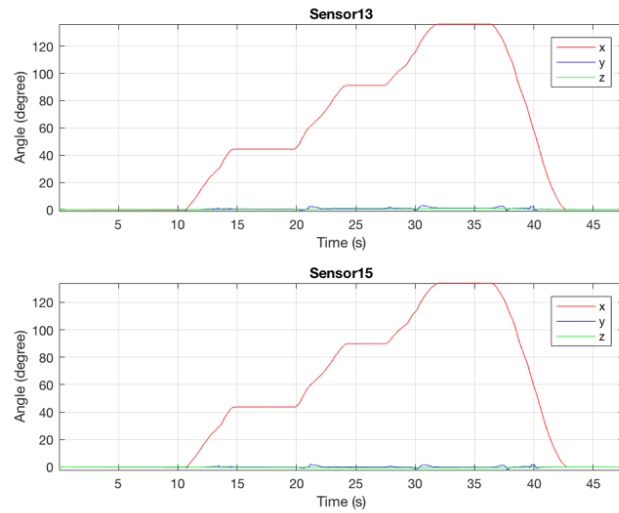


Figure 4.5: Rotational test, angular velocity in the X direction.

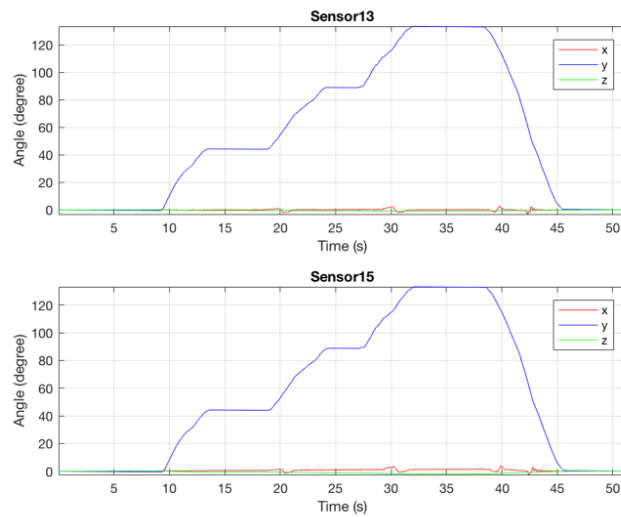


Figure 4.6: Rotational test, angular velocity in the Y direction.

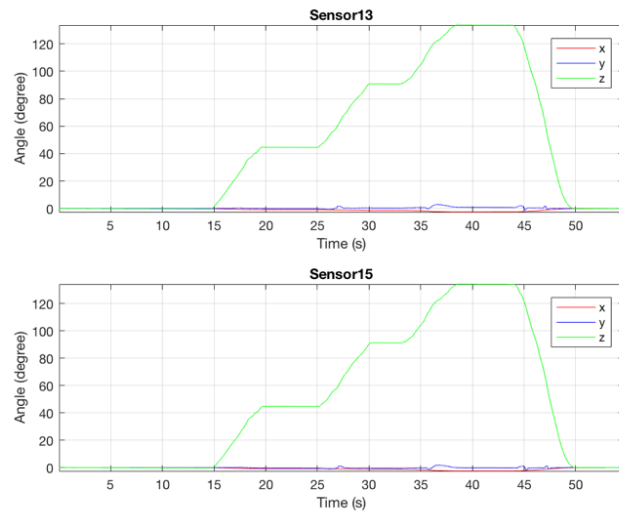


Figure 4.7: Rotational test, angular velocity in the Z direction.

Combining results obtained in this first test for each direction, a second test was carried out using the two sensors on a human being. This time, the two sensors were fixed separately, "Sensor15" on the middle forehead and "Sensor13" on the centre of the sternum and the neck range of motion respect to the torso was investigated.

During the test the subject was asked to execute movements around the anatomical axes of the head (Figure 4.8), in particular the sequence of rotations and actions was the following:

- rest with head and neck aligned in vertical position;
- three oscillations on the frontal plane (around the antero-posterior Z-axis) with his full range of motion;
- 5 seconds of rest in the vertical position;
- three oscillations on the sagittal plane (around the medio-lateral Y-axis) with his full range of motion;
- 5 seconds of rest in the vertical position;
- three oscillations on the transverse plane (around the longitudinal X-axis) with his full range of motion;
- rest with head and neck aligned in vertical position.

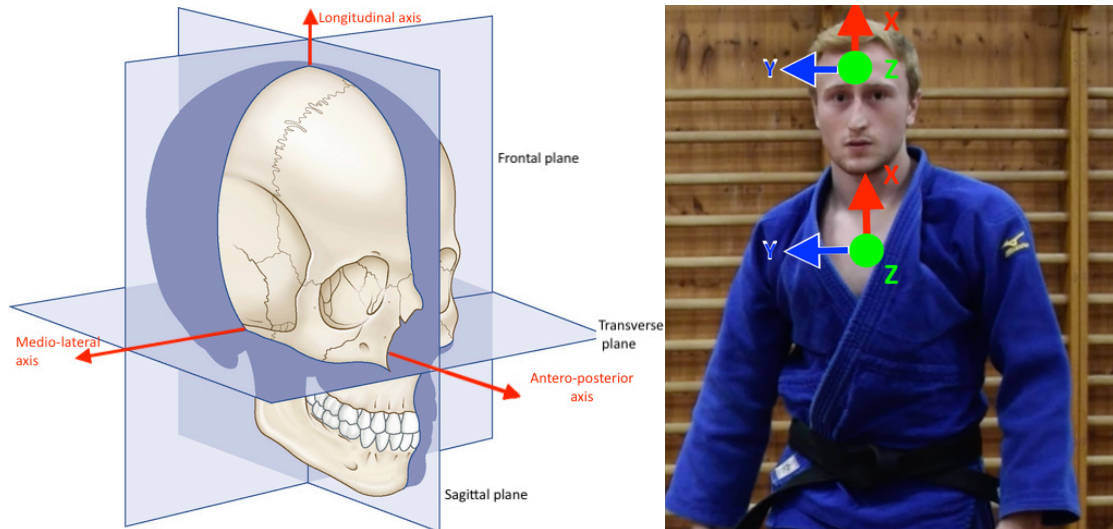


Figure 4.8: Anatomical planes and axes considered in the test.

Considering angular velocities (Figure 4.9), relatively small values close to zero were obtained for the sensor fixed to the sternum which remained in a motionless position. It can be seen also that, in particular in the first three oscillation in the frontal plane, the subject did not completely isolate the movement from others

around X and Y axes. This fact leads to an angle estimation in that direction (Figure 4.10): unwanted angular movements were found also examining the video of subject's torso.

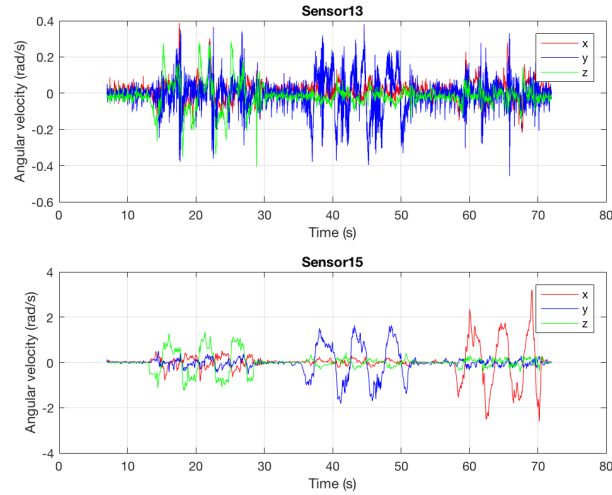


Figure 4.9: Angular velocities obtained in studying the range of motion of a human neck. “Sensor15” was placed onto forehead, while “Sensor13” on the sternum.

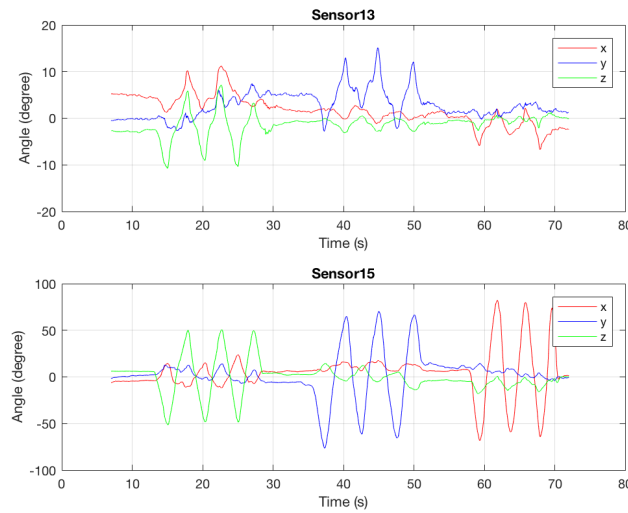


Figure 4.10: Angles gained from integration of the angular velocities presented in Figure 4.9. “Sensor15” was placed onto forehead, while “Sensor13” on the sternum.

Results obtained in this investigation proved the reliability of the sensors and the MATLAB script to estimate the angle between the accelerometers. Indeed, data gained are similar to a normal range of motion of a human cervical spine, moreover a visual inspection of the video captured during the test demonstrated the right estimation of angles in the planes. As can be seen from Figure 4.11, in which the angle between the two sensors (calculated by the integration of the difference of angular velocities of both sensors for each axis) is presented, the subject did not isolate the rotations around one axis, but the resultant movement was a rotation around three axes, as highlighted above for single sensors angles.

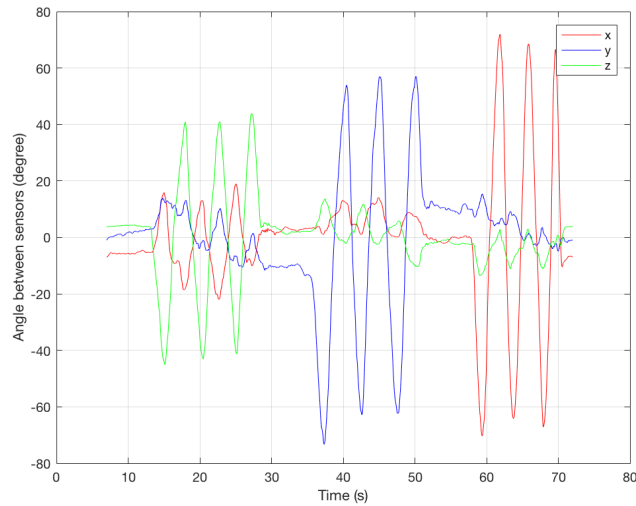


Figure 4.11: Angle between the two IMUs used in the test. Angle in the X direction represents head rotation movements, in the Y direction flexion/extension and in the Z direction lateral flexion

4.3 Initial Tests on Judo Mat

After having verified sensors functioning and algorithm reliability, many preliminary tests were conducted on Judo mat. Sensors configuration used in the following tests was full acceleration range of measurement (± 16 g), full angular velocity range (± 2000 deg/s), maximum sample rate (1000 Hz), with “Sensor13” placed on the middle forehead and “Sensor15” on the sternum. Axes here considered are: X-axis, longitudinal and directed upward; Y-axis, mediolateral and directed to the right of the subject; Z-axis, anteroposterior and directed forward.

At first a set of five backward breakfalls was performed by a black belt (I dan) with 17 years of experience (Figure 4.12).

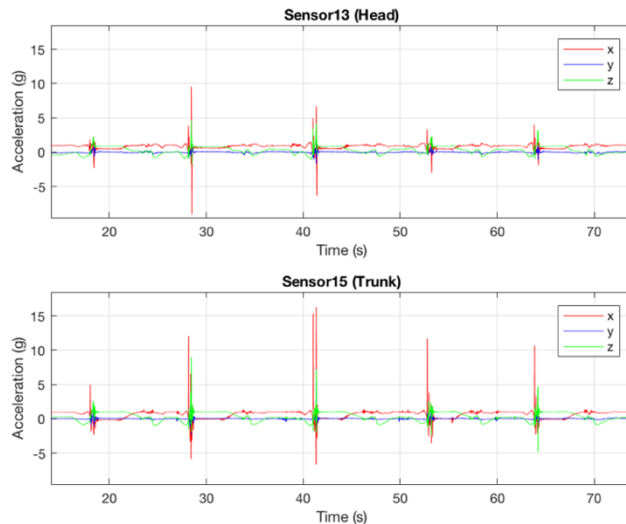


Figure 4.12: First measurement of linear acceleration during backward breakfalls.

Looking at obtained curves no repeatability could be seen in this circumstance, indeed peak values range from about 2 g to 10 g on the head and from 5 to 15 g on the trunk. In order to deeply comprehend the accelerations that head has to bear while performing this movement, a motion video analysis was successively carried out whilst measuring kinetic variables through IMUs (see Chapter 5 Breakfall Techniques Analysis).

Then some Judo techniques were tested to first notice if sensors were reliable for the scope of this study. For further information about techniques here cited refer to Appendix A.

O-soto-gari technique was first tested: five repetitions were measured using two black belt judokas, a thrower who execute the technique and a faller who wore the sensors (Figure 4.13). As can be seen from the figure, considering that sensors could measure acceleration values up to 16 g, three throws saturated the sensor on the sternum, a particular of the second throw is here reported (Figure 4.14).

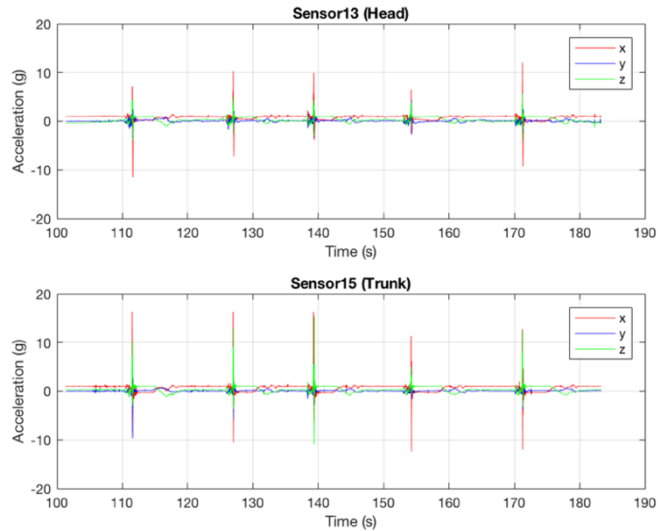


Figure 4.13: Linear acceleration obtained by o-soto-gari technique.

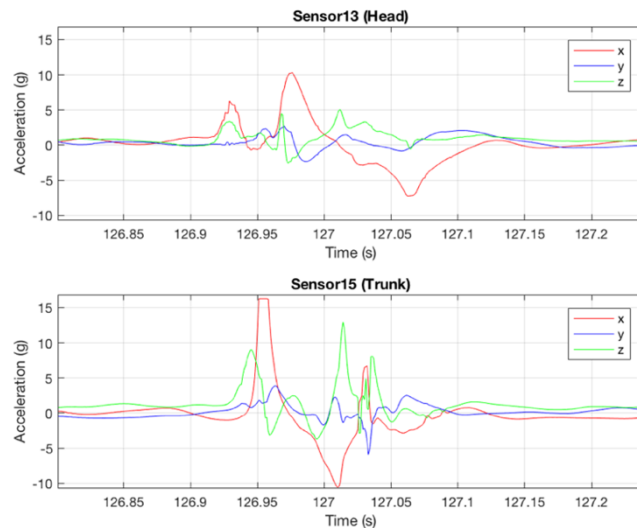


Figure 4.14: Particular of the second o-soto-gari throw.

Furthermore, a set of three tai-otoshi was performed to test another technique in order to understand if the saturation problem could be overcome (Figure 4.15).

As can be seen from Figure 4.16 in which the second peak is detailed, values of linear acceleration saturated both sensors. In particular, acceleration in the longitudinal X axis saturated on the head, while it happens for the antero-posterior Z axis on the sternum: the difference is due to the specific position assumed by faller's head and trunk while being thrown and impacting the floor, with the trunk laid on the mat and the neck flexed to not strike the head to the floor.

It has to be considered that the technical execution was not a maximal expression of thrower's force: nevertheless 16 g were not enough to precisely capture the motion. Because sensors used were already set

to their maximal capabilities, they cannot be considered appropriate for the purpose of this research, thus other sensors with an extended range of acceleration have to be employed.

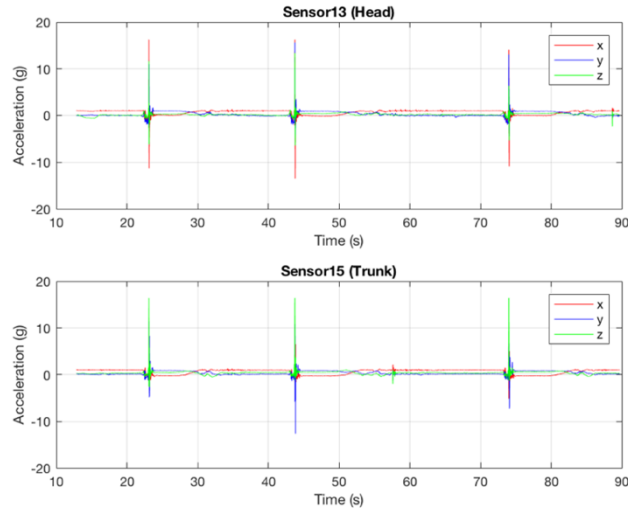


Figure 4.15: Linear acceleration measured while being thrown with tai-otoshi technique.

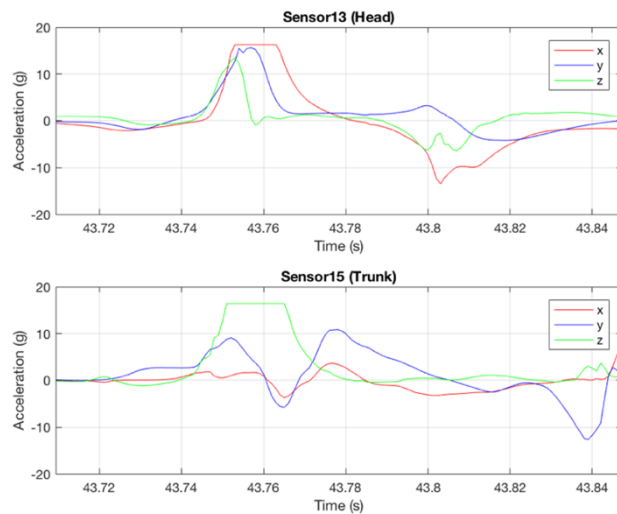


Figure 4.16: Particular of the second tai-otoshi projection. Both sensors saturated, as in the case of the first throw.

4.4 IMU Market Analysis

Due to the saturation problem, a research on the market was carried out looking for Inertial Measurement Units with proper features for the study.

Brands considered in the inquiry were APDM Wearable Technology, BTS Bioengineering, Cometa Systems, Exel, IMeasureU, LP Research, Mac-Lloyd Sport, Mide Technology, Princip, Shadow System, Shimmer, STT systems, Technaid, TecnoBody, XSense and Yost Labs. Excluding brands which propose sensors limited to 16 g or less, a comparison table was then computed considering main features such as modalities of communication with personal computers, ranges of acceleration and angular velocity, sampling rate and price (Table 4.1).

Bearing in mind that the first device reported in Table 4.1 is the one mainly used in studies cited in the state-of-the-art assessment, it cannot be used in this study because of the lack of angular information. Moreover, it has to be connected to pc by cable during the acquisition and it could be insidious in the protocol to be followed.

Last three sensors presented have a high price because of the presence of an included user-friendly software interface. Furthermore, OPAL sensor was initially excluded from the challenge because of the low sampling rate, which was meant to reduce the memory usage and to lower battery consumption. The highest rate of acquisition affordable (128 Hz) indeed does not guarantee to adequate sample acceleration or velocity peaks, which from literature have a duration of about 20 ms: one sample every 7.8 ms means that two points would be taken in the impact time, not allowing to proper reconstruct the peaks.

In the end, the selected device was 3-Space™ Sensor. Communication modality does not influence sensor performances basing on published specifications, so Bluetooth configuration was chosen for the familiarity since the previously used sensors communicate through this protocol. Main characteristics of the selected device are presented in Table 4.2.

4 Preliminary Tests

Table 4.1: IMUs on the market appropriated for the research purpose. * = Reference accelerometer used in studies found in literature, N.D. = Not Declared in available documentation.

Model	Brand	Connectivity	Acceleration range (g)	Angular velocity range (dps)	Sampling Rate (Hz)	Price	Link
Triaxial Charge Accelerometer Types 4321 *	Brüel & Kjaer	Cable	± 1000	Gyroscope absent	Up to 10000	2350 €	https://www.bksv.com/en/products/transducers/vibration/transducers/accelerometers/4321
3-Space™ Sensor Wireless (Ultra High-G)	Yost Labs	USB 2.0 or wireless 2.4 GHz DSSS	± 100 / ± 200 / ± 400	± 250 / ± 500 / ± 1000 / ± 2000	Up to 1350	\$ 265.00	https://yostlabs.com/product/3-space-wireless-2-4ghz-dsss/
3-Space™ Sensor Bluetooth (Ultra High-G)	Yost Labs	USB 2.0 or 2.4 GHz Bluetooth v2.0	± 100 / ± 200 / ± 400	± 250 / ± 500 / ± 1000 / ± 2000	Up to 1350	\$ 335.00	https://yostlabs.com/product/3-space-bluetooth/
HIGH G SENSOR	Mac-Lloyd Sport	Bluetooth	± 100 / ± 200 / ± 400	N.D.	1300	1750 €	http://mac-lloyd.com/en/products/#!/sensor
OPAL	APDM Wearable Technology	USB (to collect data)	± 16 / ± 200	± 2000	20 to 128	\$ 2400.00	https://www.apdm.com/wearable-sensors/
Slam Stick C	Mide Technology	USB (to collect data)	± 16 / ± 200	Gyroscope absent	12 to 3200	\$ 1000.00	https://www.mide.com/collections/shock-vibration-data-loggers/products/slam-stick-c

Table 4.2: Technical specifications of Yost Labs 3-Space™ Bluetooth sensors Ultra High-G. * = values obtained through the equation $\text{resolution} = \text{range} / 2^{\text{NBIT}}$, where NBIT = 12 bit for accelerometer and magnetometer, 16 bit for gyroscope (data from datasheet information).

Physical specifications	
Dimensions (mm)	35 x 60 x 15
Weight (g)	28
Data transmission/collection methods	
Radio transmission	Bluetooth 2.0 + EDR (2.4 GHz)
Memory storage (Mbyte)	-
Wired communication	USB 2.0
Mounted sensors	
Accelerometer	Sampling: up to 1350 Hz in IMU mode Acceleration range: $\pm 100 \text{ g}$, $\pm 200 \text{ g}$, $\pm 400 \text{ g}$ Acceleration resolution: 0.049 g , 0.098 g , 0.195 g *
Gyroscope	Sampling: up to 1350 Hz in IMU mode Angular velocity range: $\pm 250 \text{ dps}$, $\pm 500 \text{ dps}$, $\pm 1000 \text{ dps}$, $\pm 2000 \text{ dps}$ Angular velocity resolution: 0.008 dps , 0.015 dps , 0.030 dps , 0.061 dps *
Geomagnetic sensor	Sampling: up to 1350 Hz in IMU mode Detection range: ± 88 to $\pm 810 \mu\text{T}$ Resolution: 0.043 to $0.396 \mu\text{T}$ *

5 Breakfall Techniques Analysis

Falling techniques are the most important aspect related to Judo fights to properly ensure athletes' safety. Indeed, the different types of ukemi are the first subject involved in teaching Judo. Since the first lesson, many games and educational exercises are used to make these technical gestures as automatic movements in order to guarantee the absence of injuries during every type of falling.

Judo comprehends four types of breakfalls (see Appendix A for clarifications). During fights the technical execution of these movements is never perfect because of the particularity of each situation. The most frequent type of breakfall, which is meant for avoiding head traumas while being thrown, is the backward breakfall, named "ushiro ukemi". Thus, it was chosen for a detailed examination comprehending video and statistical analysis.

Moreover, considering that during fights technical execution is not faultless, a different type of backward breakfall was considered in the following test: "no-hands" backward breakfall, which can happen in fights due to grips or situational characteristics, was opposed to the standard breakfall technique. In this variation, hands and arms do not impact or touch the floor during the entire execution, but the general movement is equal to the standard technique.

5.1 Preliminary Test

In order to understand how quantities such as acceleration and neck flexion-extension angle are linked to human motion during falling techniques, a video was recorded while performing the movement and then processed with Kinovea program for video analysis.

Firstly, it was tested if a proper reconstruction of head trajectory could be obtained by simple double integration of filtered IMU data. In this preliminary test, sensors were fastened together and a triangular trajectory on the X-Y plane was followed counterclockwise, as shown in Figure 5.1.

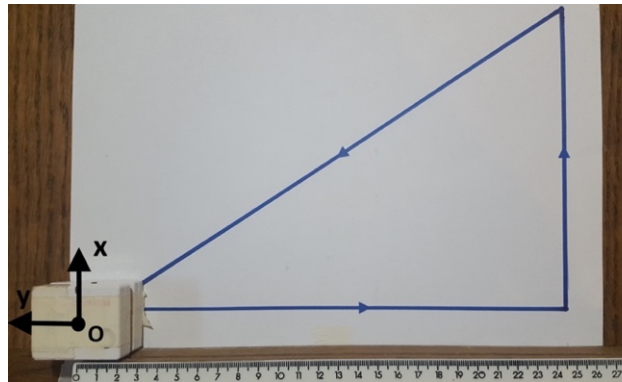


Figure 5.1: Triangular path followed for verifying trajectory reconstruction.

Data from the accelerometer were pass-band filtered, with the same filter used in Section 4.2, to avoid drift and then integrated once to obtain velocity, twice to get position data. Instead, Kinovea data were low-pass filtered with a 2nd order Butterworth filter with a cut-off frequency of 5 Hz: in this way, noise due to the derivative was closely excluded. Then, they were derived once to obtain velocity, twice for acceleration.

As can be seen from Figure 5.2 in which test results are proposed, no matches can be found between the two types of data. Kinovea positions and velocities could be considered reliable because they are close to theoretical diagrams; this cannot be said for accelerations in which noise is significantly enhanced. The noise which can be appreciated in Kinovea velocities could be connected to the manual execution of the test, but also to the derivative enhancing of noises which cannot be completely excluded.

IMU data thus cannot be considered reliable in detecting sensors path if a simple double integration is used for getting position along axes. Consequently, following tests would not contain information about velocity and position, which cannot be straightforwardly estimated from accelerometers data.

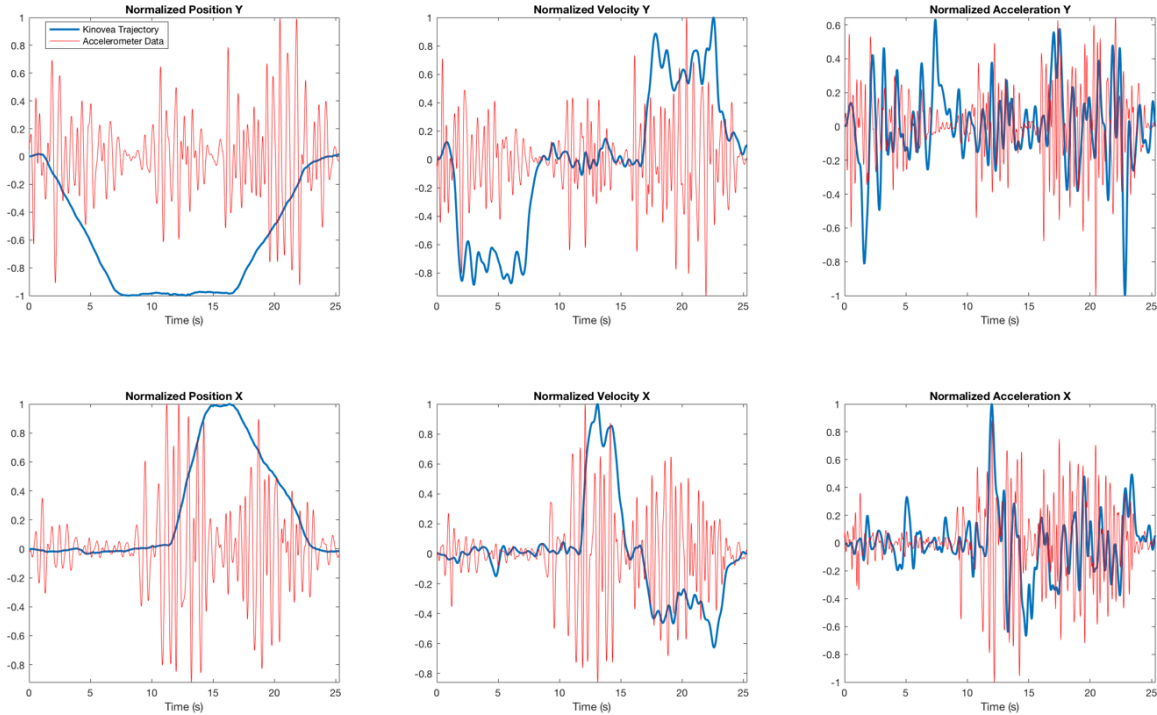


Figure 5.2: Comparison between Kinovea and IMU trajectory reconstruction. Data are normalized to the maximum of their module, because even if IMU data are in standard units of measurement, Kinovea data are exported in pixels and no comparison could be easily made. IMU data are resampled to match the lower video sampling rate.

5.2 Analysis of the Technical Gesture

Considering results obtained previously, breakfall would not imply acceleration values next to the upper limit of the acceleration range of ATR-Promotions sensors: thus, sensors exploited in this Section were ATR-Promotions TSND121, one on the middle forehead and one on the sternum. Used axes are reported in Figure 4.8.

In order to investigate the breakfall technique the experimental protocol was established as follows:

- 2 jumps
- 5 ushiro ukemi
- 2 jumps
- 5 ushiro ukemi
- 2 jumps

The protocol was repeated three days by the same subject, a 17 years of experience black belt (I dan), and every day the procedure was performed firstly with standard ukemi and then it was reiterated with “no-hands” ukemi. At the end, 30 breakfall for each type were recorded by sensors and video camera.

The two types of information were synchronized used Kinovea and MATLAB: for this purpose, jumps were executed at the beginning, in the middle and at the end of the tests. The first jump was used to synchronize the two types of information and the second to control if they were correctly matched. Data were matched using the first photograph in which feet took off and linking it to the first point acquired in which acceleration along the longitudinal X axis becomes near to zero. Jumps in the middle and at the end of the tests were instead exploited to investigate if synchronization lasted for the entire test.

At first, the two breakfall techniques were analysed in detail to well determine the movement, and to link acceleration and angle data to the particular phases of the ukemi. One repetition for each type of breakfall was chosen randomly to be investigated. Furthermore, because the movement develops on a plane, in particular on the sagittal plane (XZ-plane for the sensors placement on athlete's body), X and Z components of acceleration are reported, while the angle considered is only the flexion-extension angle (Y-angle for the sensors configuration on athlete's body). Examined breakfalls are reported in Figure 5.3 and Figure 5.4. According to acceleration curves, the standard ukemi (Japanese term for breakfall) technique can be divided into eight distinct phases corresponding to their local maxima or minima:

- A) Start position;
- B) Descending phase;
- C) Sacral contact;
- D) Lumbar contact;
- E) Thoracic contact;
- F) Head deceleration;
- G) Longitudinal deceleration;
- H) End position.

The ukemi starts in standing position with arms outstretched forward (phase A), then the movement begin with approaching the floor by bending legs and moving the head forward (phase B). Once crouched down, the first body part which contacts the floor is the sacrum (phase C): this contact is reflected to the head with a peak of acceleration on both axes due to the extension of the neck. Thus, athlete's body keeps rolling till firstly lumbar, then scapular zones hit the mat (phases D and E). Since the beginning of the breakfall, forehead follows trunk movements, so when it moves forward neck extension angle reduces bringing chin next to the sternum, while when athlete lets dropping down extension angle starts growing. Instead, since thoracic vertebrae contact the mat, head starts a counter-movement guiding the forehead upward (phase F): thanks to the activation of neck flexor muscles, head decelerates avoiding striking the floor and cerebral damages. Because of trajectory followed by athlete's centre of mass, through which a downward movement is converted into a longitudinal slipping, the last dynamic phase is a longitudinal deceleration (phase G). The technique ends in a static position with the athlete completely arrested on the floor (phase H).

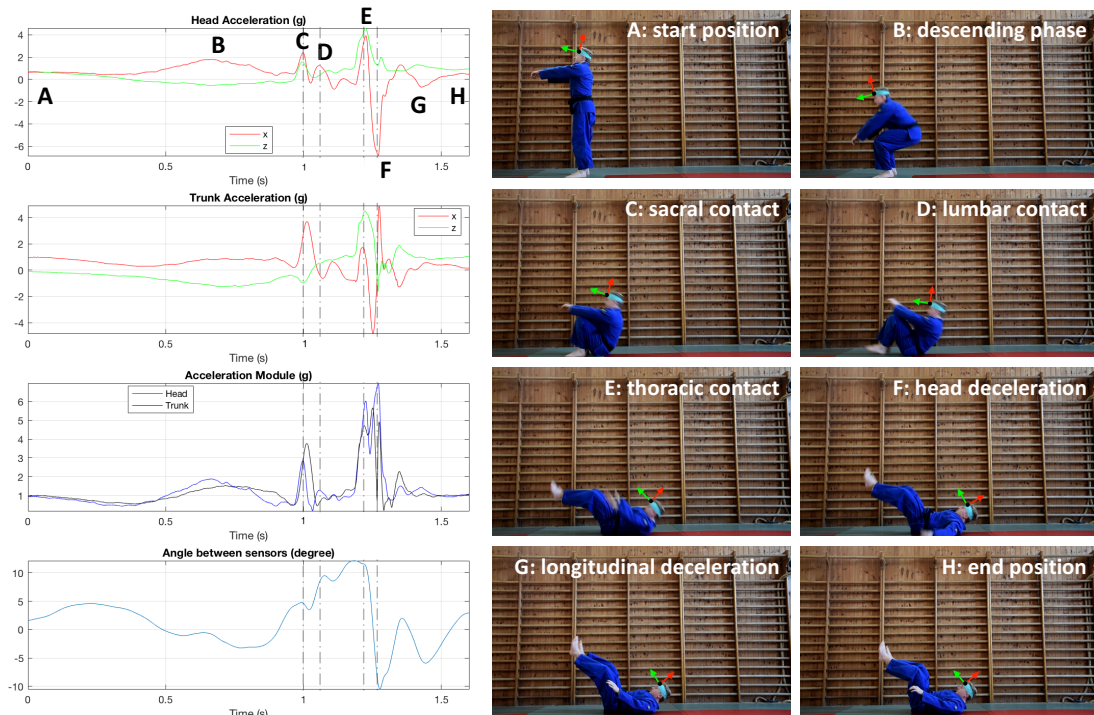


Figure 5.3: Analysis of standard backward breakfall. Positive angle values mean neck extension while negatives flexion.

Examining how breakfall develops in time, most critical instants for head injuries analyses are when the human body hits the floor, so phases C-D-E, and during head deceleration in which the peak value is acquired, represented by phase F. The four moments here identified will be further analysed for detecting repeatability and differences in the two types of breakfall examined.

As for the standard ukemi, the eight phases previously identified can be easily found also in data acquired while falling without the possibility of using hands and arms.

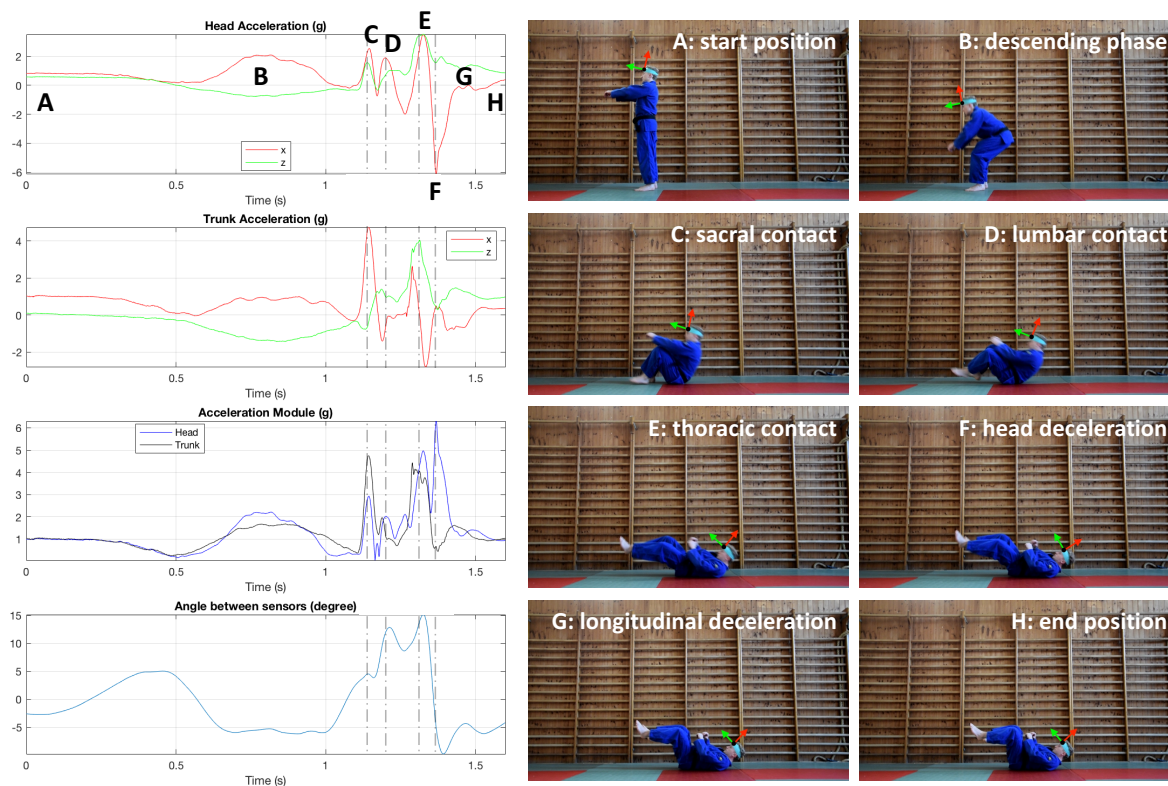


Figure 5.4: Analysis of "no-hands" backward breakfall. Positive angle values mean neck extension while negatives flexion.

Variables considered as parameters for evaluating the risk of trauma to the head or to the trunk were linear accelerations, angular velocities, angular accelerations and the angle between sternum and forehead. All the variables were measured along the three directions X, Y, Z, respectively meaning longitudinal, medio-lateral and antero-posterior axes. All three components were considered even if the movement develops on a plane: out of plane components were here examined to confirm this hypothesis.

Data were firstly analysed calculating mean and standard deviation of each variable during the whole ukemi cycle. Repetitions were aligned using the MATLAB function `findsignal()`, using Euclidean distance minimization between a prototype signal and data. The first repetition was chosen as prototype and all other signals were correctly found and divided into best matching epochs. Mean and standard deviation for each breakfall parameter were then computed considering all 30 repetitions for each type of ukemi. Results in terms of components and module are reported in Figure 5.5, Figure 5.6, Figure 5.7, Figure 5.8, Figure 5.9, Figure 5.10, Figure 5.11.

Regarding acceleration curves, the two peaks in head X-acceleration, one positive followed by one negative, correspond to the previously indicated phases E-F, evidencing that the two potentially dangerous moments always occur while performing a backward breakfall.

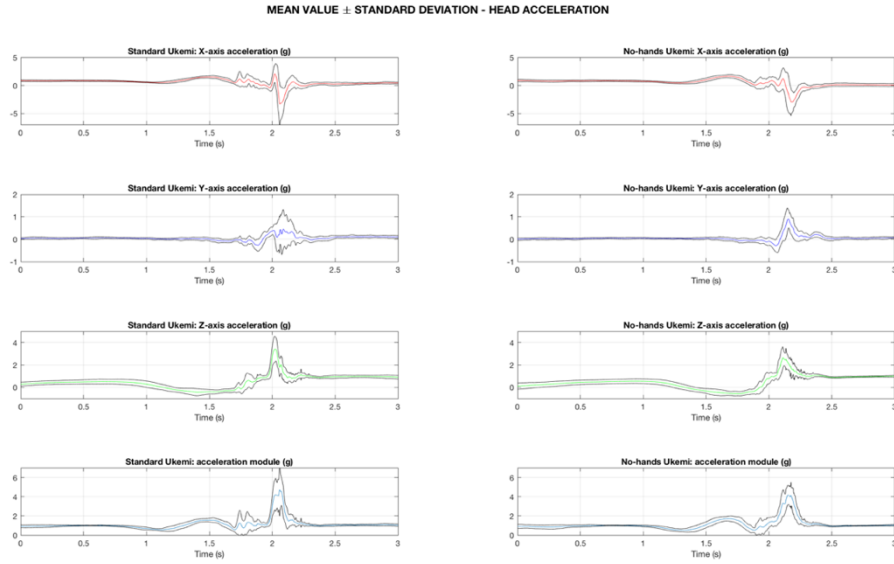


Figure 5.5: Head acceleration during backward breakfalls.

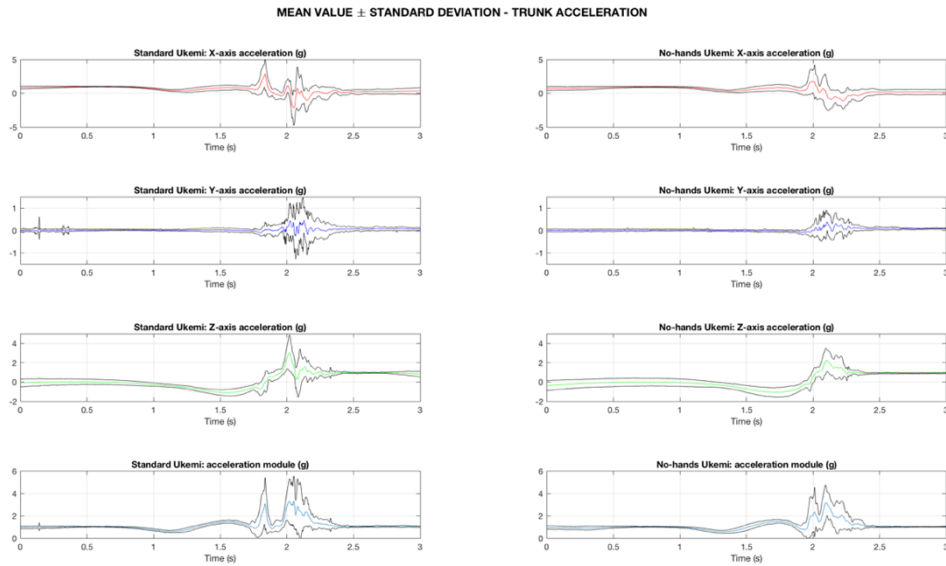


Figure 5.6: Trunk acceleration during backward breakfalls.

As can be seen from Figure 5.5 and Figure 5.6 in which linear acceleration is presented, Y component is less than or equal to 1 g: reflecting on other components values and its great variability for both types of breakfall on both sensors, the movements can be considered on a plane, so neglecting Y acceleration in previous analyses can be considered appropriate.

Furthermore, a reduced standard deviation is reported only on head Y-acceleration during “no-hands” breakfall. This fact is probably due to factors that cannot be controlled by the athlete while falling: for example, it should be addressed to a first contact between one scapula and the mat, and then the other one, instead of one hit with both scapulae at the same time. It leads to the positive peak value corresponding to head deceleration. In particular, contacting first with the left side of the body results in a positive acceleration with this Y-axes orientation. This hypothesis is additionally supported by the fact that the athlete which performs the test is right-handed while doing Judo, so in his guard position the right side of his body is placed forward. In this way, left shoulder is always back with respect to the right one, influencing his posture in real life, so more inclined to touch the floor first. Moreover, a peak value is more visible on head than trunk because of its greater distance from impact zone.

Even if passed down by Judo coaches, considering acquired data, the use of hands does not reduce acceleration, but results here reported evidences greater acceleration while performing standard ukemi. This situation may be due to athlete's inexperience in executing a breakfall without the use of arms and hands. Indeed, this type of ukemi is never taught to judokas, but may happen during fights. On the other hand, the extensive knowledge of standard breakfall allows the athlete to execute it with more impact force determining greater acceleration values.

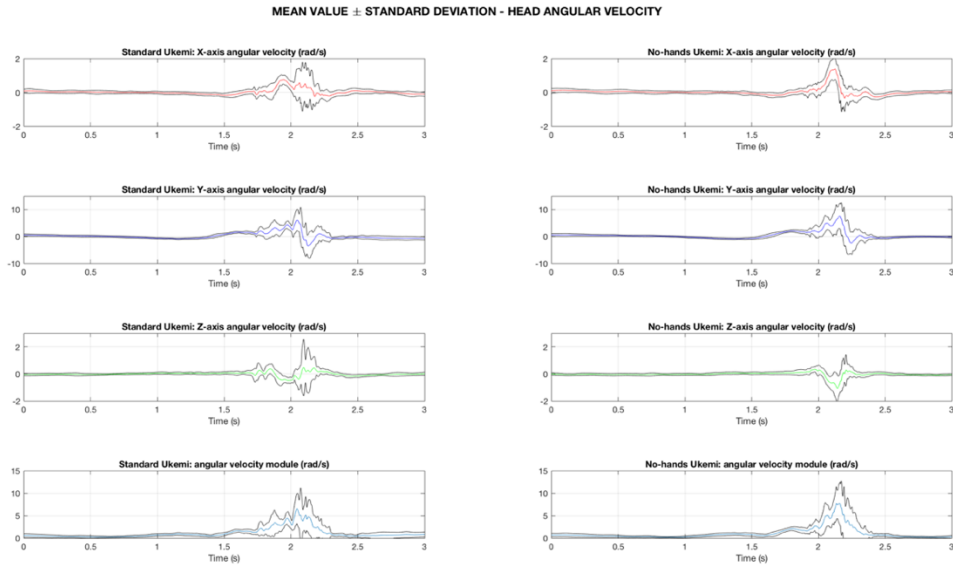


Figure 5.7: Head angular velocity during backward breakfalls.

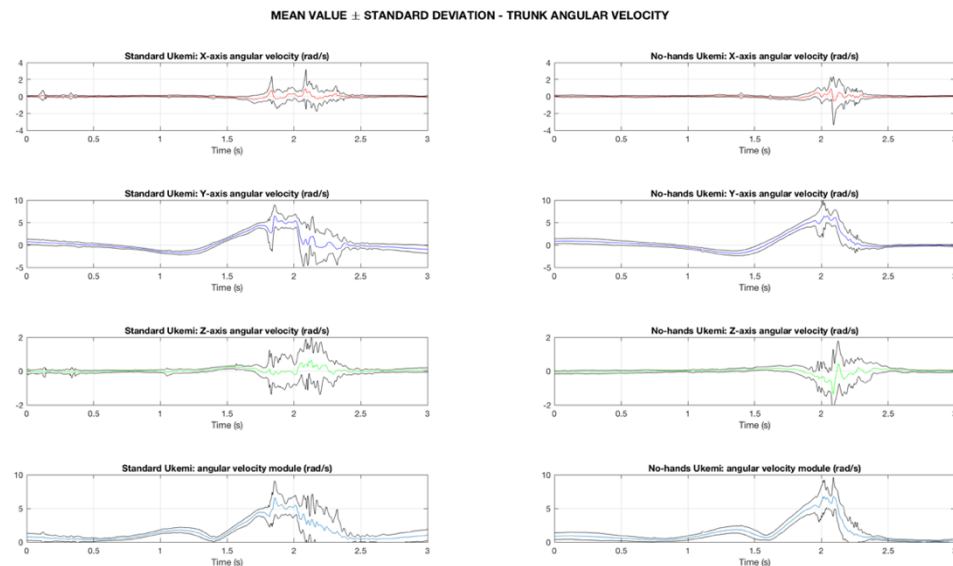


Figure 5.8: Trunk angular velocity during backward breakfalls.

As evidenced with acceleration curves, the movements are correctly considered on a plane as can be seen from Figure 5.7 and Figure 5.8, in which angular velocities are proposed: indeed, Y-angular velocity presents values next to 10 rad/s, while in other directions the great variability, which reaches 2 rad/s, demonstrates the presence of noise and not a well-determined action.

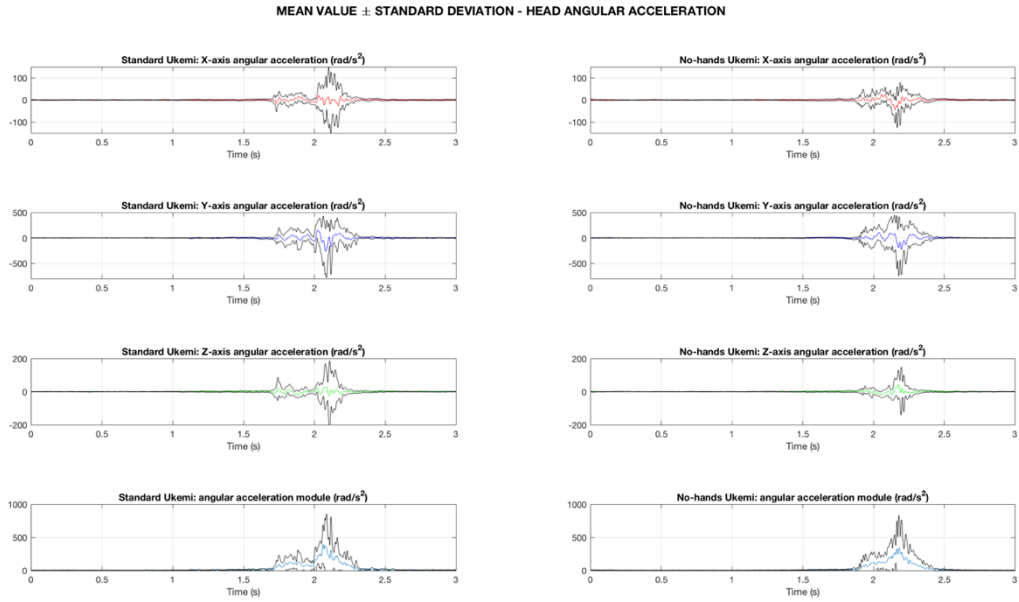


Figure 5.9: Head angular acceleration during backward breakfalls.

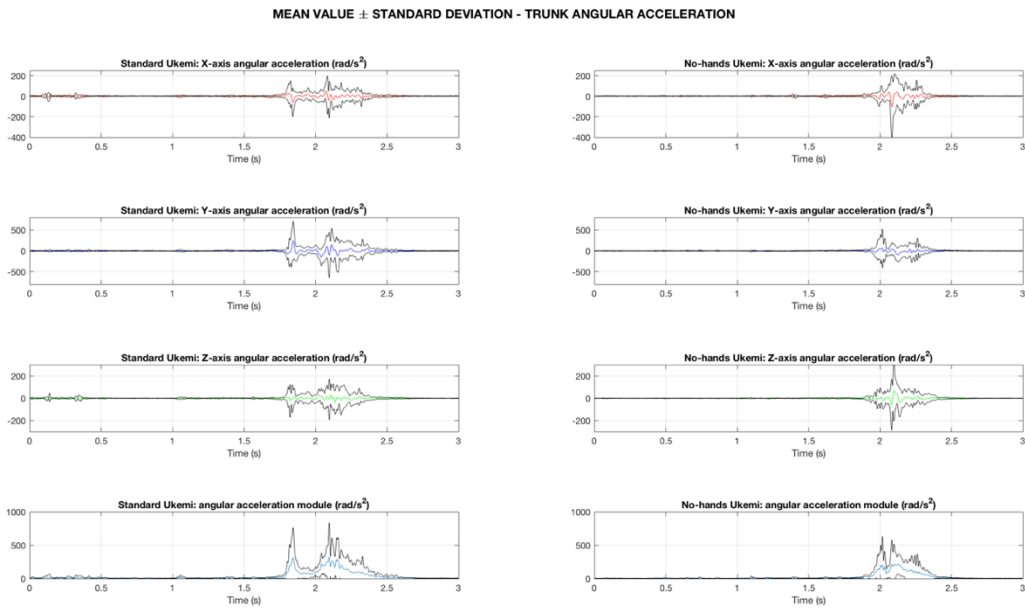


Figure 5.10: Trunk angular acceleration during backward breakfalls.

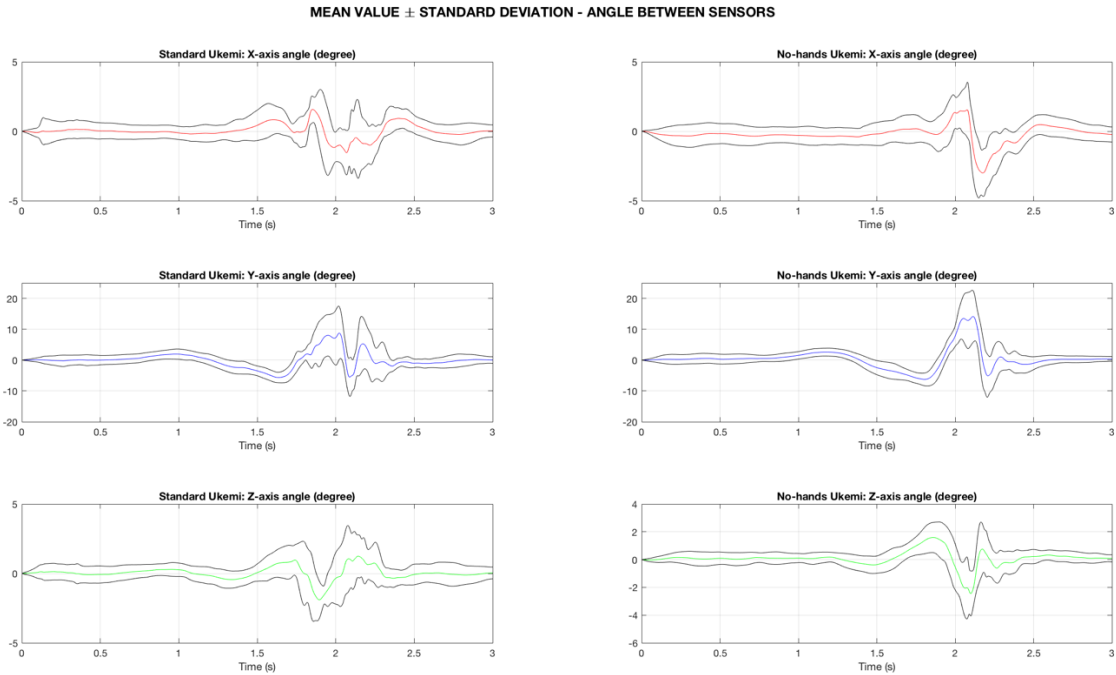


Figure 5.11: Angle between head and trunk during backward breakfalls. Neck flex-extension angle is represented by Y-angle: positive values mean neck extension, while negative denotes flexions.

As evidenced in Figure 5.11, the entity of angles variations demonstrates that the main rotation is around the medio-lateral Y-axis: in detail, the breakfalls involve a first increase of angle and then a fast decrease till negative values. It means that neck extension is followed by a rapid flexion while contacting the floor with the thoracic spine and decelerating the head to avoid striking the mat. Values here obtained lies in the error bars identified by Koshida et al. [41] for experienced judokas, even if they are relatively lower than the mean identified in the study (presented in previous Table 2.4). This fact may be caused by the assumption that sensors on the forehead and on the sternum are perfectly aligned in vertical position: it might not be so realistic because of anatomical peculiarities and bones conformation. A small offset would cause the measurement to be more aligned to the one obtained by Koshida et al.

In order to verify if a more reliable angle path could be gained from the video camera, Kinovea was used to determine neck angle while doing a standard breakfall. It was chosen the same ukemi previously analysed in detail in Figure 5.3.

Kinovea angle was obtained by calculating in MATLAB the angle between three points extracted from the video: virtual markers were placed on left ear, left shoulder and at the last fluctuant left rib (Figure 5.12).

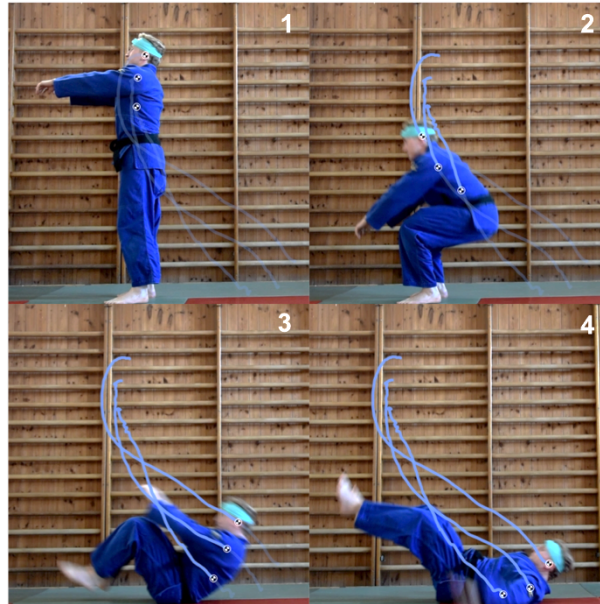


Figure 5.12: Virtual markers placement for coordinates extraction in Kinovea. Here are reported some frames used for points tracking.

Results are reported in Figure 5.13. As can be seen, values obtained in Kinovea were greater than the one gained with inertial sensors. It has to be considered that anatomical references tracking was done by hand and the point chosen are arbitrary. Moreover, points were tracked on the judogi which masks the actual position of the shoulder and of the rib: this fact led also to a difference in locating in time the neck flexion.

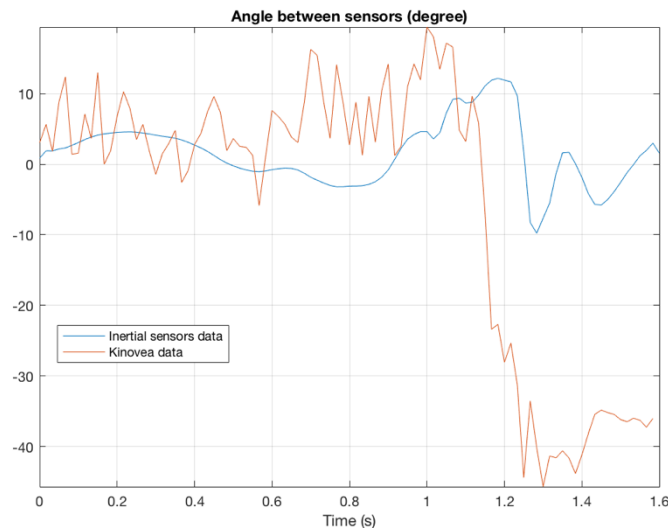


Figure 5.13: Comparison between the angle obtained by IMU and the one gained from Kinovea video analysis.

Concluding, the neck excursion angle gained by different method do not bring to potentially dangerous situations while performing a technically perfect backward breakfall, even if the ukemi is performed without the use of hands and arms.

Data gained from IMU were then analysed to find repeatability in the athlete's motion and statistical differences between the two types of ukemi.

5.3 Repeatability measures

Repeatability was quantified by calculating the Intra-class Correlation Coefficient (ICC) and the correlation. For each variable considered in the study (linear acceleration along X, Y, Z, angular velocity along X, Y, Z,

angular acceleration along X, Y, Z and flex-extension angle), values corresponding to phases C-D-E-F were extracted analysing each repetition in MATLAB: these values were isolated by manually individuating peaks zones and then through a rudimental local search algorithm the actual peaks were found. The search was done on the curves relative to the head X-acceleration in which phases are more visible and discernible. Once gained the indexes of peaks of each phase (four phases), data were extracted for each variable (ten variables), for each sensor (two sensors), for each type of breakfall (two types), for each repetition (ten repetitions), for each day (three days). A total of 4800 values were then manually exported to IBM SPSS Statistics software in order to calculate the two parameters. Values obtained are listed in Table 5.1.

ICC was calculated selecting “two-way mixed effects” model, “absolute agreement” type with a confidence interval of 95%. At the same time, inter-item correlation was selected to be estimated. They were calculated considering the ten repetitions over the three days. In this way, considering that the same athlete performed the same movement many times, the two parameters here calculated provide information only about intra-subject variability. Reflecting on ICC definition, which contemplates intra-subject and inter-subjects variability, values out of the range 0 to 1 might be due to the absence of an actual inter-subjects variability because of the presence of just one athlete. According to Koo et al. [53], ICC thresholds for discerning the level of repeatability were set as follows:

- less than 0.5, poor reliability;
- from 0.5 to 0.75, moderate reliability;
- from 0.75 to 0.9, good reliability;
- greater than 0.9, excellent reliability.

Considering correlation, thresholds were obtained from Evans [54], which defined ranges basing on correlation absolute value:

- less than 0.19, very weak correlation;
- from 0.2 to 0.39, weak correlation;
- from 0.4 to 0.59, moderate correlation;
- from 0.6 to 0.79, strong correlation;
- greater than 0.8, very strong correlation.

Once obtained and analysed all values, variables regarding the plane in which breakfalls develop were post-processed in MATLAB in order to better understand if movements could be considered repeatable. Plots hence gained are presented in Figure 5.14 and Figure 5.15.

5 Breakfall Techniques Analysis

Table 5.1: Values of ICC and correlation gained from SPSS software. Highlighted cells reflect thresholding by Koo et al. [53] for ICC and by Eoans [54] for correlation: dark green means excellent reliability or very strong correlation, light green means good reliability or strong correlation, yellow means moderate reliability or moderate correlation.

Type of ukemi	Sensor	Variable	Phase	Correlation				ICC single measures			ICC avg measures		
				mean	min	max		mean	lower	upper	mean	lower	upper
Standard	Head	linear acceleration	X	C	0,166	-0,052	0,461	0,172	-0,133	0,608	0,384	-0,545	0,823
				D	-0,23	-0,525	0,237	-0,287	-0,463	0,138	-2,018	-18,781	0,324
			E	0,395	0,242	0,57	0,382	0,01	0,758	0,65	0,03	0,904	
			F	0,407	0,042	0,658	0,383	0,005	0,759	0,65	0,014	0,904	
			C	-0,161	-0,265	-0,085	-0,166	-0,405	0,312	-0,748	-6,398	0,577	
			D	-0,028	-0,287	0,103	-0,06	-0,355	0,439	-0,206	-3,655	0,701	
		Y	E	-0,296	-0,43	-0,088	-0,192	-0,357	0,2	-0,935	-3,747	0,428	
			F	0,16	-0,11	0,433	0,14	-0,178	0,593	0,329	-0,827	0,814	
		Z	C	-0,098	-0,487	0,611	-0,096	-0,356	0,386	-0,358	-3,701	0,653	
			D	0,212	-0,089	0,505	0,193	-0,166	0,644	0,418	-0,747	0,845	
			E	0,25	0,156	0,436	0,246	-0,106	0,674	0,495	-0,402	0,861	
			F	0,376	0,171	0,731	0,293	-0,096	0,712	0,554	-0,356	0,881	
		angular velocity	X	C	-0,021	-0,122	0,072	-0,019	-0,232	0,403	-0,059	-1,297	0,67
				D	0,316	0,273	0,401	0,232	-0,056	0,637	0,475	-0,189	0,841
			E	0,076	-0,212	0,374	0,017	-0,22	0,454	0,049	-1,182	0,713	
			F	0,057	-0,127	0,22	0,048	-0,276	0,534	0,132	-1,853	0,775	
Y	C		-0,083	-0,231	0,157	-0,07	-0,301	0,379	-0,245	-2,269	0,647		
	D		-0,035	-0,475	0,568	-0,152	-0,364	0,295	-0,653	-4,01	0,557		
E	0,238		0,002	0,475	0,187	-0,124	0,62	0,409	-0,497	0,831			
F	0,504		0,382	0,599	0,427	0,057	0,781	0,691	0,154	0,914			
Z	C		0,068	-0,192	0,461	0,014	-0,291	0,499	0,04	-2,097	0,75		
	D		-0,022	-0,147	0,076	-0,057	-0,321	0,419	-0,191	-2,688	0,684		

5 Breakfall Techniques Analysis

	D	-0,122	-0,52	0,183	-0,06	-0,343	0,431	-0,206	-3,273	0,694
	E	-0,068	-0,079	-0,061	-0,06	-0,309	0,405	-0,203	-2,424	0,671
	F	0,162	-0,244	0,569	0,113	-0,234	0,588	0,276	-1,324	0,811
	C	0,133	-0,345	0,421	0,025	-0,273	0,503	0,072	-1,799	0,752
Y	D	0,043	-0,052	0,216	0,024	-0,285	0,509	0,069	-1,995	0,757
	E	-0,245	-0,618	0,215	-0,29	-0,436	0,085	-2,063	-10,147	0,218
	F	-0,312	-0,639	0,229	-0,184	-0,38	0,249	-0,875	-4,746	0,498
	C	0,174	-0,088	0,375	0,149	-0,105	0,563	0,345	-0,398	0,794
Z	D	0,196	-0,044	0,469	0,154	-0,142	0,591	0,353	-0,597	0,812
	E	0,148	-0,242	0,475	0,063	-0,238	0,531	0,168	-1,358	0,772
	F	0,387	0,243	0,521	0,364	0,006	0,744	0,632	0,018	0,897
	C	-0,058	-0,416	0,307	-0,137	-0,384	0,343	-0,564	-4,945	0,611
X	D	0,347	0,037	0,576	0,313	-0,089	0,727	0,578	-0,325	0,889
	E	-0,01	-0,183	0,276	0	-0,297	0,484	0	-2,187	0,738
	F	-0,024	-0,063	-0,002	-0,018	-0,328	0,481	-0,055	-2,869	0,735
	C	0,123	-0,23	0,519	0,131	-0,23	0,606	0,312	-1,275	0,822
angular acceleration	D	-0,07	-0,219	0,054	-0,037	-0,34	0,462	-0,12	-3,187	0,72
	E	0,122	-0,06	0,375	0,143	-0,224	0,616	0,334	-1,22	0,828
	F	-0,06	-0,335	0,24	-0,005	-0,266	0,455	-0,016	-1,708	0,715
	C	0	-0,057	0,087	-0,008	-0,29	0,469	-0,024	-2,072	0,726
Z	D	-0,306	-0,666	-0,036	-0,283	-0,447	0,12	-1,964	-12,576	0,29
	E	-0,088	-0,345	0,089	-0,04	-0,33	0,451	-0,132	-2,922	0,711
	F	-0,338	-0,534	-0,123	-0,308	-0,468	0,094	-2,406	-21,638	0,237
	C	-0,164	-0,301	0,056	-0,147	-0,352	0,291	-0,622	-3,558	0,552
Neck flex-extension angle	D	0,085	-0,354	0,729	0,06	-0,262	0,541	0,16	-1,654	0,779
	E	0,383	0,158	0,739	0,383	-0,016	0,764	0,65	-0,05	0,907
	F	0,279	0,025	0,53	0,278	-0,089	0,697	0,536	-0,324	0,874

5 Breakfall Techniques Analysis

"No-hands"	Head	linear acceleration	X	C	0,471	0,299	0,676	0,431	0,069	0,781	0,695	0,183	0,915
			D	-0,022	-0,046	0,016	-0,024	-0,305	0,456	-0,076	-2,341	0,715	
			E	0,15	0,01	0,362	0,168	-0,171	0,621	0,378	-0,781	0,831	
			F	0,035	-0,217	0,36	0,084	-0,235	0,555	0,216	-1,326	0,789	
			C	-0,081	-0,304	0,189	-0,115	-0,362	0,361	-0,447	-3,948	0,629	
			D	0,1	-0,106	0,234	0,093	-0,243	0,57	0,235	-1,423	0,799	
		angular velocity	E	0,207	-0,22	0,642	0,154	-0,166	0,603	0,354	-0,748	0,82	
			F	0,007	-0,099	0,21	-0,011	-0,318	0,483	-0,034	-2,623	0,737	
			C	-0,145	-0,495	0,218	-0,178	-0,395	0,28	-0,828	-5,658	0,539	
			D	0,374	0,029	0,872	0,318	-0,05	0,721	0,583	-0,167	0,886	
			E	0,037	-0,448	0,311	-0,081	-0,346	0,401	-0,29	-3,364	0,668	
			F	0,523	0,363	0,78	0,497	0,124	0,818	0,748	0,298	0,931	
angular acceleration	C	0,045	-0,24	0,203	0,065	-0,261	0,546	0,173	-1,632	0,783			
	D	0,179	0,086	0,326	0,192	-0,167	0,643	0,416	-0,75	0,844			
	E	0,147	-0,15	0,705	0,144	-0,203	0,608	0,336	-1,021	0,823			
	F	0,146	-0,036	0,316	0,152	-0,196	0,614	0,35	-0,969	0,827			
	C	0,58	0,424	0,83	0,437	0,056	0,789	0,7	0,151	0,918			
	D	0,093	-0,264	0,426	0,053	-0,23	0,513	0,143	-1,279	0,76			
linear acceleration	E	0,069	-0,181	0,413	0,012	-0,27	0,483	0,036	-1,761	0,737			
	F	-0,068	-0,358	0,176	0,028	-0,253	0,493	0,078	-1,536	0,745			
	C	0,278	-0,137	0,551	0,307	-0,068	0,717	0,571	-0,235	0,883			
	D	-0,278	-0,445	0,037	-0,312	-0,481	0,106	-2,485	-37,619	0,263			
	E	-0,032	-0,637	0,561	-0,092	-0,368	0,402	-0,339	-4,186	0,669			
	F	0,178	0,113	0,233	0,172	-0,177	0,626	0,383	-0,819	0,834			
angular acceleration	C	0,15	-0,328	0,82	0,064	-0,256	0,542	0,17	-1,568	0,78			
	D	0,112	-0,01	0,274	0,11	-0,247	0,591	0,271	-1,464	0,813			
	E	-0,18	-0,573	0,606	-0,311	-0,47	0,091	-2,467	-23,581	0,23			

5 Breakfall Techniques Analysis

Neck flex-extension angle	Z	E	0,616	0,484	0,833	0,624	0,253	0,877	0,833	0,504	0,955	
		F	-0,16	-0,435	0,038	-0,102	-0,346	0,367	-0,384	-3,367	0,635	
		C	0,171	-0,156	0,443	0,145	-0,194	0,605	0,337	0,337	-0,951	0,821
		D	-0,013	-0,133	0,058	-0,043	-0,329	0,446	-0,141	-0,141	-2,897	0,707
		E	-0,122	-0,582	0,37	-0,061	-0,334	0,423	-0,207	-0,207	-3,008	0,688
		F	0,162	-0,184	0,506	0,177	-0,142	0,617	0,392	0,392	-0,594	0,829
	angular acceleration	X	C	-0,178	-0,605	0,208	-0,132	-0,375	0,343	-0,537	-4,484	0,611
			D	-0,175	-0,733	0,65	-0,112	-0,359	0,363	-0,431	-3,831	0,631
			E	-0,29	-0,573	-0,12	-0,122	-0,375	0,36	-0,483	-4,492	0,628
			F	0,308	0,049	0,514	0,177	-0,202	0,641	0,392	-1,102	0,843
			C	0,141	-0,129	0,395	0,191	-0,188	0,65	0,415	-0,904	0,848
			D	0,25	-0,134	0,6	0,032	-0,211	0,469	0,09	-1,099	0,729
Z	Y	E	-0,079	-0,493	0,242	0,003	-0,24	0,447	0,008	-1,383	0,708	
		F	-0,062	-0,368	0,123	0,015	-0,31	0,511	0,042	-2,455	0,759	
		C	-0,256	-0,482	-0,061	-0,225	-0,426	0,224	-1,223	-8,663	0,464	
		D	-0,166	-0,572	0,111	-0,114	-0,347	0,348	-0,441	-3,392	0,615	
		E	-0,057	-0,377	0,146	0,014	-0,303	0,507	0,042	-2,303	0,755	
		F	0,097	-0,152	0,396	0,15	-0,212	0,618	0,346	-1,1	0,829	
Neck flex-extension angle	Z	C	0,105	-0,383	0,533	0,149	-0,209	0,616	0,344	-1,077	0,828	
		D	0,414	0,301	0,489	0,416	0,031	0,779	0,681	0,087	0,913	
		E	0,423	0,31	0,561	0,39	0,019	0,762	0,657	0,055	0,906	
		F	0,345	0,175	0,604	0,321	-0,053	0,724	0,587	-0,178	0,887	

As can be seen also from colours presented in Table 5.1, moderate correlation and reliability can be observed in some reported variables, even if the range between their maximum and minimum is very large: thus, variables reported may have an excellent reliability ($ICC > 0.9$) or a very strong correlation (> 0.8) if considering their maximum value, while reflecting about the minimum value no reliability or correlation can be identified. Given their main values, moderate repeatability can be observed while performing the standard ukemi in head X and Z-acceleration and Y-angular velocity especially in the phase F of the breakfall – i.e. head deceleration. Regarding “no-hands” ukemi, moderate repeatability can be found on the head in phase C, i.e. sacral contact, for X-acceleration and Y-angular velocity and in phase F for Z-acceleration; moreover, these variables gained moderated repeatability in trunk in phase E, i.e. thoracic contact. Results here reported demonstrate that even if the movement may appear simple and linear, its complexity makes it repeatable on a macro scale considering the entire action, but less reproducible considering the physical variables during the whole breakfall. Indeed, the moments in which the breakfall exerts its function, i.e. while contacting the floor to decrease the speed of the athlete’s body and reacting to the deceleration (phases E-F), gained the maximum values for correlation and ICC, proving that some movements always happen approximately in the same way in order to prevent injuries. Furthermore, to support this hypothesis, the information about neck flex-extension angle should be closely noted: for both types of ukemi, angle obtained relatively large values in comparison with others, especially during phases E and F, when the rapid decreasing of extension angle avoids the head to contact the mat and permits its deceleration. Even if with not excellent values of the two indicators, it proves the reliability of the technical gesture in order to preserve the human body health.

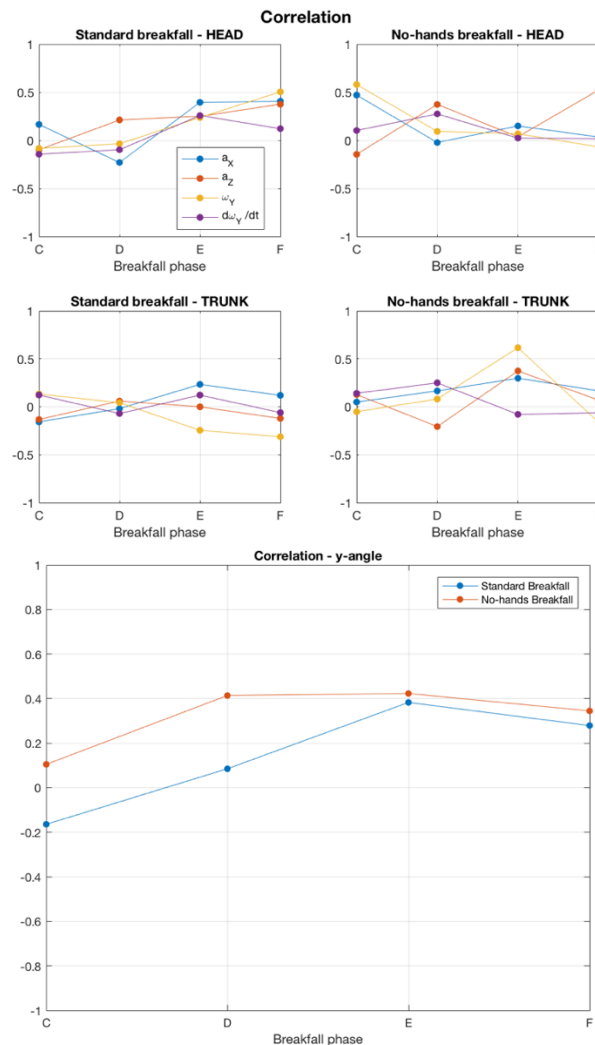


Figure 5.14: Correlation mean values of principal variables involved in breakfalls movement.

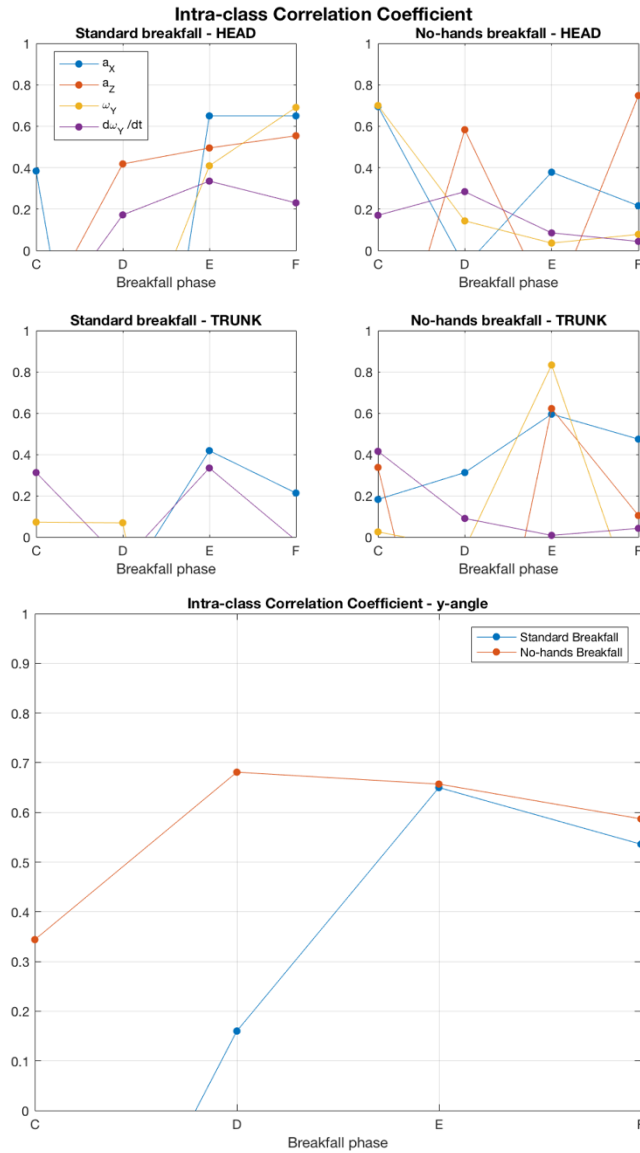


Figure 5.15: ICC values for main variables cited in the ukemi analysis. Negative values are not presented because of the lack of physical meaning.

5.4 Differences between Breakfalls Techniques

Same database was then tested for statistical differences between the two types of breakfall. Data were organized in days, and for each one the Wilcoxon signed rank test was exploited. This test was chosen because ten repetitions are not enough to define the population as normally distributed, so a non-parametric test was used to decide if there are differences between the two situations, repetition per repetition each of the three days. Moreover, a paired test was chosen because the same subjects repeated the movements and no other subjects were involved in the study. The null hypothesis was that the differences between the two samples came from a symmetric distribution centred in zero. Considering a level of significance of 5%, a p-value gained from the test lower than 0.05 means that the null hypothesis is rejected, so there is a statistical difference. Other values here considered for detecting stronger statistical significance are $p < 0.01$ and $p < 0.001$ [55].

Results obtained from MATLAB function `signrank()` are listed in Table 5.2.

Table 5.2: P-values obtained with the Wilcoxon signed rank test. Highlighted cells reflect significance level: light green means $p < 0.05$, dark green means $p < 0.01$. No values with $p < 0.001$ were found.

Day	Sensor	Phase	Variable								
			X-acceleration	Y-acceleration	Z-acceleration	X-angular velocity	Y-angular velocity	Z-angular velocity	X-angular acceleration	Y-angular acceleration	Z-angular acceleration
1	Head	C	0,0488	0,9219	0,1934	0,0371	0,1602	0,625	0,0039	0,0371	0,3223
		D	0,0137	0,1309	0,0645	0,2754	0,375	0,0645	0,084	0,4316	0,6953
		E	0,3223	0,2754	0,0039	0,2324	1	0,1309	0,2324	0,2324	0,9219
		F	0,1055	0,3223	0,7695	0,1934	0,625	0,6953	0,6953	1	0,2754
	Trunk	C	0,4316	0,3223	0,0039	0,6953	0,375	0,0039	0,625	0,1602	0,0371
		D	0,0645	0,2402	0,002	0,0371	1	0,8262	1	0,0645	0,7695
		E	0,1055	0,5566	0,0195	1	0,9219	0,375	0,8457	0,7695	0,1055
		F	0,6953	0,1602	0,625	0,084	0,0645	0,2324	0,4316	0,4316	0,1309
2	Head	C	0,002	0,4316	1	0,0371	0,0039	0,0195	0,1602	0,084	0,0039
		D	0,4922	0,3223	0,002	0,0137	0,002	0,6953	0,1602	0,8457	0,0137
		E	0,7695	0,6953	0,0273	0,002	0,1309	0,0273	0,3223	0,625	0,084
		F	0,6953	0,0195	0,8457	0,084	0,5566	0,0488	0,5566	0,1602	0,5566
	Trunk	C	0,4922	0,8457	0,1309	0,0645	0,0039	0,084	0,7695	0,3223	0,3223
		D	0,1602	1	0,0039	0,5566	0,1602	0,5566	0,9219	0,2324	0,084
		E	0,1934	0,9219	0,5566	0,4922	0,0195	0,7695	0,1602	0,2754	0,9219
		F	0,2324	0,4316	0,6953	0,084	0,2324	0,1309	0,375	0,375	0,1934
3	Head	C	0,0645	0,5566	0,4922	0,002	0,0195	0,1934	0,5566	0,002	0,0137
		D	0,0488	0,084	0,375	0,0098	0,084	0,6953	0,1055	0,6953	0,0137
		E	0,5566	0,7695	0,0645	0,002	0,8457	0,0137	0,6953	1	0,084
		F	0,4922	0,1602	0,002	1	0,9219	0,1055	0,084	0,375	0,4922
	Trunk	C	0,4316	0,1055	0,1055	0,1309	0,002	0,0645	0,3223	0,375	1
		D	0,3223	0,0039	0,002	0,1934	0,5566	0,0195	0,4316	0,5566	0,3223
		E	0,8457	0,6953	0,1055	0,7188	0,0371	0,6953	0,3223	0,625	0,1934
		F	0,0098	1	0,0645	0,1055	0,084	0,0273	0,8457	0,9219	0,7695

Neck flex-extension angle			
Phase	Day		
	1	2	3
C	0,0371	0,0273	0,0195
D	0,8457	0,0039	0,0039
E	0,0840	0,0273	0,1309
F	0,5566	0,1055	0,8457

P-values lower than 0.05 gained for principal variables are plotted in Figure 5.16. As can be seen from Table 5.2, some differences can be found on variables, such as X and Z-angular velocity, X and Z-angular acceleration or Y-linear acceleration: considering that these variables are out of the plane on which the movement develops, their impact on the whole movement can be neglected. Moreover, the differences here found may be due to minimal alterations in athlete's body position while contacting the floor, which bring variations on rotational variables out of the XZ-plane.

Differences in Z-acceleration (antero-posterior direction) were found on head and trunk, in particular in phases D-E, demonstrating that the use of hands implies a different force on the body. As told before, in this case, the acceleration absolute value was greater while performing the standard breakfall, so the great

experience of the athlete in performing just one type of the breakfalls analysed might play an essential role. This fact can be seen also evaluating the information obtained with angle data. A statistical difference with $p < 0.05$, and in some cases $p < 0.01$, was found in phases C-D for the angle curves: C and D are the preliminary contact phases in which the body initially touches the floor. Moreover, considering curves reported in Figure 5.11, in which mean values and standard deviations of the angles are plotted, the entity of the differences here discovered can be evaluated. Figure 5.17 clarify these words: as can be seen, peak values identified in the angle curves demonstrate that, in the phases where significance between the two breakfalls was discovered, i.e. C and D, the angle for “no-hands” ukemi is more positive (it reaches 5 to 10 degrees) than what happens in standard breakfall (values are near to zero). It means that during the falling phase, neck is more extended proving the inability to control head movements in a perfect way. Instead, values obtained while performing standard breakfall demonstrates a higher control of head position allowing it to move slightly. It might confirm the hypothesis of significant differences in the two breakfalls due to the lack of experience in performing the “no-hands” breakfall.

Another hypothesis should be addressed to the role of arms and shoulders muscles whose contraction for striking hands to the floor in the standard breakfall may help the stabilization of the neck due to contraction and contributed to body stiffening during the fall.

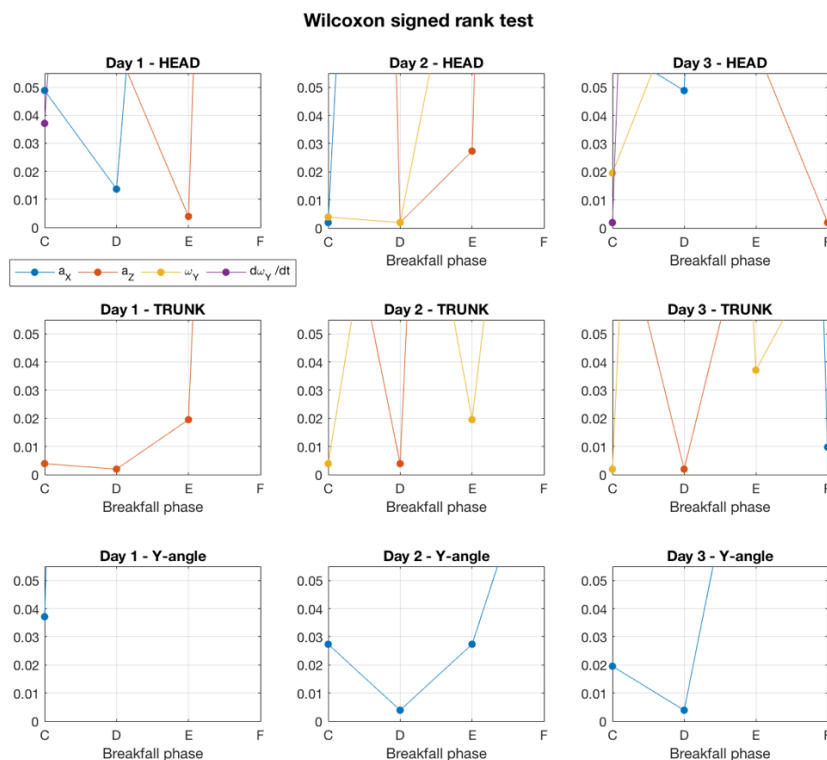


Figure 5.16: Wilcoxon signed rank test results. P -values < 0.05 are presented for main variables used in the comparison between standard and “no-hands” backward breakfall.

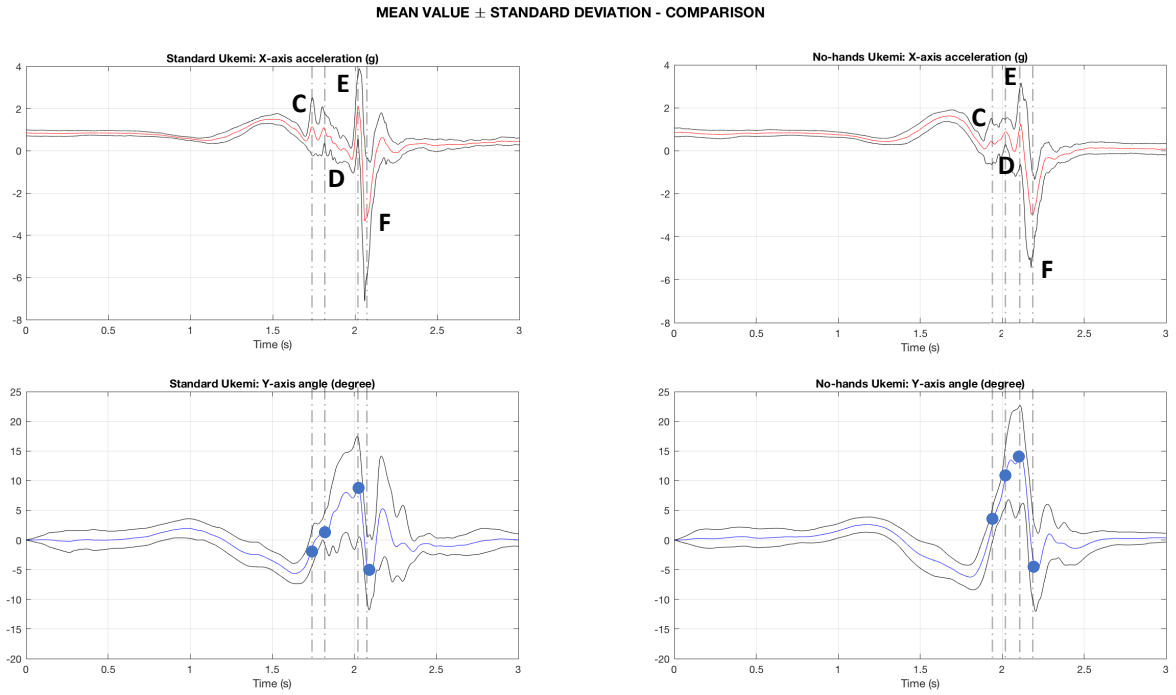


Figure 5.17: Comparison of neck angle gained by IMU. Values of the four phases statistically analysed are here evidenced. The time instant for each phase is respectively selected from the X-acceleration curve of the head for each type of breakfall. As previous figures, means and standard deviations were computed from all 30 breakfalls for the two breakfalls types. Values obtained in phases C and D demonstrate statistical differences with $p < 0.05$ and $p < 0.01$ respectively.

6 Head Injury Risk Assessment

Considering studies proposed in Section 2.2.2 where articles on injuries related to Judo were analysed, a deeper comprehension of the strategies adopted by judokas for avoiding any kind of head and neck traumas emerged. For this purpose, after having examined in detail the most common falling technique which athletes have to master to not strike their head to the floor while being thrown (Section 5 of the current study), an analysis on linear and angular acceleration levels which judokas' body has to bear during throws was carried out. In particular, the main topics of interest were differences in values obtained on subjects of different ages and levels of experience and with different techniques, so in determining which technique brings higher values near to the concussion threshold. These aspects were studied for the first time also in children, to analyse levels of acceleration on their body which have to tolerate in trainings and competitions. Axes configuration exploited in this Section is the one previously used in Chapter 4 Preliminary Tests and Chapter 5 Breakfall Analysis, reported in Figure 4.8.

6.1 Preliminary Analysis

In order to better define the protocol to be followed, a preliminary test, aimed to detect if faller may adapt his body position to being repetitively thrown with the same technique, was held.

In this phase of the study, one technique (o-soto-gari) was tested: two black belts (one I dan and one II dan) were selected to perform the investigation, with attention to not saturate sensors: thus, a woman of 57 kg was selected to throw a man weighing 73 kg. The number of consecutive projections was chosen in order to not exert the thrower: eight throws were selected to be the best trade-off between fatigue and repetition of the same movement. The test was repeated on three different days.

Test results are reported in Figure 6.1, Figure 6.2 and Figure 6.3.

Considering the mean of the peak values calculated for each repetition among the three days (Figure 6.1), no accommodation took place: indeed, the trend demonstrates that, in last falls, head and trunk of faller underwent to greater accelerations than the previous throws.

This fact is also supported by Figure 6.2, in which almost all best fit lines tend to grow, on the contrary of what might happen if faller had adapted his body to the specific technique. On the first day, trunk acceleration seems to decrease basing on the trend line: it has to be said that best fit lines have a very poor r-squared coefficient, so in general data do not behave as a straight line. Moreover, the module of the angular coefficient of the line is very low, so the tendency is near to be constant.

Reflecting on Figure 6.3, no specific trends can be observed in the three days of test, even if standard deviations are relatively large in comparison with the relative mean values. This fact could be attributed to the difficulty on performing exactly the same gesture every time, but also to the specific reactions of the faller in that specific situation. The two causes here identified can be minimized, but not completely excluded in a complex and open-skills sport such as Judo.

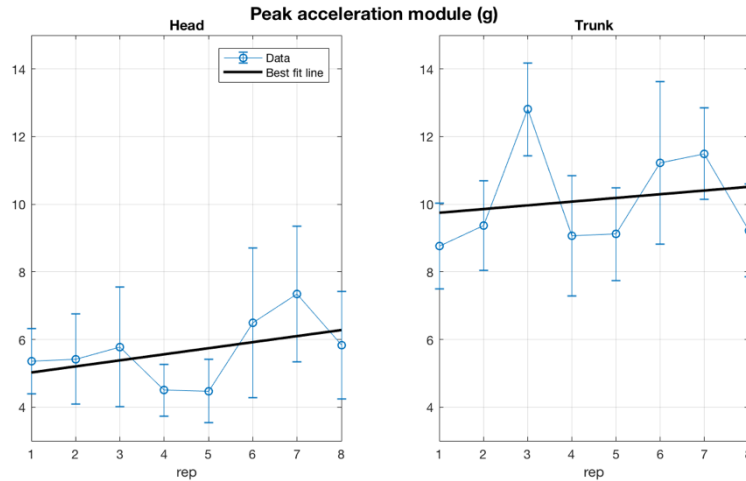


Figure 6.1: Mean values and standard deviations for each repetition among the three days of test. Means are interpolated with a linear regression.

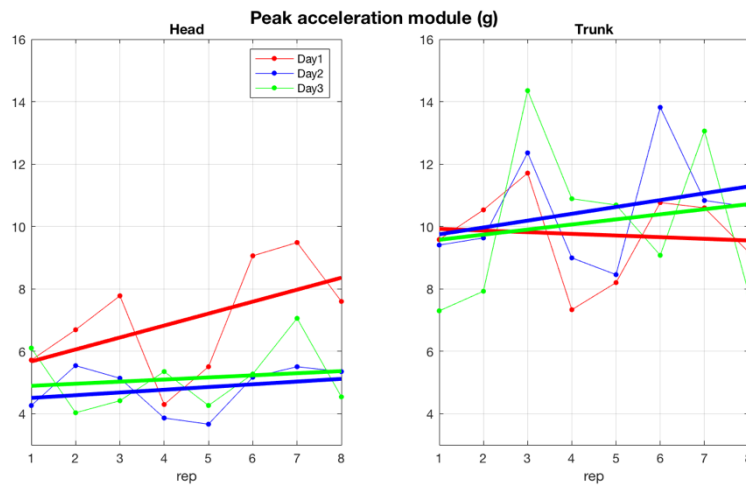


Figure 6.2: Peak values for every repetition. Best fit lines for each day are calculated on peak values gained in each daily repetition.

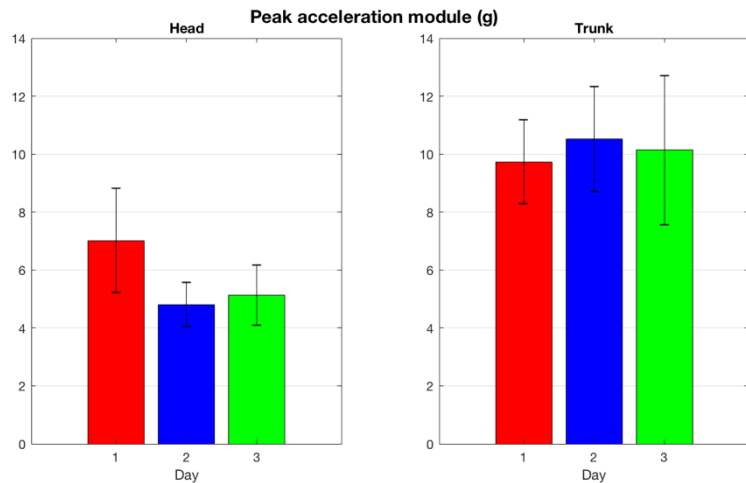


Figure 6.3: Mean values and standard deviations calculated among all eight repetitions for each day.

Considering results achieved in this preliminary test, a completely random order of techniques repetitions might not be needed. Thus, the protocol will be constituted of many different techniques repeated each three times, to not exert the thrower and also the faller, but to have a statistical relevance. A random order of the type of techniques was selected to not let the faller to get prepared by seeing previous tests.

6.1.1 Sensors Calibration and Comparison

In this Section, preliminary tests conducted with the new sensors of Yost Labs, purchased in order to adequately perform the protocol, are presented. A wide list of all efforts and attempts that have been made to better exploit the new devices is reported in Appendix B.

Because the 3-Space™ Sensors did not meet the specifications they were selected for, many changes had to be done in order to fix the problems. Firstly, Bluetooth connection could not be considered anymore due to the meagre sample rate of about 50 Hz and to the random working time. Secondly, the acquisition program provided by Yost Labs could not be used because of its tendency to change sensors settings.

Thus, wired connection had to be used in the protocol, with all related problems. Moreover, a general serial port terminal application was chosen to meet a larger sample rate: CoolTerm 1.5 for Mac was selected from web.

Sensors were firstly tested as done in Section 4.1: accelerations in the three directions were proved leaving fastened sensors on a stable surface to measure the value of gravitational acceleration on their three axes.

The sequence of axes sense followed in the test was, as previously:

- X-axis upward;
- Z-axis upward;
- X-axis downward;
- Z-axis downward;
- Y-axis upward;
- Y-axis downward.

Each position was maintained for about 5 seconds. A jump with both sensors was used to synchronize the two acquisition: as for breakfall analysis of Section 5, the first point near to zero acceleration was chosen to synchronize sensors.

First acquisition is presented in Figure 6.4. As can be observed, axes order is respected in sensors, even if values different from 1 g, -1 g or zero are gained in stationary conditions. To overcome this issue, the “Gradient Descent Wizard” of the 3-Space Sensor Suite was used, by which all orientations around three axes were tested and used for the calibration process.

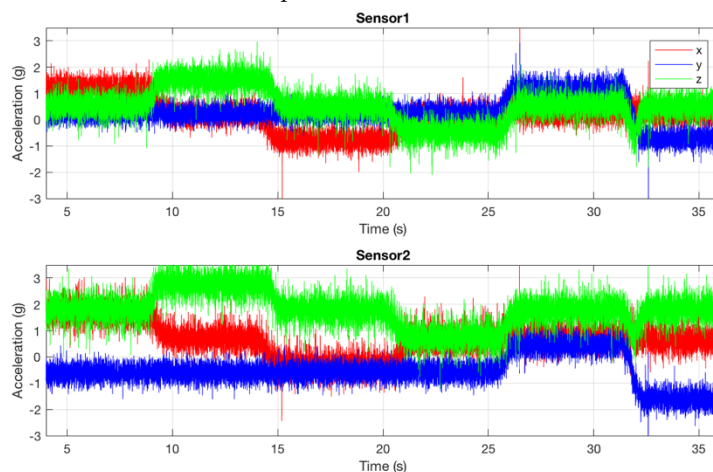


Figure 6.4: Acquisitions while performing the static test before calibration.

Once the calibration process was completed, the previous test was repeated in order to demonstrate if the problem was fixed. Results are presented in Figure 6.5. As can be seen, the axes order was respected, and also actual values of acceleration were acquired in the three directions. This fact can be observed in Figure 6.6, in which data acquired from the test were low-pass filtered at 5 Hz to remove the high variability and the presence of noise.

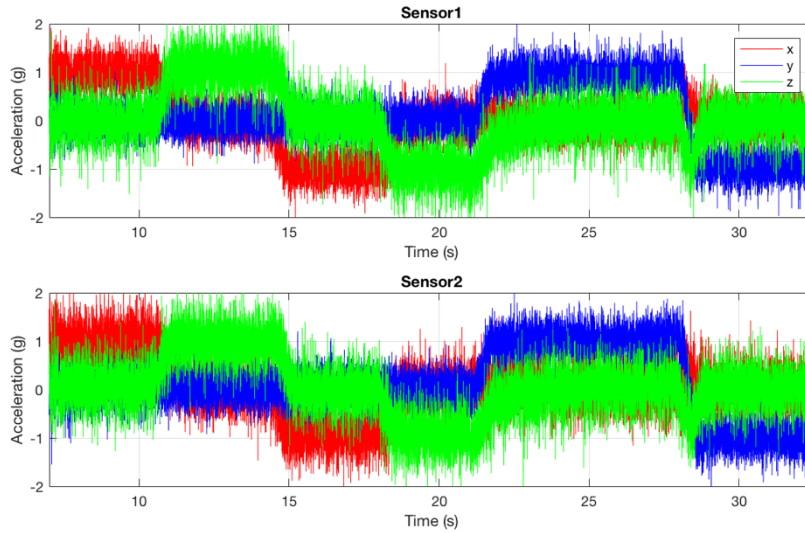


Figure 6.5: Linear acceleration gained in the static test after sensors calibration.

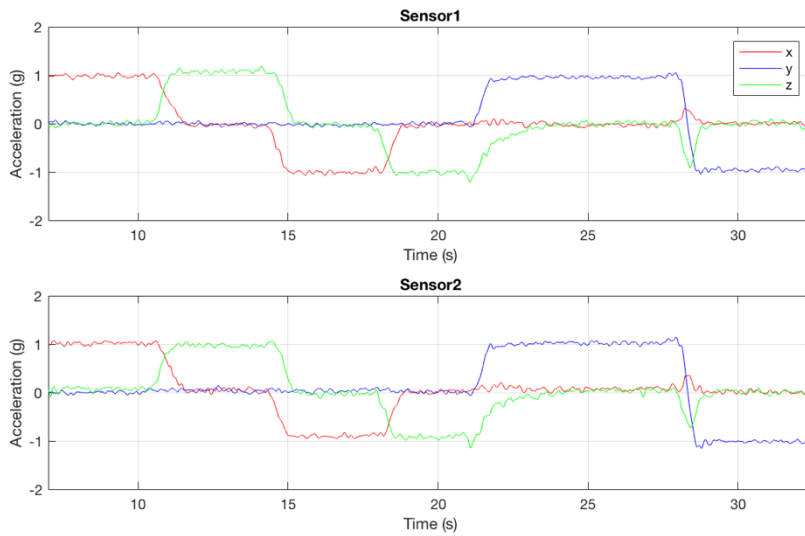


Figure 6.6: Filtered acceleration values obtained after calibration.

Moreover, angular rate was monitored in order to discover the presence of any bias: on the contrary of what happened for linear acceleration, values of angular velocity could be considered reliable. Indeed, each rotation was around one axis, as can be seen from Figure 6.7, and while sensors were in rest condition the value of angular rate in the three directions was zero.

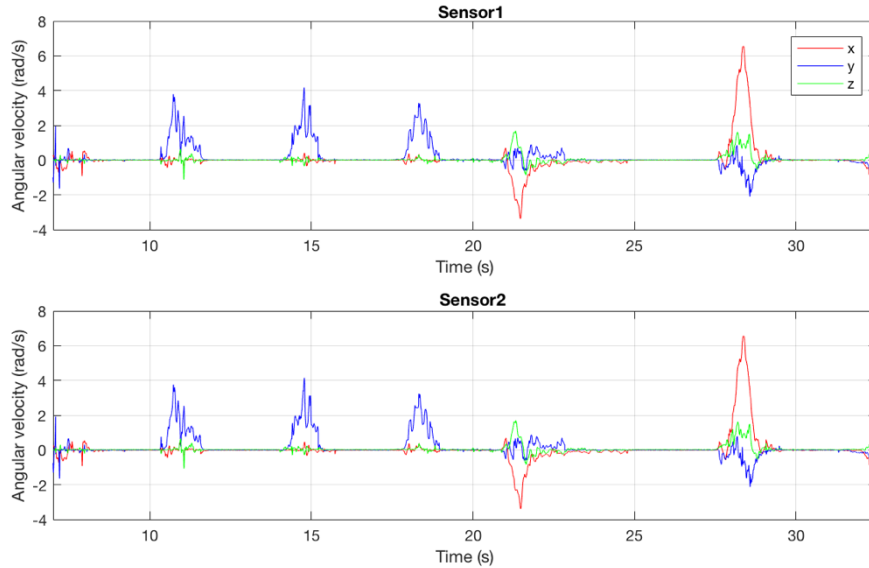


Figure 6.7: Angular velocity gained in the static test before calibration.

3-Space™ sensors were then tested to verify the differences with sensors used previously in the current study. Moreover, the aim of the test was to identify if the lower sample rate might bring wrong valuations about accelerations and variables gained by integration and differentiation of the angular rate.

The test was planned as follows: the subject wore at the same time one sensor on the forehead and one on the sternum for each brand. In this way, data gained by the two types of devices could be compared in time. ATR-Promotions sensors were connected via Bluetooth to the pc, while 3-Space™ sensors were linked through USB cable. The subject performed one jump, to synchronize the sensors as in the other tests, then three backward breakfalls followed by a final jump to verify the time synchronization.

A particular of the third ukemi is reported in Figure 6.8, Figure 6.9 and Figure 6.10.

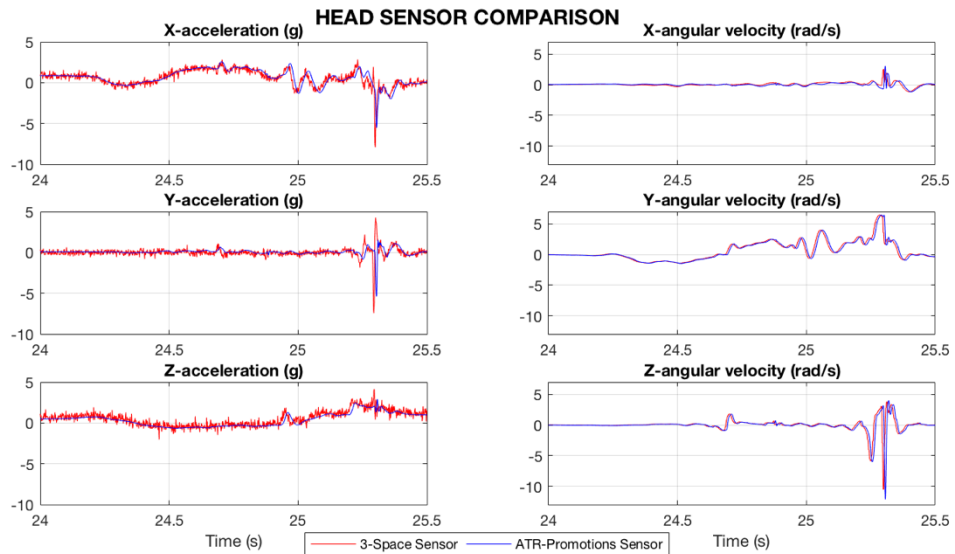


Figure 6.8: Comparison of data gained simultaneously by the two sensors placed on subject's head.

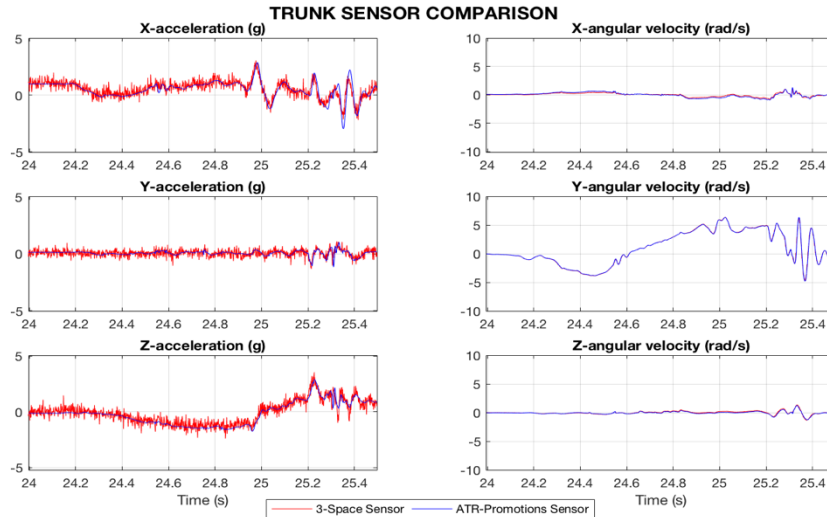


Figure 6.9: Comparison of data gained by the two sensors placed on subject's trunk.

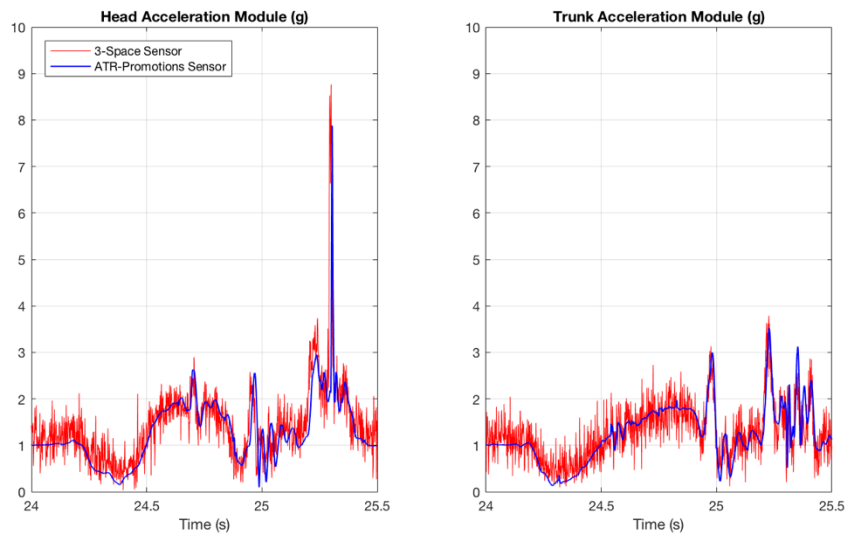


Figure 6.10: Comparison of the acceleration module calculated from data acquired by the sensors placed on subject's head and trunk.

As can be seen, the pattern of the curve is maintained even if a greater variability involves new sensors in comparison to ATR-Promotions ones. The variability involves accelerations data and not the angular velocity: this might be due to the greater full scale of the sensors, 100 g in contrast to 16 g, and to the lower features of the Yost Labs sensors in comparison to the others (as seen in Table 4.2). Another aspect that can be evidenced, in particular considering the angular velocity which lacks in variability between the two types of sensors, is the delay in time. The fact is due to the difficulty in synchronizing the initial jump for 3-Space sensors: indeed, even if the thresholding for finding the flight phase is done considering a 5 Hz low-pass filtered version of the acquired signal, which brings more reliable results for the 3-Space sensor, a more accurate identification is done with the ATR-Promotions sensors thanks to the greater sample rate. It will not bring any problem in the following analysis because even if the two types of devices are not synchronized, the same sensors of each brand are synchronized.

6.2 Methods

Concluded preliminary tests, the protocol was designed in order to study the most common techniques in Judo competitions, to get results to be compared with scientific literature on head injuries, to get statistically reliable results and to avoid wrong conclusions due to thrower's fatigue or faller's accommodation.

6.2.1 Subjects

Considering that scientific articles do not deal with acceleration measures on younger people, the study was thought to analyse both children and adults, contemplating different years of experience in practicing Judo. Thus, groups were created with the support of the entire team of DLF Judo Alessandria: subjects, who accepted to enrol the tests with their written consent, were listed and the groups generated. Athletes were divided into Agonists and Not-Agonists with the age threshold imposed by the Italian Judo federation (Federazione Italiana Judo Lotta Karate Arti Marziali, FIJLKAM): 12 years is the discriminant between these two categories, so people under 12 were labelled as Not-Agonists while subjects 12 years old or older were put into the Agonists group.

Moreover, two sub-groups were made for each division by means of experience: for the Not-Agonists group, 3 years of Judo practice was chosen as the limit to define a child as "Expert", while 10 years were hypothesized as the threshold for "Expert" Agonists. Experience was chosen as the main factor discriminating performances and capabilities level, because most articles found in literature used this criterion, and others such as belt are highly related to experience as for example its transition occurs every one to three years (excepted for the black belt). No distinctions were made on sex, weight and height, because in the training phase two athletes of different sex, weight and height may fight each other, so a plausible situation which happens in everyday training would be simulated. A total of 40 athletes were examined, ten for each of the four created groups. Features of the subjects involved in the study are reported in Table 6.1, while mean physical characteristics are presented in Table 6.2.

Table 6.1: Age and experience years of the subjects involved in the study. Groups: Aex = Expert Agonists, An = Not-expert Agonists, NAex = Expert Not-agonists, NAn = Not-expert Not-Agonists. Belts order is the following: white, yellow, orange, green, blue, brown and black (I dan, II dan, III dan and so on).

Subject Number	Sex (M/F)	Age (years)	Experience (years)	Belt	Group
1	F	34	28	Black (III dan)	Aex
2	M	24	17	Black (I dan)	
3	F	22	15	Black (II dan)	
4	F	22	15	Black (I dan)	
5	M	18	12	Brown	
6	M	18	11	Brown	
7	M	15	11	Brown	
8	M	19	11	Black (I dan)	
9	F	16	11	Brown	
10	M	22	10	Black (I dan)	
1	M	13	9	Blue	An
2	F	13	9	Blue	
3	M	14	9	Brown	
4	M	35	8	Brown	
5	F	15	8	Brown	
6	M	16	7	Brown	
7	M	12	5	Blue	
8	M	12	5	Blue	
9	F	14	5	Brown	
10	M	16	2	Orange	

1	F	11	5	Blue	NAex
2	M	9	4	Green	
3	M	8	4	Green	
4	M	8	3	Orange	
5	M	8	3	Orange	
6	M	8	3	Orange	
7	M	9	3	Orange	
8	M	9	3	Orange	
9	M	7	3	Orange	
10	M	7	3	Orange	
1	M	6	2	Yellow	NAn
2	F	7	2	Yellow	
3	M	7	2	Orange	
4	M	10	2	Orange	
5	F	8	2	Orange	
6	M	8	1	Yellow	
7	F	6	1	Yellow	
8	M	9	1	Yellow	
9	M	5	1	White	
10	M	5	1	White	

Table 6.2: Mean values and standard deviations (std) of height and weight of the different groups involved in the study. Groups: Aex = Expert Agonists, An = Not-expert Agonists, NAex = Expert Not-agonists, NAn = Not-expert Not-Agonists.

Group	Height (m)		Weight (kg)	
	mean	std	mean	std
Aex	1.73	0.05	66.10	5.97
An	1.63	0.11	56.40	13.11
NAex	1.37	0.08	32.10	9.62
NAn	1.26	0.14	25.90	8.39

Two throwers were chosen to perform the test, one for each age category: people were selected among subjects in their group basing on technical skills and competitions outcomes. Furthermore, they were chosen as the best individuals in performing always the same technical gesture in the most reliable fashion, for having reproducibility of the movements exerted by the thrower. In this way, fallers of the same age category should have been subjected to the same circumstances. Main characteristics of throwers are summarized in Table 6.3.

Table 6.3: Physical and Judo-related characteristics of selected throwers.

	Thrower Not-Agonists	Thrower Agonists
Age (years)	9	30
Sex	M	M
Height (m)	1.36	1.77
Weight (kg)	31	80
Experience (years)	4	24
Belt	Green	Black (II dan)

6.2.2 Protocol

Techniques to be tested were selected among the large number of movements comprised in competitive Judo for different reasons:

- T1)** o-soto-gari, the most cited technique for provoking traumas on faller's head due to the backward breakfall, but additionally one of the most common and instinctive techniques that also children use in competitions;
- T2)** o-uchi-gari, the second most studied judo technique in which a whiplash-like movement involves faller's head;
- T3)** ippon-seoi-nage, one of the most common technique in Judo competitions and one of the firsts taught to children;
- T4)** tai-otoshi, one of the quickest and powerful technique used by athletes of all ages, similar versions of this technique are unconsciously used by children in many competitions.

They have been selected as a trade-off among velocity, power, knowledge of the technique by all people involved in the study, frequency of use and possibility of applying the technique in competition for both categories. Furthermore, the first two are techniques in which the faller falls backward, while in the third and in the fourth the breakfall is forward. Details and explanations about the selected techniques are reported in Appendix A.

Due to the presence of cables (6 meters of wires were employed), two assistants were used to follow faller's path in order to not interrupt the connection because of wire damages: one followed head trajectory while the second moved the wire connected to the trunk sensor in order to not twist on subjects' legs and arms (Figure 6.11).



Figure 6.11: Experiment setup used in the protocol. Two collaborators were exploited to avoid stresses on the cables.

The protocol was restricted to the cited four techniques to not exert the thrower and to not make the test last more than 5 minutes, especially since children were involved in the study and their attention span is limited to few minutes in doing the same movement. In this way, last throws would not have greater acceleration values due to faller's fatigue in contracting always the same muscular groups.

Each technique was repeated three times, but the order of execution of the four techniques was randomly generated by the MATLAB function `randperm(4)` (Table 6.4). The same order was used for both categories.

A complete rest was used to avoid fatigue episodes in throwers, so they rested 5 minutes before testing another subject. Moreover, a maximum number of four people was tested for each session. Tests lasted five days for both Agonists and Not-Agonists and each day random people from the two respective categories were examined.

Table 6.4: Techniques order used in the tests. for both categories. 1 = T1 (o-soto-gari), 2 = T2 (o-uchi-gari), 3 = T3 (ippon-seoi-nage), 4 = T4 (tai-otoshi).

Subject number	Technique #1	Technique #2	Technique #3	Technique #4
1	1	3	2	4
2	3	4	1	2
3	3	2	4	1
4	4	2	3	1
5	2	3	4	1
6	4	3	1	2
7	1	4	2	3
8	2	4	1	3
9	1	2	3	4
10	1	4	3	2
11	2	4	3	1
12	4	3	1	2
13	4	1	2	3
14	3	4	2	1
15	1	3	4	2
16	1	3	2	4
17	4	3	1	2
18	3	1	4	2
19	3	4	1	2
20	3	1	4	2

Data gained for each subject were pre-processed in order to cancel out spurious peaks not aligned with the maximum of linear and angular acceleration. Groups of three peaks were selected on MATLAB and, after a visual inspection to verify the correct selection of the values, each block was mapped with the proposed Table 6.4 to a matrix containing each data ordered for the four techniques here studied. Signals from both sensors were then divided into epochs lasting 1 second centred on the index of the peak of linear acceleration module of the respective sensor: for each throw thus two indexes were computed, due to the different sample rates of the two sensors which shift signals in time, to be sure that a correct peaks analysis would take place.

Data were then post-processed in order to compare and contrast results obtained by the four groups. Variables considered for the analysis were mean of peak values among the three repetition for each technique for head and trunk linear and angular acceleration, for neck angle, and for impact duration. Scripts here used are reported in Appendix C.

6.3 Results and Discussion

At first, data acquired were generally analysed to detect which levels of accelerations Agonists' and Not-Agonists' heads had to bear. Results are presented in Figure 6.12. Even if most values were above 60 g and 2500 rad/s², in some cases Agonists acquisitions reached dangerous levels near to and above the limits evidenced in curves presented in Chapter 2.1.1. Data were gained by the two sensors at sample rates of 836 ± 235 Hz and 883 ± 212 Hz, respectively for head sensor and trunk sensor.

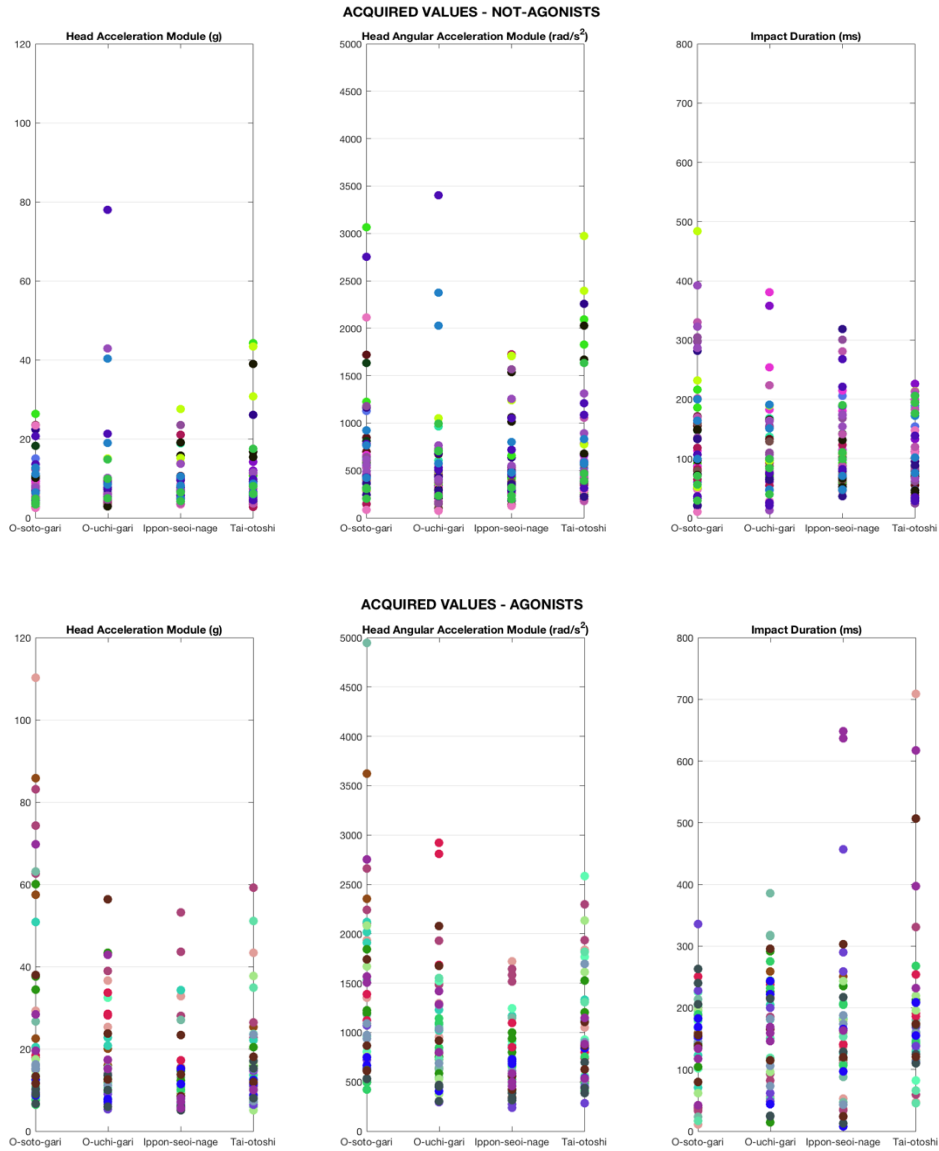


Figure 6.12: Values experimentally gained through the tested protocol. Values on the head are here displayed for the two groups analysed.

Linear and angular acceleration were analysed considering just their module, instead of the three components, because of the high three-dimensionality of the tested techniques.

Impact duration was obtained by thresholding the acceleration module of each repetition to the 10% of its maximum value and then measuring the time interval between the first and the last samples above the threshold. Considering that obtained peak values were also inferior to 10 g (value for which the threshold on the acceleration module becomes 1 g), it was thought to set the threshold to 1 g if the peak value was below 10 g to not count for the entire portion of signal which would bring to an impact duration of 1 second. It is interesting to note that values obtained are much greater than the 20 ms reported in literature and also that range is very similar for Agonists and Not-Agonists.

In the further analyses, neck angle was calculated in two ways: while studying differences among techniques, extension and flexion angle were calculated respectively as the maximum and the minimum values in the angle path during the fall, while looking for differences due to experience also the corresponding value gained at the time in which the peak value of head acceleration module occurred was analysed. This distinction was made in order to study in the first case the excursion of the neck during the

entire technique and to verify if dangerous values were reached, in the second case for searching differences at the impact time among subjects with different level of experience.

As told before, differences were searched among subjects belonging to the Agonists groups or to the Not-Agonists groups because no comparison can be achieved in matching novices Agonists to novices Not-Agonists or any other combination involving the two main categories. Thus, differences for age related and experience factors were searched between Expert and Not-expert groups for each category.

At first, data were verified for being normally distributed with the one-sample Kolmogorov-Smirnov test (MATLAB function `kstest()`): p-values far below 0.001 (near to 10^{-15}) were obtained so the null hypothesis of data normally distributed was rejected, due to the low number of subjects for each category. Mann-Whitney test (executed through the MATLAB function `ranksum()`) was employed in this case for studying differences among individuals because of different athletes employed in the measures, meaning that an unpaired test was required.

6.3.1 Techniques Analysis

Acquired data were proved for verifying the presence of any differences in head impact features when being thrown with different techniques. Significant differences were searched with the aid of the Friedman's test, chosen for comparing variables from the four movements in a paired way because the same subject was thrown with the four techniques. When statistical differences were found, a post hoc test was employed to verify which techniques differed. MATLAB functions hence used were `friedman()` and `multcompare()`.

Differences were looked for in the all Agonists and Not-Agonists categories, neglecting the distinction between Experts and Not-experts. This choice was done for evaluating the differences in the average execution of the specific technique, so considering when any subject is thrown with that technique: in this way the overall technique is evaluated, not the particular behaviour of the faller.

Each of the four techniques was compared with others considering the main variables of the analysis involving the head and the neck: linear and angular acceleration module, neck flexion and extension angles and impact duration. Data tested are presented in Figure 6.13, while results of the test in form of matrices for each variable are proposed in Table 6.5

As can be seen from matrices, two observations are remarkable: firstly, no differences in duration of the impact on the head were found meaning that for each technique the time spent for decelerating the head is almost the same, but secondly, and it is the most interesting, no significant differences were found on the falls subsequent any techniques in the Not-Agonist group. This means that main parameters here considered for studying the throws do not change even if the technique is different, thus the faller moves his head almost in the same way every time: it can be due to a particular ability in doing breakfalls or to a sub-maximal execution of the technique by the thrower bringing no alterations on movements of the faller's head.

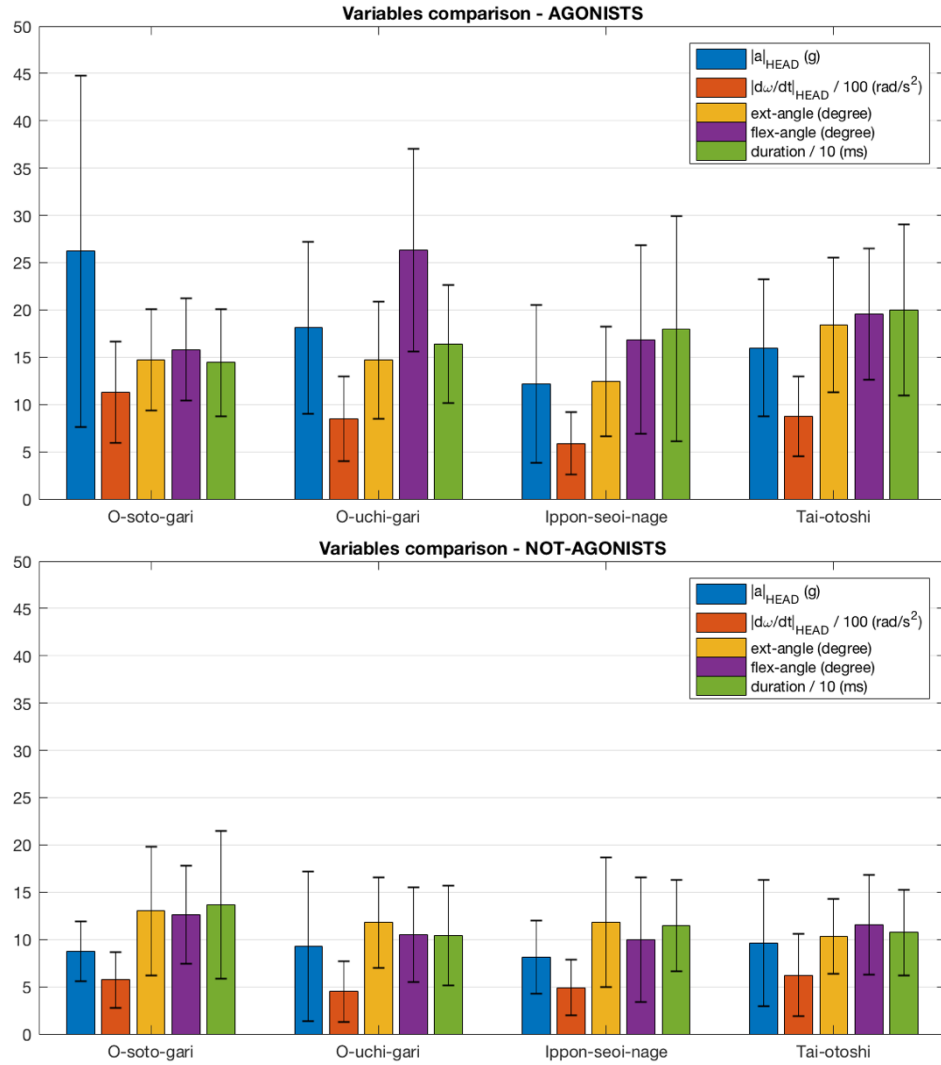


Figure 6.13: Mean values and standard deviation of variables considered for finding significant differences among the four tested techniques. Values divided for the two group are here presented. Head angular acceleration is represented divided per 100 and duration divided per 10 to increase images readability.

Table 6.5: Results of the post hoc test. All values are reported even if Friedman's test found differences just in accelerations and angles for the Agonist category. Cells are evidenced in colours corresponding to the p-value found: very light green means $p < 0.05$, light green $p < 0.01$ and dark green $p < 0.001$.

AGONISTS					NOT-AGONISTS				
HEAD ACCELERATION MODULE									
	T1	T2	T3	T4		T1	T2	T3	T4
T1	1	0,6111	0,0005	0,1219	T1	1	0,8831	0,8831	0,9614
T2	0,6111	1	0,0355	0,7160	T2	0,8831	1	1,0000	0,9948
T3	0,0005	0,0355	1	0,3159	T3	0,8831	1,0000	1	0,9948
T4	0,1219	0,7160	0,3159	1	T4	0,9614	0,9948	0,9948	1
HEAD ANGULAR ACCELERATION MODULE									
	T1	T2	T3	T4		T1	T2	T3	T4
T1	1	0,5327	0,0003	0,7610	T1	1	0,4559	0,2035	1,0000
T2	0,5327	1	0,0355	0,9831	T2	0,4559	1	0,9614	0,4559
T3	0,0003	0,0355	1	0,0118	T3	0,2035	0,9614	1	0,2035
T4	0,7610	0,9831	0,0118	1	T4	1,0000	0,4559	0,2035	1

EXTENSION ANGLE									
	T1	T2	T3	T4		T1	T2	T3	T4
T1	1	1,0000	0,3159	0,1219	T1	1	0,9614	0,9282	0,9831
T2	1,0000	1	0,3159	0,1219	T2	0,9614	1	0,6881	0,8268
T3	0,3159	0,3159	1	0,0005	T3	0,9282	0,6881	1	0,9948
T4	0,1219	0,1219	0,0005	1	T4	0,9831	0,8268	0,9948	1
FLEXION ANGLE									
	T1	T2	T3	T4		T1	T2	T3	T4
T1	1	0,0079	0,9993	0,5327	T1	1	0,9614	0,3159	0,9948
T2	0,0079	1	0,0052	0,2559	T2	0,9614	1	0,6111	0,9948
T3	0,9993	0,0052	1	0,4559	T3	0,3159	0,6111	1	0,4559
T4	0,5327	0,2559	0,4559	1	T4	0,9948	0,9948	0,4559	1
DURATION									
	T1	T2	T3	T4		T1	T2	T3	T4
T1	1	0,8831	0,9282	0,1589	T1	1	0,6881	0,6111	0,6881
T2	0,8831	1	0,9993	0,5327	T2	0,6881	1	0,9993	1,0000
T3	0,9282	0,9993	1	0,4559	T3	0,6111	0,9993	1	0,9993
T4	0,1589	0,5327	0,4559	1	T4	0,6881	1,0000	0,9993	1

Considering Agonists, on the contrary, many significant differences were found among techniques, some with a p-value < 0.001 meaning strong differences between samples: a graphic representation of significant differences is given in Figure 6.14. This dissimilarity is due to the higher expression of force in adults than in children which brings the human body to react in a defensive manner: it does not happen while being gently thrown as occurred for Not-Agonists category.

Differences were found among almost all techniques for Agonists: these are due to the specific features of each technique, which bring the head to move in a particular way. For example, neck extension angle gained low p-values ($p < 0.001$) between the third and the fourth technique due to the greater stress produced by the throw velocity. However, this angle did not reach insidious levels which could produce neck injuries because of the presence of the mat which avoids extending maximally the neck, limiting the values that can be obtained (mean values about 10 to 15 degree for the two groups). Instead, flexion angle which is not limited by obstacles could reach higher values and it is guided by subject experience: in particular, in the second technique, o-uchi-gari, the flexion angle reached values higher than others ($p < 0.01$), due to the whiplash-like movement involved in the technique and determined by the muscular reaction to the head acceleration directed to the floor.

Head linear acceleration differed among almost all techniques but, in particular, greater values were obtained while being thrown with o-soto-gari demonstrating its superior possibility of reaching dangerous levels and the motivation for which it was studied the most among all articles reviewed in Section 2.2.

Head rotational acceleration, instead, gained the lowest values for the third technique, ippon-seoi-nage: indeed, as can be seen from Figure A.6 of Appendix A in which this technique is presented, it is a technique in which the faller is thrown forward, so the head has to bear lower values of linear and angular acceleration due to the particular impact. The latter techniques, even if the throw is forward, gained higher values than ippon-seoi-nage due to the faster movement involved.

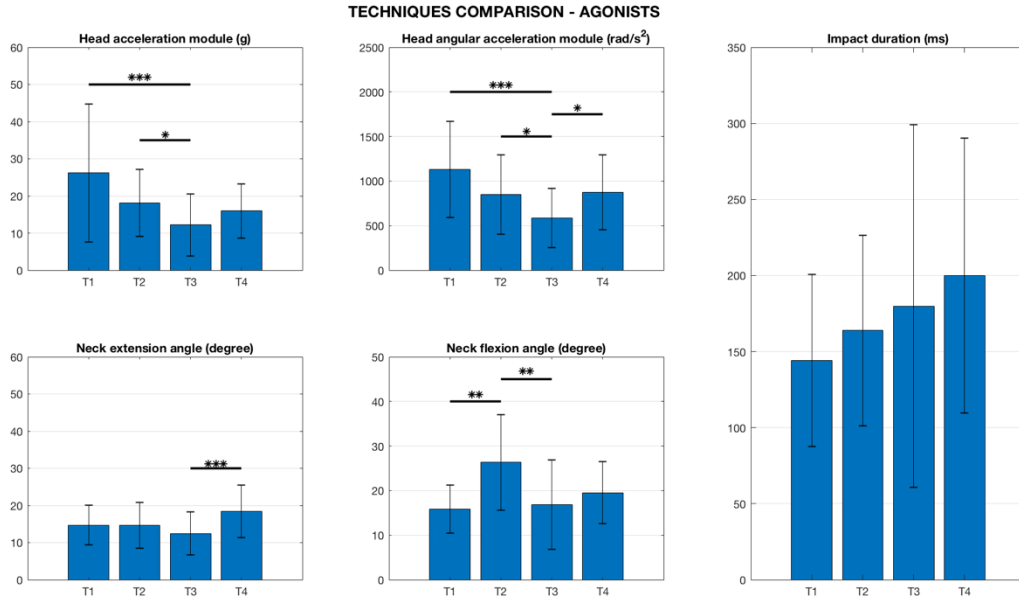


Figure 6.14: Comparison of variables among the four techniques for the Agonists group: T1 = o-soto-gari, T2 = o-uchi-gari, T3 = ippon-seoi-nage, T4 = tai-otoshi. All significant p-values obtained with the Friedman and post hoc tests are highlighted, one star means $p < 0.05$, two stars $p < 0.01$ and three stars $p < 0.001$.

6.3.2 Not-Agonists

After having verified differences among the techniques chosen for the protocol, an analysis was carried out looking for differences among the groups previously identified.

After having verified that no particular trends due to fatigue or adaption were present in the linear and rotational accelerations values across repetitions (Figure 6.15), differences were looked for. Results of the Mann-Whitney test are reported in Figure 6.16. As can be observed, no values below the 0.05 threshold were found meaning that no significant difference were present in the variables experimentally acquired in the protocol for the Not-Agonist category. Variables tested were all those mentioned till this Section, i.e. mean peak values of head linear and rotational acceleration, of trunk linear and rotational acceleration, of neck flexion and extension angles and mean impact duration.

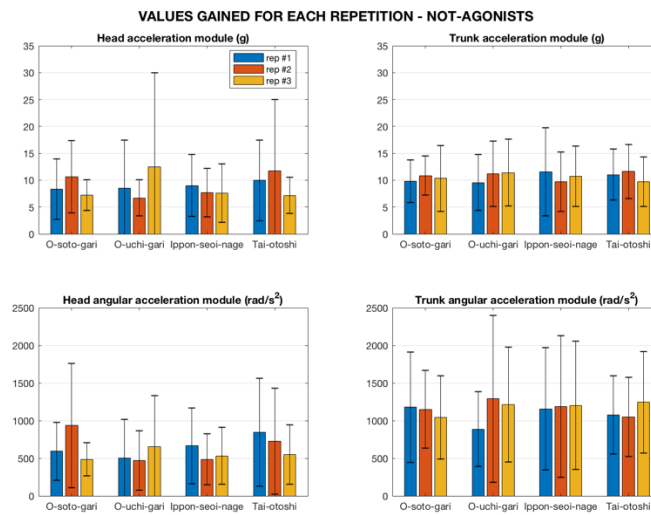


Figure 6.15: Accelerations values grouped for repetitions. Fatigue or adaption may be visible by particular trends in all techniques.

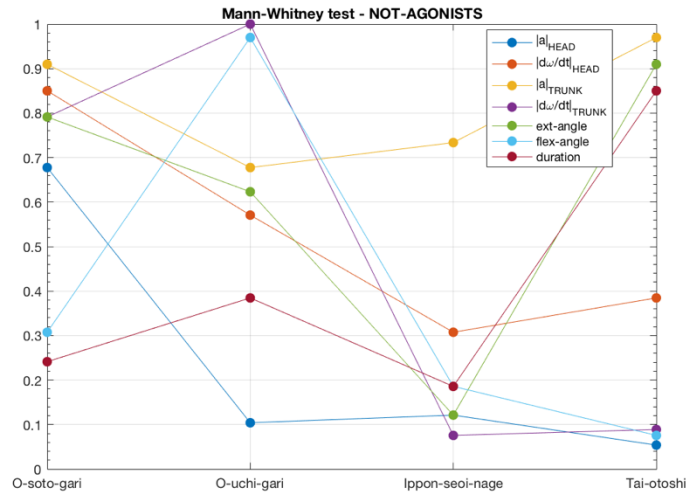


Figure 6.16: Results of the Mann-Whitney test for main variables involved in the study. The lowest value obtained is 0.055.

Results of the significance test are presented in Figure 6.16, while values tested for statistical differences are proposed in Figure 6.18, Figure 6.19 and Figure 6.20. No statistical differences were found between Expert and Not-expert for any variable gained from experimentation. The fact means that parameters do not differ so much among Not-Agonists: it could be attributed to a sub-maximal expression of force applied by the thrower, which brought all subjects to react in the same way for preventing head traumas because they were not exposed to extreme levels of acceleration and so, also most inexpert athletes had the time to correctly execute the breakfall technique. Another hypothesis for these results is that the two sub-groups mastered good breakfall skills: in this way, it has to be said that the division basing on 3 years of experience might be inappropriate for children: Kamitani et al. [29] distinguished novice people on this basis, but their analysis did not comprehend children which have greater learning abilities.

A further analysis was so conducted on subjects belonging to the Not-expert Not-Agonist group, considering that these subjects had one or two years of experience. Statistical differences were looked for between these two sub sub-groups: unfortunately, no differences were found, so it can be stated that thanks to their elastic memory capabilities, both muscular and intellectual, one year of experience in performing Judo is enough for children to learn and master breakfalls in an adequate way (Figure 6.17).

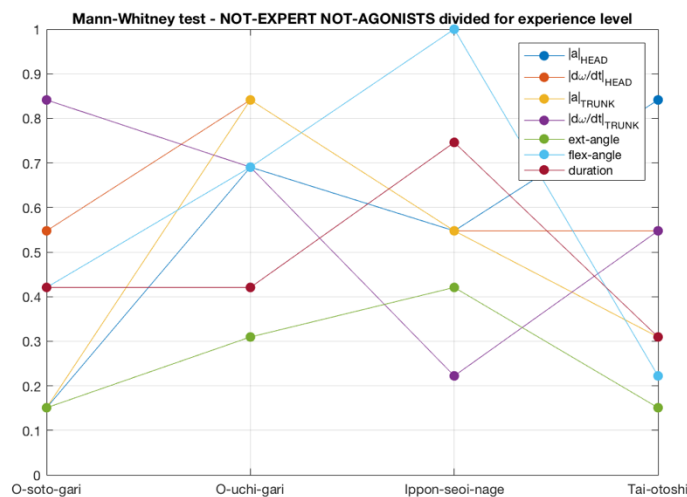


Figure 6.17: Results of the Mann-Whitney test conducted between Not-Agonists with one or two years of experience in practicing Judo.

No significant differences found in the trunk linear and rotational accelerations between Experts and Not-experts Not-Agonists means that the thrower executed each technique almost with same force and in the

same way. A reliability analysis was not performed on throws because the low values gained in Chapter 5 Breakfall Techniques Analysis would surely decrease due to the three-dimensional movements and the numerous ways of moving faller's body in the space when the two subjects collides.

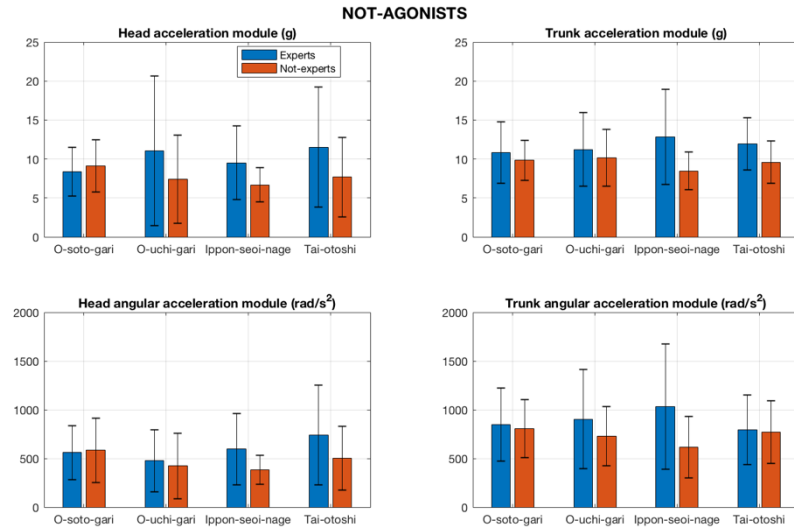


Figure 6.18: Mean values and standard deviation of linear and rotational accelerations for the Not-Agonists category. Values are compared between Expert and Not-expert groups.

Considering head linear acceleration values, low levels were measured in the Not-Agonists category: mean values on the head and on the trunk were about 10 g, far from the threshold of about 80 g, but it has to reflect on the fact that 10 g elapsed in 100 ms on a child body weighting 25 kg might be thought to be dangerous. The Gadd Severity Index (GSI) was calculated for these mean impact features leading to a value of about 30. GSI was chosen to take in account the entire impact event, and to consider the acceleration-duration relationship. It is defined as the integral over the time span, in which the impact occurs, of the acceleration curve to the 2.5: GSI considered dangerous for the human body are greater than 1000, so no danger could be found considering mean values. It has to be told that these calculations have been made hypothesizing the mean value of the curve lasting for the entire impact, so no reliability to this calculated index can be given. However, considering each single repetition the maximum value of the GSI obtained is about 175, very far from the threshold of 1000 even if scaling factor would be used accounting for age, weight and height differences (about 0.8 for a 6 years old subject while dealing with HIC measures).

Neck angle did not reach insidious levels: an excursion in the sagittal plane of about 40° can be considered normal also for children. For further analysis on trauma risks, shear forces on the neck vertebrae should be taken into account verifying different neck injury criteria.

Impact duration obtained in Not-Agonists was greater than the 20 ms cited in literature, demonstrating a slower motion which implies a longer impact on the mat. However, a different method for measuring the time span could had been employed by other researchers leading undoubtedly to different results.

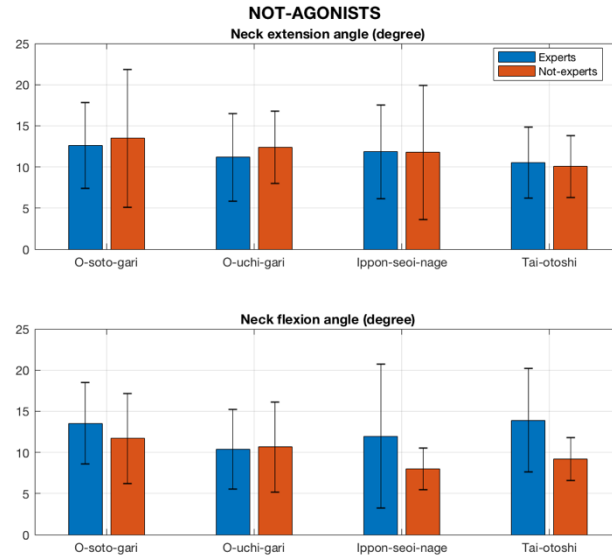


Figure 6.19: Mean values and standard deviation of neck extension and flexion angles for the Not-Agonists category. Values are compared between Expert and Not-expert groups.

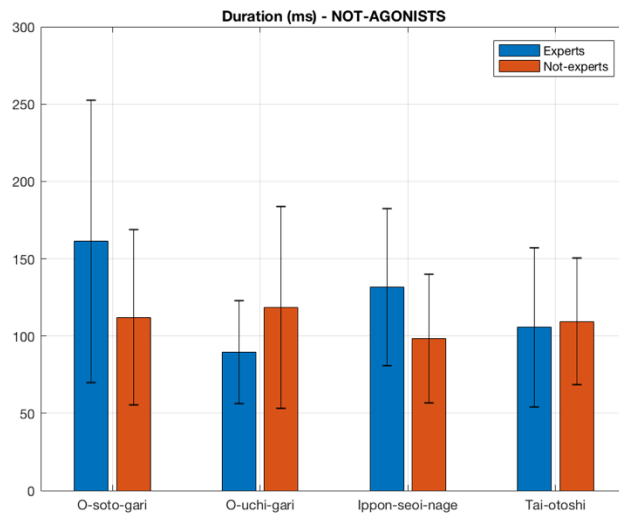


Figure 6.20: Mean values and standard deviation of impact duration for the Not-Agonists category. Values are compared between Expert and Not-expert groups.

A further analysis was conducted for verifying if there were any differences in the value of the neck angle in the instant in which the peak value of the module acceleration occurred for both categories. As can be seen from Figure 6.21 in which values of the angle and the corresponding p-value are presented, no statistical differences were found meaning that both categories respond in the same way to acceleration peaks while being thrown.

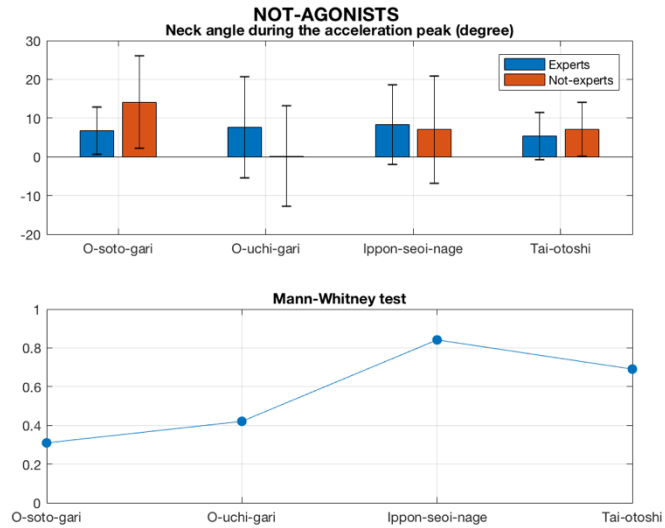


Figure 6.21: Mean values and standard deviations of the neck angle at the acceleration peak time. Positive values mean neck extension, negative correspond to flexion. Results for the significance test are proposed below.

6.3.3 Agonists

Same analysis conducted on the Not-Agonists category were managed on the Agonists group. As can be seen from the previous Figure 6.12 and Figure 6.13, greater values were acquired than the ones gained from Not-Agonists. Values above the 80 g limit identified for Judo throws were measured demonstrating the potential risk involved in Agonists' Judo. As for Not-Agonists, GSI was calculated for each fall for identifying potential risks: the maximum value here obtained is 530 (for a peak value of the head acceleration module of 86 g in the first technique considered), half of the tolerance limit but enough for thinking about the potential risks. Moreover, the limit of 80 g has been overcome many times in the protocol for the Agonists category, suggesting an increased risk of head traumas. However, the duration of the impact was greater than the one published in many researches, indeed about 150 ms was the mean value found for the Agonists category (Figure 6.27).

At first fatigue or adaption was searched looking for specific trends in head and trunk accelerations grouped for repetition among subjects (Figure 6.22). No particular and repetitive trends were present among all repetitions of the tested techniques, so three repetitions were rightly chosen to not exert the thrower or the faller.

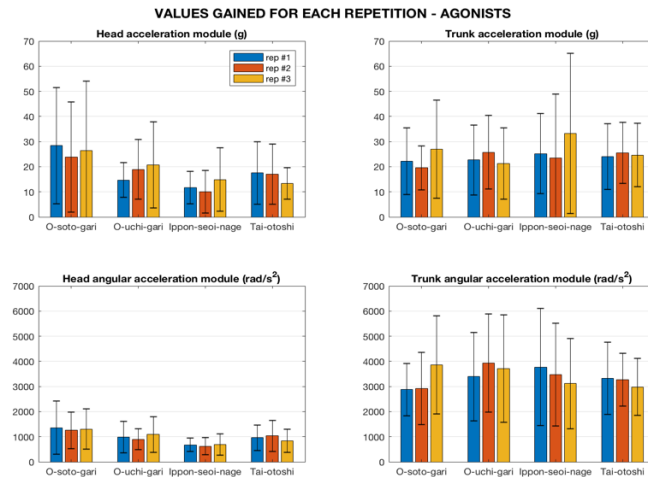


Figure 6.22: Accelerations values grouped for the three repetition among subjects.

As previously done, statistical differences were searched between Experts and Not-experts through the Mann-Whitney test (Figure 6.23). As not happened for the Not-Agonists group, significant differences were found on head linear and rotational accelerations, trunk linear acceleration and impact duration.

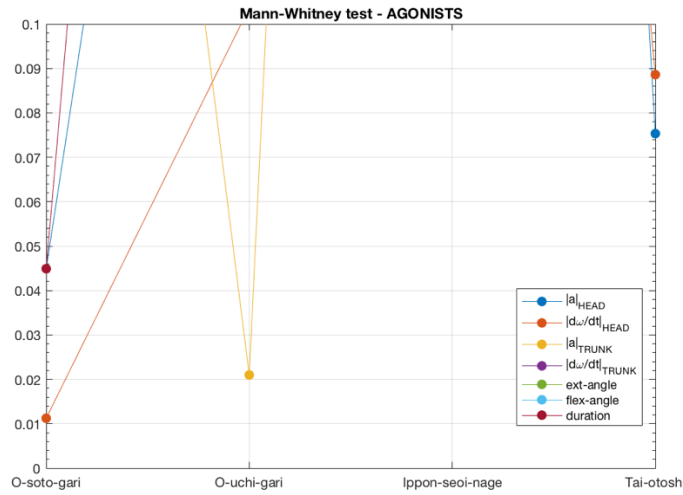


Figure 6.23: Mann-Whitney test results for the main variables involved in the study for Agonists category. P-values lower than 0.1 are presented.

Differences in linear acceleration values were found in o-soto-gari, the technique which gained the greatest values of acceleration demonstrating its superior chances of determining head injuries (Figure 6.24): combining this difference with the one obtained on the rotational acceleration for this technique, a note on the different behaviour of Expert and Not-expert subjects can be made. In this technique, the higher levels of accelerations make subjects to react in different manner basing on their experience, in particular Experts succeed in lowering these values by a gradual activation of neck flexors and abdomen muscles and by a correct body shape.

Variances of the trunk linear acceleration in the second tested throw technique could be addressed to a different level of force used by the thrower: it might be possible because thrower force cannot be controlled without measures about him, but it could be also addressed to a different position gained by fallers which lead to not dissipate correctly the acceleration imparted by the thrower.

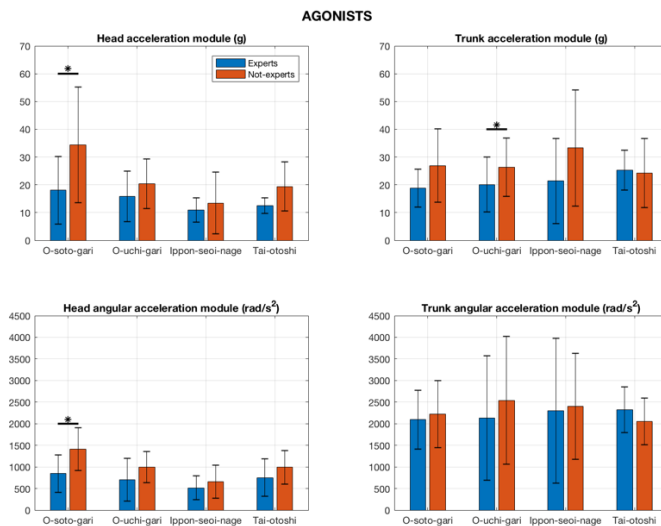


Figure 6.24: Mean values and standard deviation of linear and rotational accelerations for the Agonists category. Values are compared between Expert and Not-expert groups. Statistical differences are highlighted by star sign, one meaning $p < 0.05$.

P-values obtained for the neck angles demonstrate that no variations in the range of motion occurred during the test due to inexperience. As previously done for the Not-Agonist category, an analysis of the value acquired concomitantly with the acceleration peak was carried out for verifying further differences: results are proposed in Figure 6.26. As can be observed, no significant differences were found between Expert and Not-expert Agonists, thus their head reached a specific value of flexion/extension angle independently from the experience level. However, it can be seen how o-uchi-gari technique implies a flexion of the neck while being thrown: this fact can be explained by the great pushing action exerted by the thrower and directed to uke's back, which makes the faller to react in a conservative way for avoiding head striking. Mean negatives values were acquired also in the third technique, ippon-seoi-nage, probably because of the forward throw causing the head to flex as in the forward rolling breakfall (see Appendix A for further information).

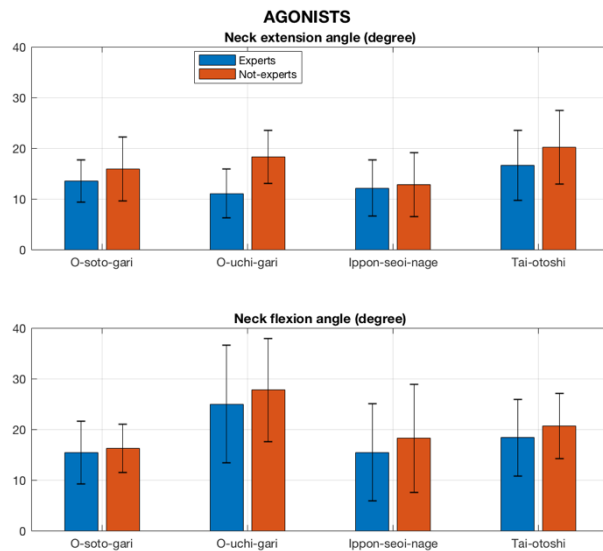


Figure 6.25: Mean values and standard deviation of neck extension and flexion angles for the Agonists category. Values are compared between Expert and Not-expert groups.

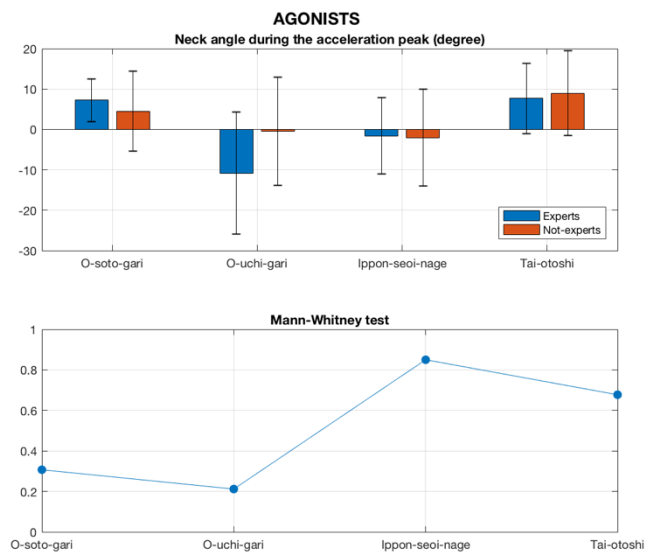


Figure 6.26: Mean values and standard deviations of the neck angle at the acceleration peak time. Positive values mean neck extension, negative correspond to flexion. Results of the significance test are proposed below.

Impact duration, presented in Figure 6.27 gained statistical differences in the first tested technique, meaning that Expert fallers extend the time duration of the impact to dissipate more energy than Not-expert subjects.

This fact might be caused by a wrong body shape assumed by novice judokas leading them to accuse higher values of linear and rotational acceleration, as found previously in Figure 6.24.

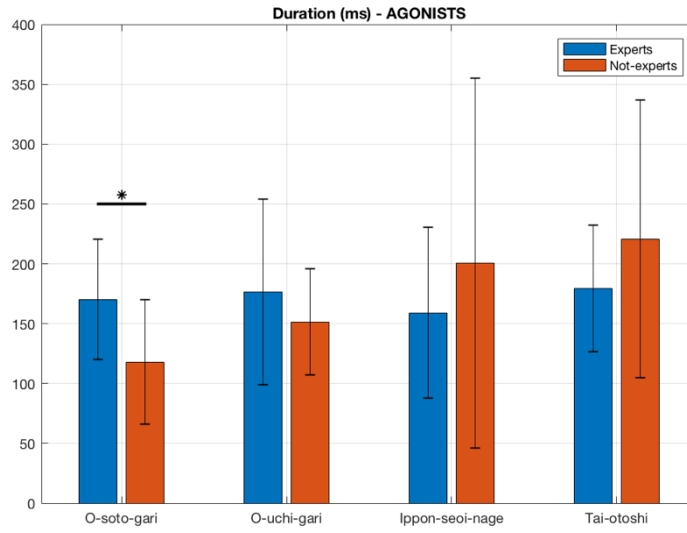


Figure 6.27: Mean values and standard deviation of impact duration for the Agonists category. Values are compared between Expert and Not-expert groups. P -value < 0.05 is highlighted with star sign.

7 Conclusions and Future Developments

Judo was investigated with scientific methods through the aid of technologies slightly exploited in the Sport Science field. It was proved that reliable information can be obtained from these devices and that the sport here considered can be analysed with technologies different from optoelectronic systems with all their related disadvantages (markers, high costs, experimental setup, etc). By the way, also both IMUs exploited in this study had related problems in dealing with a sport as Judo: low full scale for linear acceleration measures or low sample rate which varies among samples and between identical devices of the same brand. Considering that literature about acceleration levels to which judokas are exposed every day is not as broad as happens for other topics, such as American Football, more research about this sport should be done in order to correctly define associated risks. In particular, it has also to be considered the increasing number of people who starts Judo classes thanks to the mass media diffusion of such a sport. Moreover, considering that in Japan most students have to master Judo as national sport activity, a great number of subjects who could encounter injuries is present. The research here conducted was aimed to identify potential risks while doing Judo, in particular referring to head traumas.

At first, one strategy adopted by judokas for avoiding head injuries was examined, giving details about how the mechanism involved in the backward breakfall works and comparing it to the typical variation which happens during fights, the “no-hands” ukemi. Differences about the acceleration along the antero-posterior axis were found, but more important was the difference in the neck angle path. Higher values of the extension angle were found while performing the variation of the standard ukemi technique in the phases of sacral, lumbar and thoracic contact, demonstrating the increased risk of striking the head to the floor leading to major TBIs cited in Section 2.3.

Thereafter, an analysis on the main techniques practiced by children and adults was conducted aiming to detect which levels of linear and rotational acceleration judokas have to bear and to determine if they could be considered injurious to the human body. The analysis was carried out considering also distinctions based on age and experience in practicing Judo.

Firstly, it has to be said that values of the impact duration here obtained differed by a factor about eight from the ones cited in literature [5] [38]: because no information on how they measured the time span over which the impact occurs, a standard technique was adopted in the study and, in this way, longer impacts were acquired in both categories here reviewed. However, even if peak values in some cases reached and overcame the 80 g limit for concussion cited in many studies, the calculation of the Gadd Severity Index, which accounts for the entire acceleration curve, reveals that no harmful levels were met, even if caution should be addressed in practicing Judo techniques due to the high GSI values.

Counting for the Not-Agonists category, no differences were found neither among techniques, neither between Expert and Not-expert subjects. It might be due to the low force level exerted by the thrower and to the greater time in which fallers can plan the movement to be performed in order to fall correctly avoiding traumas.

Considering Agonists, by contrast, many differences between techniques were found demonstrating that most dangerous techniques for the head among the ones tested are o-soto-gari and o-uchi-gari, in which the faller executes a backward breakfall as the one previously tested. In particular, greater values of linear and rotational acceleration were gained for o-soto-gari, while a greater excursion of the neck angle was acquired with o-uchi-gari technique. Differences between Expert and Not-expert were discovered likewise in these two techniques, in particular the first exhibits higher values of linear acceleration and angular acceleration of the head but lower impact duration, demonstrating the low efficacy of the breakfall executed by novice subjects.

As also concluded by many articles reviewed in Chapter 2.2, the practice of breakfall techniques is mandatory for preventing head traumas and only when breakfalls have been mastered techniques study can begin. Furthermore, more attention must be employed in dealing with novice adults in comparison to novice children, because of the greater levels of acceleration developed by Agonists and their lower mental flexibility than the one owned by children.

Further analyses are required for proving results here obtained, in particular a common criterion for assessing the impact force and linking the clinical results during throws should be elected for standardizing the data obtained by different researchers.

Moreover, analyses should be performed exploiting wireless technology for avoiding artefacts due to the presence and the encumbrance of cables. A greater sample rate should be employed for capturing actual peak values, but also it should be stable and reproducible for each sensor used in the tests. Furthermore, it was never thought till this moment that a performance study, conducted with sensors placed on the thrower, can be combined to an injury assessment research by measuring data from the faller. In this way, data for injury analysis could be extracted from sensors placed on the faller, while from the devices placed on thrower's body important information on reliability and reproducibility of the technical gesture could be obtained. For example, just one limb of the thrower could be analysed basing on the typology of technique tested, i.e. one leg or one foot for leg throws, one hand for hand throws, etc. Thus, information about the level of force used by the thrower for each technique should be acquired, and also comparisons between adults and child could be achieved by normalizing data, for example by thrower's limb acceleration or angular velocity peak value.

Another analysis that could be performed is about the difference in experience considering more levels, for example enrolling elite judokas (for example Olympic Games contestants or National teams) for examining if there are any differences in head acceleration or neck angle path.

At last, an observation about what was tested regarding Judo has to be made: Judo, as stated in Chapter 2.2, is dynamic open-skill sport which involves two people fighting against each other. The way in which techniques were tested in this study, but also in which they were always tested in literature, is the one used in training for learning and improving execution, i.e. from a standing position with the faller not opposing. As stated, this is a particular situation which did not happen during fights, so an analysis of what happens during fight may be necessary: a video should be recorded in order to verify the origin of each signal peak. Furthermore, during fights, due to the open-skill nature of this sport, variations of the standard techniques linked to the particular situation, the particular opponent, the agonism or to personal adaptations occur. This might be the fact leading to precise situation bringing to traumas that cannot be evidenced while analysing the standard execution.

In addition to this, other techniques, not tested in this study, exist in Judo: they were not chosen because children cannot exploit them in competitions, so neither in trainings, and because of the particular risk involved for the faller. These techniques are frequently used in competition and may be one of main causes for head traumas (an example, Figure 7.1).

In conclusion, this study proved the differences on head variables between athletes with distinctive experience levels while being thrown with Judo techniques from a standing position. Results here found demonstrate that the risk of head injury has to be considered even if rarely thought by coaches to be probable: indeed, the head impact index here considered, even if head collision to the mat hardly had happened, proved for the Agonists group to be next to a hypothetical threshold for younger Agonists. Thus, more studies are needed to elucidate the possibility of head injuries while practicing Judo, but the risk must

not be underestimated by judokas, physicians, clinicians and all personal involved in Judo trainings and competitions.

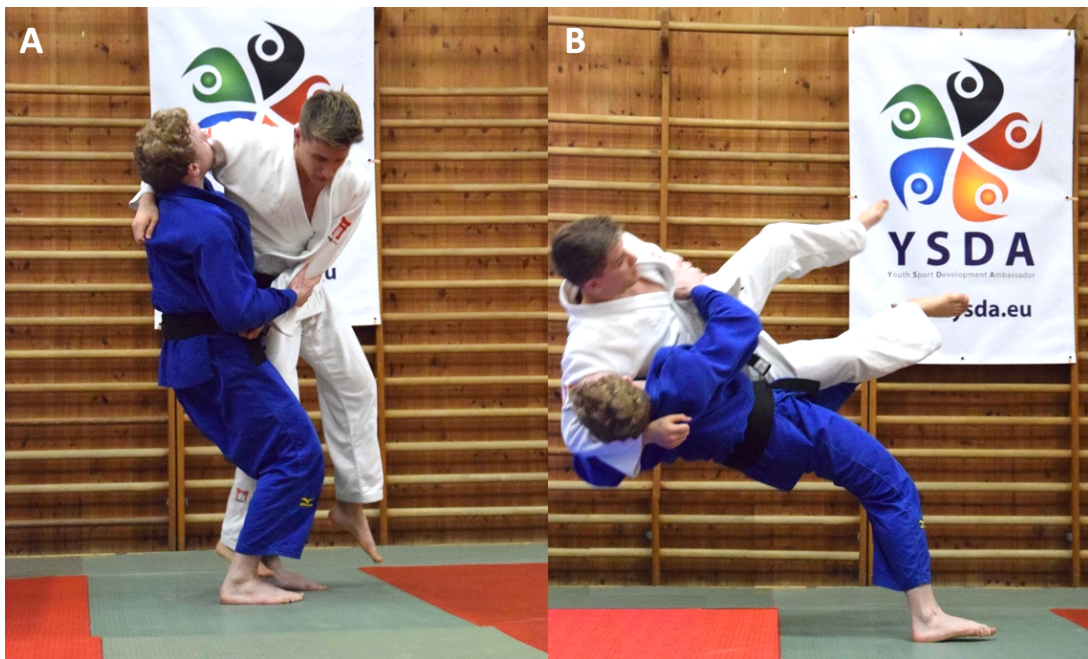


Figure 7.1: Ura-nage technique.

References

- [1] E. Polak, J. Kulasa, A. Vencesbrito, M. A. Castro and O. Fernandes, "Motion Analysis Systems as Optimization Training Tools in Combat Sports and Martial Arts," *Revista de Artes Marciales Asiáticas*, vol. 10, no. 2, pp. 105-123, 2016.
- [2] K. L. O'Connor, S. Rowson, S. M. Duma and S. P. Broglio, "Head-Impact-Measurement Devices: A Systematic Review," *Journal of Athletic Training*, vol. 52, no. 3, pp. 206-227, 2017.
- [3] N. Hammammi, S. Hattabi, A. Salhi, T. Rezgui, M. Oueslati and A. Bouassida, "Combat Sport Injuries Profile: A Review," *Science & Sports*, 2017.
- [4] R. C. Cantu, "Head Injuries in Sport," *British Journal of Sports Medicine*, vol. 30, pp. 289-296, 1996.
- [5] T. B. Hoshizaki, A. Post, M. Kendall, J. Cournoyer, P. Rousseau, M. D. Gilchrist, S. Brien, M. Cusimano and S. Marshall, "The Development of a Threshold Curve for the Understanding of Concussion in Sport," *Trauma*, vol. 19, no. 3, pp. 196-206, 2016.
- [6] C. Z. Cory, M. D. Jones, D. S. James, S. Leadbeatter and L. D. M. Nokes, "The Potential and Limitations of Utilising Head Impact Injury Models to Assess the Likelihood of Significant Head Injury in Infants after a Fall," *Forensic Science International*, vol. 123, pp. 89-106, 2001.
- [7] R. Graham, F. P. Rivara, M. A. Ford and C. M. Spicer, Sports-related Concussions in Youth: Improving the Science, Changing the Culture, I. o. M. (. a. N. R. C. (NRC), Ed., Washington, D.C.: The National Academies Press, 2014.
- [8] H. Gao, Z. Han, R. Bai, S. Huang, X. Ge, F. Chen and P. Lei, "The Accumulation of Brain Injury Leads to Severe Neuropathological and Neurobehavioral Changes After Repetitive Mild Traumatic Brain Injury," *Brain Research*, vol. 1, no. 8, 2017.
- [9] T. McAllister, L. Flashman, A. Maerlender, R. Greenwald, J. Beckwith, T. Tosteson, J. Crisco, P. Brolinson, S. Duma, A. Duhaime, M. Grove and J. Turco, "Cognitive Effects of One Season of Head Impacts in a Cohort of Collegiate Contact Sport Athletes," *Neurology*, vol. 78, pp. 1777-1784, 2012.
- [10] J. D. Schmidt, K. M. Guskiewicz, J. P. Mihalik, J. T. Blackburn, G. P. Sigmund and S. W. Marshall, "Head Impact Magnitude in American High School Football," *Pediatrics*, vol. 138, no. 2, 2016.
- [11] R. M. Greenwald, J. T. Gwin, J. J. Chu and J. J. Crisco, "Head Impact Severity Measures for Evaluating Mild Traumatic Brain Injury Risk Exposure," *Neurosurgery*, vol. 62, no. 4, pp. 789-798, 2008.
- [12] S. M. Duma, S. J. Manoogian, W. R. Bussone, G. P. Brolinson, M. W. Goforth, J. J. Donnenwerth, R. M. Greenwald, J. J. Chu and J. J. Crisco, "Analysis of Real-time Head Accelerations in Collegiate Football Players," *Clinical Journal of Sport Medicine*, vol. 15, no. 1, pp. 3-8, 2005.
- [13] S. P. Broglio, J. T. Eckner, D. Martini, J. J. Sosnoff, J. S. Kutcher and C. Randolph, "Cumulative Head Impact Burden in High School Football," *Journal of Neurotrauma*, vol. 18, pp. 2069-2078, 2011.
- [14] J. T. Eckner, M. Sabin, J. S. Kutcher and S. P. Broglio, "No Evidence for a Cumulative Impact Effect on Concussion Injury Threshold," *Journal of Neurotrauma*, vol. 28, pp. 2079-2090, 2011.

- [15] K. L. O'Connor, T. Peeters, S. Szymanski and S. P. Broglio, "Individual Impact Magnitude vs. Cumulative Magnitude for Estimating Concussion Odds," *Annals of Biomedical Engineering*, vol. 45, no. 8, pp. 1985-1992, 2017.
- [16] B. B. Reynolds, J. Patrie, E. J. Henry, H. P. Goodkin, D. K. Broshek, M. Wintermark and T. J. Druzgal, "Comparative Analysis of Head Impact in Contact and Collision Sports," *Journal of Neurotrauma*, vol. 34, pp. 38-49, 2017.
- [17] R. T. Imamura, M. Iteya, A. Hreljac and R. F. Escamilla, "A Kinematic Comparison of the Judo Throw Harai-goshi During Competitive and Non-competitive conditions," *Journal of Sports Science and Medicine*, vol. 6, pp. 15-22, 2007.
- [18] M. Exton and Y. Iura, "A Biomechanical Study on Tomoe-nage of Judo Techniques," *Resear Journal of Budo*, vol. 23, no. 3, pp. 24-34, 1991.
- [19] T. Ishii, M. Ae, S. Koshida and N. Fujii, "The Centre of Mass Kinematics for Elite Women Judo Athletes in Seoi-nage," in *XXXIV International Conference on Biomechanics in Sports*, Tsukuba, Japan, July 18-22, 2016.
- [20] T. Ishii, M. Ae, Y. Suzuki and Y. Kobayashi, "Kinematic Comparison of the Seoi-nage Judo Technique between Elite and College Athletes," *Sports Biomechanics*, 2017.
- [21] S. Frassinelli, A. Niccolai, T. Marzi, M. Aghaei, M. Mussetta and R. Zich, "Event-based Measurement of Power in Sport Activities by Means of Distributed Wireless Sensors," in *International Conference on Event-based Control, Communication, and Signal Processing*, June 2015.
- [22] S. Frassinelli, "Design and Development of Technologies for the Measurement of Biomechanical Performance in Athletes Practicing Judo".
- [23] L. Blais, F. Trilles and P. Lacouture, "Validation of a Specific Machine to the Strength Training of Judokas," *Journal of Strength and Conditioning Research*, vol. 21, no. 2, pp. 409-412, 2007.
- [24] M. Hassmann, M. Buchegger, K.-P. Stollberg, A. Sever and A. Sabo, "Motion Analysis of Performance Tests Using a Pulling Force Device (PFD) Simulating a Judo Throw," *Procedia Engineering*, vol. 2, pp. 3329-3334, 2010.
- [25] G. Lech, W. Chwala, T. Ambrozy and S. Sterkowicz, "Muscle Torque and Its Relation to Technique, Tactics, Sport Level and Age Group in Judo Contestants," *Journal of Human Kinetics*, vol. 45, pp. 167-175, 2015.
- [26] L. Blais, F. Trilles and P. Lacouture, "Three-dimensional Joint Dynamics and Energy Expenditure During the Execution of a Judo Throwing Technique (Morote Seoi Nage)," *Journal of Sports Sciences*, vol. 25, no. 11, pp. 1211-1220, 2007.
- [27] N. Dimitrova, "Biodynamic Analysis of the Uki-goshi Technique in Judo," *The Exercise of Quality of Life Journal*, pp. 38-41, 2009.
- [28] E. Pocecco, G. Ruedl, N. Stankovic, S. Sterkowicz, F. Boscolo Del Vecchio, C. Gutierrez-Garcia, R. Rousseau, M. Wolf, M. Kopp, B. Miarka, V. Menz, P. Krusmann, M. Calmet and Malliaropoul, "Injuries in Judo: A Systematic Literature Review Including Suggestion for Prevention," *British Journal of Sports Medicine*, vol. 47, pp. 1139-1143, 2013.

- [29] T. Kamitani, Y. Nimura, S. Nagahiro, S. Miyazaki and T. Tomatsu, "Catastrophic head and Neck Injuries in Judo Players in Japan from 2003 to 2010," *The American Journal of Sports Medicine*, vol. 41, no. 8, pp. 1915-1921, 2013.
- [30] S. Nagahiro and Y. Mizobuchi, "Current Topics in Sport-Related Head Injuries: A Review," *Neurologia Medico-Chirurgica (Tokio)*, vol. 54, pp. 878-886, 2014.
- [31] K. Nishimura, K. Fujii, R. Maeyama, I. Saiki, S. Sakata and K. Kitamura, "Acute Subdural Hematoma in Judo Practitioners," *Neurologia Medico Chirurgica (Tokio)*, vol. 28, pp. 991-993, 1988.
- [32] H. Yokota and Y. Ida, "Acute Subdural Hematoma in a Judo Player with Repeated Head Injuries," *World Neurosurgery*, vol. 91, pp. 671.e1-671.e3, 2016.
- [33] E. E. Zusman, P. Zopfi, J. Kuluva and S. Zuckerman, "Can Ideas from United States Youth Sports Reduce Judo-related Head Injuries in Japan?," *World Neurosurgery*, vol. 97, pp. 725-727, 2017.
- [34] T. Piuccio and S. G. Dos Santos, "Magnitude and Duration of the Impact Generated on the Athletes' Body During Training in Ippon Seoi-nage," *Motricidade*, vol. 6, no. 1, pp. 71-83, 2010.
- [35] S. G. Dos Santos, C. R. De Melo Roesler and S. Iberes Lopes Melo, "Inquiry of the Discomfort Offered for Different Tatamis Used in the Practical of the Judo," *Revista Brasileira de Cineantropometria & Desempenho Humano*, vol. 9, no. 4, pp. 358-365, 2007.
- [36] T. K. Florentin, C. Snodgrass and S. O. Henry, "Head Acceleration Associated with Six Standard Judo Throws and Break Falls," *International Journal of Exercise Science: Conference Proceedings*, vol. 8, no. 5, 2017.
- [37] H. Murayama, M. Hitosugi, Y. Motozawa, M. Ogino and K. Koyama, "Rotational Head Acceleration of Thrown Person with Break-fall Skills by Judo Throwing Techniques," *Medicine & Science in Sports & Exercise*, vol. 49, 2017.
- [38] M. Hitosugi, H. Murayama, Y. Motozawa, K. Ishii, M. Ogino and K. Koyama, "Biomechanical Analysis of Acute Subdural Hematoma Resulting from Judo," *Biomedical Research (Tokio)*, vol. 35, no. 5, pp. 339-344, 2014.
- [39] S. Koshida, T. Ishii, T. Matsuda and T. Hashimoto, "Biomechanics of Judo Backward Breakfall for Different Throwing Techniques in Novice Judokas," *European Journal of Sport Science*, vol. 17, no. 4, pp. 417-424, 2017.
- [40] S. Koshida, T. Ishii, T. Matsuda and T. Hashimoto, "Kinematics of Judo Breakfall for Osoto-gari: Considerations for Head Injury Prevention," *Journal of Sports Sciences*, vol. 35, no. 11, pp. 1059-1065, 2016.
- [41] S. Koshida and T. Matsuda, "Neck and Trunk Kinematics and Electromyographic Activity During Judo Backward Breakfalls," in *XXX Annual Conference of Biomechanics in Sports*, Melbourne, 2012.
- [42] H. Murayama, M. Hitosugi, Y. Motozawa, M. Ogino and K. Koyama, "Simple Strategy to Prevent Severe Head Trauma in Judo," *Neurologia Medico Chirurgica (Tokio)*, vol. 53, pp. 580-584, 2013.
- [43] H. Murayama, M. Hitosugi, Y. Motozawa, M. Ogino and K. Koyama, "Rotational Acceleration During Head Impact Resulting from Different Judo Throwing Techniques," *Neurologia Medico Chirurgica (Tokio)*, vol. 54, pp. 374-378, 2014.

- [44] A. C. McKee, D. H. Daneshvar, V. E. Alvarez and T. D. Stein, "The Neuropathology of Sport," *Acta Neuropathol*, vol. 127, pp. 29-51, 2014.
- [45] B. D. Jordan, "The Clinical Spectrum of Sport-related Traumatic Brain Injury," *Nature Reviews Neurology*, vol. 9, no. 4, pp. 222-230, 2013.
- [46] Y. Mizobuchi and S. Nagahiro, "A Review of Sport-Related Head Injuries," *Korean J Neurotrauma*, vol. 12, no. 1, pp. 1-5, 2016.
- [47] A. White, "Sports-Related Head Injuries," *Journal of Emergency Nursing*, vol. 38, no. 5, pp. 463-465, 2012.
- [48] L. Mainwaring, K. M. F. Pennock, S. Mylabathula and B. Z. Alavie, "Subconcussive Head Impact in Sport: A Systematic Review of the Evidence," *International Journal of Psychophysiology*, 2018.
- [49] R. C. Cantu, "Dysautoregulation/Second-Impact Syndrome with Recurrent Athletic Head Injury," *World Neurosurgery*, vol. 95, pp. 601-602, 2016.
- [50] V. Agostini, L. Antenucci, G. Lisco, L. Gastaldi, S. Tadano and M. Knaflitz, "Wearable sensors for gait analysis: Comparison between a MIMUs system and a gold standard electromechanical system," in *IEEE International Symposium on Medical Measurements and Applications*, Torino, 2015.
- [51] A. J. Wheeler and A. R. Ganji, *Introduction to Engineering Experimentation*, Pearson, 2010.
- [52] S. Kandekar, T. Chaudhari, A. Chopde and Y. Kapgade, "Anatomy of MEMS Capacitive Accelerometer," *International Journal for Research in Applied Science & Engineering Technology*, vol. 6, no. 8, pp. 532-539, 2018.
- [53] T. K. Koo and M. Y. Li, "A Guideline of Selecting and Reporting Intraclass Correlation Coefficients for Reliability Research," *Journal of Chiropractic Medicine*, vol. 15, pp. 155-163, 2016.
- [54] J. D. Evans, *Straightforward statistics for the behavioral sciences*, Pacific Grove, California, USA: Brooks/Cole Publishing, 1996.
- [55] T. Dahiru, "P-value, a True Test of Statistical Significance? A Cautionary Note," *Annals of Ibadan Postgraduate Medicine*, vol. 6, no. 1, pp. 21-26, 2008.

Appendix A: Judo Breakfalls and Techniques

In this section, words, breakfalls and techniques used in the study are briefly exposed with the aid of photos to clarify the phases of each movement. This Appendix is meant to explain in poor words the mechanism behind each movement, so no technicalities are mentioned, and no specific details are discussed.

Judo is a Martial Art developed by Jigoro Kano in 1882. Originally thought as a physical, mental and moral pedagogy in Japan by its founder, it was introduced in Tokyo 1964 Olympic Games. Judo matches involve two contestants (same age group, same weight category) wearing the typical Judo uniform, the judogi, fighting each other with the possibility of using grip fighting, throwing techniques, ground fighting with holding, joint lever and strangulation techniques. The match victory is assigned to the one who throws the opponent on his back, pins the opponent to the floor or submitted him by the use of levers or strangulations. Before practicing any throwing technique, fallers have to master the right way of falling without injury risk: these movements are called breakfalls (ukemi in Japanese) and involve the head not to touch the floor at any time, for preserving health and life. Four types of breakfalls were taught by Judo founder:

- rear breakfall (ushiro ukemi);
- side breakfall (yoko ukemi);
- rolling breakfall (zempo kaiten ukemi);
- front breakfall (mae ukemi).

Ushiro ukemi, the one studied in Section 5 Breakfall Techniques Analysis, involves a leg flexion to approach the floor, then a phase of rolling on the back till hands and arms are used to stop the movement by contacting the mat (Figure A.1). The movement develops on the sagittal plane and it is the most important breakfall for avoiding traumas to the back of the head. Moreover, it is taught to novice judokas from their first experience, in order to systematise the movement for preserving subject's health. This breakfall is used while fighting when being throw backward, even if the thrower may hold one opponent's arm preventing from contacting both on the floor.

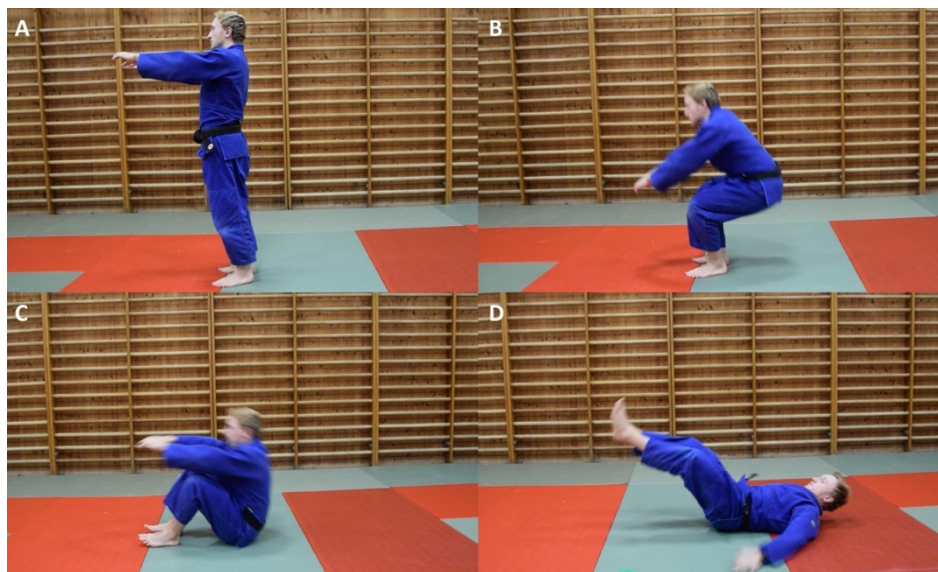


Figure A.1: Ushiro ukemi execution.

Yoko ukemi is probably the most likely final position when being thrown. The whole movement is seen very rarely, but one side laid on the floor with one arm contacting it is the arriving position for several techniques. Indeed, yoko ukemi from a standing position brings the body to rotate in the frontal plane while

approaching the floor till one side of the body touches the floor together with one arm and one hand (Figure A.2).

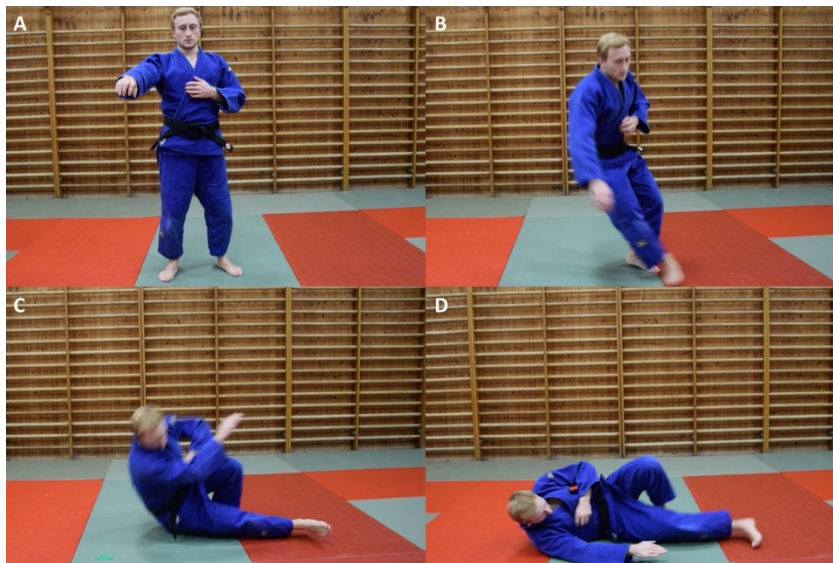


Figure A.2: Yoko ukemi.

Zempo kaiten ukemi is a forward breakfall similar to a simple somersault starting from a standing position: hands are precisely placed in order to not hurt elbows and wrists and then, through a rolling movement on one shoulder, a position similar to the one of yoko ukemi is reached, with one arm and one side in contact with the floor (Figure A.3). Due to the rotation on one shoulder the movement does not develop on a plane, but it is more likely to be three-dimensional differing from others breakfalls. This type of ukemi is common when being thrown forward and if correctly executed avoids any neck injury due to a frontal impact of the head against the mat.

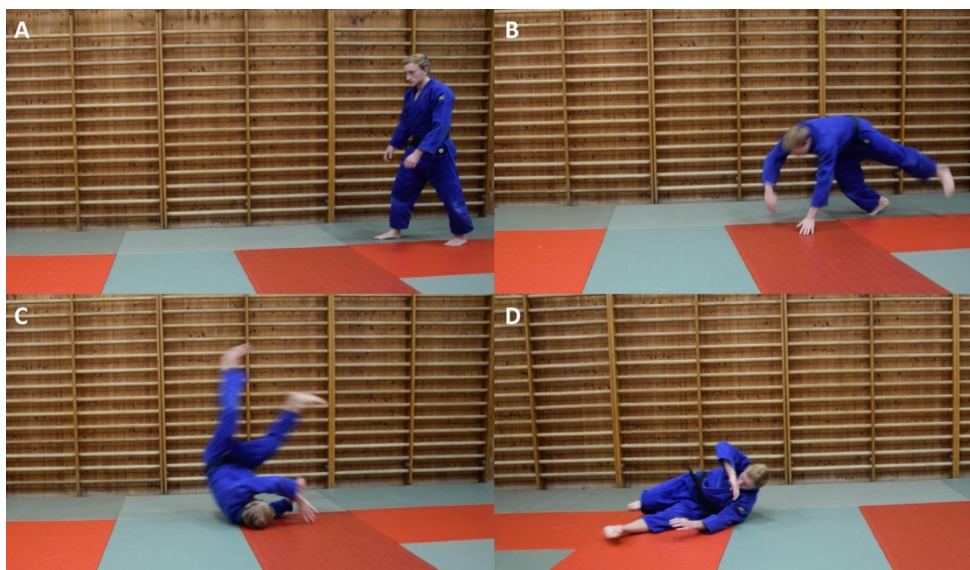


Figure A.3: Zempo kaiten ukemi.

Mae ukemi is not used and not practiced in the competitive version of Judo because it involves contacting the floor with stomach bringing no scores for the thrower. It starts from a kneeling or standing position and is used when there are no chance of rolling. Hands and arms are employed to avoid striking the face to the floor.

While breakfalls can be done singularly, throwing techniques need two people: one thrower and one faller, in Japanese respectively tori and uke. Each technique (in Japanese nage-waza) is composed of four phases subsequent in time:

- 1) kumi kata, establishing firm grip or grips;
- 2) kuzushi, breaking opponent's balance;
- 3) tsukuri, turning in and fitting the throw;
- 4) kake, completing the throw.

The first phase is mandatory only during matches, while in studying techniques can be neglected by starting with grips already prepared.

Official techniques are 68 (40 initially developed by Jigoro kano), even if variations and personal modifications to get a more efficient throw in a specific situation are permitted in competition. Traditionally, nage-waza are categorised into five groups depending on which part of tori body is used for throwing uke:

- te-waza (hand techniques);
- koshi-waza (hip techniques);
- ashi-waza (foot and leg techniques);
- ma-sutemi-waza (backward sacrifice techniques);
- yoko-sutemi-waza (side sacrifice techniques).

Last two group of techniques, named sutemi, are not taken into consideration in this brief guide because they are not employed in the study due to their prohibition in competition for Not-Agonists, so children under 12 years do not know how to perform them and how to correctly fall when thrown with this type of techniques.

As explained in Section 6.2 of the Chapter Head Injury Risk Assessment, four techniques were selected for the tests:

- T1** o-soto-gari (big outer reap);
- T2** o-uchi-gari (big inner reap);
- T3** ippon-seoi-nage (one arm shoulder throw);
- T4** tai-otoshi (body drop).

O-soto-gari is a technique from the ashi-waza group, indeed tori employs his leg to throw uke onto his back (Figure A.4). The movement starts with a great pulling action of tori to one side of uke, breaking his balance by driving him on one foot, and at the same time tori steps forward to uke getting closer to him. Then tori reaps from the outer uke's leg which is his unique support, driving him to the floor. Due to the rear breakfall that uke is forced to perform, it is considered by the scientific literature as the most dangerous technique responsible for head injuries.

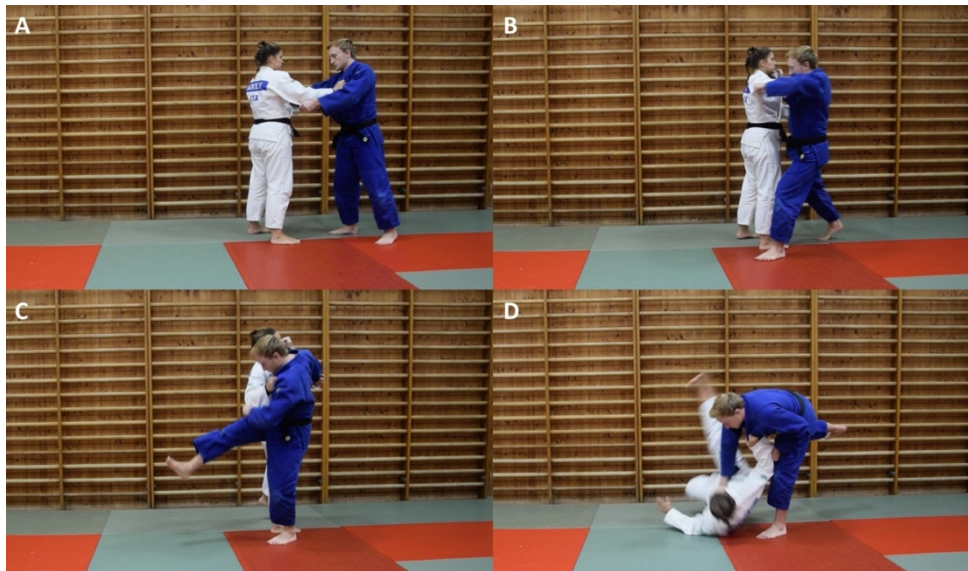


Figure A.4: O-soto-gari.

O-uchi-gari comes from the group of ashi-waza techniques: tori reaps uke's leg from the inner with one leg while hands are used to pull down the opponent where the support is removed (Figure A.5). Faller's head is free of touching the mat and muscles action lead to a whiplash-like movement potentially dangerous for both head and neck.

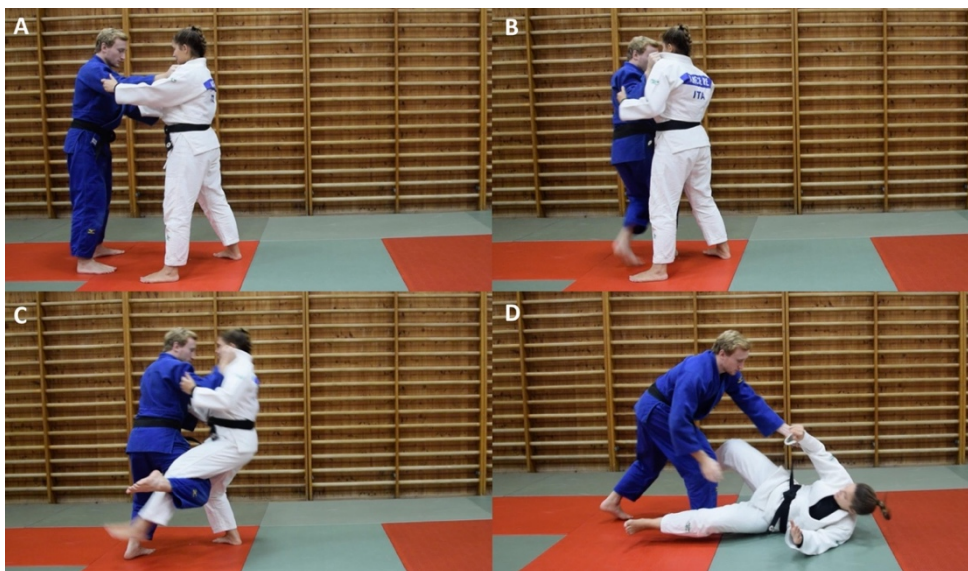


Figure A.5: O-uchi-gari.

Ippon-seoi-nage is a te-waza in which the opponent is thrown over tori by using one arm (Figure A.6). While pulling forward, tori approaches uke by dropping inside his feet and giving him his back. One arm is used by tori to grip uke's arm and with a great pulling action uke is thrown forward over tori's head. The faller uses in this case a breakfall similar to zempo kaiten ukemi.



Figure A.6: Ippon-seoi-nage.

Tai-otoshi is equally a technique from the te-waza group. The movement is similar to the one of ippon-seoi-nage, but standard grips are not broken, so one hand remain on the sleeve and the other on the lapel. Moreover, a leg is spread to avoid uke escaping by going around tori. As before, the great pulling action exerted by tori makes uke going over tori's head, falling analogously to zempo kaiten ukemi.

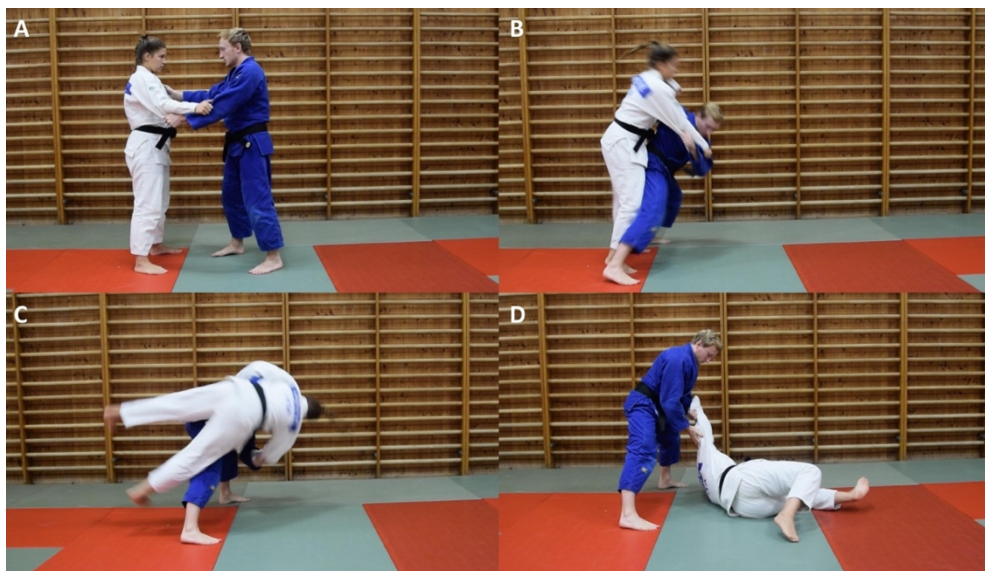


Figure A.7: Tai-otoshi.

Appendix B: Testing 3-Space™ Sensors

Yost Labs devices were selected to perform the analysis essentially for the adequate range of acceleration and for the Bluetooth 2.1 EDR SPP connectivity.

The first connection to a pc went wrong: a MacBook Pro (Early 2015, 2.7 GHz Intel Core i5, Bluetooth 4.2) was used for connecting the devices, but the 3-Space Suite provided by Yost Labs did not recognize both sensors (Figure B.1). As happened with ATR-Promotions sensors, the second step was to try using the virtual machine installed on that computer: even if in Yost Labs website and User's Manual the compatibility with Mac platform was cited and the Suite was designed for both Windows and Mac, this decision was made because it worked out with old sensors. Thus, a connection through a virtual platform with Windows 10 Education installed was carried out, but no advancement occurred.

It was thought that the problem might be related to Bluetooth drivers, so a research on the web was made for downloading and installing them. After having found and installed the correct versions of them, on both Mac platform and Windows, and having tried again to connect the devices, there were no improvements.

Then, connection problems might be caused by a wrong or old firmware version installed on the sensors. In this way, sensors were connected via USB to update the firmware: this time the wired connection worked with Mac, but not on Windows platform. Once connected, the firmware of both sensors was updated using the Suite tab "Sensor" -> "Update Firmware" -> "Update Firmware from Web". The connection was then re-tested firstly on Mac, then on Windows but unfortunately there were no progresses.

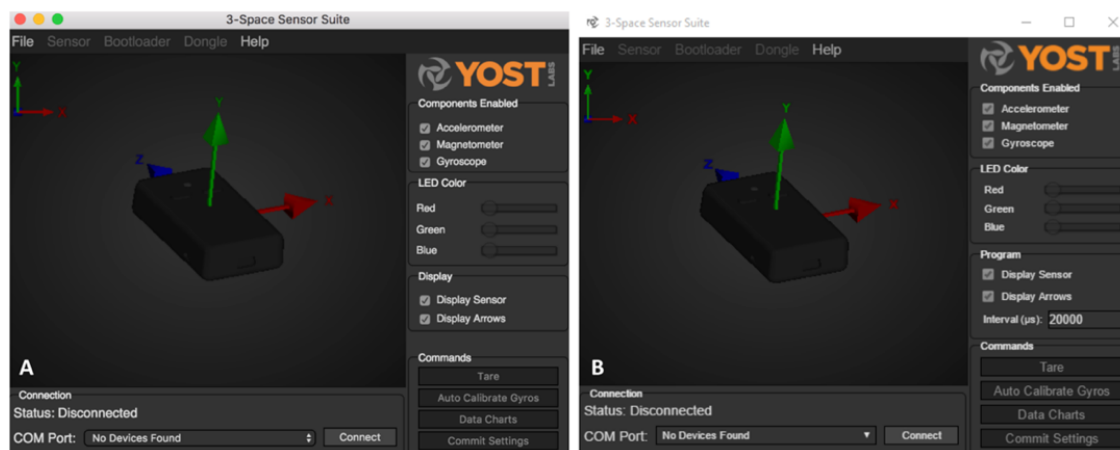


Figure B.1: Initial windows of the 3-Space Suite by Yost Labs. A) Mac version. B) Windows version.

The connection problem seemed not to be resolved: assuming that the issue might be due to an incompatibility between the sensors and the Mac Bluetooth, they were tested on another pc. An Acer laptop, Intel Core i7-5500U 2.4 GHz (dual core) Bluetooth 4.2 with Windows 10, was used: after having installed the Suite, one sensor was successfully connected via Bluetooth. To connect both sensors, the second sensor was reset through the Suite commands "Sensor" -> "Reset Sensor" and after "Sensor" -> "Restore Factory Settings". No ameliorations took place but finally, after upgrading its firmware as previously done, also the second sensor got connected to a second window of the Suite. Sensors were then calibrated for the first time through the command "Sensors" -> "Run Gradient Descent Wizard". Thus, signals from one sensor were acquired for the first time and an extract of the results was the following:

```
# Data format:
"%int(ChipTimeUS),%float(CorrectedGyroX),%float(CorrectedGyroY),%float(CorrectedGyroZ),%float(
CorrectedAccelX),%float(CorrectedAccelY),%float(CorrectedAccelZ)"
```

1830045514,0.1233330,1.8139255,0.1023896,0.9277344,0.1953125,0.6347656
 1830065675,0.0302515,3.2613428,0.1407858,1.4160156,-0.0488281,0.3906250
 1830105931,-0.5933945,5.3719654,0.0104717,1.3671875,0.0976563,0.7812500
 1830126071,-0.7376708,5.2602677,0.0267609,1.4160156,0.7324219,1.8066406
 1830166286,-0.5852499,-0.0546854,-0.1000626,0.9765625,0.0488281,0.1953125
 1830205477,0.1640561,0.9924814,0.2780809,1.6113281,0.2929688,0.4882813
 1830225597,-0.1035532,2.0361576,0.0814463,2.0507813,-0.1953125,-0.3906250
 1830265858,-0.3188041,1.0471668,-0.3874517,0.7324219,0.4882813,0.6835938
 1830326193,0.0581759,-0.6434258,-0.4444641,0.4882813,0.0488281,0.1464844
 1830346324,0.1314776,-1.8779191,-0.0674841,0.8789063,0.1464844,0.8789063

As can be seen from the first column which represents the internal time of the sensor in microseconds, the interval between two subsequent samples is 20 to 60 milliseconds, representing a sample rate from 50 to 17 Hz. This frequency is too far from sensors specifications and absolutely not suitable for the current study in terms of low value and great variability. Moreover, if two sensors were connected at the same time to the pc, the interval between samples increased till 80 ms, i.e. a sample rate of 12.5 Hz.

At this stage, considering that there were no settings involving frequencies and that the box "Interval (us):", present in the right of Windows 3-Space Suite (part B of Figure B.1), even if set to values different from 20000, turned into 20000 when a sensor was connected and became disabled, the Terminal Mode of the Suite was used to change sensors settings. Here commands are sent through string of numbers preceded by colon: it was chosen to use a repetitive way of setting parameter, so for each change in settings firstly the set value was asked to the sensor, then it was changed and thus re-asked for the actual value. Particular values of the language are zero which means "as fast as possible" and 255 which means "none".

The sequence of commands used for setting parameters to increase the sample rate was the following:

- to change the values related to interval timing (interval, length of transmission, delay before start)
 - : 83
 - : 82, 0, -1, 0
 - : 83
- to change the eight available streaming slots (38 = gyroscope vector, 39 = accelerometer vector)
 - : 81
 - : 80, 255, 38, 39, 255, 255, 255, 255, 255
 - : 81
- to change the header string into internal timestamp
 - : 222
 - : 221, 2
 - : 222
- to change the desired update rate
 - : 132
 - : 103, 0
 - : 146
- to commit the settings
 - : 225

Due to the lack of a command to write files from the terminal mode and due to the limited buffer of the terminal window which did not memorize all values returned, after committed the settings the data transmission had to be started in the classic Suite GUI. Unfortunately, there were no improvements in sample rate, and when got back to Terminal Mode the settings previously committed had changed to their previous values demonstrating the uselessness of that mode. Moreover, through the command : 132 which displays the time spent in the last cycle, it was discovered that sensors spent less than 1 ms in completing the internal processes. In this way, sensors could hypothetically ensure 1 kHz of sample rate. The problem might be due so to the Bluetooth connection or the CPU performance.

Many attempts had then been conducted to make sensors useful for the main application of this study: firstly, a Bluetooth 2 USB Trust adapter was used on pcs tested before, but no connection took place. Then, the devices connection and performances were experienced on different laptops and home computers with various hardware and software features. Devices tested are listed below:

- Home computer (2013), Window 8.1, AMD Phenom II X4 925 Processor 2.8 GHz (quad core), Bluetooth 2 USB Trust adapter;
- Fujitsu Esprimo (2008), Windows XP, Intel Core T5850 2.16 GHz (dual core), Bluetooth 2.1;
- Fujitsu Siemens (2002), Windows XP, Pentium III 1 GHz, Bluetooth 2 USB Trust adapter;
- Fujitsu Esprimo (2018), Windows 10 Pro, Intel Core i5-5200U 2.2 GHz, Bluetooth 4.0;
- Dell (2002), Windows XP, Intel Core T5600 1.83 GHz (dual core), Bluetooth 2 USB adapter;
- Fujitsu (2016), Windows 10, Intel Core i7-7600U 2.9 GHz (dual core), Bluetooth 4.0;
- Ankermann (2016), Windows 10, Intel Core i3-6100 3.7 GHz (dual core), Bluetooth 4.0 USB adapter;
- Alantik (2017), Windows 10, Intel Core i5-4460 3.2 GHz (quad core), Bluetooth 4.0 USB adapter;
- Asus (2017), Windows 10 Home, AMD A9-9420 Radeon R5 3.0 GHz (dual core), Bluetooth 4.2;
- Fujitsu (2018), Windows 10, Intel Core i7-8750H 4.1 GHz (hexa core), Bluetooth 5.0.

After having connected sensors to each computer listed, when the connection worked out the interval between samples did not reach values lower than 20 ms via Bluetooth.

Using the Suite, values about 5-7 ms were measured via USB cable. Those values are not appropriate for impact assessments, but no improvements took place after all these preliminary tests: this fact can be seen in Figure B.2, where the last of a set of three backward breakfalls is reported while sampling at about 50 Hz with one 3-Space™ sensor on the head. Those values are compared with data acquired from an ATR-Promotion sensor placed at the same time on subject's head.

The issue might so be restricted to the Bluetooth protocol because different hardware and CPUs were tested, from older systems to the most recent hexa core technology.

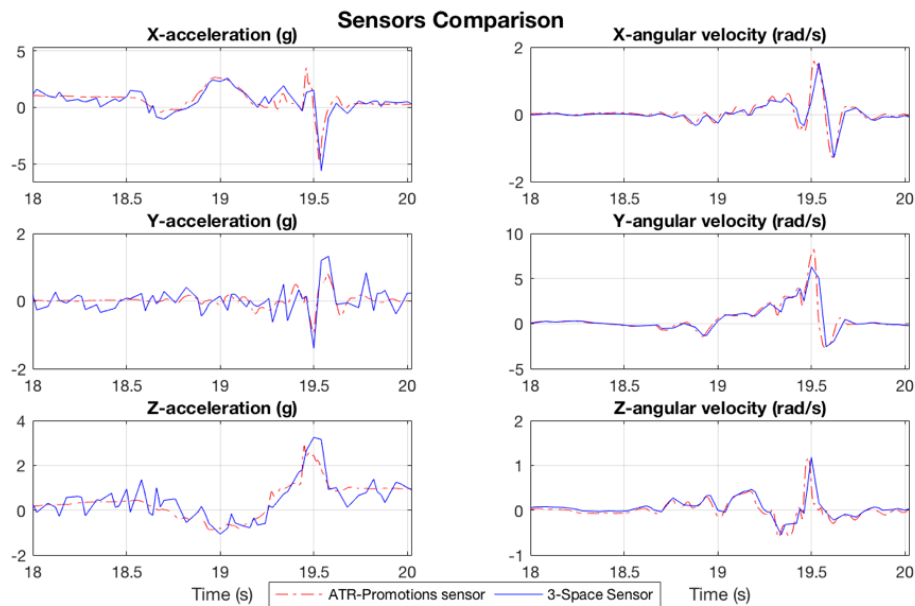


Figure B.2: Comparison between ATR-Promotions and 3-Space™ sensors, with a sample rate of respectively 1000 Hz and about 50 Hz, while doing three consecutive breakfalls (the last is here reported). The positive peaks in X-acceleration and Y-angular velocity were missed by Yost Labs sensor due to the low sample rate.

Considering that no answers were received from the Yost Labs support, a last attempt was done by direct connecting a memory to the USB mini port of the sensors in order to override Bluetooth connection which seems to be the bottleneck of the transmission. It did not work probably because of the lack of possibility of choosing the correct path where to save the generated .txt file, or due to the absence of a suitable power supply for the USB flash drive.

Contacted the developer of the 3-Space Suite on his private email, he revealed that there is a bug in the Suite which automatically modifies some acquisition parameters to display the correct orientation on the GUI, and that it would be fixed as soon as possible. Moreover, he suggested to use an all-purpose terminal for serial communications to increase the sample rate, even if the Bluetooth connection would still limit it.

The software RealTerm was suggested, so a first acquisition with it was accomplished. At this time a part of the .txt file was the following:

```
946783246,-0.23852,-0.83424,0.00349
1.51367,-0.09766,-0.19531
946788585,-0.24550,-0.75396,0.00233
1.61133,-0.24414,0.00000
946793933,-0.25714,-0.66553,0.01164
1.46484,0.68359,0.04883
946799308,-0.27343,-0.57478,0.01396
1.51367,0.34180,0.19531
946804876,-0.28506,-0.49682,0.01288,-0.03956,-0.01513
1.36719,-0.24414,0.00000
947167438,-0.99830,-0.00582,-0.01396
1.75781,0.09766,0.58594
947172811,-1.01342,0.02443,-0.01862
1.22070,0.48828,-0.48828
947178186,-1.02506,0.05236,-0.01862
0.78125,0.19531,0.24414
947183557,-1.03204,0.08726,-0.02443
0.63477,0.19531,-0.58594
947188920,-1.03320,0.11053,-0.02792
1.17188,0.63477,0.53711
```

As can be seen, the interval between samples was about 5 ms, meaning a sample rate of 200 Hz. Furthermore, the format was different (two lines for each timestamp) and some errors occurred while reading data from sensors, such as in line 9 of the proposed extract where two extra data were added after the gyroscope vector. This issue was overcome through a specific MATLAB script developed for such a purpose and reported in Appendix C. Other errors found in those files were lines without timestamp, timestamp added in random position, lines with a number of elements different from three or four, data acquisitions not composed of two consecutive lines: they were always passed over, those lines neglected and not used for retrieving data. The 200 Hz available with RealTerm are not the most appropriate sample rate for studying impacts in Judo because two acquired samples would be spaced of 5 ms: considering that impact lasts about 20 ms, the peaks values might be missed, and injury risk might be underestimated.

Moreover, an additional issue arose: the connection with a terminal different from the 3-Space Suite stopped after a random interval of acquisition, from few seconds (one or two) to tens of minutes. This is a major problem because the randomness of the acquisition duration makes Bluetooth connection useless for acquiring data in a protocol; if connection would stop after a determined interval, the protocol would have been resized in order to be entirely acquired, or it would have been split up into sub-protocols.

Presuming that the problem might be related to RealTerm, other software were searched on the net and tried out to verify if connection lasted a defined interval of time. Software and applications were searched for Windows pcs, Mac computers, Android tablets and Android smartphones. Thus, they were tested on the Asus pc listed before, on the MacBook Pro used for the first test, on a tablet Huawei MediaPad M2 (2016, Android 5.1, octa core 2.0 GHz, Bluetooth 4.0 LE/EDR), on a tablet Samsung Galaxy Tab A (2015, Android 7.1.1, quad core 1.2 GHz, Bluetooth 4.0), on a Samsung Galaxy S6 edge (2016, Android 7.0, octa core 1.6 GHz, Bluetooth 4.0 LE/EDR) and a Samsung Galaxy S7 (2017, Android 6.0.1 Marshmallow, octa core 2.0 GHz, Bluetooth 4.2 LE/EDR). Software hence exploited were the following:

- BLE Terminal;
- BlueTerm +;
- Bluetooth Terminal by Alexander Vozjennikov;
- Bluetooth Terminal by HAFTLabs;

- Bluetooth Terminal by SONWORKS;
- Bluetooth Terminal Controller (SPP Terminal);
- Communication Serial Bluetooth;
- CoolTerm.
- CuteCom;
- DTerm Open;
- FTDI UART Terminal;
- S2 Terminal for Bluetooth;
- Serial Bluetooth Terminal;
- Terminal for Bluetooth;
- TerminalBT2;
- TerminalBT3;
- VisualLogger (Terminal/Graph);
- YAT – Yet Another Terminal;

None of these software worked out for an unlimited interval of time or for a determined interval of time, but after a random duration connection stopped. A MATLAB script was developed for trying to overcome this issue, using the function `Bluetooth()` to create a Bluetooth object and connect to it. No improvements took place and recorded data were similar to the previous ones. The few lines of the script are here reported:

```
a=instrhwinfo('Bluetooth'); % get info on bluetooth devices connected to pc
a.RemoteNames;
instrhwinfo('Bluetooth','Yost_3SpaceBT-DE41'); % get info on Yost_3SpaceBT-DE41
bt1=Bluetooth('Yost_3SpaceBT-DE41',1); % Creation of the bluetooth object
bt1.RecordName='record.txt';
bt1.RecordDetail='verbose'; % write all received data
bt1.Timeout=0.001; % time to wait for data
bt1.TimerPeriod=0.001; % duration of the cycle
bt1.InputBufferSize=4096; % size of the buffer memory

fopen(bt1); % Start the bluetooth connection
record(bt1, 'on'); % record data
fprintf(bt1, ';85'); % Start command
i=0;
while i==0
    a=fscanf(bt1, '%s'); % read data
    if isempty(a)
        i=1;
    end
end
end
fprintf(bt1, ';86'); % Stop command
record(bt1, 'off');
fclose(bt1); % Close the connection
```

A last attempt was then completed employing USB cables and one of the previously cited terminal software on the MacBook Pro (CoolTerm was chosen). In this way, a sample rate of about 800 Hz was achieved, greater than previously obtained with USB and the Suite, as shown below:

```
1292085778,-0.03258,-0.00582,-0.01164
-1.23185,0.02407,0.45603
1292087109,-0.03025,-0.00931,-0.01513
-0.98525,0.38317,0.23154
1292088431,-0.03025,-0.01047,-0.01862
-1.08868,0.11632,0.70128
1292089753,-0.02676,-0.01745,-0.02443
-1.13330,0.38364,0.27672
1292091086,-0.02676,-0.01745,-0.02443
-1.03435,0.17803,0.32044
1292092416,-0.02560,-0.02676,-0.02560
-0.92981,-0.22175,0.07073
1292093739,-0.02327,-0.03607,-0.02676
```

-0.49825,0.57382,0.43824
 1292095073,-0.02327,-0.03607,-0.02676
 -0.68356,0.18807,-0.15226
 1292096404,-0.02327,-0.03956,-0.03258
 -0.92913,-0.11741,-0.02208
 1292097729,-0.02094,-0.04421,-0.03840
 -0.93894,0.68540,0.28935

In conclusion, the tests for verifying the correct functioning of the purchased sensors demonstrate the non-conformity to the specifications proposed on the datasheets in Yost Labs website and user manuals.

Three solutions were thus proposed to continue the project:

- 1) use the 50 Hz sample rate through Bluetooth connection to the Suite;
- 2) use the 200 Hz sample rate through Bluetooth connection to a terminal application;
- 3) use the 800 Hz sample rate through USB cable and terminal application.

Main aspects related to each proposal are listed in Table B.1. Considering that the Bluetooth connection could not be assumed reliable for the entire test, USB connection was chosen for performing the test, bearing in mind the presence of troubles related to cable connection.

Table B.1: Pros and cons of proposed solutions.

Proposals (sample rate, connection, software)	Pros	Cons
50 Hz, Bluetooth, Suite	- Stable connection - Ease of use	- Extremely low sample rate, not suitable for the analysis
200 Hz, Bluetooth, Terminal	- Higher sample rate - Ease of use	- Connection not stable
800 Hz, USB, Terminal	- Higher sample rate, suitable for the application - Stable connection	- Cables

Appendix C: MATLAB Scripts

C.1 ATR-Promotions data reading and elaborating

```

% Sensors data reading and elaborating if a jump is used as trigger for
starting and ending the signal record.
% by Luca Vacca
clc
clear all
close all

% Acquisition parameters
f_acc=1/0.001; % Accelerometer sampling rate (Hz)
f_mag=1/0.020; % Magnetometer sampling rate (Hz)
g=9.81; % Gravitational acceleration (m/s^2)

% Obtain organized data from accelerometers files
[DATA, L]=RSTWosens(f_acc,f_mag);

% Extraction of wanted signal and synchronization
j_ind1=find(DATA(:,2,1)<=0.01*g);
j_ind1=unique([j_ind1(1); j_ind1(diff(j_ind1)~=1); j_ind1(end)]);
j_ind2=find(DATA(:,2,2)<=0.01*g);
j_ind2=unique([j_ind2(1); j_ind2(diff(j_ind2)~=1); j_ind2(end)]);

plot(DATA(:,1,1),DATA(:,2,1)/g,'k',DATA(j_ind1,1,1),DATA(j_ind1,2,1)/g,'.r',DA
TA(:,1,2),DATA(:,2,2)/g,'b',DATA(j_ind2,1,2),DATA(j_ind2,2,2)/g,'.r')
pause()

data=zeros(size(DATA,1)-min([j_ind1(1),j_ind2(1)]),size(DATA,2),size(DATA,3));
data(:, :, 1)=DATA(j_ind1(1):end-1, :, 1);
data(1:size(DATA,1)-j_ind2(1), :, 2)=DATA(j_ind2(1):end-1, :, 2);

t=0:1/f_acc:(size(data,1)-1)/f_acc;
%% PLOT DATA GAINED FROM SENSORS
figure()
ax1=subplot(2,1,1);
plot(t,data(:,2,1)/g,'r',t,data(:,3,1)/g,'b',t,data(:,4,1)/g,'g')
title('Sensor13 (Head)'), legend('x','y','z'), grid on, xlabel('Time (s)'),
ylabel('Acceleration (g)')
ax2=subplot(2,1,2);
plot(t,data(:,2,2)/g,'r',t,data(:,3,2)/g,'b',t,data(:,4,2)/g,'g')
title('Sensor15 (Trunk)'), legend('x','y','z'), grid on, xlabel('Time (s)'),
ylabel('Acceleration (g)')
linkaxes([ax1,ax2], 'xy')

lacc_tot(:, :)=sqrt(data(:,2, :).^2+data(:,3, :).^2+data(:,4, :).^2)/g;
figure()
subplot(2,1,1)
plot(t,lacc_tot(:,1))
title('Sensor13'), grid on, xlabel('Time (s)'), ylabel('Acceleration module
(g)')
subplot(2,1,2)
plot(t,lacc_tot(:,2))
title('Sensor15'), grid on, xlabel('Time (s)'), ylabel('Acceleration module
(g)')

% Angular velocity
figure()
subplot(2,1,1)
plot(t,data(:,5,1),'r',t,data(:,6,1),'b',t,data(:,7,1),'g')
title('Sensor13'), legend('x','y','z'), grid on, xlabel('Time (s)'),
ylabel('Angular velocity (rad/s)')

```

```

subplot(2,1,2)
plot(t,data(:,5,2),'r',t,data(:,6,2),'b',t,data(:,7,2),'g')
title('Sensor15'), legend('x','y','z'), grid on, xlabel('Time (s)'),
ylabel('Angular velocity (rad/s)')

%% DATA ELABORATION
%-----
% Filter parameters for integration and differentiation
ft1=1; % start of passband zone (Hz)
ft2=50; % end of passband zone (Hz)
ord=4; % filter order
[b,a]=butter(ord,[ft1/(f_acc/2),ft2/(f_acc/2)]);
freqz(b,a,2048,2048)
% Signal to analyse
plot(data(:,2:4,1)/g),title('Choose begin and end of analysis zone: ')
coord=ginput(2);
coord=round(coord);
data=data(coord(1,1):coord(2,1),:,:);
t=t(coord(1,1):coord(2,1))-t(coord(1,1));
%-----

% Angular acceleration estimation
omega_f=filtfilt(b,a,data(:,5:7,:));
aacc=diff(omega_f)*f_acc;
aacc_tot=sqrt(aacc(:,1,:).^2+aacc(:,2,:).^2+aacc(:,3,:).^2);

figure()
subplot(2,1,1)
plot(t(1:end-1),aacc(:,1,1),'r',t(1:end-1),aacc(:,2,1),'b',t(1:end-1),aacc(:,3,1),'g')
title('Sensor13'), legend('x','y','z'), grid on, xlabel('Time (s)'),
ylabel('Angular acceleration (rad/s^2)'), axis tight
subplot(2,1,2)
plot(t(1:end-1),aacc(:,1,2),'r',t(1:end-1),aacc(:,2,2),'b',t(1:end-1),aacc(:,3,2),'g')
title('Sensor15'), legend('x','y','z'), grid on, xlabel('Time (s)'),
ylabel('Angular acceleration (rad/s^2)'), axis tight

figure()
subplot(2,1,1)
plot(t(1:end-1),aacc_tot(:,1))
title('Sensor13'), grid on, xlabel('Time (s)'), ylabel('Angular acceleration module (rad/s^2)')
subplot(2,1,2)
plot(t(1:end-1),aacc_tot(:,2))
title('Sensor15'), grid on, xlabel('Time (s)'), ylabel('Angular acceleration module (rad/s^2)')

% Angle between the two sensors
a2s=cumtrapz(t,omega_f(:, :, 2)-omega_f(:, :, 1))*180/pi;

figure()
plot(t,a2s(:,1),'r',t,a2s(:,2),'b',t,a2s(:,3),'g')
xlabel('Time (s)'), ylabel('Angle between sensors (degree)'), grid on,
legend('x','y','z')

```

C.2 Function for reading ATR-Promotions .csv files

```

function [matr] = readsensor_new_lg(filename,facc,fmag)

% Function to read .csv file from inertial sensor and create a matrix
% [time accx accy accz omegax omegay omegaz magx magy magz].
% Acceleration data are in m/s^2, angular velocity omega in rad/s, mag in
microTesla.
% CSV files begin with acceleration or magnetometer: rows must be read
% carefully and well organized.
% Sampling frequencies are used to give a matrix with all corresponding
% values of magnetometer even if its samplig frequency is lower than the
% one of the accelerometer (interpolation is used to increase number of
% samples)
% Prototype: [matr] = readsensor_new_lg(filename,facc,fmag)
% Input:      filename = Name of the .csv file to be read
%            facc = Accelerometer sampling rate (Hz)
%            fmag = Magnetometer sampling rate (Hz)
% Output:     matr = [time accx accy accz omegax omegay omegaz magx magy magz]

Sensor=csvread(char(filename),0,1); % file reading
flag=0;
index=1;

% CSV file has seven column of numbers: excluding the first which is time,
% if last three are zero than data from magnetometer are reported,
% otherwise data from accelerometer are presented
while flag==0
    if Sensor(index,5)== 0 && Sensor(index,6)==0 && Sensor (index,7)==0
        index=index+1;
    else
        flag=1;
    end
end

j=1;
k=1;
for i=index:1:size(Sensor(:,1)) % start reading from first acceleration data
found previously
    if Sensor(i,5)== 0 && Sensor(i,6)==0 && Sensor (i,7)==0 % Magnetometer
data
        tmag(j)=Sensor(i,1);
        mag_x0(j)=Sensor(i,2);
        mag_y0(j)=Sensor(i,3);
        mag_z0(j)=Sensor(i,4);
        j=j+1;
    else % Accelerometer data
        tacc(k)=Sensor(i,1);
        acc_x0(k)=Sensor(i,2);
        acc_y0(k)=Sensor(i,3);
        acc_z0(k)=Sensor(i,4);
        omega_x0(k)=Sensor(i,5);
        omega_y0(k)=Sensor(i,6);
        omega_z0(k)=Sensor(i,7);
        k=k+1;
    end
end

% conversion of acc to m/s^2, angular velocity omega to dps, mag to microTesla
acc_x_Mob=acc_x0.*0.001;
acc_y_Mob=acc_y0.*0.001;
acc_z_Mob=acc_z0.*0.001;
omega_x_Mob=omega_x0.*0.01;
omega_y_Mob=omega_y0.*0.01;
omega_z_Mob=omega_z0.*0.01;
mag_x_Mob=mag_x0.*0.1;
mag_y_Mob=mag_y0.*0.1;

```

```
mag_z_Mob=mag_z0.*0.1;
time=tacc;

acc_Mob=[acc_x_Mob' acc_y_Mob' acc_z_Mob'];
omega_Mob=[omega_x_Mob' omega_y_Mob' omega_z_Mob']*(pi/180);
mag_Mob_temp=[mag_x_Mob' mag_y_Mob' mag_z_Mob'];
mag_Mob=resample(mag_Mob_temp,facc,fmag); % Resampling to obtain the same
number of samples for acc and mag

% Data organization for being all of the same length for matrix construction
if size(acc_Mob,1)> size(mag_Mob,1)
    aaa=size(mag_Mob,1);
    acc_Mob= acc_Mob(1:aaa,:);
    omega_Mob=omega_Mob(1:aaa,:);
    time=time(1:aaa);
end
if size(acc_Mob,1)< size(mag_Mob,1)
    bbb=size(acc_Mob,1);
    mag_Mob= mag_Mob(1:bbb,:);
    omega_Mob=omega_Mob(1:bbb,:);
    time=time(1:bbb);
end

matr=[time' acc_Mob omega_Mob mag_Mob];
end
```

C.3 Specific function for reading and synchronize data from two ATR-Promotions sensors

```
function [SENSORS_DATA, LIST] = RSTWosens(f_acc,f_mag,n1)

% Function to Read and Synchronize data from TWO inertial sensors. CSV files
% must be in the same directory of the script, files are alphabetically
% ordered and the ones read are
% the n1 file and the corresponding file of other sensor. Information about
% files read are
% returned in LIST
%
% Prototype: SENSORS_DATA = RSTWosens(f_acc,f_mag,n1)
% Input:     f_acc = Accelerometer sampling rate (Hz)
%           f_mag = Magnetometer sampling rate (Hz)
%           n1 = first file to be read (optionally, default value is 1 so the
% first file for each sensor is read)
% Output:    SENSORS_DATA = [time acc_x acc_y acc_z omega_x omega_y omega_z
% mag_x mag_y mag_z], third dimensions is sensor number
%           LIST = list of .csv files to be read in the script directory
% by Luca Vacca

% DATA READING
dati_imuPath = cd('.'); % identify the script path
LIST=dir('*.csv'); % List all .csv files in the folder, files will be listed
in crescent order following sensor number
if nargin<3
    n1=1;
end
n2=size(LIST,1)/2+n1;

trial1name=char(LIST(n1).name);
trial2name=char(LIST(n2).name);
LIST=LIST([n1,n2]);
% Reading data to obtain [time acc_x acc_y acc_z omega_x omega_y
% omega_z mag_x mag_y mag_z]
[trial01raw]=readsensor_new_lg(fullfile(dati_imuPath,trial1name),f_acc,f_mag);
[trial02raw]=readsensor_new_lg(fullfile(dati_imuPath,trial2name),f_acc,f_mag);

%DATA SINCHRONIZATION
trialtime01=trial01raw(:,1)*0.1; % to obtain a float number
trialtime01=round(trialtime01);
trialtime01ini=round(trialtime01(1,1)); % to get the temporal succession
trialtime02=trial02raw(:,1)*0.1; % to obtain a float number
trialtime02=round(trialtime02);
trialtime02ini=round(trialtime02(1,1)); % to get the temporal succession

trialtimeini=max([trialtime01ini trialtime02ini]);
if trialtimeini==trialtime02ini
    flag=0;
    while flag==0
        [trial01detx]=find(trialtime01==trialtimeini); % initial time
coordinates
        if isempty(trial01detx)==1
            trialtimeini=trialtimeini+1;
        else
            flag=1;
        end
    end
    trial01rawl=trial01raw(trial01detx:end, 2:end);
    trial02rawl=trial02raw(:, 2:end);
else
    flag=0;
    while flag==0
        [trial02detx]=find(trialtime02==trialtimeini); % initial time
coordinates
```

```
        if isempty(trial02detx)==1
            trialtimeini=trialtimeini+1;
        else
            flag=1;
        end
    end
    trial01rawl=trial01raw(:, 2:end);
    trial02rawl=trial02raw(trial02detx:end, 2:end);
end
% obtain same size matrices
s=min([size(trial01rawl,1) size(trial02rawl,1)]);
trial01=trial01rawl(1:s,:);
trial02=trial02rawl(1:s,:);

% Time vector
t=(1:size(trial01,1))/f_acc;

% DATA MATRIX CONSTRUCTION
SENSORS_DATA(:, :, 1)=[t' trial01(:, :)];
SENSORS_DATA(:, :, 2)=[t' trial02(:, :)];
end
```

C.4 Script used for Section 5 Breakfall Techniques Analysis

```

clc
clear all
close all

% DATA LOADING
d1=load('ukemi_final1.mat'); % day 1
data1=d1.alldata; % sample * data(10 columns) * sensor number(1 or 2) *
condition(1=standard or 2=no hands)
t1=d1.allt;
d2=load('ukemi_final2.mat'); % day 2
data2=d2.alldata; % sample * data(10 columns) * sensor number(1 or 2) *
condition(1=standard or 2=no hands)
t2=d2.allt;
d3=load('ukemi_final3.mat'); % day 3
data3=d3.alldata; % sample * data(10 columns) * sensor number(1 or 2) *
condition(1=standard or 2=no hands)
t3=d3.allt;

% Parameters
f_acc=1000; %Hz
g=9.81; %m/s^2
nu=30; % total number of performed ukemi

% Moving averaging parameter
coeff=201-1;
b=ones(coeff,1)/coeff;
a=1;

% Filter parameters for integration and differentiation
ft1=1; % start of passband zone (Hz)
ft2=50; % end of passband zone (Hz)
ord=2; % filter order
[bb,aa]=butter(ord,[ft1/(f_acc/2),ft2/(f_acc/2)]);

% DATA ORGANIZATION
data1(:,2:4,:,:) = data1(:,2:4,:,:)/g;
data2(:,2:4,:,:) = data2(:,2:4,:,:)/g;
data3(:,2:4,:,:) = data3(:,2:4,:,:)/g;
data=cat(1,data1,data2,data3);
%data=cat(1,data2,data3);
t=0:1/f_acc:(size(data,1)-1)/f_acc;

%% DAY 1-2-3 ANALYSIS

figure()
s1=subplot(2,2,1);
plot(t,data(:,2,1,1),'r',t,data(:,3,1,1),'b',t,data(:,4,1,1),'g'),title('Stand
ard Ukemi - HEAD')
ylabel('Acceleration (g)'), xlabel('Time (s)'), grid
on,legend('x','y','z','Location','best')
s3=subplot(2,2,3);
plot(t,data(:,2,2,1),'r',t,data(:,3,2,1),'b',t,data(:,4,1,1),'g'),title('Stand
ard Ukemi - TRUNK')
ylabel('Acceleration (g)'), xlabel('Time (s)'), grid on
s2=subplot(2,2,2);
plot(t,data(:,2,1,2),'r',t,data(:,3,1,2),'b',t,data(:,4,1,2),'g'),title('No
Hands Ukemi - HEAD')
ylabel('Acceleration (g)'), xlabel('Time (s)'), grid on
s4=subplot(2,2,4);
plot(t,data(:,2,2,2),'r',t,data(:,3,2,2),'b',t,data(:,4,2,2),'g'),title('No
Hands Ukemi - TRUNK')
ylabel('Acceleration (g)'), xlabel('Time (s)'), grid on
linkaxes([s1 s3],'x'),linkaxes([s2 s4],'x')
annotation('textbox',[0 0 1 1],'String','DAY 1-2-3','FontSize',14,
'FontWeight','bold','EdgeColor','none','HorizontalAlignment','center')

```

```

acc_module=sqrt(data(:,2,:,:) .^2+data(:,3,:,:) .^2+data(:,4,:,:) .^2);
omega_module=sqrt(data(:,5,:,:) .^2+data(:,6,:,:) .^2+data(:,7,:,:) .^2);

% STANDARD UKEMI
% Find epochs of the signal by the use of a prototype signal portion
acc_module_s_f=filtfilt(b,a,acc_module(:,:,:),1));
PS=5000; % prototype ukemi starting point
PE=8000; % prototype ukemi ending point
findsignal(acc_module_s_f(:,:,:),1),acc_module_s_f(PS:PE,:,:),1), 'Metric', 'euclidean',
'MaxNumSegments', nu);
[first_s,last_s]=findsignal(acc_module_s_f(:,:,:),1),acc_module_s_f(PS:PE,:,:),1), 'Metric', 'euclidean', 'MaxNumSegments', nu);

figure()
for i=1:length(first_s) % for each epoch
    s_epoch(:,:,:,1,i)=data(first_s(i):last_s(i),:,:,:),1);% sample * data(10
columns) * sensor number(1 or 2) * condition(1=standard or 2=no hands) *
epoch(1to30)
    acc_module_epoch(:,:,:,1,i)=acc_module(first_s(i):last_s(i),:,:,:),1);
    omega_module_epoch(:,:,:,1,i)=omega_module(first_s(i):last_s(i),:,:,:),1);
    s_epoch_f(:,:,:,1,i)=filtfilt(bb,aa,s_epoch(:,:,:,1,i));
    aacc_epoch(:,:,:,1,i)=diff(s_epoch_f(:,5:7,:,:),1,i))*f_acc;

aacc_module_epoch(:,:,:,1,i)=sqrt(aacc_epoch(:,1,:,:),1,i).^2+aacc_epoch(:,2,:,:),1,
i).^2+aacc_epoch(:,3,:,:),1,i).^2);
    a2s_epoch(:,:,:,1,i)=cumtrapz(t(1:PE-PS+1),s_epoch_f(:,5:7,2,1,i))-
s_epoch_f(:,5:7,1,1,i))*180/pi;

    subplot(2,1,1)
    plot(t(1:PE-PS+1),s_epoch(:,2,1,1,i)),hold on
end
mean_data(:,:,:,1)=mean(s_epoch(:,:,:,1,:),5);
std_data(:,:,:,1)=std(s_epoch(:,:,:,1,:),0,5);
plot(t(1:PE-PS+1),mean_data(:,2,1,1),'k','LineWidth',1.5)
hold off
subplot(2,1,2)
plot(t(1:PE-PS+1),std_data(:,2,1,1),'k','LineWidth',1.5)

mean_acc_module(:,:,:,1)=mean(acc_module_epoch(:,:,:,1,:),5);
std_acc_module(:,:,:,1)=std(acc_module_epoch(:,:,:,1,:),0,5);
mean_omega_module(:,:,:,1)=mean(omega_module_epoch(:,:,:,1,:),5);
std_omega_module(:,:,:,1)=std(omega_module_epoch(:,:,:,1,:),0,5);
mean_aacc(:,:,:,1)=mean(aacc_epoch(:,:,:,1,:),5);
std_aacc(:,:,:,1)=std(aacc_epoch(:,:,:,1,:),0,5);
mean_aacc_module(:,:,:,1)=mean(aacc_module_epoch(:,:,:,1,:),5);
std_aacc_module(:,:,:,1)=std(aacc_module_epoch(:,:,:,1,:),0,5);
mean_a2s(:,:,:,1)=mean(a2s_epoch(:,:,:,1,:),5);
std_a2s(:,:,:,1)=std(a2s_epoch(:,:,:,1,:),0,5);
% NO-HANDS UKEMI
% Find epochs of the signal by the use of a prototype signal portion
acc_module_nh_f=filtfilt(b,a,acc_module(:,:,:),2));
PS=5000; % prototype ukemi starting point
PE=8000; % prototype ukemi ending point
findsignal(acc_module_nh_f(:,:,:),1),acc_module_nh_f(PS:PE,:,:),1), 'Metric', 'euclidean',
'MaxNumSegments', nu);
[first_nh,last_nh]=findsignal(acc_module_nh_f(:,:,:),1),acc_module_nh_f(PS:PE,:,:),1),
'Metric', 'euclidean', 'MaxNumSegments', nu);

figure()
for i=1:length(first_nh) % for each epoch
    s_epoch(:,:,:,2,i)=data(first_nh(i):last_nh(i),:,:,:),2);
    acc_module_epoch(:,:,:,2,i)=acc_module(first_nh(i):last_nh(i),:,:,:),2);
    omega_module_epoch(:,:,:,2,i)=omega_module(first_nh(i):last_nh(i),:,:,:),2);
    s_epoch_f(:,:,:,2,i)=filtfilt(bb,aa,s_epoch(:,:,:,2,i));
    aacc_epoch(:,:,:,2,i)=diff(s_epoch_f(:,5:7,:,:),2,i))*f_acc;

aacc_module_epoch(:,:,:,2,i)=sqrt(aacc_epoch(:,1,:,:),2,i).^2+aacc_epoch(:,2,:,:),2,
i).^2+aacc_epoch(:,3,:,:),2,i).^2);

```

```

    a2s_epoch(:,:,:,2,i)=cumtrapz(t(1:PE-PS+1),s_epoch_f(:,5:7,2,2,i)-
s_epoch_f(:,5:7,1,2,i))*180/pi;

    subplot(2,1,1)
    plot(t(1:PE-PS+1),s_epoch(:,2,1,2,i)),hold on
end
mean_data(:,:,:,2)=mean(s_epoch(:,:,:,2,:),5);
std_data(:,:,:,2)=std(s_epoch(:,:,:,2,:),0,5);
plot(t(1:PE-PS+1),mean_data(:,2,1,2),'k','LineWidth',1.5),hold off
subplot(2,1,2)
plot(t(1:PE-PS+1),std_data(:,2,1,2),'k','LineWidth',1.5)

mean_acc_module(:,:,:,2)=mean(acc_module_epoch(:,:,:,2,:),5);
std_acc_module(:,:,:,2)=std(acc_module_epoch(:,:,:,2,:),0,5);
mean_omega_module(:,:,:,2)=mean(omega_module_epoch(:,:,:,2,:),5);
std_omega_module(:,:,:,2)=std(omega_module_epoch(:,:,:,2,:),0,5);
mean_aacc(:,:,:,2)=mean(aacc_epoch(:,:,:,2,:),5);
std_aacc(:,:,:,2)=std(aacc_epoch(:,:,:,2,:),0,5);
mean_aacc_module(:,:,:,2)=mean(aacc_module_epoch(:,:,:,2,:),5);
std_aacc_module(:,:,:,2)=std(aacc_module_epoch(:,:,:,2,:),0,5);
mean_a2s(:,:,:,2)=mean(a2s_epoch(:,:,:,2,:),5);
std_a2s(:,:,:,2)=std(a2s_epoch(:,:,:,2,:),0,5);

%% GRAPHIC COMPARISON
figure() % acc,head
s1=subplot(4,2,1);
plot(t(1:PE-PS+1),mean_data(:,2,1,1),'r',t(1:PE-
PS+1),mean_data(:,2,1,1)+std_data(:,2,1,1),'k',t(1:PE-
PS+1),mean_data(:,2,1,1)-std_data(:,2,1,1),'k')
title('Standard Ukemi: X-axis acceleration (g)'), xlabel('Time (s)'),grid on
s3=subplot(4,2,3);
plot(t(1:PE-PS+1),mean_data(:,3,1,1),'b',t(1:PE-
PS+1),mean_data(:,3,1,1)+std_data(:,3,1,1),'k',t(1:PE-
PS+1),mean_data(:,3,1,1)-std_data(:,3,1,1),'k')
title('Standard Ukemi: Y-axis acceleration (g)'), xlabel('Time (s)'),grid on
s5=subplot(4,2,5);
plot(t(1:PE-PS+1),mean_data(:,4,1,1),'g',t(1:PE-
PS+1),mean_data(:,4,1,1)+std_data(:,4,1,1),'k',t(1:PE-
PS+1),mean_data(:,4,1,1)-std_data(:,4,1,1),'k')
title('Standard Ukemi: Z-axis acceleration (g)'), xlabel('Time (s)'),grid on
s7=subplot(4,2,7);
plot(t(1:PE-PS+1),mean_acc_module(:, :, 1, 1),t(1:PE-
PS+1),mean_acc_module(:, :, 1, 1)+std_acc_module(:, :, 1, 1),'k',t(1:PE-
PS+1),mean_acc_module(:, :, 1, 1)-std_acc_module(:, :, 1, 1),'k')
title('Standard Ukemi: acceleration module (g)'), xlabel('Time (s)'),grid on
s2=subplot(4,2,2);
plot(t(1:PE-PS+1),mean_data(:,2,1,2),'r',t(1:PE-
PS+1),mean_data(:,2,1,2)+std_data(:,2,1,2),'k',t(1:PE-
PS+1),mean_data(:,2,1,2)-std_data(:,2,1,2),'k')
title('No-hands Ukemi: X-axis acceleration (g)'), xlabel('Time (s)'),grid on
s4=subplot(4,2,4);
plot(t(1:PE-PS+1),mean_data(:,3,1,2),'b',t(1:PE-
PS+1),mean_data(:,3,1,2)+std_data(:,3,1,2),'k',t(1:PE-
PS+1),mean_data(:,3,1,2)-std_data(:,3,1,2),'k')
title('No-hands Ukemi: Y-axis acceleration (g)'), xlabel('Time (s)'),grid on
s6=subplot(4,2,6);
plot(t(1:PE-PS+1),mean_data(:,4,1,2),'g',t(1:PE-
PS+1),mean_data(:,4,1,2)+std_data(:,4,1,2),'k',t(1:PE-
PS+1),mean_data(:,4,1,2)-std_data(:,4,1,2),'k')
title('No-hands Ukemi: Z-axis acceleration (g)'), xlabel('Time (s)'),grid on
s8=subplot(4,2,8);
plot(t(1:PE-PS+1),mean_acc_module(:, :, 1, 2),t(1:PE-
PS+1),mean_acc_module(:, :, 1, 2)+std_acc_module(:, :, 1, 2),'k',t(1:PE-
PS+1),mean_acc_module(:, :, 1, 2)-std_acc_module(:, :, 1, 2),'k')
title('No-hands Ukemi: acceleration module (g)'), xlabel('Time (s)'),grid on
annotation('textbox', [0 0 1 1], 'String', 'MEAN VALUE \pm STANDARD DEVIATION
- HEAD ACCELERATION', 'FontSize', 14, 'FontWeight', 'bold', 'EdgeColor',
'none', 'HorizontalAlignment', 'center')

```

```

linkaxes([s1,s3,s5,s7], 'x'), linkaxes([s2,s4,s6,s8], 'x')
savefig('HEAD ACCELERATION.fig')

figure() % acc, trunk
s1=subplot(4,2,1);
plot(t(1:PE-PS+1),mean_data(:,2,2,1), 'r', t(1:PE-
PS+1),mean_data(:,2,2,1)+std_data(:,2,2,1), 'k', t(1:PE-
PS+1),mean_data(:,2,2,1)-std_data(:,2,2,1), 'k')
title('Standard Ukemi: X-axis acceleration (g)'), xlabel('Time (s)'),grid on
s3=subplot(4,2,3);
plot(t(1:PE-PS+1),mean_data(:,3,2,1), 'b', t(1:PE-
PS+1),mean_data(:,3,2,1)+std_data(:,3,2,1), 'k', t(1:PE-
PS+1),mean_data(:,3,2,1)-std_data(:,3,2,1), 'k')
title('Standard Ukemi: Y-axis acceleration (g)'), xlabel('Time (s)'),grid on
s5=subplot(4,2,5);
plot(t(1:PE-PS+1),mean_data(:,4,2,1), 'g', t(1:PE-
PS+1),mean_data(:,4,2,1)+std_data(:,4,2,1), 'k', t(1:PE-
PS+1),mean_data(:,4,2,1)-std_data(:,4,2,1), 'k')
title('Standard Ukemi: Z-axis acceleration (g)'), xlabel('Time (s)'),grid on
s7=subplot(4,2,7);
plot(t(1:PE-PS+1),mean_acc_module(:, :, 2, 1), t(1:PE-
PS+1),mean_acc_module(:, :, 2, 1)+std_acc_module(:, :, 2, 1), 'k', t(1:PE-
PS+1),mean_acc_module(:, :, 2, 1)-std_acc_module(:, :, 2, 1), 'k')
title('Standard Ukemi: acceleration module (g)'), xlabel('Time (s)'),grid on
s2=subplot(4,2,2);
plot(t(1:PE-PS+1),mean_data(:,2,2,2), 'r', t(1:PE-
PS+1),mean_data(:,2,2,2)+std_data(:,2,2,2), 'k', t(1:PE-
PS+1),mean_data(:,2,2,2)-std_data(:,2,2,2), 'k')
title('No-hands Ukemi: X-axis acceleration (g)'), xlabel('Time (s)'),grid on
s4=subplot(4,2,4);
plot(t(1:PE-PS+1),mean_data(:,3,2,2), 'b', t(1:PE-
PS+1),mean_data(:,3,2,2)+std_data(:,3,2,2), 'k', t(1:PE-
PS+1),mean_data(:,3,2,2)-std_data(:,3,2,2), 'k')
title('No-hands Ukemi: Y-axis acceleration (g)'), xlabel('Time (s)'),grid on
s6=subplot(4,2,6);
plot(t(1:PE-PS+1),mean_data(:,4,2,2), 'g', t(1:PE-
PS+1),mean_data(:,4,2,2)+std_data(:,4,2,2), 'k', t(1:PE-
PS+1),mean_data(:,4,2,2)-std_data(:,4,2,2), 'k')
title('No-hands Ukemi: Z-axis acceleration (g)'), xlabel('Time (s)'),grid on
s8=subplot(4,2,8);
plot(t(1:PE-PS+1),mean_acc_module(:, :, 2, 2), t(1:PE-
PS+1),mean_acc_module(:, :, 2, 2)+std_acc_module(:, :, 2, 2), 'k', t(1:PE-
PS+1),mean_acc_module(:, :, 2, 2)-std_acc_module(:, :, 2, 2), 'k')
title('No-hands Ukemi: acceleration module (g)'), xlabel('Time (s)'),grid on
annotation('textbox', [0 0 1 1], 'String', 'MEAN VALUE \pm STANDARD DEVIATION
- TRUNK ACCELERATION', 'FontSize', 14, 'FontWeight', 'bold', 'EdgeColor',
'none', 'HorizontalAlignment', 'center')
linkaxes([s1,s3,s5,s7], 'x'), linkaxes([s2,s4,s6,s8], 'x')
savefig('TRUNK ACCELERATION.fig')

figure() % omega, head
s1=subplot(4,2,1);
plot(t(1:PE-PS+1),mean_data(:,5,1,1), 'r', t(1:PE-
PS+1),mean_data(:,5,1,1)+std_data(:,5,1,1), 'k', t(1:PE-
PS+1),mean_data(:,5,1,1)-std_data(:,5,1,1), 'k')
title('Standard Ukemi: X-axis angular velocity (rad/s)'), xlabel('Time
(s)'),grid on
s3=subplot(4,2,3);
plot(t(1:PE-PS+1),mean_data(:,6,1,1), 'b', t(1:PE-
PS+1),mean_data(:,6,1,1)+std_data(:,6,1,1), 'k', t(1:PE-
PS+1),mean_data(:,6,1,1)-std_data(:,6,1,1), 'k')
title('Standard Ukemi: Y-axis angular velocity (rad/s)'), xlabel('Time
(s)'),grid on
s5=subplot(4,2,5);
plot(t(1:PE-PS+1),mean_data(:,7,1,1), 'g', t(1:PE-
PS+1),mean_data(:,7,1,1)+std_data(:,7,1,1), 'k', t(1:PE-
PS+1),mean_data(:,7,1,1)-std_data(:,7,1,1), 'k')
title('Standard Ukemi: Z-axis angular velocity (rad/s)'), xlabel('Time
(s)'),grid on

```

```

s7=subplot(4,2,7);
plot(t(1:PE-PS+1),mean_omega_module(:,:,1,1),t(1:PE-
PS+1),mean_omega_module(:,:,1,1)+std_omega_module(:,:,1,1),'k',t(1:PE-
PS+1),mean_omega_module(:,:,1,1)-std_omega_module(:,:,1,1),'k')
title('Standard Ukemi: angular velocity module (rad/s)'), xlabel('Time
(s)'),grid on
s2=subplot(4,2,2);
plot(t(1:PE-PS+1),mean_data(:,5,1,2),'r',t(1:PE-
PS+1),mean_data(:,5,1,2)+std_data(:,5,1,2),'k',t(1:PE-
PS+1),mean_data(:,5,1,2)-std_data(:,5,1,2),'k')
title('No-hands Ukemi: X-axis angular velocity (rad/s)'), xlabel('Time
(s)'),grid on
s4=subplot(4,2,4);
plot(t(1:PE-PS+1),mean_data(:,6,1,2),'b',t(1:PE-
PS+1),mean_data(:,6,1,2)+std_data(:,6,1,2),'k',t(1:PE-
PS+1),mean_data(:,6,1,2)-std_data(:,6,1,2),'k')
title('No-hands Ukemi: Y-axis angular velocity (rad/s)'), xlabel('Time
(s)'),grid on
s6=subplot(4,2,6);
plot(t(1:PE-PS+1),mean_data(:,7,1,2),'g',t(1:PE-
PS+1),mean_data(:,7,1,2)+std_data(:,7,1,2),'k',t(1:PE-
PS+1),mean_data(:,7,1,2)-std_data(:,7,1,2),'k')
title('No-hands Ukemi: Z-axis angular velocity (rad/s)'), xlabel('Time
(s)'),grid on
s8=subplot(4,2,8);
plot(t(1:PE-PS+1),mean_omega_module(:,:,1,2),t(1:PE-
PS+1),mean_omega_module(:,:,1,2)+std_omega_module(:,:,1,2),'k',t(1:PE-
PS+1),mean_omega_module(:,:,1,2)-std_omega_module(:,:,1,2),'k')
title('No-hands Ukemi: angular velocity module (rad/s)'), xlabel('Time
(s)'),grid on
annotation('textbox', [0 0 1 1], 'String', 'MEAN VALUE \pm STANDARD DEVIATION
- HEAD ANGULAR VELOCITY','FontSize', 14, 'FontWeight', 'bold', 'EdgeColor',
'none', 'HorizontalAlignment', 'center')
linkaxes([s1,s3,s5,s7],'x'),linkaxes([s2,s4,s6,s8],'x')
savefig('HEAD ANGULAR VELOCITY.fig')

figure() % omega,trunk
s1=subplot(4,2,1);
plot(t(1:PE-PS+1),mean_data(:,5,2,1),'r',t(1:PE-
PS+1),mean_data(:,5,2,1)+std_data(:,5,2,1),'k',t(1:PE-
PS+1),mean_data(:,5,2,1)-std_data(:,5,2,1),'k')
title('Standard Ukemi: X-axis angular velocity (rad/s)'), xlabel('Time
(s)'),grid on
s3=subplot(4,2,3);
plot(t(1:PE-PS+1),mean_data(:,6,2,1),'b',t(1:PE-
PS+1),mean_data(:,6,2,1)+std_data(:,6,2,1),'k',t(1:PE-
PS+1),mean_data(:,6,2,1)-std_data(:,6,2,1),'k')
title('Standard Ukemi: Y-axis angular velocity (rad/s)'), xlabel('Time
(s)'),grid on
s5=subplot(4,2,5);
plot(t(1:PE-PS+1),mean_data(:,7,2,1),'g',t(1:PE-
PS+1),mean_data(:,7,2,1)+std_data(:,7,2,1),'k',t(1:PE-
PS+1),mean_data(:,7,2,1)-std_data(:,7,2,1),'k')
title('Standard Ukemi: Z-axis angular velocity (rad/s)'), xlabel('Time
(s)'),grid on
s7=subplot(4,2,7);
plot(t(1:PE-PS+1),mean_omega_module(:,:,2,1),t(1:PE-
PS+1),mean_omega_module(:,:,2,1)+std_omega_module(:,:,2,1),'k',t(1:PE-
PS+1),mean_omega_module(:,:,2,1)-std_omega_module(:,:,2,1),'k')
title('Standard Ukemi: angular velocity module (rad/s)'), xlabel('Time
(s)'),grid on
s2=subplot(4,2,2);
plot(t(1:PE-PS+1),mean_data(:,5,2,2),'r',t(1:PE-
PS+1),mean_data(:,5,2,2)+std_data(:,5,2,2),'k',t(1:PE-
PS+1),mean_data(:,5,2,2)-std_data(:,5,2,2),'k')
title('No-hands Ukemi: X-axis angular velocity (rad/s)'), xlabel('Time
(s)'),grid on
s4=subplot(4,2,4);

```

```

plot(t(1:PE-PS+1),mean_data(:,6,2,2),'b',t(1:PE-
PS+1),mean_data(:,6,2,2)+std_data(:,6,2,2),'k',t(1:PE-
PS+1),mean_data(:,6,2,2)-std_data(:,6,2,2),'k')
title('No-hands Ukemi: Y-axis angular velocity (rad/s)'), xlabel('Time
(s)'),grid on
s6=subplot(4,2,6);
plot(t(1:PE-PS+1),mean_data(:,7,2,2),'g',t(1:PE-
PS+1),mean_data(:,7,2,2)+std_data(:,7,2,2),'k',t(1:PE-
PS+1),mean_data(:,7,2,2)-std_data(:,7,2,2),'k')
title('No-hands Ukemi: Z-axis angular velocity (rad/s)'), xlabel('Time
(s)'),grid on
s8=subplot(4,2,8);
plot(t(1:PE-PS+1),mean_omega_module(:, :,2,2),t(1:PE-
PS+1),mean_omega_module(:, :,2,2)+std_omega_module(:, :,2,2),'k',t(1:PE-
PS+1),mean_omega_module(:, :,2,2)-std_omega_module(:, :,2,2),'k')
title('No-hands Ukemi: angular velocity module (rad/s)'), xlabel('Time
(s)'),grid on
annotation('textbox', [0 0 1 1], 'String', 'MEAN VALUE \pm STANDARD DEVIATION
- TRUNK ANGULAR VELOCITY','FontSize', 14, 'FontWeight', 'bold', 'EdgeColor',
'none', 'HorizontalAlignment', 'center')
linkaxes([s1,s3,s5,s7], 'x'),linkaxes([s2,s4,s6,s8], 'x')
savefig('TRUNK ANGULAR VELOCITY.fig')

figure() % angular acceleration,head
s1=subplot(4,2,1);
plot(t(1:PE-PS),mean_aacc(:,1,1,1),'r',t(1:PE-
PS),mean_aacc(:,1,1,1)+std_aacc(:,1,1,1),'k',t(1:PE-PS),mean_aacc(:,1,1,1)-
std_aacc(:,1,1,1),'k')
title('Standard Ukemi: X-axis angular acceleration (rad/s^2)'), xlabel('Time
(s)'),grid on
s3=subplot(4,2,3);
plot(t(1:PE-PS),mean_aacc(:,2,1,1),'b',t(1:PE-
PS),mean_aacc(:,2,1,1)+std_aacc(:,2,1,1),'k',t(1:PE-PS),mean_aacc(:,2,1,1)-
std_aacc(:,2,1,1),'k')
title('Standard Ukemi: Y-axis angular acceleration (rad/s^2)'), xlabel('Time
(s)'),grid on
s5=subplot(4,2,5);
plot(t(1:PE-PS),mean_aacc(:,3,1,1),'g',t(1:PE-
PS),mean_aacc(:,3,1,1)+std_aacc(:,3,1,1),'k',t(1:PE-PS),mean_aacc(:,3,1,1)-
std_aacc(:,3,1,1),'k')
title('Standard Ukemi: Z-axis angular acceleration (rad/s^2)'), xlabel('Time
(s)'),grid on
s7=subplot(4,2,7);
plot(t(1:PE-PS),mean_aacc_module(:, :,1,1),t(1:PE-
PS),mean_aacc_module(:, :,1,1)+std_aacc_module(:, :,1,1),'k',t(1:PE-
PS),mean_aacc_module(:, :,1,1)-std_aacc_module(:, :,1,1),'k')
title('Standard Ukemi: angular acceleration module (rad/s^2)'), xlabel('Time
(s)'),grid on
s2=subplot(4,2,2);
plot(t(1:PE-PS),mean_aacc(:,1,1,2),'r',t(1:PE-
PS),mean_aacc(:,1,1,2)+std_aacc(:,1,1,2),'k',t(1:PE-PS),mean_aacc(:,1,1,2)-
std_aacc(:,1,1,2),'k')
title('No-hands Ukemi: X-axis angular acceleration (rad/s^2)'), xlabel('Time
(s)'),grid on
s4=subplot(4,2,4);
plot(t(1:PE-PS),mean_aacc(:,2,1,2),'b',t(1:PE-
PS),mean_aacc(:,2,1,2)+std_aacc(:,2,1,2),'k',t(1:PE-PS),mean_aacc(:,2,1,2)-
std_aacc(:,2,1,2),'k')
title('No-hands Ukemi: Y-axis angular acceleration (rad/s^2)'), xlabel('Time
(s)'),grid on
s6=subplot(4,2,6);
plot(t(1:PE-PS),mean_aacc(:,3,1,2),'g',t(1:PE-
PS),mean_aacc(:,3,1,2)+std_aacc(:,3,1,2),'k',t(1:PE-PS),mean_aacc(:,3,1,2)-
std_aacc(:,3,1,2),'k')
title('No-hands Ukemi: Z-axis angular acceleration (rad/s^2)'), xlabel('Time
(s)'),grid on
s8=subplot(4,2,8);

```

```

plot(t(1:PE-PS),mean_aacc_module(:,:,1,2),t(1:PE-
PS),mean_aacc_module(:,:,1,2)+std_aacc_module(:,:,1,2),'k',t(1:PE-
PS),mean_aacc_module(:,:,1,2)-std_aacc_module(:,:,1,2),'k')
title('No-hands Ukemi: angular acceleration module (rad/s^2)'), xlabel('Time
(s)'),grid on
annotation('textbox', [0 0 1 1], 'String', 'MEAN VALUE \pm STANDARD DEVIATION
- HEAD ANGULAR ACCELERATION','FontSize', 14, 'FontWeight', 'bold',
'EdgeColor', 'none', 'HorizontalAlignment', 'center')
linkaxes([s1,s3,s5,s7],'x'),linkaxes([s2,s4,s6,s8],'x')
savefig('HEAD ANGULAR ACCELERATION.fig')

figure() % angular acceleration,trunk
s1=subplot(4,2,1);
plot(t(1:PE-PS),mean_aacc(:,1,2,1),'r',t(1:PE-
PS),mean_aacc(:,1,2,1)+std_aacc(:,1,2,1),'k',t(1:PE-PS),mean_aacc(:,1,2,1)-
std_aacc(:,1,2,1),'k')
title('Standard Ukemi: X-axis angular acceleration (rad/s^2)'), xlabel('Time
(s)'),grid on
s3=subplot(4,2,3);
plot(t(1:PE-PS),mean_aacc(:,2,2,1),'b',t(1:PE-
PS),mean_aacc(:,2,2,1)+std_aacc(:,2,2,1),'k',t(1:PE-PS),mean_aacc(:,2,2,1)-
std_aacc(:,2,2,1),'k')
title('Standard Ukemi: Y-axis angular acceleration (rad/s^2)'), xlabel('Time
(s)'),grid on
s5=subplot(4,2,5);
plot(t(1:PE-PS),mean_aacc(:,3,2,1),'g',t(1:PE-
PS),mean_aacc(:,3,2,1)+std_aacc(:,3,2,1),'k',t(1:PE-PS),mean_aacc(:,3,2,1)-
std_aacc(:,3,2,1),'k')
title('Standard Ukemi: Z-axis angular acceleration (rad/s^2)'), xlabel('Time
(s)'),grid on
s7=subplot(4,2,7);
plot(t(1:PE-PS),mean_aacc_module(:,:,2,1),t(1:PE-
PS),mean_aacc_module(:,:,2,1)+std_aacc_module(:,:,2,1),'k',t(1:PE-
PS),mean_aacc_module(:,:,2,1)-std_aacc_module(:,:,2,1),'k')
title('Standard Ukemi: angular acceleration module (rad/s^2)'), xlabel('Time
(s)'),grid on
s2=subplot(4,2,2);
plot(t(1:PE-PS),mean_aacc(:,1,2,2),'r',t(1:PE-
PS),mean_aacc(:,1,2,2)+std_aacc(:,1,2,2),'k',t(1:PE-PS),mean_aacc(:,1,2,2)-
std_aacc(:,1,2,2),'k')
title('No-hands Ukemi: X-axis angular acceleration (rad/s^2)'), xlabel('Time
(s)'),grid on
s4=subplot(4,2,4);
plot(t(1:PE-PS),mean_aacc(:,2,2,2),'b',t(1:PE-
PS),mean_aacc(:,2,2,2)+std_aacc(:,2,2,2),'k',t(1:PE-PS),mean_aacc(:,2,2,2)-
std_aacc(:,2,2,2),'k')
title('No-hands Ukemi: Y-axis angular acceleration (rad/s^2)'), xlabel('Time
(s)'),grid on
s6=subplot(4,2,6);
plot(t(1:PE-PS),mean_aacc(:,3,2,2),'g',t(1:PE-
PS),mean_aacc(:,3,2,2)+std_aacc(:,3,2,2),'k',t(1:PE-PS),mean_aacc(:,3,2,2)-
std_aacc(:,3,2,2),'k')
title('No-hands Ukemi: Z-axis angular acceleration (rad/s^2)'), xlabel('Time
(s)'),grid on
s8=subplot(4,2,8);
plot(t(1:PE-PS),mean_aacc_module(:,:,2,2),t(1:PE-
PS),mean_aacc_module(:,:,2,2)+std_aacc_module(:,:,2,2),'k',t(1:PE-
PS),mean_aacc_module(:,:,2,2)-std_aacc_module(:,:,2,2),'k')
title('No-hands Ukemi: angular acceleration module (rad/s^2)'), xlabel('Time
(s)'),grid on
annotation('textbox', [0 0 1 1], 'String', 'MEAN VALUE \pm STANDARD DEVIATION
- TRUNK ANGULAR ACCELERATION','FontSize', 14, 'FontWeight', 'bold',
'EdgeColor', 'none', 'HorizontalAlignment', 'center')
linkaxes([s1,s3,s5,s7],'x'),linkaxes([s2,s4,s6,s8],'x')
savefig('TRUNK ANGULAR ACCELERATION.fig')

figure() % angle between sensors
s1=subplot(3,2,1);

```

```

plot(t(1:PE-PS+1),mean_a2s(:,1,:,1),'r',t(1:PE-
PS+1),mean_a2s(:,1,:,1)+std_a2s(:,1,:,1),'k',t(1:PE-PS+1),mean_a2s(:,1,:,1)-
std_a2s(:,1,:,1),'k')
title('Standard Ukemi: X-axis angle (degree)'), xlabel('Time (s)'),grid on
s3=subplot(3,2,3);
plot(t(1:PE-PS+1),mean_a2s(:,2,:,1),'b',t(1:PE-
PS+1),mean_a2s(:,2,:,1)+std_a2s(:,2,:,1),'k',t(1:PE-PS+1),mean_a2s(:,2,:,1)-
std_a2s(:,2,:,1),'k')
title('Standard Ukemi: Y-axis angle (degree)'), xlabel('Time (s)'),grid on
s5=subplot(3,2,5);
plot(t(1:PE-PS+1),mean_a2s(:,3,:,1),'g',t(1:PE-
PS+1),mean_a2s(:,3,:,1)+std_a2s(:,3,:,1),'k',t(1:PE-PS+1),mean_a2s(:,3,:,1)-
std_a2s(:,3,:,1),'k')
title('Standard Ukemi: Z-axis angle (degree)'), xlabel('Time (s)'),grid on
s2=subplot(3,2,2);
plot(t(1:PE-PS+1),mean_a2s(:,1,:,2),'r',t(1:PE-
PS+1),mean_a2s(:,1,:,2)+std_a2s(:,1,:,2),'k',t(1:PE-PS+1),mean_a2s(:,1,:,2)-
std_a2s(:,1,:,2),'k')
title('No-hands Ukemi: X-axis angle (degree)'), xlabel('Time (s)'),grid on
s4=subplot(3,2,4);
plot(t(1:PE-PS+1),mean_a2s(:,2,:,2),'b',t(1:PE-
PS+1),mean_a2s(:,2,:,2)+std_a2s(:,2,:,2),'k',t(1:PE-PS+1),mean_a2s(:,2,:,2)-
std_a2s(:,2,:,2),'k')
title('No-hands Ukemi: Y-axis angle (degree)'), xlabel('Time (s)'),grid on
s6=subplot(3,2,6);
plot(t(1:PE-PS+1),mean_a2s(:,3,:,2),'g',t(1:PE-
PS+1),mean_a2s(:,3,:,2)+std_a2s(:,3,:,2),'k',t(1:PE-PS+1),mean_a2s(:,3,:,2)-
std_a2s(:,3,:,2),'k')
title('No-hands Ukemi: Z-axis angle (degree)'), xlabel('Time (s)'),grid on
annotation('textbox',[0 0 1 1],'String','MEAN VALUE \pm STANDARD DEVIATION
- ANGLE BETWEEN SENSORS','FontSize',14,'FontWeight','bold','EdgeColor',
'none','HorizontalAlignment','center')
linkaxes([s1,s3,s5],'x'),linkaxes([s2,s4,s6],'x')
savefig('ANGLE BETWEEN SENSORS.fig')

%% STATISTICS
% variables extraction
npoints=4;

figure('units','normalized','outerposition',[0 0 1 1])
for c=1:2 % for each condition
    for e=1:30 % for each epoch
        subplot(2,1,1),plot(s_epoch(1000:2500,2,1,c,e)),xlim([0
1500]),title(['a_x condition=',num2str(c),' epoch=',num2str(e)])
        subplot(2,1,2),plot(a2s_epoch(1000:2500,2,:,c,e)),xlim([0
1500]),title('a2s')

        coord=ginput(npoints);
        coord=round(coord)+1000;
        % real maximum local search
        for ii=1:npoints
            maximum=abs(s_epoch(coord(ii,1),2,1,c,e));
            for i=0:30
                if abs(s_epoch(coord(ii,1)-15+i,2,1,c,e))>=maximum
                    coordn(ii,1)=coord(ii,1)-15+i;
                    maximum=abs(s_epoch(coordn(ii,1),2,1,c,e));
                end
            end
            end
            extract(:,1:6,:,c,e)=s_epoch(coordn(:,1),2:7,:,c,e);% linear
acceleration and omega
            extract(:,7:9,:,c,e)=aacc_epoch(coordn(:,1),:,:,c,e);% angular
acceleration
            angle(:,c,e)=a2s_epoch(coordn(:,1),2,:,c,e);% y angle
            indexes(:,e,c)=coordn(:,1);
        end
    end
end
save('Variables_for_Statistics.mat','extract','angle','indexes')

```

```

% INTRA-CLASS CORRELATION COEFFICIENT AND CORRELATION
% Data organization for SPSS importing
for c=1:2 % for each condition
    for s=1:2 % for each sensor
        for v=1:9 % for each variable
            for p=1:4 % for each phase
                e(:,1)=extract(p,v,s,c,1:10);
                e(:,2)=extract(p,v,s,c,11:20);
                e(:,3)=extract(p,v,s,c,21:30);
                fprintf('%f\t%f\t%f\n',e);
                pause()
            end
        end
    end
end
for c=1:2 % for each condition
    for p=1:4 % for each phase
        an(:,1)=angle(p,c,1:10);
        an(:,2)=angle(p,c,11:20);
        an(:,3)=angle(p,c,21:30);
        fprintf('%f\t%f\t%f\n',an);
        pause()
    end
end
% --> TEST ON SPSS
% Importing and saving SPSS output (ICC and correlation) to MATLAB, then re-
organizing it (from 144*9 to 4*9*9*2*2)
save('stat_output.mat','stat_out_variables','stat_out_angle')

for c=1:2 % for each condition
    for s=1:2 % for each sensor
        for v=1:9 % for each variable
            if s==1 && c==1
                start=0; % first 36 rows
            else if s==2 && c==1
                start=4*9; % second 36 rows
            else if s==1 && c==2
                start=4*9*2; % third 36 rows
            else if s==2 && c==2
                start=4*9*3; % last 36 rows
            end
        end
    end
end
    sov(:,:,v,s,c)=stat_out_variables(1+4*(v-
1)+start:4*v+start,:); % stat. output variables
end
end
    soa(:,:,1)=stat_out_angle(1:4,:); %stat. output angle
    soa(:,:,2)=stat_out_angle(5:8,:);
    save('rearranged_stat_output.mat','sov','soa')

% ICC
figure()
subplot(2,2,1)
for v=1:9
    plot(sov(:,7,v,1,1),'.-','MarkerSize',15),hold on
end
ylim([0 1]),xticks([1 2 3 4]),xticklabels({'C','D','E','F'})
xlabel('Breakfall phase'), title('Standard breakfall - HEAD')
legend('a_X','a_Y','a_Z','\omega_X','\omega_Y','\omega_Z','d\omega_X
/dt','d\omega_Y /dt','d\omega_Z /dt','Location','NorthWest')
subplot(2,2,2)
for v=1:9
    plot(sov(:,7,v,1,2),'.-','MarkerSize',15),hold on
end
ylim([0 1]),xticks([1 2 3 4]),xticklabels({'C','D','E','F'})

```

```

xlabel('Breakfall phase'), title('No-hands breakfall - HEAD')
subplot(2,2,3)
for v=1:9
    plot(sov(:,7,v,2,1),'.-','MarkerSize',15),hold on
end
ylim([0 1]),xticks([1 2 3 4]),xticklabels({'C','D','E','F'})
xlabel('Breakfall phase'), title('Standard breakfall - TRUNK')
subplot(2,2,4)
for v=1:9
    plot(sov(:,7,v,2,2),'.-','MarkerSize',15),hold on
end
ylim([0 1]),xticks([1 2 3 4]),xticklabels({'C','D','E','F'})
xlabel('Breakfall phase'), title('No-hands breakfall - TRUNK')
annotation('textbox', [0 0 1 1], 'String', 'Intra-class Correlation
Coefficient', 'FontSize', 14, 'FontWeight', 'bold', 'EdgeColor', 'none',
'HorizontalAlignment', 'center')

% corr
figure()
subplot(2,2,1)
for v=1:9
    plot(sov(:,1,v,1,1),'.-','MarkerSize',15),hold on
end
ylim([-1 1]),xticks([1 2 3 4]),xticklabels({'C','D','E','F'})
xlabel('Breakfall phase'), title('Standard breakfall - HEAD')
legend('a_X','a_Y','a_Z','\omega_X','\omega_Y','\omega_Z','d\omega_X
/dt','d\omega_Y /dt','d\omega_Z /dt','Location','NorthWest')
subplot(2,2,2)
for v=1:9
    plot(sov(:,1,v,1,2),'.-','MarkerSize',15),hold on
end
ylim([-1 1]),xticks([1 2 3 4]),xticklabels({'C','D','E','F'})
xlabel('Breakfall phase'), title('No-hands breakfall - HEAD')
subplot(2,2,3)
for v=1:9
    plot(sov(:,1,v,2,1),'.-','MarkerSize',15),hold on
end
ylim([-1 1]),xticks([1 2 3 4]),xticklabels({'C','D','E','F'})
xlabel('Breakfall phase'), title('Standard breakfall - TRUNK')
subplot(2,2,4)
for v=1:9
    plot(sov(:,1,v,2,2),'.-','MarkerSize',15),hold on
end
ylim([-1 1]),xticks([1 2 3 4]),xticklabels({'C','D','E','F'})
xlabel('Breakfall phase'), title('No-hands breakfall - TRUNK')
annotation('textbox', [0 0 1 1], 'String', 'Correlation', 'FontSize', 14,
'FontWeight', 'bold', 'EdgeColor', 'none', 'HorizontalAlignment', 'center')

% ICC angle
figure()
plot(soa(:,7,1),'.-','MarkerSize',15),hold on
plot(soa(:,7,2),'.-','MarkerSize',15),hold off
ylim([0 1]),xticks([1 2 3 4]),xticklabels({'C','D','E','F'})
xlabel('Breakfall phase'), title('Intra-class Correlation Coefficient - y-
angle')
legend('Standard Breakfall','No-hands Breakfall')

% corr angle
figure()
plot(soa(:,1,1),'.-','MarkerSize',15),hold on
plot(soa(:,1,2),'.-','MarkerSize',15),hold off
ylim([-1 1]),xticks([1 2 3 4]),xticklabels({'C','D','E','F'})
xlabel('Breakfall phase'), title('Correlation - y-angle')
legend('Standard Breakfall','No-hands Breakfall')

% ICC of interest
figure()
subplot(2,2,1)
for v=[1 3 5 8]

```

```

        plot(sov(:,7,v,1,1),'.-','MarkerSize',15),hold on
    end
    ylim([0 1]),xticks([1 2 3 4]),xticklabels({'C','D','E','F'})
    xlabel('Breakfall phase'), title('Standard breakfall - HEAD')
    legend('a_X','a_Z','\omega_Y','d\omega_Y /dt'),hold off
    subplot(2,2,2)
    for v=[1 3 5 8]
        plot(sov(:,7,v,1,2),'.-','MarkerSize',15),hold on
    end
    ylim([0 1]),xticks([1 2 3 4]),xticklabels({'C','D','E','F'})
    xlabel('Breakfall phase'), title('No-hands breakfall - HEAD'),hold off
    subplot(2,2,3)
    for v=[1 3 5 8]
        plot(sov(:,7,v,2,1),'.-','MarkerSize',15),hold on
    end
    ylim([0 1]),xticks([1 2 3 4]),xticklabels({'C','D','E','F'})
    xlabel('Breakfall phase'), title('Standard breakfall - TRUNK'),hold off
    subplot(2,2,4)
    for v=[1 3 5 8]
        plot(sov(:,7,v,2,2),'.-','MarkerSize',15),hold on
    end
    ylim([0 1]),xticks([1 2 3 4]),xticklabels({'C','D','E','F'})
    xlabel('Breakfall phase'), title('No-hands breakfall - TRUNK'),hold off
    annotation('textbox', [0 0 1 1], 'String', 'Intra-class Correlation
Coefficient','FontSize', 14, 'FontWeight', 'bold', 'EdgeColor', 'none',
'HorizontalAlignment', 'center')

% corr of interest
figure()
subplot(2,2,1)
for v=[1 3 5 8]
    plot(sov(:,1,v,1,1),'.-','MarkerSize',15),hold on
end
ylim([0 1]),xticks([1 2 3 4]),xticklabels({'C','D','E','F'})
xlabel('Breakfall phase'), title('Standard breakfall - HEAD')
legend('a_X','a_Z','\omega_Y','d\omega_Y /dt'),hold off
subplot(2,2,2)
for v=[1 3 5 8]
    plot(sov(:,1,v,1,2),'.-','MarkerSize',15),hold on
end
ylim([0 1]),xticks([1 2 3 4]),xticklabels({'C','D','E','F'})
xlabel('Breakfall phase'), title('No-hands breakfall - HEAD'),hold off
subplot(2,2,3)
for v=[1 3 5 8]
    plot(sov(:,1,v,2,1),'.-','MarkerSize',15),hold on
end
ylim([0 1]),xticks([1 2 3 4]),xticklabels({'C','D','E','F'})
xlabel('Breakfall phase'), title('Standard breakfall - TRUNK'),hold off
subplot(2,2,4)
for v=[1 3 5 8]
    plot(sov(:,1,v,2,2),'.-','MarkerSize',15),hold on
end
ylim([0 1]),xticks([1 2 3 4]),xticklabels({'C','D','E','F'})
xlabel('Breakfall phase'), title('No-hands breakfall - TRUNK'),hold off
annotation('textbox', [0 0 1 1], 'String', 'Correlation','FontSize', 14,
'FontWeight', 'bold', 'EdgeColor', 'none', 'HorizontalAlignment', 'center')

% WILCOXON SIGNED RANK TEST
for s=1:2 % for each sensor
    for v=1:9 % for each variable
        for p=1:4 % for each phase
            W(p,v,s,1)=signrank(reshape(extract(p,v,s,1,1:10),10,1),reshape(extract(p,v,s,
2,1:10),10,1));
            W(p,v,s,2)=signrank(reshape(extract(p,v,s,1,11:20),10,1),reshape(extract(p,v,s
,2,11:20),10,1));
            W(p,v,s,3)=signrank(reshape(extract(p,v,s,1,21:30),10,1),reshape(extract(p,v,s
,2,21:30),10,1));
        end
    end
end
end

```

```

end
for p=1:4

W_angle(p,1)=signrank(reshape(angle(p,1,1:10),10,1),reshape(angle(p,2,1:10),10,1));

W_angle(p,2)=signrank(reshape(angle(p,1,11:20),10,1),reshape(angle(p,2,11:20),10,1));

W_angle(p,3)=signrank(reshape(angle(p,1,21:30),10,1),reshape(angle(p,2,21:30),10,1));
end

% Wilcoxon results
figure()
subplot(3,3,1)
for v=1:9
    plot(W(:,v,1,1),'.-','MarkerSize',15),hold on
end
ylim([0 0.055]),xticks([1 2 3 4]),xticklabels({'C','D','E','F'}),xlim([1 4])
xlabel('Breakfall phase'), title('Day 1 - HEAD')
legend('a_X','a_Y','a_Z','\omega_X','\omega_Y','\omega_Z','d\omega_X/dt','d\omega_Y/dt','d\omega_Z/dt','Location','Best')
subplot(3,3,2)
for v=1:9
    plot(W(:,v,1,2),'.-','MarkerSize',15),hold on
end
ylim([0 0.055]),xticks([1 2 3 4]),xticklabels({'C','D','E','F'}),xlim([1 4])
xlabel('Breakfall phase'), title('Day 2 - HEAD')
subplot(3,3,3)
for v=1:9
    plot(W(:,v,1,3),'.-','MarkerSize',15),hold on
end
ylim([0 0.055]),xticks([1 2 3 4]),xticklabels({'C','D','E','F'}),xlim([1 4])
xlabel('Breakfall phase'), title('Day 3 - HEAD')
subplot(3,3,4)
for v=1:9
    plot(W(:,v,2,1),'.-','MarkerSize',15),hold on
end
ylim([0 0.055]),xticks([1 2 3 4]),xticklabels({'C','D','E','F'}),xlim([1 4])
xlabel('Breakfall phase'), title('Day 1 - TRUNK')
subplot(3,3,5)
for v=1:9
    plot(W(:,v,2,2),'.-','MarkerSize',15),hold on
end
ylim([0 0.055]),xticks([1 2 3 4]),xticklabels({'C','D','E','F'}),xlim([1 4])
xlabel('Breakfall phase'), title('Day 2 - TRUNK')
subplot(3,3,6)
for v=1:9
    plot(W(:,v,2,3),'.-','MarkerSize',15),hold on
end
ylim([0 0.055]),xticks([1 2 3 4]),xticklabels({'C','D','E','F'}),xlim([1 4])
xlabel('Breakfall phase'), title('Day 3 - TRUNK')
subplot(3,3,7)
plot(W_angle(:,1),'.-','MarkerSize',15)
ylim([0 0.055]),xticks([1 2 3 4]),xticklabels({'C','D','E','F'}),xlim([1 4])
xlabel('Breakfall phase'), title('Day 1 - y-angle')
subplot(3,3,8)
plot(W_angle(:,2),'.-','MarkerSize',15)
ylim([0 0.055]),xticks([1 2 3 4]),xticklabels({'C','D','E','F'}),xlim([1 4])
xlabel('Breakfall phase'), title('Day 2 - y-angle')
subplot(3,3,9)
plot(W_angle(:,3),'.-','MarkerSize',15)
ylim([0 0.055]),xticks([1 2 3 4]),xticklabels({'C','D','E','F'}),xlim([1 4])
xlabel('Breakfall phase'), title('Day 3 - y-angle')
annotation('textbox', [0 0 1 1], 'String', 'Wilcoxon signed rank test', 'FontSize', 14, 'FontWeight', 'bold', 'EdgeColor', 'none', 'HorizontalAlignment', 'center')

```

```

% Wilcoxon, angle
figure()
plot(W_angle(:,1),'.-','MarkerSize',15),hold on
plot(W_angle(:,2),'.-','MarkerSize',15)
plot(W_angle(:,3),'.-','MarkerSize',15),hold off
ylim([0 0.055]),xticks([1 2 3 4]),xticklabels({'C','D','E','F'}),xlim([1 4])
xlabel('Breakfall phase'), title('Wilcoxon signed rank test - y-angle')
legend('Day 1','Day 2','Day 3')

% Wilcoxon results of interest
figure()
subplot(3,3,1)
for v=[1 3 5 8]
    plot(W(:,v,1,1),'.-','MarkerSize',15),hold on
end
ylim([0 0.055]),xticks([1 2 3 4]),xticklabels({'C','D','E','F'}),xlim([1 4])
xlabel('Breakfall phase'), title('Day 1 - HEAD')
legend('a_X','a_Z','\omega_Y','d\omega_Y /dt','Location','SouthWest'),hold off
subplot(3,3,2)
for v=[1 3 5 8]
    plot(W(:,v,1,2),'.-','MarkerSize',15),hold on
end
ylim([0 0.055]),xticks([1 2 3 4]),xticklabels({'C','D','E','F'}),xlim([1 4])
xlabel('Breakfall phase'), title('Day 2 - HEAD')
subplot(3,3,3)
for v=[1 3 5 8]
    plot(W(:,v,1,3),'.-','MarkerSize',15),hold on
end
ylim([0 0.055]),xticks([1 2 3 4]),xticklabels({'C','D','E','F'}),xlim([1 4])
xlabel('Breakfall phase'), title('Day 3 - HEAD')
subplot(3,3,4)
for v=[1 3 5 8]
    plot(W(:,v,2,1),'.-','MarkerSize',15),hold on
end
ylim([0 0.055]),xticks([1 2 3 4]),xticklabels({'C','D','E','F'}),xlim([1 4])
xlabel('Breakfall phase'), title('Day 1 - TRUNK')
subplot(3,3,5)
for v=[1 3 5 8]
    plot(W(:,v,2,2),'.-','MarkerSize',15),hold on
end
ylim([0 0.055]),xticks([1 2 3 4]),xticklabels({'C','D','E','F'}),xlim([1 4])
xlabel('Breakfall phase'), title('Day 2 - TRUNK')
subplot(3,3,6)
for v=[1 3 5 8]
    plot(W(:,v,2,3),'.-','MarkerSize',15),hold on
end
ylim([0 0.055]),xticks([1 2 3 4]),xticklabels({'C','D','E','F'}),xlim([1 4])
xlabel('Breakfall phase'), title('Day 3 - TRUNK')
subplot(3,3,7)
plot(W_angle(:,1),'.-','MarkerSize',15)
ylim([0 0.055]),xticks([1 2 3 4]),xticklabels({'C','D','E','F'}),xlim([1 4])
xlabel('Breakfall phase'), title('Day 1 - y-angle')
subplot(3,3,8)
plot(W_angle(:,2),'.-','MarkerSize',15)
ylim([0 0.055]),xticks([1 2 3 4]),xticklabels({'C','D','E','F'}),xlim([1 4])
xlabel('Breakfall phase'), title('Day 2 - y-angle')
subplot(3,3,9)
plot(W_angle(:,3),'.-','MarkerSize',15)
ylim([0 0.05]),xticks([1 2 3 4]),xticklabels({'C','D','E','F'}),xlim([1 4])
xlabel('Breakfall phase'), title('Day 3 - y-angle')
annotation('textbox',[0 0 1 1],'String','Wilcoxon signed rank
test','FontSize',14,'FontWeight','bold','EdgeColor','none',
'HorizontalAlignment','center')

```

C.5 Script used for video analysis in Section 5 Breakfall Techniques Analysis

```

clc
clear all
close all

% Acquisition parameters
f_acc=1/0.001; % Accelerometer sampling rate (Hz)
f_mag=1/0.020; % Magnetometer sampling rate (Hz)
g=9.81; % Gravitational acceleration (m/s^2)

% Obtain organized data from accelerometers files
[DATA, L]=RSTWOSens(f_acc,f_mag);

% Extraction of wanted signal
j_ind=find(DATA(:,2,1)<=0.01*g);
j_ind=unique([j_ind(1); j_ind(diff(j_ind)~=1); j_ind(end)]);

%% Video Analysis
Video=input('Video filename: ','s');
vobj = VideoReader(Video);
ratio=(f_acc/vobj.FrameRate);
first=j_ind(1);
ti=DATA(first,1,1); % initial time of video
k=1;

% set figure and output video
fig=figure();
writerObj=VideoWriter('video&plot.avi');
writerObj.FrameRate=vobj.FrameRate;
open(writerObj);

while hasFrame(vobj)
    subplot(5,2,[1,2,3,4,5,6])
    this_frame = readFrame(vobj);
    image(this_frame), axis image off

    subplot(5,2,[7,8,9,10])
    kf=round(k*ratio);
    if k<=vobj.FrameRate
        s=first; % first data to be plotted
        e=first+kf; % last data to be plotted
    else % one second expired
        ki=round((k-vobj.FrameRate)*ratio); %one second of data displayed
        s=first+ki;
        e=first+kf;
    end
    plot(DATA(s:e,1,1)-ti,DATA(s:e,2,1)/g,'r',DATA(s:e,1,1)-
ti,DATA(s:e,3,1)/g,'b',DATA(s:e,1,1)-ti,DATA(s:e,4,1)/g,'g')
    title('Sensor13 (Head)'), legend('x','y','z','Location','NorthWest'),
    grid on, xlabel('Time (s)'), ylabel('Acceleration (g)'), axis tight

    drawnow;
    k=k+1;

    % Video writing
    frame=getframe(fig);
    writeVideo(writerObj,frame);
end
close(writerObj); % Video saving

```

C.6 Script used for accommodation tests in Section 6.1 Preliminary Analysis

```

clc
clear all
close all

% Acquisition parameters
f_acc=1/0.001; % Accelerometer sampling rate (Hz)
f_mag=1/0.020; % Magnetometer sampling rate (Hz)
g=9.81; % Gravitational acceleration (m/s^2)

% Moving averaging parameter
coeff=201-1;
b=ones(coeff,1)/coeff;
a=1;

% Filter parameters for integration and differentiation
ft1=1; % start of passband zone (Hz)
ft2=50; % end of passband zone (Hz)
ord=2; % filter order
[bb,aa]=butter(ord,[ft1/(f_acc/2),ft2/(f_acc/2)]);

% DATA LOADING
for n=1:3
    [DATA, L]=RSTW0sens(f_acc,f_mag,n);

    % Synchronize data at the event
    threshold=0.01*g;
    direction=1; % 1=X, 2=Y, 3=Z
    j_ind1=find(DATA(:,direction+1,1)<=threshold);
    j_ind1=unique([j_ind1(1); j_ind1(diff(j_ind1)~=1); j_ind1(end)]);
    j_ind2=find(DATA(:,direction+1,2)<=threshold);
    j_ind2=unique([j_ind2(1); j_ind2(diff(j_ind2)~=1); j_ind2(end)]);
    if n==1
        data=zeros(round(1.5*(size(DATA,1)-
min([j_ind1(1),j_ind2(1)]))),size(DATA,2),size(DATA,3));
        end
        data(1:size(DATA,1)-j_ind1(1),:,1,n)=DATA(j_ind1(1):end-1, :, 1); % sample *
data(10 columns) * sensor number(1 or 2) * day(1,2,3)
        data(1:size(DATA,1)-j_ind2(1), :, 2, n)=DATA(j_ind2(1):end-1, :, 2); % sample *
data(10 columns) * sensor number(1 or 2) * day(1,2,3)
        end
        data(:,2:4, :, :)=data(:,2:4, :, :)/g;
        t=0:1/f_acc:(size(data,1)-1)/f_acc;

    figure()
    s1=subplot(3,2,1);
    plot(t,data(:,2,1,1),'r',t,data(:,3,1,1),'b',t,data(:,4,1,1),'g'),title('HEAD'
))
    ylabel('Acceleration (g)'), xlabel('Time (s)'), grid
    on, legend('x','y','z','Location','best')
    s3=subplot(3,2,3);
    plot(t,data(:,2,1,2),'r',t,data(:,3,1,2),'b',t,data(:,4,1,2),'g')
    ylabel('Acceleration (g)'), xlabel('Time (s)'), grid on
    s5=subplot(3,2,5);
    plot(t,data(:,2,1,3),'r',t,data(:,3,1,3),'b',t,data(:,4,1,3),'g')
    ylabel('Acceleration (g)'), xlabel('Time (s)'), grid on
    s2=subplot(3,2,2);
    plot(t,data(:,2,2,1),'r',t,data(:,3,2,1),'b',t,data(:,4,2,1),'g'),title('TRUNK
')
    ylabel('Acceleration (g)'), xlabel('Time (s)'), grid on
    s4=subplot(3,2,4);
    plot(t,data(:,2,2,2),'r',t,data(:,3,2,2),'b',t,data(:,4,2,2),'g')
    ylabel('Acceleration (g)'), xlabel('Time (s)'), grid on
    s6=subplot(3,2,6);
    plot(t,data(:,2,2,3),'r',t,data(:,3,2,3),'b',t,data(:,4,2,3),'g')

```

```

ylabel('Acceleration (g)'), xlabel('Time (s)'), grid on

acc_m=sqrt(data(:,2, :, :).^2+data(:,3, :, :).^2+data(:,4, :, :).^2); % sample *
value(1 columns) * sensor number(1 or 2) * day(1,2,3)
acc_m_f=filtfilt(b,a,acc_m);

figure()
s1=subplot(3,2,1);
plot(t,acc_m(:, :, 1, 1)), title('HEAD')
ylabel('Acceleration module (g)'), xlabel('Time (s)'), grid on
s3=subplot(3,2,3);
plot(t,acc_m(:, :, 1, 2))
ylabel('Acceleration module (g)'), xlabel('Time (s)'), grid on
s5=subplot(3,2,5);
plot(t,acc_m(:, :, 1, 3))
ylabel('Acceleration module (g)'), xlabel('Time (s)'), grid on
s2=subplot(3,2,2);
plot(t,acc_m(:, :, 2, 1)), title('TRUNK')
ylabel('Acceleration module (g)'), xlabel('Time (s)'), grid on
s4=subplot(3,2,4);
plot(t,acc_m(:, :, 2, 2))
ylabel('Acceleration module (g)'), xlabel('Time (s)'), grid on
s6=subplot(3,2,6);
plot(t,acc_m(:, :, 2, 3))
ylabel('Acceleration module (g)'), xlabel('Time (s)'), grid on

PS=5000; % fall prototype starting point
PE=7000; % fall prototype ending point
nf=8; % number of falls for each day
figure()
for n=1:3

findsignal(acc_m_f(:, :, 1, n), acc_m_f(PS:PE, :, 1, 1), 'Metric', 'euclidean', 'MaxNumS
gments', nf);

[first(:, n), last(:, n)]=findsignal(acc_m_f(:, :, 1, n), acc_m_f(PS:PE, :, 1, 1), 'Metri
c', 'euclidean', 'MaxNumSegments', nf);
    pause()
    first(:, n)=unique(first(:, n));
    last(:, n)=unique(last(:, n));

    for rep=1:nf
        peaks(rep, :, n)=max(acc_m(first(rep, n):last(rep, n), :, :, n)); % rep *
sensor * day
        % plot(acc_m(first(rep, n):last(rep, n), :, 1, n))
        % pause()
    end
end

% PLOT mean and std.dev for each repetition
mean_peaks=mean(peaks, 3);
std_peaks=std(peaks, 0, 3);
p(:, 1)=polyfit((1:nf)', mean_peaks(:, 1), 1);
p(:, 2)=polyfit((1:nf)', mean_peaks(:, 2), 1);
pp(:, 1)=polyval(p(:, 1), 1:nf);
pp(:, 2)=polyval(p(:, 2), 1:nf);
r=rsquared(mean_peaks(:, 1:2), pp(:, 1:2))

figure()
subplot(1,2,1)
errorbar(1:nf, mean_peaks(:, 1), std_peaks(:, 1), '-o'), hold on
plot(1:nf, pp(:, 1), 'k', 'LineWidth', 2), hold off, legend('Data', 'Best fit line')
title('Head'), xlabel('rep')
subplot(1,2,2)
errorbar(1:nf, mean_peaks(:, 2), std_peaks(:, 2), '-o'), hold on
plot(1:nf, pp(:, 2), 'k', 'LineWidth', 2), hold off
title('Trunk'), xlabel('rep')

```

```

annotation('textbox', [0 0 1 1], 'String', 'Peak acceleration module
(g)', 'FontSize', 14, 'FontWeight', 'bold', 'EdgeColor', 'none',
'HorizontalAlignment', 'center')

% PLOT peak values
clear p pp r;
p(:,1,1)=polyfit((1:nf)', peaks(:,1,1), 1);
p(:,1,2)=polyfit((1:nf)', peaks(:,1,2), 1);
p(:,1,3)=polyfit((1:nf)', peaks(:,1,3), 1);
pp(:,1,1)=polyval(p(:,1,1), 1:nf);
pp(:,1,2)=polyval(p(:,1,2), 1:nf);
pp(:,1,3)=polyval(p(:,1,3), 1:nf);
p(:,2,1)=polyfit((1:nf)', peaks(:,2,1), 1);
p(:,2,2)=polyfit((1:nf)', peaks(:,2,2), 1);
p(:,2,3)=polyfit((1:nf)', peaks(:,2,3), 1);
pp(:,2,1)=polyval(p(:,2,1), 1:nf);
pp(:,2,2)=polyval(p(:,2,2), 1:nf);
pp(:,2,3)=polyval(p(:,2,3), 1:nf);
r=rsquared(peaks(:,1:2,1:3), pp(:,1:2,1:3))

figure()
subplot(1,2,1)
plot(1:nf, peaks(:,1,1), 'r.-', 'MarkerSize', 10), hold on
plot(1:nf, peaks(:,1,2), 'b.-', 'MarkerSize', 10)
plot(1:nf, peaks(:,1,3), 'g.-', 'MarkerSize', 10)
plot(1:nf, pp(:,1,1), 'r', 'LineWidth', 3), hold on
plot(1:nf, pp(:,1,2), 'b', 'LineWidth', 3)
plot(1:nf, pp(:,1,3), 'g', 'LineWidth', 3), hold off
title('Head'), xlabel('rep'), legend('Day1', 'Day2', 'Day3', 'Location', 'best')
subplot(1,2,2)
plot(1:nf, peaks(:,2,1), 'r.-', 'MarkerSize', 10), hold on
plot(1:nf, peaks(:,2,2), 'b.-', 'MarkerSize', 10)
plot(1:nf, peaks(:,2,3), 'g.-', 'MarkerSize', 10)
plot(1:nf, pp(:,2,1), 'r', 'LineWidth', 3), hold on
plot(1:nf, pp(:,2,2), 'b', 'LineWidth', 3)
plot(1:nf, pp(:,2,3), 'g', 'LineWidth', 3), hold off
title('Trunk'), xlabel('rep')
annotation('textbox', [0 0 1 1], 'String', 'Peak acceleration module
(g)', 'FontSize', 14, 'FontWeight', 'bold', 'EdgeColor', 'none',
'HorizontalAlignment', 'center')

% PLOT mean and std.dev for each day
daily_mean_peaks=mean(peaks,1);
daily_std_peaks=std(peaks,0,1);

figure()
subplot(1,2,1)
bar(1, daily_mean_peaks(:,1,1), 'r'), hold on
errorbar(1, daily_mean_peaks(:,1,1), daily_std_peaks(:,1,1), 'k')
bar(2, daily_mean_peaks(:,1,2), 'b'), hold on
errorbar(2, daily_mean_peaks(:,1,2), daily_std_peaks(:,1,2), 'k')
bar(3, daily_mean_peaks(:,1,3), 'g'), hold on
errorbar(3, daily_mean_peaks(:,1,3), daily_std_peaks(:,1,3), 'k'), hold off
title('Head'), xlabel('Day'), xticks([1,2,3]), xticklabels({'1' '2' '3'})
subplot(1,2,2)
bar(1, daily_mean_peaks(:,2,1), 'r'), hold on
errorbar(1, daily_mean_peaks(:,2,1), daily_std_peaks(:,2,1), 'k')
bar(2, daily_mean_peaks(:,2,2), 'b'), hold on
errorbar(2, daily_mean_peaks(:,2,2), daily_std_peaks(:,2,2), 'k')
bar(3, daily_mean_peaks(:,2,3), 'g'), hold on
errorbar(3, daily_mean_peaks(:,2,3), daily_std_peaks(:,2,3), 'k'), hold off
title('Trunk'), xlabel('Day'), xticks([1,2,3]), xticklabels({'1' '2' '3'})
annotation('textbox', [0 0 1 1], 'String', 'Peak acceleration module
(g)', 'FontSize', 14, 'FontWeight', 'bold', 'EdgeColor', 'none',
'HorizontalAlignment', 'center')

```

C.7 Yost Labs sensors data visualization and organization for Section 6 Head Injury Risk Assessment (pre-processing)

```

% Sensors data reading and elaborating if a jump is used
% as trigger for starting and ending the signal record.
% by Luca Vacca
clc
clear all
close all

%% FILES LOADING
NA=input('Not Agonist? (YES=1, NO=0) '); % Parameter to define if axes
rotation is required
tic
[DATA, L,f_mean,f_std]=YOSTreading(); % Data loading
toc
f_r=round(mean(f_mean)); % Mean sample frequency

if NA==1
    DATA(:,[2,3,5,6],:)=~DATA(:,[2,3,5,6],:); % Axes rotation
end

% Extraction of wanted signal and synchronization
[b,a]=butter(5,5/(f_r/2),'low');
DATAf=filtfilt(b,a,DATA(:,2,:));

j_ind1=find(DATAf(:,1,1)<=0.1); % Find start of fligth phase on head sensor
j_ind1=unique([j_ind1(1); j_ind1(diff(j_ind1)~=1); j_ind1(end)]);
j_ind2=find(DATAf(:,1,2)<=0.1); % Find start of fligth phase on trunk sensor
j_ind2=unique([j_ind2(1); j_ind2(diff(j_ind2)~=1); j_ind2(end)]);

plot(DATA(:,1,1)-DATA(1,1,1),DATAf(:,1,1),'k',DATA(j_ind1(1),1,1)-
DATA(1,1,1),DATAf(j_ind1(1),1,1),'r',DATA(:,1,2)-
DATA(1,1,2),DATAf(:,1,2),'b',DATA(j_ind2(1),1,2)-
DATA(1,1,2),DATAf(j_ind2(1),1,2),'r');
xlim([0,max(max([DATA(:,1,1)-DATA(1,1,1),DATA(:,1,2)-DATA(1,1,2)]))]);
pause()

% Matrix construction
data=zeros(size(DATA,1)-min([j_ind1(1),j_ind2(1)]),size(DATA,2),size(DATA,3));
data(1:size(DATA,1)-j_ind1(1),:,1)=DATA(j_ind1(1):end-1,1);
data(1:size(DATA,1)-j_ind2(1),:,2)=DATA(j_ind2(1):end-1,2);

t1=data(:,1,1)-data(1,1,1);
t2=data(:,1,2)-data(1,1,2);
for i=2:length(t1)
    if t1(i)<=0
        t1(i)=t1(i-1)+1/f_mean(1);
    end
    if t2(i)<=0
        t2(i)=t2(i-1)+1/f_mean(2);
    end
end
end

%% PLOT DATA GAINED FROM SENSORS
% Linear acceleration
figure()
ax1=subplot(2,1,1);
plot(t1,data(:,2,1),'r',t1,data(:,4,1),'b',t1,data(:,3,1),'g')
title('Sensor1 (Head)', legend('x','y','z'), grid on, xlabel('Time (s)'),
ylabel('Acceleration (g)'))
ax2=subplot(2,1,2);
plot(t2,data(:,2,2),'r',t2,data(:,4,2),'b',t2,data(:,3,2),'g')
title('Sensor2 (Trunk)', legend('x','y','z'), grid on, xlabel('Time (s)'),
ylabel('Acceleration (g)'))
linkaxes([ax1,ax2],'xy')

```

```

% Acceleration Module
lacc_tot(:,:)=sqrt(data(:,2,:).^2+data(:,3,:).^2+data(:,4,:).^2);
figure()
ax1=subplot(2,1,1);
plot(t1,lacc_tot(:,1))
title('Sensor1 (Head)'), grid on, xlabel('Time (s)'), ylabel('Acceleration
module (g)')
ax2=subplot(2,1,2);
plot(t2,lacc_tot(:,2))
title('Sensor2 (Trunk)'), grid on, xlabel('Time (s)'), ylabel('Acceleration
module (g)')
linkaxes([ax1,ax2], 'xy')

% Angular velocity
figure()
ax1=subplot(2,1,1);
plot(t1,data(:,5,1), 'r', t1,data(:,6,1), 'b', t1,data(:,7,1), 'g')
title('Sensor1 (Head)'), legend('x', 'y', 'z'), grid on, xlabel('Time (s)'),
ylabel('Angular velocity (rad/s)')
ax2=subplot(2,1,2);
plot(t2,data(:,5,2), 'r', t2,data(:,6,2), 'b', t2,data(:,7,2), 'g')
title('Sensor2 (Trunk)'), legend('x', 'y', 'z'), grid on, xlabel('Time (s)'),
ylabel('Angular velocity (rad/s)')
linkaxes([ax1,ax2], 'xy')

%% DATA ELABORATION
%-----
% Signal to analyse (define a rest condition)
figure()
plot(t1(1:round(15*f_r)),data(1:round(15*f_r),2,1),t1(1:round(15*f_r)),data(1:
round(15*f_r),6,1),t2(1:round(15*f_r)),data(1:round(15*f_r),6,2))
title('Choose begin of analysis zone: '), legend('a_x HEAD', '\omega_y
HEAD', '\omega_y TRUNK')
coord=ginput(1);
coord=round(coord);
data=data(coord(1,1):end,:,:)
t=t1(coord(1,1):end)-t1(coord(1,1)); % Refer measures to head acquisition time
t1=t1(coord(1,1):end)-t1(coord(1,1));
t2=t2(coord(1,1):end)-t2(coord(1,1));
f=round(f_mean(1));

% Filter parameters for integration and differentiation
ft1=1; % start of passband zone (Hz)
ft2=30; % end of passband zone (Hz)
ord=4; % filter order
[b,a]=butter(ord,[ft1/(f/2),ft2/(f/2)]);
%freqz(b,a,2048,2048)

omega_f=filtfilt(b,a,data(:,5:7,:)); % Angular rate filtering
omega_f(:,2)=interp1(t2,omega_f(:,2),t); % Interpolation of trunk data at
head acquisition time to have the same instant to calculate values
%-----
% ANGULAR ACCELERATION ESTIMATION
aacc=diff(omega_f)*f; % Differentiation
aacc(:,2)=interp1(t(1:end-1),aacc(:,2),t2(1:end-1)); % Interpolation of
trunk data at trunk acquisition time
aacc_tot=sqrt(aacc(:,1,:).^2+aacc(:,2,:).^2+aacc(:,3,:).^2); % Module

% Angular acceleration
figure()
subplot(2,1,1)
plot(t(1:end-1),aacc(:,1,1), 'r', t(1:end-1),aacc(:,2,1), 'b', t(1:end-
1),aacc(:,3,1), 'g')
title('Sensor1'), legend('x', 'y', 'z'), grid on, xlabel('Time (s)'),
ylabel('Angular acceleration (rad/s^2)'), axis tight
subplot(2,1,2)
plot(t(1:end-1),aacc(:,1,2), 'r', t(1:end-1),aacc(:,2,2), 'b', t(1:end-
1),aacc(:,3,2), 'g')

```

```

title('Sensor2'), legend('x','y','z'), grid on, xlabel('Time (s)'),
ylabel('Angular acceleration (rad/s^2)'), axis tight

% Angular acceleration module
figure()
subplot(2,1,1)
plot(t(1:end-1),aacc_tot(:,1))
title('Sensor1'), grid on, xlabel('Time (s)'), ylabel('Angular acceleration
module (rad/s^2)')
subplot(2,1,2)
plot(t(1:end-1),aacc_tot(:,2))
title('Sensor2'), grid on, xlabel('Time (s)'), ylabel('Angular acceleration
module (rad/s^2)')

% ANGLE BETWEEN THE TWO SENSORS (HYP: angles=0° in rest condition)
a2s=cumtrapz(t,omega_f(:,2)-omega_f(:,1))*180/pi; % Integration of the
difference of angular rate

% Three components of the angle
figure()
plot(t,a2s(:,1),'r',t,a2s(:,2),'b',t,a2s(:,3),'g')
xlabel('Time (s)'), ylabel('Angle between sensors (degree)'), grid on,
legend('x','y','z')

% Neck flex/extension angle
figure()
plot(t,a2s(:,2),'b')
xlabel('Time (s)'), ylabel('Angle (degree)'), grid on, title('Neck
flex/extension angle')
%% REMOVING WRONG PARTS (if needed)
figure()
subplot(2,1,1),plot(lacc_tot(coord(1):end-1,1)),hold on,
plot(aacc_tot(:,1)/100), title('Head')
cut=ginput(2);
cut=round(cut);
data(coord(1)+cut(1,1):coord(1)+cut(2,1),2:end,1)=0;
lacc_tot(coord(1)+cut(1,1):coord(1)+cut(2,1),1)=0;
aacc_tot(cut(1,1):cut(2,1),1)=0;
a2s(cut(1,1):cut(2,1),:)=0;
subplot(2,1,2),plot(lacc_tot(coord(1):end-1,1)),hold on,
plot(aacc_tot(:,1)/100)
figure()
subplot(2,1,1),plot(lacc_tot(coord(1):end-1,2)),hold on,
plot(aacc_tot(:,2)/100),title('Trunk')
cut=ginput(2);
cut=round(cut);
data(coord(1)+cut(1,1):coord(1)+cut(2,1),2:end,2)=0;
lacc_tot(coord(1)+cut(1,1):coord(1)+cut(2,1),2)=0;
aacc_tot(cut(1,1):cut(2,1),2)=0;
subplot(2,1,2),plot(lacc_tot(coord(1):end-1,2)),hold on,
plot(aacc_tot(:,2)/100)
%
% figure()
% plot(t1(1:end-1),lacc_tot(coord(1):end-1,1),t2(1:end-
1),lacc_tot(coord(1):end-1,2),t1(1:end-1),aacc_tot(:,1)/100,t2(1:end-
1),aacc_tot(:,2)/100)

%% DATA SAVING IN A BINARY FILE (quicker loading) AND SECTIONS INDIVIDUATION

MATR=cat(3,[t1(1:end-1),data(1:end-1,2,1),data(1:end-1,4,1),data(1:end-
1,3,1),lacc_tot(coord(1):end-1,1),data(1:end-
1,5:7,1),aacc(:,1:3,1),aacc_tot(:,1),a2s(1:end-1,1:3)],...
[t2(1:end-1),data(1:end-1,2:4,2),lacc_tot(coord(1):end-1,2),data(1:end-
1,5:7,2),aacc(:,1:3,2),aacc_tot(:,2),a2s(1:end-1,1:3)]);
save('A20.mat','MATR','f_r');

% load('A16m.mat')
figure(),subplot(2,1,1),plot(MATR(:,5,1)),hold on, plot(MATR(:,12,1)/100)
l=ginput(5);

```

```
l=round(l(:,1));
MATR(1,5,1)=-1;
subplot(2,1,2),plot(MATR(:,5,1))

figure(),subplot(2,1,1),plot(MATR(:,5,2)),hold on, plot(MATR(:,12,2)/100)
l=ginput(5);
l=round(l(:,1));
MATR(1,5,2)=-1;
subplot(2,1,2),plot(MATR(:,5,2))

% Cut wrong parts
figure()
subplot(2,1,1),plot(MATR(:,5,1)),hold on, plot(MATR(:,12,1)/100),
title('Head')
cut=ginput(2);
cut=round(cut);
MATR(cut(1,1):cut(2,1),2:end,1)=0;
subplot(2,1,2),plot(MATR(:,5,1)),hold on, plot(MATR(:,12,1)/100)

figure()
subplot(2,1,1),plot(MATR(:,5,2)),hold on, plot(MATR(:,12,2)/100),
title('Trunk')
cut=ginput(2);
cut=round(cut);
MATR(cut(1,1):cut(2,1),2:end,2)=0;
subplot(2,1,2),plot(MATR(:,5,2)),hold on, plot(MATR(:,12,2)/100)

save('A20m.mat','MATR','f_r')
```

C.8 Function for reading data from two Yost Labs sensors

```
function [DATA,LIST,f_mean,f_std]=YOSTreading(n1)

% Function for reading data from two 3-Space Sensors via USB connection and
% CoolTerm application.
% Input: - n1 = number of first file to be read in the current folder
% (default = 1)
% Output: - DATA = matrix
% sample*[time,acc_vector(g),gyro_vector(rad/s)]*sensors
% - LIST = files read
% - f_mean = mean of sample rate of the all acquisitions for both
% sensors
% - f_std = standard deviation of sample rate of the all acquisitions
% for both sensors
% by Luca Vacca

LIST=dir('*.txt'); % List all .csv files in the folder, files will be listed
in crescent order following sensor number
if nargin==0
    n1=1;
end
n2=size(LIST,1)/2+n1;
if n2==1.5
    n2=1;
end

LIST=LIST([n1,n2]);

%% FILE SENSOR #1
f=fopen(char(LIST(n1).name));

flag=0;
i=1;
pos=0;
tprec=0;
while flag==0
line(1,1:4)=textscan(f,'%f,%f,%f,%f',1,'HeaderLines',pos);
line(2,1:4)=textscan(f,'%f,%f,%f,%f',1);
if length(find(cellfun(@isempty,line(2,:))))==1 &&
length(find(cellfun(@isempty,line(1,:))))==0 ...
    && abs(sum(cell2mat(line(1,1))))>1e+4 &&
abs(sum(cell2mat(line(2,1))))<1e+4 ...
    && sum(sum(abs(cell2mat([line(:,2:3);line(2,1) line(1,4)]))))<500 ...
    && abs(sum(cell2mat(line(2,1))))~=tprec% lines without mistakes
    d(i,1:4)=line(1,1:4);
    d(i+1,1:3)=line(2,1:3);
    tprec=cell2mat(d(i,1));
    i=i+2;
    pos=0;
else
    pos=pos+1;
end
if sum(sum(~cellfun(@isempty,line))))==0
    flag=1;
end
end
fclose(f);

odd=1:2:size(d,1);
even=2:2:size(d,1);
data_resized=[d(odd,:) d(even,:)];
data_matrix=cell2mat(data_resized);

t=round(data_matrix(:,1)/1000)/1000;
t_diff=diff(t);
f_ist=1./t_diff;
```

```

f_mean(1)=mean(f_ist);
f_std(1)=std(f_ist,0,1);
DATA_n1(:,1)=t;
DATA_n1(:,2:4)=data_matrix(:,5:7);
DATA_n1(:,5:7)=data_matrix(:,2:4);

clear d data_resized data_matrix t t_diff f_ist

%% FILE SENSOR #2
if n2~=1
    f=fopen(char(LIST(n2).name));

    flag=0;
    i=1;
    pos=0;
    tprec=0;
    while flag==0
        line(1,1:4)=textscan(f,'%f,%f,%f,%f',1,'HeaderLines',pos);
        line(2,1:4)=textscan(f,'%f,%f,%f,%f',1);
        if length(find(cellfun(@isempty,line(2,:))))==1 &&
length(find(cellfun(@isempty,line(1,:))))==0 ...
        && abs(sum(cell2mat(line(1,1))))>1e+4 ...
        && abs(sum(cell2mat(line(2,1))))<1e+4 ...
        && sum(sum(abs(cell2mat([line(:,2:3);line(2,1)
line(1,4)]))))<500 ...
        && abs(sum(cell2mat(line(2,1))))~=tprec% lines without
mistakes
            d(i,1:4)=line(1,1:4);
            d(i+1,1:3)=line(2,1:3);
            tprec=cell2mat(d(i,1));
            i=i+2;
            pos=0;
        else
            pos=pos+1;
        end
        if sum(sum(~cellfun(@isempty,line))))==0
            flag=1;
        end
    end
    fclose(f);

    odd=1:2:size(d,1);
    even=2:2:size(d,1);
    data_resized=[d(odd,:) d(even,:)];
    data_matrix=cell2mat(data_resized);

    t=round(data_matrix(:,1)/1000)/1000;
    t_diff=diff(t);
    f_ist=1./t_diff;
    f_mean(2)=mean(f_ist);
    f_std(2)=std(f_ist,0,1);
    DATA_n2(:,1)=t;
    DATA_n2(:,2:4)=data_matrix(:,5:7);
    DATA_n2(:,5:7)=data_matrix(:,2:4);
else
    DATA_n2=DATA_n1;
    f_mean(2)=f_mean(1);
    f_std(2)=f_std(1);
end
%% MATRIX CONSTRUCTION
s=min([size(DATA_n1,1) size(DATA_n2,1)]);
DATA=zeros(round(s*1.1),7,2);
DATA(1:min([size(DATA_n1,1),size(DATA,1)]),:,1)=DATA_n1(1:min([size(DATA_n1,1)
,size(DATA,1)]),:);
DATA(1:min([size(DATA_n2,1),size(DATA,1)]),:,2)=DATA_n2(1:min([size(DATA_n2,1)
,size(DATA,1)]),:);
end

```

C.9 Script for data analysis in Section 6 Head Injury Risk Assessment

```

clc
clear all
close all

NA=input('Not Agonist? (YES=1, NO=0) ');
if NA==1
    l=dir('NA*.mat');
else if NA==0
    l=dir('A*.mat');
end
end
ns_max=5*60*900; % max number of samples acquired (min*sec/min*freq)
ns=size(l,1); % number of subjects tested
nt=4; % number of techniques tested
nr=3; % number of repetitions for each technique tested

%% DATA LOADING AND EPOCHS SPLITTING
data=NaN(ns_max,15,2,ns);
for s=1:ns % For each subject tested
    load(char(l(s).name))
    data_matrix(1:size(MATR,1),:,:,s)=MATR;
    frequencies(s)=f_r;
    clear MATR f_r
end
ord=load('techniques_order.mat');
o=ord.o;
f=round(mean(frequencies(s)));
o(18,:)= [4,3,1,2];
o(19,:)= [1,3,2,4];
o(20,:)= [2,4,1,3];

% Dividing signal into blocks of 3 throws
blocks=zeros(round(ns_max/3),15,2,ns,nt);
for s=1:ns
    coord(:,1,s)=find(data_matrix(:,5,1,s)==-1);
    coord(:,2,s)=find(data_matrix(:,5,2,s)==-1);
    blocks(1:coord(2,1,s)-
coord(1,1,s),:,1,s,1)=data_matrix(coord(1,1,s):coord(2,1,s)-1,(:,1,s);
    blocks(1:coord(3,1,s)-
coord(2,1,s),:,1,s,2)=data_matrix(coord(2,1,s):coord(3,1,s)-1,(:,1,s);
    blocks(1:coord(4,1,s)-
coord(3,1,s),:,1,s,3)=data_matrix(coord(3,1,s):coord(4,1,s)-1,(:,1,s);
    blocks(1:coord(5,1,s)-
coord(4,1,s),:,1,s,4)=data_matrix(coord(4,1,s):coord(5,1,s)-1,(:,1,s);

    blocks(1:coord(2,2,s)-
coord(1,2,s),:,2,s,1)=data_matrix(coord(1,2,s):coord(2,2,s)-1,(:,2,s);
    blocks(1:coord(3,2,s)-
coord(2,2,s),:,2,s,2)=data_matrix(coord(2,2,s):coord(3,2,s)-1,(:,2,s);
    blocks(1:coord(4,2,s)-
coord(3,2,s),:,2,s,3)=data_matrix(coord(3,2,s):coord(4,2,s)-1,(:,2,s);
    blocks(1:coord(5,2,s)-
coord(4,2,s),:,2,s,4)=data_matrix(coord(4,2,s):coord(5,2,s)-1,(:,2,s);
end

% Identify the peaks of head and trunk acceleration module
for s=1:ns
    for t=1:nt
        for sens=1:2
            [p,ind]=findpeaks(blocks(:,5,sens,s,t),'MinPeakProminence',2,'MinPeakDistance',
frequencies(s));
            p_d=sort(p,'descend');

```

```

indexes(:,sens,o(s,t),s)=sort([ind(p==p_d(1));ind(p==p_d(2));ind(p==p_d(3))], '
ascend');
%      fprintf(['sens=',num2str(sens),' o(s,t)=',num2str(o(s,t)), '
s=',num2str(s),'\n']);
%      plot(blocks(:,5,sens,s,t)),hold on,
plot(indexes(1,sens,o(s,t),s),blocks(indexes(1,sens,o(s,t),s),5,sens,s,t),'ro'
),
%
% plot(indexes(2,sens,o(s,t),s),blocks(indexes(2,sens,o(s,t),s),5,sens,s,t),'bo'
),
plot(indexes(3,sens,o(s,t),s),blocks(indexes(3,sens,o(s,t),s),5,sens,s,t),'go'
), hold off
%      pause
%      end
end
end

% Divide each blocks into 3 epochs
for s=1:ns % for each subject
    for t=1:nt % for each technique
        for r=1:nr % for each repetition
            for sens=1:2
                epochs(:, :, sens, s, t, r)=blocks(indexes(r, sens, t, s)-
round(f/2):indexes(r, sens, t, s)+round(f/2), :, sens, s, find(o(s, :)==t));
                % samples-variables-sensors-subjects-techniques-repetitions
            end
        end
    end
end

%% DATA POST-PROCESSING
for s=1:ns
    m(s)=nanmean(data_matrix(find(data_matrix(:,14,1,s)~=0),14,1,s));
    epochs(:,14,1,s,:)=epochs(:,14,1,s,:)-m(s);
end
subjects_mean=mean(epochs,6); % samples-variables-sensors-subjects-techniques
subjects_std=std(epochs,0,6);
subjects_max=max(max(epochs,[],6),[],1);
subjects_min=min(min(epochs,[],6),[],1);
techniques_mean=mean(subjects_mean,4); % samples-variables-sensors-techniques
techniques_std=std(subjects_mean,0,4);
techniques_max=max(max(max(epochs,[],6),[],4),[],1);
techniques_min=min(min(min(epochs,[],6),[],4),[],1);

mean_rep=mean(max(epochs,[],1),4);
std_rep=std(max(epochs,[],1),[],4);
size(mean_rep)
figure()
subplot(2,2,1)
barwitherr(permute([std_rep(:,5,1,:,:),1),std_rep(:,5,1,:,:),2),std_rep(:,5,1,:,:),
:3],[5,2,1,3,4]),...

permute([mean_rep(:,5,1,:,:),1),mean_rep(:,5,1,:,:),2),mean_rep(:,5,1,:,:),3],[5
,2,1,3,4]),
legend('rep #1','rep #2','rep #3'), title('Head acceleration module (g)')
xticks([1,2,3,4]), xticklabels({'O-soto-gari','O-uchi-gari','Ippon-seoi-
nage','Tai-otoshi'})
subplot(2,2,2)
barwitherr(permute([std_rep(:,5,2,:,:),1),std_rep(:,5,2,:,:),2),std_rep(:,5,2,:,:),
:3],[5,2,1,3,4]),...

permute([mean_rep(:,5,2,:,:),1),mean_rep(:,5,2,:,:),2),mean_rep(:,5,2,:,:),3],[5
,2,1,3,4])
xticks([1,2,3,4]), xticklabels({'O-soto-gari','O-uchi-gari','Ippon-seoi-
nage','Tai-otoshi'})
title('Trunk acceleration module (g)')
subplot(2,2,3)

```

```

barwitherr(permute([std_rep(:,12,1,::,1),std_rep(:,12,1,::,2),std_rep(:,12,1,
::,3)],[5,2,1,3,4]),...

permute([mean_rep(:,12,1,::,1),mean_rep(:,12,1,::,2),mean_rep(:,12,1,::,3)]
,[5,2,1,3,4]))
xticks([1,2,3,4]), xticklabels({'O-soto-gari','O-uchi-gari','Ippon-seoi-
nage','Tai-otoshi'})
title('Head angular acceleration module (rad/s^2)')
subplot(2,2,4)
barwitherr(permute([std_rep(:,12,2,::,1),std_rep(:,12,2,::,2),std_rep(:,12,2,
::,3)],[5,2,1,3,4]),...

permute([mean_rep(:,12,2,::,1),mean_rep(:,12,2,::,2),mean_rep(:,12,2,::,3)]
,[5,2,1,3,4]))
xticks([1,2,3,4]), xticklabels({'O-soto-gari','O-uchi-gari','Ippon-seoi-
nage','Tai-otoshi'})
title('Trunk angular acceleration module (rad/s^2)')
annotation('textbox',[0 0 1 1],'String','VALUES GAINED FOR EACH REPETITION
- NOT-AGONISTS','FontSize',14,'FontWeight','bold','EdgeColor','none',
'HorizontalAlignment','center')

indexes=NaN(f,ns,nt,nr);
duration=NaN(1,ns,nt,nr);
sens=1;
for s=1:ns
    for t=1:4
        for r=1:nr
            if max(epochs(:,5,sens,s,t,r),[],1)<=10
                level=1;
            else
                level=0.1*max(epochs(:,5,sens,s,t,r),[],1);
            end
            a=find(epochs(:,5,sens,s,t,r)==max(epochs(:,5,sens,s,t,r),[],1));
            i=1;
            while epochs(a-i,5,sens,s,t,r)>level && a-i>1
                i=i+1;
            end
            first=a-i;
            i=1;
            while epochs(a+i,5,sens,s,t,r)>level && a+i<f
                i=i+1;
            end
            last=a+i;

            ind=first:1:last;
            indexes(1:length(ind),s,t,r)=ind;
            % plot(epochs(:,5,sens,s,t,r),hold on,
            plot(ind,epochs(ind,5,sens,s,t,r),hold off,pause()
                duration(1,s,t,r)=(epochs(ind(end),1,sens,s,t,r)-
            epochs(ind(1),1,sens,s,t,r))*1000;

            GSI(s,t,r)=max(cumtrapz(epochs(ind,1,sens,s,t,r),epochs(ind,5,sens,s,t,r).^2.5
            ));
        end
    end
end
max(max(max(GSI)))

% dispersions
figure()
a=rand(ns,3);
subplot(1,3,1)
for s=1:ns
    for t=1:4

plot(t,reshape(max(epochs(:,5,1,s,t,:),[],1),3,1),'.','MarkerSize',30,'Color',
a(s,:)), hold on
end

```

```

end
hold off, xticks([1,2,3,4]),xticklabels({'O-soto-gari','O-uchi-gari','Ippon-
seoi-nage','Tai-otoshi'})
title('Head Acceleration Module (g)'), set(gca, 'YGrid', 'on', 'XGrid', 'off')
subplot(1,3,2)
for s=1:ns
    for t=1:4

plot(t,reshape(max(epochs(:,12,1,s,t,:),[],1),3,1),'.','MarkerSize',30,'Color'
,a(s,:)), hold on
    end
end
hold off, xticks([1,2,3,4]),xticklabels({'O-soto-gari','O-uchi-gari','Ippon-
seoi-nage','Tai-otoshi'})
title('Head Angular Acceleration Module (rad/s^2)'), set(gca, 'YGrid', 'on',
'XGrid', 'off')
subplot(1,3,3)
for s=1:ns
    for t=1:4
        plot(t,reshape(duration(:,s,t,:),3,1),'.','MarkerSize',30,'Color',a(s,:)),
hold on
    end
end
hold off, xticks([1,2,3,4]),xticklabels({'O-soto-gari','O-uchi-gari','Ippon-
seoi-nage','Tai-otoshi'})
title('Impact Duration (ms)'), set(gca, 'YGrid', 'on', 'XGrid',
'off'),set(gca, 'YGrid', 'on', 'XGrid', 'off')
annotation('textbox', [0 0 1 1], 'String', 'ACQUIRED VALUES','FontSize', 14,
'FontWeight', 'bold', 'EdgeColor', 'none', 'HorizontalAlignment', 'center')

% head acceleration module
figure()
obj=5;
subplot(1,4,1)
for s=1:ns
    for r=1:nr
        plot(epochs(:,obj,1,s,1,r)),hold on
    end
end
plot(techniques_mean(:,obj,1,1),'k','LineWidth',3),hold off, title('O-soto-
gari'),xlim([0.3*f 0.7*f]),xlabel('Samples')
subplot(1,4,2)
for s=1:ns
    for r=1:nr
        plot(epochs(:,obj,1,s,2,r)),hold on
    end
end
plot(techniques_mean(:,obj,1,2),'k','LineWidth',3),hold off, title('O-uchi-
gari'),xlim([0.3*f 0.7*f]),xlabel('Samples')
subplot(1,4,3)
for s=1:ns
    for r=1:nr
        plot(epochs(:,obj,1,s,3,r)),hold on
    end
end
plot(techniques_mean(:,obj,1,3),'k','LineWidth',3),hold off, title('Ippon-
seoi-nage'),xlim([0.3*f 0.7*f]),xlabel('Samples')
subplot(1,4,4)
for s=1:ns
    for r=1:nr
        plot(epochs(:,obj,1,s,4,r)),hold on
    end
end
plot(techniques_mean(:,obj,1,4),'k','LineWidth',3),hold off, title('Tai-
otoshi'),xlim([0.3*f 0.7*f]),xlabel('Samples')
annotation('textbox', [0 0 1 1], 'String', 'HEAD ACCELERATION MODULE
(g)','FontSize', 14, 'FontWeight', 'bold', 'EdgeColor', 'none',
'HorizontalAlignment', 'center')

```

```

% head angular acceleration module
figure()
obj=12;
subplot(1,4,1)
for s=1:ns
    for r=1:nr
        plot(epochs(:,obj,1,s,1,r),hold on
    end
end
plot(techniques_mean(:,obj,1,1),'k','LineWidth',3),hold off, title('O-soto-
gari'),xlim([0.3*f 0.6*f]),xlabel('Samples')
subplot(1,4,2)
for s=1:ns
    for r=1:nr
        plot(epochs(:,obj,1,s,2,r),hold on
    end
end
plot(techniques_mean(:,obj,1,2),'k','LineWidth',3),hold off, title('O-uchi-
gari'),xlim([0.3*f 0.6*f]),xlabel('Samples')
subplot(1,4,3)
for s=1:ns
    for r=1:nr
        plot(epochs(:,obj,1,s,3,r),hold on
    end
end
plot(techniques_mean(:,obj,1,3),'k','LineWidth',3),hold off, title('Ippon-
seoi-nage'),xlim([0.3*f 0.6*f]),xlabel('Samples')
subplot(1,4,4)
for s=1:ns
    for r=1:nr
        plot(epochs(:,obj,1,s,4,r),hold on
    end
end
plot(techniques_mean(:,obj,1,4),'k','LineWidth',3),hold off, title('Tai-
otoshi'),xlim([0.3*f 0.6*f]),xlabel('Samples')
annotation('textbox', [0 0 1 1], 'String', 'HEAD ANGULAR ACCELERATION MODULE
(rad/s^2)', 'FontSize', 14, 'FontWeight', 'bold', 'EdgeColor', 'none',
'HorizontalAlignment', 'center')

% neck angle
figure()
obj=14;
subplot(1,4,1)
for s=1:ns
    for r=1:nr
        plot(epochs(:,obj,1,s,1,r),hold on
    end
end
plot(techniques_mean(:,obj,1,1),'k','LineWidth',3),hold off, title('O-soto-
gari'),xlim([0.3*f 0.7*f]),xlabel('Samples')
subplot(1,4,2)
for s=1:ns
    for r=1:nr
        plot(epochs(:,obj,1,s,2,r),hold on
    end
end
plot(techniques_mean(:,obj,1,2),'k','LineWidth',3),hold off, title('O-uchi-
gari'),xlim([0.3*f 0.7*f]),xlabel('Samples')
subplot(1,4,3)
for s=1:ns
    for r=1:nr
        plot(epochs(:,obj,1,s,3,r),hold on
    end
end
plot(techniques_mean(:,obj,1,3),'k','LineWidth',3),hold off, title('Ippon-
seoi-nage'),xlim([0.3*f 0.7*f]),xlabel('Samples')
subplot(1,4,4)
for s=1:ns

```

```

    for r=1:nr
        plot(epochs(:,obj,1,s,4,r)),hold on
    end
end
plot(techniques_mean(:,obj,1,4),'k','LineWidth',3),hold off, title('Tai-otoshi'),xlim([0.3*f 0.7*f]),xlabel('Samples')
annotation('textbox', [0 0 1 1], 'String', 'NECK FLEX/EXTENSION ANGLE (degree)', 'FontSize', 14, 'FontWeight', 'bold', 'EdgeColor', 'none', 'HorizontalAlignment', 'center')

% Acceleration module
obj=5;
figure()
subplot(2,4,1)
plot(techniques_mean(:,obj,1,1)),hold on
plot(techniques_mean(:,obj,1,1)+techniques_std(:,obj,1,1),'k')
plot(techniques_mean(:,obj,1,1)-techniques_std(:,obj,1,1),'k'),hold off,title('O-soto-gari - HEAD')
subplot(2,4,2)
plot(techniques_mean(:,obj,1,2)),hold on
plot(techniques_mean(:,obj,1,2)+techniques_std(:,obj,1,2),'k')
plot(techniques_mean(:,obj,1,2)-techniques_std(:,obj,1,2),'k'),hold off,title('O-uchi-gari - HEAD')
subplot(2,4,3)
plot(techniques_mean(:,obj,1,3)),hold on
plot(techniques_mean(:,obj,1,3)+techniques_std(:,obj,1,3),'k')
plot(techniques_mean(:,obj,1,3)-techniques_std(:,obj,1,3),'k'),hold off,title('Ippon-seoi-nage - HEAD')
subplot(2,4,4)
plot(techniques_mean(:,obj,1,4)),hold on
plot(techniques_mean(:,obj,1,4)+techniques_std(:,obj,1,4),'k')
plot(techniques_mean(:,obj,1,4)-techniques_std(:,obj,1,4),'k'),hold off,title('Tai-otoshi - HEAD')
subplot(2,4,5)
plot(techniques_mean(:,obj,2,1)),hold on
plot(techniques_mean(:,obj,2,1)+techniques_std(:,obj,2,1),'k')
plot(techniques_mean(:,obj,2,1)-techniques_std(:,obj,2,1),'k'),hold off,title('O-soto-gari - TRUNK')
subplot(2,4,6)
plot(techniques_mean(:,obj,2,2)),hold on
plot(techniques_mean(:,obj,2,2)+techniques_std(:,obj,2,2),'k')
plot(techniques_mean(:,obj,2,2)-techniques_std(:,obj,2,2),'k'),hold off,title('O-uchi-gari - TRUNK')
subplot(2,4,7)
plot(techniques_mean(:,obj,2,3)),hold on
plot(techniques_mean(:,obj,2,3)+techniques_std(:,obj,2,3),'k')
plot(techniques_mean(:,obj,2,3)-techniques_std(:,obj,2,3),'k'),hold off,title('Ippon-seoi-nage - TRUNK')
subplot(2,4,8)
plot(techniques_mean(:,obj,2,4)),hold on
plot(techniques_mean(:,obj,2,4)+techniques_std(:,obj,2,4),'k')
plot(techniques_mean(:,obj,2,4)-techniques_std(:,obj,2,4),'k'),hold off,title('Tai-otoshi - TRUNK')
annotation('textbox', [0 0 1 1], 'String', 'MEAN VALUE  $\pm$  STANDARD DEVIATION - ACCELERATION MODULE (g)', 'FontSize', 14, 'FontWeight', 'bold', 'EdgeColor', 'none', 'HorizontalAlignment', 'center')

% Angular acceleration module
obj=12;
figure()
subplot(2,4,1)
plot(techniques_mean(:,obj,1,1)),hold on
plot(techniques_mean(:,obj,1,1)+techniques_std(:,obj,1,1),'k')
plot(techniques_mean(:,obj,1,1)-techniques_std(:,obj,1,1),'k'),hold off,title('O-soto-gari - HEAD')
subplot(2,4,2)
plot(techniques_mean(:,obj,1,2)),hold on
plot(techniques_mean(:,obj,1,2)+techniques_std(:,obj,1,2),'k')

```

```

plot(techniques_mean(:,obj,1,2)-techniques_std(:,obj,1,2), 'k'),hold
off,title('O-uchi-gari - HEAD')
subplot(2,4,3)
plot(techniques_mean(:,obj,1,3)),hold on
plot(techniques_mean(:,obj,1,3)+techniques_std(:,obj,1,3), 'k')
plot(techniques_mean(:,obj,1,3)-techniques_std(:,obj,1,3), 'k'),hold
off,title('Ippon-seoi-nage - HEAD')
subplot(2,4,4)
plot(techniques_mean(:,obj,1,4)),hold on
plot(techniques_mean(:,obj,1,4)+techniques_std(:,obj,1,4), 'k')
plot(techniques_mean(:,obj,1,4)-techniques_std(:,obj,1,4), 'k'),hold
off,title('Tai-otoshi - HEAD')
subplot(2,4,5)
plot(techniques_mean(:,obj,2,1)),hold on
plot(techniques_mean(:,obj,2,1)+techniques_std(:,obj,2,1), 'k')
plot(techniques_mean(:,obj,2,1)-techniques_std(:,obj,2,1), 'k'),hold
off,title('O-soto-gari - TRUNK')
subplot(2,4,6)
plot(techniques_mean(:,obj,2,2)),hold on
plot(techniques_mean(:,obj,2,2)+techniques_std(:,obj,2,2), 'k')
plot(techniques_mean(:,obj,2,2)-techniques_std(:,obj,2,2), 'k'),hold
off,title('O-uchi-gari - TRUNK')
subplot(2,4,7)
plot(techniques_mean(:,obj,2,3)),hold on
plot(techniques_mean(:,obj,2,3)+techniques_std(:,obj,2,3), 'k')
plot(techniques_mean(:,obj,2,3)-techniques_std(:,obj,2,3), 'k'),hold
off,title('Ippon-seoi-nage - TRUNK')
subplot(2,4,8)
plot(techniques_mean(:,obj,2,4)),hold on
plot(techniques_mean(:,obj,2,4)+techniques_std(:,obj,2,4), 'k')
plot(techniques_mean(:,obj,2,4)-techniques_std(:,obj,2,4), 'k'),hold
off,title('Tai-otoshi - TRUNK')
annotation('textbox', [0 0 1 1], 'String', 'MEAN VALUE  $\pm$  STANDARD DEVIATION
- ANGULAR ACCELERATION MODULE (rad/s2)', 'FontSize', 14, 'FontWeight', 'bold',
'EdgeColor', 'none', 'HorizontalAlignment', 'center')

% Neck angle
obj=14;
figure()
subplot(1,4,1)
plot(techniques_mean(:,obj,1,1)),hold on
plot(techniques_mean(:,obj,1,1)+techniques_std(:,obj,1,1), 'k')
plot(techniques_mean(:,obj,1,1)-techniques_std(:,obj,1,1), 'k'),hold
off,title('O-soto-gari')
subplot(1,4,2)
plot(techniques_mean(:,obj,1,2)),hold on
plot(techniques_mean(:,obj,1,2)+techniques_std(:,obj,1,2), 'k')
plot(techniques_mean(:,obj,1,2)-techniques_std(:,obj,1,2), 'k'),hold
off,title('O-uchi-gari')
subplot(1,4,3)
plot(techniques_mean(:,obj,1,3)),hold on
plot(techniques_mean(:,obj,1,3)+techniques_std(:,obj,1,3), 'k')
plot(techniques_mean(:,obj,1,3)-techniques_std(:,obj,1,3), 'k'),hold
off,title('Ippon-seoi-nage')
subplot(1,4,4)
plot(techniques_mean(:,obj,1,4)),hold on
plot(techniques_mean(:,obj,1,4)+techniques_std(:,obj,1,4), 'k')
plot(techniques_mean(:,obj,1,4)-techniques_std(:,obj,1,4), 'k'),hold
off,title('Tai-otoshi')
annotation('textbox', [0 0 1 1], 'String', 'MEAN VALUE  $\pm$  STANDARD DEVIATION
- NECK FLEX/EXTENSION ANGLE (degree)', 'FontSize', 14, 'FontWeight', 'bold',
'EdgeColor', 'none', 'HorizontalAlignment', 'center')

figure()
obj=12;
subplot(1,4,1)
for s=1:ns
    for r=1:nr

```

```

        plot(epochs(:,obj,2,s,1,r)),hold on
    end
end
plot(techniques_mean(:,obj,2,1),'k','LineWidth',3),hold off, title('O-soto-
gari'),xlim([0 f]),xlabel('Samples')
subplot(1,4,2)
for s=1:ns
    for r=1:nr
        plot(epochs(:,obj,2,s,2,r)),hold on
    end
end
plot(techniques_mean(:,obj,2,2),'k','LineWidth',3),hold off, title('O-uchi-
gari'),xlim([0 f]),xlabel('Samples')
subplot(1,4,3)
for s=1:ns
    for r=1:nr
        plot(epochs(:,obj,2,s,3,r)),hold on
    end
end
plot(techniques_mean(:,obj,2,3),'k','LineWidth',3),hold off, title('Ippon-
seoi-nage'),xlim([0 f]),xlabel('Samples')
subplot(1,4,4)
for s=1:ns
    for r=1:nr
        plot(epochs(:,obj,2,s,4,r)),hold on
    end
end
plot(techniques_mean(:,obj,2,4),'k','LineWidth',3),hold off, title('Tai-
otoshi'),xlim([0 f]),xlabel('Samples')
annotation('textbox', [0 0 1 1], 'String', 'TRUNK ANGULAR ACCELERATION MODULE
(rad/s^2)', 'FontSize', 14, 'FontWeight', 'bold', 'EdgeColor', 'none',
'HorizontalAlignment', 'center')

%% RESULTS ANALYSIS
M3r=max(subjects_mean,[],1); % peak value of the mean curve of the three
repetitions
m3r=min(subjects_mean,[],1); % negative peak value of the mean curve of the
three repetitions

if NA==0
    Aex=[1,6,7,9,13,14,16,17,18,19];
    An=[2,3,4,5,8,10,11,12,15,20];

    MEAN_TECHNIQUES=NaN(1,4,1,1,4,2);
    MEAN_TECHNIQUES(:,1:3,:,:,1)=mean(M3r(:,[5,12,14],1,Aex,:),4);
    MEAN_TECHNIQUES(:,1:3,:,:,2)=mean(M3r(:,[5,12,14],1,An,:),4);
    MEAN_TECHNIQUES(:,4,:,:,1)=mean(m3r(:,14,1,Aex,:),4);
    MEAN_TECHNIQUES(:,4,:,:,2)=mean(m3r(:,14,1,An,:),4);
    MEAN_TECHNIQUES=permute(MEAN_TECHNIQUES,[5,2,6,1,3,4]);
    MEAN_TECHNIQUES_trunk=NaN(1,2,1,1,4,2);
    MEAN_TECHNIQUES_trunk(:,:,:,:,1)=mean(M3r(:,[5,12],2,Aex,:),4);
    MEAN_TECHNIQUES_trunk(:,:,:,:,2)=mean(M3r(:,[5,12],2,An,:),4);
    MEAN_TECHNIQUES_trunk=permute(MEAN_TECHNIQUES_trunk,[5,2,6,1,3,4]);
    MEAN_DURATION(:,1)=mean(mean(duration(:,Aex,:),4),2);
    MEAN_DURATION(:,2)=mean(mean(duration(:,An,:),4),2);

    MEAN_ang(:,1)=permute(mean(subjects_mean(431,14,1,Aex,:),4),[4,5,1,2,3]);
    MEAN_ang(:,2)=permute(mean(subjects_mean(431,14,1,An,:),4),[4,5,1,2,3]);

    STD_TECHNIQUES=NaN(1,4,1,1,4,2);
    STD_TECHNIQUES(:,1:3,:,:,1)=std(M3r(:,[5,12,14],1,Aex,:),0,4);
    STD_TECHNIQUES(:,1:3,:,:,2)=std(M3r(:,[5,12,14],1,An,:),0,4);
    STD_TECHNIQUES(:,4,:,:,1)=std(m3r(:,14,1,Aex,:),0,4);
    STD_TECHNIQUES(:,4,:,:,2)=std(m3r(:,14,1,An,:),0,4);
    STD_TECHNIQUES=permute(STD_TECHNIQUES,[5,2,6,1,3,4]);
    STD_TECHNIQUES_trunk=NaN(1,2,1,1,4,2);
    STD_TECHNIQUES_trunk(:,:,:,:,1)=std(M3r(:,[5,12],2,Aex,:),0,4);
    STD_TECHNIQUES_trunk(:,:,:,:,2)=std(M3r(:,[5,12],2,An,:),0,4);

```

```

STD_TECHNIQUES_trunk=permute(STD_TECHNIQUES_trunk,[5,2,6,1,3,4]);
STD_DURATION(:,1)=std(mean(duration(:,Aex,:),:),4,0,2);
STD_DURATION(:,2)=std(mean(duration(:,An,:),:),4,0,2);

STD_ang(:,1)=permute(std(subjects_mean(431,14,1,Aex,:),:),[4,5,1,2,3]);
STD_ang(:,2)=permute(std(subjects_mean(431,14,1,An,:),:),[4,5,1,2,3]);

% STATISTICAL DIFFERENCES (Mann-Whitney test)
for t=1:nt
    for v=[5,12,14];

W_M(t,v)=ranksum(reshape(M3r(:,v,1,Aex,t),length(Aex),1),reshape(M3r(:,v,1,An,t),length(An),1)));

W_m(t,v)=ranksum(reshape(m3r(:,v,1,Aex,t),length(Aex),1),reshape(m3r(:,v,1,An,t),length(An),1)));

W_M_t(t,v)=ranksum(reshape(M3r(:,v,2,Aex,t),length(Aex),1),reshape(M3r(:,v,2,An,t),length(An),1)));

W_d(t)=ranksum(reshape(mean(duration(:,Aex,t,:),:),4,length(Aex),1),reshape(mean(duration(:,An,t,:),:),4,length(An),1)));

W_a(t)=ranksum(permute(subjects_mean(431,14,1,Aex,t),[4,3,2,1]),permute(subjects_mean(431,14,1,An,t),[4,3,2,1]));
    end
end

figure()
plot(W_M(:,[5,12,14]),'.-','MarkerSize',20),hold on
plot(W_M_t(:,[5,12]),'.-','MarkerSize',20)
plot(W_m(:,14),'.-','MarkerSize',20)
plot(W_d,'.-','MarkerSize',20)

legend('|a|_H_E_A_D','d\omega/dt|_H_E_A_D','|a|_T_R_U_N_K','d\omega/dt|_T_R_U_N_K','ext-angle','flex-angle','duration'),xticks([1,2,3,4]),
xticklabels({'O-soto-gari','O-uchi-gari','Ippon-seoi-nage','Tai-otoshi'})
title('Mann-Whitney test - AGONISTS'),grid on, ylim([0,0.1])

figure()
subplot(2,1,1),barwitherr(STD_ang,MEAN_ang);
legend('Experts','Not-experts'),xticklabels({'O-soto-gari','O-uchi-gari','Ippon-seoi-nage','Tai-otoshi'})
title('Neck angle during the acceleration peak (degree)'), grid on
subplot(2,1,2),plot(W_a,'.-','MarkerSize',20),ylim([0,1])
xticks([1,2,3,4]),xticklabels({'O-soto-gari','O-uchi-gari','Ippon-seoi-nage','Tai-otoshi'})
title('Mann-Whitney test'), grid on
annotation('textbox',[0 0 1 1],'String','AGONISTS','FontSize',14,'FontWeight','bold','EdgeColor','none','HorizontalAlignment','center')

% BAR DIAGRAMS
figure()
subplot(2,2,1)

b1=barwitherr([STD_TECHNIQUES(:,1,1),STD_TECHNIQUES(:,1,2)],[MEAN_TECHNIQUES(:,1,1),MEAN_TECHNIQUES(:,1,2)]);
hold on, plot([1-0.15;1+0.15],[60;60],'-k','LineWidth',2),plot(1,60*1.03,'*k')
legend(b1,{'Experts','Not-experts'}),xticklabels({'O-soto-gari','O-uchi-gari','Ippon-seoi-nage','Tai-otoshi'})
title('Head acceleration module (g)'), grid on
subplot(2,2,3)

barwitherr([STD_TECHNIQUES(:,2,1),STD_TECHNIQUES(:,2,2)],[MEAN_TECHNIQUES(:,2,1),MEAN_TECHNIQUES(:,2,2)]),title('Head angular acceleration module (rad/s^2)'), grid on

```

```

    xticklabels({'O-soto-gari', 'O-uchi-gari', 'Ippon-seoi-nage', 'Tai-otoshi'})
    hold on, plot([1-0.15;1+0.15],[2000;2000], '-k', 'LineWidth', 2), plot(1,
2000*1.05, '*k'), hold off
    subplot(2,2,2)

barwitherr([STD_TECHNIQUES_trunk(:,1,1),STD_TECHNIQUES_trunk(:,1,2)],[MEAN_TEC
HNiques_trunk(:,1,1),MEAN_TECHNIQUES_trunk(:,1,2)]),title('Trunk acceleration
module (g)'), grid on
    xticklabels({'O-soto-gari', 'O-uchi-gari', 'Ippon-seoi-nage', 'Tai-otoshi'})
    hold on, plot([2-0.15;2+0.15],[40;40], '-k', 'LineWidth', 2), plot(2,
40*1.04, '*k'), hold off
    subplot(2,2,4)

barwitherr([STD_TECHNIQUES_trunk(:,2,1),STD_TECHNIQUES_trunk(:,2,2)],[MEAN_TEC
HNiques_trunk(:,2,1),MEAN_TECHNIQUES_trunk(:,2,2)]),title('Trunk angular
acceleration module (rad/s^2)'), grid on
    xticklabels({'O-soto-gari', 'O-uchi-gari', 'Ippon-seoi-nage', 'Tai-otoshi'})
    annotation('textbox', [0 0 1 1], 'String', 'AGONISTS', 'FontSize', 14,
'FontWeight', 'bold', 'EdgeColor', 'none', 'HorizontalAlignment', 'center')

    figure()
    subplot(2,1,1)

barwitherr([STD_TECHNIQUES(:,3,1),STD_TECHNIQUES(:,3,2)],[MEAN_TECHNIQUES(:,3,
1),MEAN_TECHNIQUES(:,3,2)]),title('Neck extension angle (degree)'), grid on
    legend('Experts', 'Not-experts', 'Location', 'Best'), xticklabels({'O-soto-
gari', 'O-uchi-gari', 'Ippon-seoi-nage', 'Tai-otoshi'}), ylim([0,50])
    subplot(2,1,2)

barwitherr([STD_TECHNIQUES(:,4,1),STD_TECHNIQUES(:,4,2)],[abs(MEAN_TECHNIQUES(
:,4,1)),abs(MEAN_TECHNIQUES(:,4,2))]),title('Neck flexion angle (degree)'),
grid on
    xticklabels({'O-soto-gari', 'O-uchi-gari', 'Ippon-seoi-nage', 'Tai-
otoshi'}), ylim([0,50])
    annotation('textbox', [0 0 1 1], 'String', 'AGONISTS', 'FontSize', 14,
'FontWeight', 'bold', 'EdgeColor', 'none', 'HorizontalAlignment', 'center')

    figure()
    b1=barwitherr(STD_DURATION,MEAN_DURATION);
    hold on, plot([1-0.15;1+0.15],[250;250], '-k', 'LineWidth', 2), plot(1,
250*1.03, '*k'), hold off
    legend(b1,{'Experts', 'Not-experts'}), xticklabels({'O-soto-gari', 'O-uchi-
gari', 'Ippon-seoi-nage', 'Tai-otoshi'})
    title('Duration (ms) - AGONISTS'), grid on

    % BOXPLOTS
    figure()
    v=5;

subplot(1,4,1),boxplot([[reshape(M3r(1,v,1,Aex,1),length(Aex),1);NaN(length(An
)-length(Aex),1)],reshape(M3r(1,v,1,An,1),length(An),1)]),
xticklabels({'Experts', 'Not-experts'}), ylabel('Acceleration Module (g)'),
ylim([0,80]), title('O-soto-gari')

subplot(1,4,2),boxplot([[reshape(M3r(1,v,1,Aex,2),length(Aex),1);NaN(length(An
)-length(Aex),1)],reshape(M3r(1,v,1,An,2),length(An),1)]),
xticklabels({'Experts', 'Not-experts'}), ylim([0,80]), title('O-uchi-gari')

subplot(1,4,3),boxplot([[reshape(M3r(1,v,1,Aex,3),length(Aex),1);NaN(length(An
)-length(Aex),1)],reshape(M3r(1,v,1,An,3),length(An),1)]),
xticklabels({'Experts', 'Not-experts'}), ylim([0,80]), title('Ippon-seoi-
nage')

subplot(1,4,4),boxplot([[reshape(M3r(1,v,1,Aex,4),length(Aex),1);NaN(length(An
)-length(Aex),1)],reshape(M3r(1,v,1,An,4),length(An),1)]),
xticklabels({'Experts', 'Not-experts'}), ylim([0,80]), title('Tai-otoshi')

```

```

    annotation('textbox', [0 0 1 1], 'String', 'HEAD ACCELERATION COMPARISION
- AGONISTS', 'FontSize', 14, 'FontWeight', 'bold', 'EdgeColor', 'none',
'HorizontalAlignment', 'center')

    figure()
    v=12;

subplot(1,4,1),boxplot([[reshape(M3r(1,v,1,Aex,1),length(Aex),1);NaN(length(An)
)-length(Aex),1)],reshape(M3r(1,v,1,An,1),length(An),1)]),
xticklabels({'Experts', 'Not-experts'}), ylabel('Angular Acceleration Module
(rad/s^2)'), ylim([0,2500]), title('O-soto-gari')

subplot(1,4,2),boxplot([[reshape(M3r(1,v,1,Aex,2),length(Aex),1);NaN(length(An)
)-length(Aex),1)],reshape(M3r(1,v,1,An,2),length(An),1)]),
xticklabels({'Experts', 'Not-experts'}), ylim([0,2500]), title('O-uchi-gari')

subplot(1,4,3),boxplot([[reshape(M3r(1,v,1,Aex,3),length(Aex),1);NaN(length(An)
)-length(Aex),1)],reshape(M3r(1,v,1,An,3),length(An),1)]),
xticklabels({'Experts', 'Not-experts'}), ylim([0,2500]), title('Ippon-seoi-
nage')

subplot(1,4,4),boxplot([[reshape(M3r(1,v,1,Aex,4),length(Aex),1);NaN(length(An)
)-length(Aex),1)],reshape(M3r(1,v,1,An,4),length(An),1)]),
xticklabels({'Experts', 'Not-experts'}), ylim([0,2500]), title('Tai-otoshi')
    annotation('textbox', [0 0 1 1], 'String', 'HEAD ANGULAR ACCELERATION
COMPARISION - AGONISTS', 'FontSize', 14, 'FontWeight', 'bold', 'EdgeColor',
'none', 'HorizontalAlignment', 'center')

    figure()
    v=14;

subplot(2,4,1),boxplot([[reshape(M3r(1,v,1,Aex,1),length(Aex),1);NaN(length(An)
)-length(Aex),1)],reshape(M3r(1,v,1,An,1),length(An),1)]),
xticklabels({'Experts', 'Not-experts'}), ylabel('Angle (degree)'), ylim([-
25,35]), title('O-soto-gari')

subplot(2,4,2),boxplot([[reshape(M3r(1,v,1,Aex,2),length(Aex),1);NaN(length(An)
)-length(Aex),1)],reshape(M3r(1,v,1,An,2),length(An),1)]),
xticklabels({'Experts', 'Not-experts'}), ylim([-25,35]), title('O-uchi-gari')

subplot(2,4,3),boxplot([[reshape(M3r(1,v,1,Aex,3),length(Aex),1);NaN(length(An)
)-length(Aex),1)],reshape(M3r(1,v,1,An,3),length(An),1)]),
xticklabels({'Experts', 'Not-experts'}), ylim([-25,35]), title('Ippon-seoi-
nage')

subplot(2,4,4),boxplot([[reshape(M3r(1,v,1,Aex,4),length(Aex),1);NaN(length(An)
)-length(Aex),1)],reshape(M3r(1,v,1,An,4),length(An),1)]),
xticklabels({'Experts', 'Not-experts'}), ylim([-25,35]), title('Tai-otoshi')
    annotation('textbox', [0 0 1 1], 'String', 'NECK EXTENSION ANGLE
COMPARISION - AGONISTS', 'FontSize', 14, 'FontWeight', 'bold', 'EdgeColor',
'none', 'HorizontalAlignment', 'center')

subplot(2,4,5),boxplot([[reshape(m3r(1,v,1,Aex,1),length(Aex),1);NaN(length(An)
)-length(Aex),1)],reshape(m3r(1,v,1,An,1),length(An),1)]),
xticklabels({'Experts', 'Not-experts'}), ylabel('Angle (degree)'), ylim([-
70,0]), title('O-soto-gari')

subplot(2,4,6),boxplot([[reshape(m3r(1,v,1,Aex,2),length(Aex),1);NaN(length(An)
)-length(Aex),1)],reshape(m3r(1,v,1,An,2),length(An),1)]),
xticklabels({'Experts', 'Not-experts'}), ylim([-70,0]), title('O-uchi-gari')

subplot(2,4,7),boxplot([[reshape(m3r(1,v,1,Aex,3),length(Aex),1);NaN(length(An)
)-length(Aex),1)],reshape(m3r(1,v,1,An,3),length(An),1)]),
xticklabels({'Experts', 'Not-experts'}), ylim([-70,0]), title('Ippon-seoi-
nage')

subplot(2,4,8),boxplot([[reshape(m3r(1,v,1,Aex,4),length(Aex),1);NaN(length(An)
)-length(Aex),1)],reshape(m3r(1,v,1,An,4),length(An),1)]),
xticklabels({'Experts', 'Not-experts'}), ylim([-70,0]), title('Tai-otoshi')

```

```

    annotation('textbox', [0 0.5 1 0], 'String', 'NECK FLEXION ANGLE
    COMPARISION - AGONISTS', 'FontSize', 14, 'FontWeight', 'bold', 'EdgeColor',
    'none', 'HorizontalAlignment', 'center')

    % Technique analysis
    tech=M3r(:, [5 12 14], 1, :, :);
    tech=cat(2, tech, m3r(:, 14, 1, :, :));
    tech=permute(tech, [4, 2, 5, 1, 3]);
    tech=cat(2, tech, permute(mean(duration, 4), [2, 1, 3])); % 20 subjects in rows
    * 5variables in column(lacc,aacc,ext,flex,time) * 4 techniques

    % Friedman's test
    for v=1:5

[F_t(v), ~, stats(v)] = friedman([tech(:, v, 1), tech(:, v, 2), tech(:, v, 3), tech(:, v, 4)]
);
        d(:, :, v) = multcompare(stats(v));
    end

    figure()

    bl = barwitherr([permute(std(tech(:, 1, :)), 0, 1), [3, 2, 1]], permute(std(tech(:, 2, :)), 0,
    1)/100, [3, 2, 1]), ...

    permute(std(tech(:, 3, :)), 0, 1), [3, 2, 1]), permute(std(tech(:, 4, :)), 0, 1), [3, 2, 1]), pe
    rmute(std(tech(:, 5, :)), 0, 1), [3, 2, 1])/10], ...

    [permute(mean(tech(:, 1, :)), [3, 2, 1]), permute(mean(tech(:, 2, :))/100, [3, 2, 1]), ...
        permute(mean(tech(:, 3, :)), [3, 2, 1]), permute(-
    mean(tech(:, 4, :)), [3, 2, 1]), permute(mean(tech(:, 5, :)), [3, 2, 1])/10]);
        xticks([1, 2, 3, 4]), xticklabels({'O-soto-gari', 'O-uchi-gari', 'Ippon-seoi-
    nage', 'Tai-otoshi'})
        title('Variables comparison - AGONISTS')
        legend(bl, {'|a|_H_E_A_D (g)', '|d\omega/dt|_H_E_A_D / 100 (rad/s^2)', 'ext-
    angle (degree)', 'flex-angle (degree)', 'duration / 10 (ms)'}))

    figure()
    s = permute(std(tech(:, :, :)), 0, 1), [2, 3, 1]);
    m = permute(mean(tech(:, :, :)), [2, 3, 1]);
    subplot(2, 3, 1)
    barwitherr(s(1, :), m(1, :));
    xticklabels({'T1', 'T2', 'T3', 'T4'})
    hold on, plot([1; 3], [50; 50], '-k', 'LineWidth', 2), plot(2+0.15, 50*1.04,
    '*k'), plot(2, 50*1.04, '*k'), plot(2-0.15, 50*1.04, '*k')
        plot([2; 3], [35; 35], '-k', 'LineWidth', 2), plot(2.5, 35*1.04, '*k'),
    hold off
    title('Head acceleration module (g)'),
    subplot(2, 3, 2)
    barwitherr(s(2, :), m(2, :));
    xticklabels({'T1', 'T2', 'T3', 'T4'})
    hold on, plot([1; 3], [2000; 2000], '-k', 'LineWidth', 2), plot(2+0.15,
    2000*1.04, '*k'), plot(2, 2000*1.04, '*k'), plot(2-0.15, 2000*1.04, '*k')
        plot([3; 4], [1750; 1750], '-k', 'LineWidth', 2), plot(3.5, 1750*1.04,
    '*k')
        plot([2; 3], [1500; 1500], '-k', 'LineWidth', 2), plot(2.5, 1500*1.04,
    '*k'), hold off
    title('Head angular acceleration module (rad/s^2)')
    subplot(2, 3, 4)
    barwitherr(s(3, :), m(3, :));
    xticklabels({'T1', 'T2', 'T3', 'T4'})
    title('Neck extension angle (degree)'), ylim([0, 60])
    hold on, plot([3; 4], [30; 30], '-k', 'LineWidth', 2), plot(3.5+0.15, 30*1.04,
    '*k'), plot(3.5, 30*1.04, '*k'), plot(3.5-0.15, 30*1.04, '*k'), hold off
    subplot(2, 3, 5)
    barwitherr(s(4, :), -m(4, :));
    xticklabels({'T1', 'T2', 'T3', 'T4'})
    hold on, plot([1; 2], [40; 40], '-k', 'LineWidth', 2), plot(1.5+0.07, 40*1.04,
    '*k'), plot(1.5-0.07, 40*1.04, '*k')

```

```

        plot([2;3],[45;45], '-k', 'LineWidth',2),plot(2.5+0.07, 45*1.04,
'*k'),plot(2.5-0.07, 45*1.04, '*k'), hold off
    title('Neck flexion angle (degree)')
    subplot(2,3,[3,6])
    barwitherr(s(5,:),m(5,:));
    xticklabels({'T1','T2','T3','T4'})
    title('Impact duration (ms)')
    annotation('textbox', [0 0 1 1], 'String', 'TECHNIQUES COMPARISON -
AGONISTS', 'FontSize', 14, 'FontWeight', 'bold', 'EdgeColor', 'none',
'HorizontalAlignment', 'center')

% Controlling for not-normally distributed data (Kolmogorov-Smirnov test)
for v=1:5
    for t=1:4
        KS(v,t,1)=kstest(tech(:,v,t));
        KS(v,t,2)=kstest(reshape(M3r(:,v,1,Aex,t),length(Aex),1));
        KS(v,t,3)=kstest(reshape(M3r(:,v,1,An,t),length(An),1));
        KS(v,t,4)=kstest(reshape(m3r(:,v,1,Aex,t),length(Aex),1));
        KS(v,t,5)=kstest(reshape(m3r(:,v,1,An,t),length(An),1));
        KS(v,t,6)=kstest(reshape(M3r(:,v,2,Aex,t),length(Aex),1));
        KS(v,t,7)=kstest(reshape(M3r(:,v,2,An,t),length(An),1));

KS(v,t,8)=kstest(reshape(mean(duration(:,Aex,t,:),4),length(Aex),1));

KS(v,t,9)=kstest(reshape(mean(duration(:,An,t,:),4),length(An),1));

KS(v,t,10)=kstest(permute(subjects_mean(431,14,1,Aex,t),[4,3,2,1]));

KS(v,t,11)=kstest(permute(subjects_mean(431,14,1,An,t),[4,3,2,1]));
        end
    end

else if NA==1
    NAex=[2,4,5,12,13,15,16,17,18,20];
    NAn=[1,3,6,7,8,9,10,11,14,19];
    %     NAex=[1,6,7,8,11]; % experience = 1 year
    %     NAn=[3,9,10,14,19]; % experience = 2 years

    MEAN_TECHNIQUES=NaN(1,4,1,1,4,2);
    MEAN_TECHNIQUES(:,1:3, :, :, 1)=mean(M3r(:, [5,12,14],1,NAex,:),4);
    MEAN_TECHNIQUES(:,1:3, :, :, 2)=mean(M3r(:, [5,12,14],1,NAn,:),4);
    MEAN_TECHNIQUES(:,4, :, :, 1)=mean(m3r(:,14,1,NAex,:),4);
    MEAN_TECHNIQUES(:,4, :, :, 2)=mean(m3r(:,14,1,NAn,:),4);
    MEAN_TECHNIQUES=permute(MEAN_TECHNIQUES,[5,2,6,1,3,4]);
    MEAN_TECHNIQUES_trunk=NaN(1,2,1,1,4,2);
    MEAN_TECHNIQUES_trunk(:, :, :, :, 1)=mean(M3r(:, [5,12],2,NAex,:),4);
    MEAN_TECHNIQUES_trunk(:, :, :, :, 2)=mean(M3r(:, [5,12],2,NAn,:),4);
    MEAN_TECHNIQUES_trunk=permute(MEAN_TECHNIQUES_trunk,[5,2,6,1,3,4]);
    MEAN_DURATION(:,1)=mean(mean(duration(:,NAex,:),4),2);
    MEAN_DURATION(:,2)=mean(mean(duration(:,NAn,:),4),2);

MEAN_ang(:,1)=permute(mean(subjects_mean(431,14,1,NAex,:),4),[4,5,1,2,3]);
MEAN_ang(:,2)=permute(mean(subjects_mean(431,14,1,NAn,:),4),[4,5,1,2,3]);

    STD_TECHNIQUES=NaN(1,4,1,1,4,2);
    STD_TECHNIQUES(:,1:3, :, :, 1)=std(M3r(:, [5,12,14],1,NAex,:),0,4);
    STD_TECHNIQUES(:,1:3, :, :, 2)=std(M3r(:, [5,12,14],1,NAn,:),0,4);
    STD_TECHNIQUES(:,4, :, :, 1)=std(m3r(:,14,1,NAex,:),0,4);
    STD_TECHNIQUES(:,4, :, :, 2)=std(m3r(:,14,1,NAn,:),0,4);
    STD_TECHNIQUES=permute(STD_TECHNIQUES,[5,2,6,1,3,4]);
    STD_TECHNIQUES_trunk=NaN(1,2,1,1,4,2);
    STD_TECHNIQUES_trunk(:, :, :, :, 1)=std(M3r(:, [5,12],2,NAex,:),0,4);
    STD_TECHNIQUES_trunk(:, :, :, :, 2)=std(M3r(:, [5,12],2,NAn,:),0,4);
    STD_TECHNIQUES_trunk=permute(STD_TECHNIQUES_trunk,[5,2,6,1,3,4]);
    STD_DURATION(:,1)=std(mean(duration(:,NAex,:),4),0,2);
    STD_DURATION(:,2)=std(mean(duration(:,NAn,:),4),0,2);

```

```

STD_ang(:,1)=permute(std(subjects_mean(431,14,1,NAex, :, :),0,4),[4,5,1,2,3]);
STD_ang(:,2)=permute(std(subjects_mean(431,14,1,NaN, :, :),0,4),[4,5,1,2,3]);

% STATISTICAL DIFFERENCES (Mann-Whitney test)
for t=1:nt
    for v=[5,12,14];

W_M(t,v)=ranksum(reshape(M3r(:,v,1,NAex,t),length(NAex),1),reshape(M3r(:,v,1,NaN,t),length(NAN),1));

W_m(t,v)=ranksum(reshape(m3r(:,v,1,NAex,t),length(NAex),1),reshape(m3r(:,v,1,NaN,t),length(NAN),1));

W_M_t(t,v)=ranksum(reshape(M3r(:,v,2,NAex,t),length(NAex),1),reshape(M3r(:,v,2,NaN,t),length(NAN),1));

W_d(t)=ranksum(reshape(mean(duration(:,NAex,t,:),4),length(NAex),1),reshape(mean(duration(:,NaN,t,:),4),length(NAN),1));

W_a(t)=ranksum(permute(subjects_mean(431,14,1,NAex,t),[4,3,2,1]),permute(subjects_mean(431,14,1,NaN,t),[4,3,2,1]));
        end
    end

figure()
plot(W_M(:,[5,12,14]),'-.','MarkerSize',20),hold on
plot(W_M_t(:,[5,12]),'-.','MarkerSize',20)
plot(W_m(:,14),'-.','MarkerSize',20)
plot(W_d,'-.','MarkerSize',20)

legend('|a|_H_E_A_D','|d\omega/dt|_H_E_A_D','|a|_T_R_U_N_K','|d\omega/dt|_T_R_U_N_K','ext-angle','flex-angle','duration'),xticks([1,2,3,4]),
xticklabels({'O-soto-gari','O-uchi-gari','Ippon-seoi-nage','Tai-otoshi'})
title('Mann-Whitney test - NOT-AGONISTS'),grid on

figure()
subplot(2,1,1),barwitherr(STD_ang,MEAN_ang);
legend('Experts','Not-experts'),xticklabels({'O-soto-gari','O-uchi-gari','Ippon-seoi-nage','Tai-otoshi'})
title('Neck angle during the acceleration peak (degree)'), grid on
subplot(2,1,2),plot(W_a,'-.','MarkerSize',20),ylim([0,1])
xticks([1,2,3,4]),xticklabels({'O-soto-gari','O-uchi-gari','Ippon-seoi-nage','Tai-otoshi'})
title('Mann-Whitney test'), grid on
annotation('textbox',[0 0 1 1],'String','NOT-AGONISTS','FontSize',14,'FontWeight','bold','EdgeColor','none','HorizontalAlignment','center')

% BAR DIAGRAMS
figure()
subplot(2,2,1)

b1=barwitherr([STD_TECHNIQUES(:,1,1),STD_TECHNIQUES(:,1,2)],[MEAN_TECHNIQUES(:,1,1),MEAN_TECHNIQUES(:,1,2)]);
legend(b1,{'Experts','Not-experts'}),xticklabels({'O-soto-gari','O-uchi-gari','Ippon-seoi-nage','Tai-otoshi'})
title('Head acceleration module (g)'), grid on
subplot(2,2,3)

barwitherr([STD_TECHNIQUES(:,2,1),STD_TECHNIQUES(:,2,2)],[MEAN_TECHNIQUES(:,2,1),MEAN_TECHNIQUES(:,2,2)]),title('Head angular acceleration module (rad/s^2)'), grid on
xticklabels({'O-soto-gari','O-uchi-gari','Ippon-seoi-nage','Tai-otoshi'})

```

```

subplot(2,2,2)

barwitherr([STD_TECHNIQUES_trunk(:,1,1),STD_TECHNIQUES_trunk(:,1,2)],[MEAN_TEC
HNIQUES_trunk(:,1,1),MEAN_TECHNIQUES_trunk(:,1,2)]),title('Trunk acceleration
module (g)'), grid on
    xticklabels({'O-soto-gari', 'O-uchi-gari', 'Ippon-seoi-nage', 'Tai-
otoshi'})
subplot(2,2,4)

barwitherr([STD_TECHNIQUES_trunk(:,2,1),STD_TECHNIQUES_trunk(:,2,2)],[MEAN_TEC
HNIQUES_trunk(:,2,1),MEAN_TECHNIQUES_trunk(:,2,2)]),title('Trunk angular
acceleration module (rad/s^2)'), grid on
    xticklabels({'O-soto-gari', 'O-uchi-gari', 'Ippon-seoi-nage', 'Tai-
otoshi'})
    annotation('textbox', [0 0 1 1], 'String', 'NOT-AGONISTS', 'FontSize',
14, 'FontWeight', 'bold', 'EdgeColor', 'none', 'HorizontalAlignment',
'center')

figure()
subplot(2,1,1)

barwitherr([STD_TECHNIQUES(:,3,1),STD_TECHNIQUES(:,3,2)],[MEAN_TECHNIQUES(:,3,
1),MEAN_TECHNIQUES(:,3,2)]),title('Neck extension angle (degree)'), grid on
    legend('Experts', 'Not-experts', 'Location', 'Best'), xticklabels({'O-
soto-gari', 'O-uchi-gari', 'Ippon-seoi-nage', 'Tai-otoshi'}), ylim([0,50])
subplot(2,1,2)

barwitherr([STD_TECHNIQUES(:,4,1),STD_TECHNIQUES(:,4,2)],[abs(MEAN_TECHNIQUES(
:,4,1)),abs(MEAN_TECHNIQUES(:,4,2))]),title('Neck flexion angle (degree)'),
grid on
    xticklabels({'O-soto-gari', 'O-uchi-gari', 'Ippon-seoi-nage', 'Tai-
otoshi'}), ylim([0,50])
    annotation('textbox', [0 0 1 1], 'String', 'NOT-AGONISTS', 'FontSize',
14, 'FontWeight', 'bold', 'EdgeColor', 'none', 'HorizontalAlignment',
'center')

figure()
b1=barwitherr(STD_DURATION,MEAN_DURATION);
legend(b1,{'Experts', 'Not-experts'}), xticklabels({'O-soto-gari', 'O-
uchi-gari', 'Ippon-seoi-nage', 'Tai-otoshi'})
title('Duration (ms) - NOT-AGONISTS'), grid on

% BOXPLOTS
figure()
v=5;

subplot(1,4,1), boxplot([[reshape(M3r(1,v,1,NAex,1),length(NAex),1);NaN(length(
NAN)-length(NAex),1)],reshape(M3r(1,v,1,NAN,1),length(NAN),1)]),
xticklabels({'Experts', 'Not-experts'}), ylabel('Acceleration Module (g)'),
ylim([0,80]), title('O-soto-gari')

subplot(1,4,2), boxplot([[reshape(M3r(1,v,1,NAex,2),length(NAex),1);NaN(length(
NAN)-length(NAex),1)],reshape(M3r(1,v,1,NAN,2),length(NAN),1)]),
xticklabels({'Experts', 'Not-experts'}), ylim([0,80]), title('O-uchi-gari')

subplot(1,4,3), boxplot([[reshape(M3r(1,v,1,NAex,3),length(NAex),1);NaN(length(
NAN)-length(NAex),1)],reshape(M3r(1,v,1,NAN,3),length(NAN),1)]),
xticklabels({'Experts', 'Not-experts'}), ylim([0,80]), title('Ippon-seoi-
nage')

subplot(1,4,4), boxplot([[reshape(M3r(1,v,1,NAex,4),length(NAex),1);NaN(length(
NAN)-length(NAex),1)],reshape(M3r(1,v,1,NAN,4),length(NAN),1)]),
xticklabels({'Experts', 'Not-experts'}), ylim([0,80]), title('Tai-otoshi')
    annotation('textbox', [0 0 1 1], 'String', 'HEAD ACCELERATION
COMPARISION - NOT-AGONISTS', 'FontSize', 14, 'FontWeight', 'bold', 'EdgeColor',
'none', 'HorizontalAlignment', 'center')

figure()

```

```

v=12;

subplot(1,4,1),boxplot([[reshape(M3r(1,v,1,NAex,1),length(NAex),1);NaN(length(
NAn)-length(NAex),1)],reshape(M3r(1,v,1,NAn,1),length(NAn),1)]),
xticklabels({'Experts', 'Not-experts'}), ylabel('Angular Acceleration Module
(rad/s^2)'), ylim([0,2500]), title('O-soto-gari')

subplot(1,4,2),boxplot([[reshape(M3r(1,v,1,NAex,2),length(NAex),1);NaN(length(
NAn)-length(NAex),1)],reshape(M3r(1,v,1,NAn,2),length(NAn),1)]),
xticklabels({'Experts', 'Not-experts'}), ylim([0,2500]), title('O-uchi-gari')

subplot(1,4,3),boxplot([[reshape(M3r(1,v,1,NAex,3),length(NAex),1);NaN(length(
NAn)-length(NAex),1)],reshape(M3r(1,v,1,NAn,3),length(NAn),1)]),
xticklabels({'Experts', 'Not-experts'}), ylim([0,2500]), title('Ippon-seoi-
nage')

subplot(1,4,4),boxplot([[reshape(M3r(1,v,1,NAex,4),length(NAex),1);NaN(length(
NAn)-length(NAex),1)],reshape(M3r(1,v,1,NAn,4),length(NAn),1)]),
xticklabels({'Experts', 'Not-experts'}), ylim([0,2500]), title('Tai-otoshi')
    annotation('textbox', [0 0 1 1], 'String', 'HEAD ANGULAR ACCELERATION
COMPARISION - NOT-AGONISTS','FontSize', 14, 'FontWeight', 'bold', 'EdgeColor',
'none', 'HorizontalAlignment', 'center')

figure()
v=14;

subplot(2,4,1),boxplot([[reshape(M3r(1,v,1,NAex,1),length(NAex),1);NaN(length(
NAn)-length(NAex),1)],reshape(M3r(1,v,1,NAn,1),length(NAn),1)]),
xticklabels({'Experts', 'Not-experts'}), ylabel('Angle (degree)'), ylim([-
25,35]), title('O-soto-gari')

subplot(2,4,2),boxplot([[reshape(M3r(1,v,1,NAex,2),length(NAex),1);NaN(length(
NAn)-length(NAex),1)],reshape(M3r(1,v,1,NAn,2),length(NAn),1)]),
xticklabels({'Experts', 'Not-experts'}), ylim([-25,35]), title('O-uchi-gari')

subplot(2,4,3),boxplot([[reshape(M3r(1,v,1,NAex,3),length(NAex),1);NaN(length(
NAn)-length(NAex),1)],reshape(M3r(1,v,1,NAn,3),length(NAn),1)]),
xticklabels({'Experts', 'Not-experts'}), ylim([-25,35]), title('Ippon-seoi-
nage')

subplot(2,4,4),boxplot([[reshape(M3r(1,v,1,NAex,4),length(NAex),1);NaN(length(
NAn)-length(NAex),1)],reshape(M3r(1,v,1,NAn,4),length(NAn),1)]),
xticklabels({'Experts', 'Not-experts'}), ylim([-25,35]), title('Tai-otoshi')
    annotation('textbox', [0 0 1 1], 'String', 'NECK EXTENSION ANGLE
COMPARISION - NOT-AGONISTS','FontSize', 14, 'FontWeight', 'bold', 'EdgeColor',
'none', 'HorizontalAlignment', 'center')

subplot(2,4,5),boxplot([[reshape(m3r(1,v,1,NAex,1),length(NAex),1);NaN(length(
NAn)-length(NAex),1)],reshape(m3r(1,v,1,NAn,1),length(NAn),1)]),
xticklabels({'Experts', 'Not-experts'}), ylabel('Angle (degree)'), ylim([-
70,0]), title('O-soto-gari')

subplot(2,4,6),boxplot([[reshape(m3r(1,v,1,NAex,2),length(NAex),1);NaN(length(
NAn)-length(NAex),1)],reshape(m3r(1,v,1,NAn,2),length(NAn),1)]),
xticklabels({'Experts', 'Not-experts'}), ylim([-70,0]), title('O-uchi-gari')

subplot(2,4,7),boxplot([[reshape(m3r(1,v,1,NAex,3),length(NAex),1);NaN(length(
NAn)-length(NAex),1)],reshape(m3r(1,v,1,NAn,3),length(NAn),1)]),
xticklabels({'Experts', 'Not-experts'}), ylim([-70,0]), title('Ippon-seoi-
nage')

subplot(2,4,8),boxplot([[reshape(m3r(1,v,1,NAex,4),length(NAex),1);NaN(length(
NAn)-length(NAex),1)],reshape(m3r(1,v,1,NAn,4),length(NAn),1)]),
xticklabels({'Experts', 'Not-experts'}), ylim([-70,0]), title('Tai-otoshi')
    annotation('textbox', [0 0.5 1 0], 'String', 'NECK FLEXION ANGLE
COMPARISION - NOT-AGONISTS','FontSize', 14, 'FontWeight', 'bold', 'EdgeColor',
'none', 'HorizontalAlignment', 'center')

```

```

% Technique analysis
tech=M3r(:,[5 12 14],1,:);
tech=cat(2,tech,m3r(:,14,1,:));
tech=permute(tech,[4,2,5,1,3]);
tech=cat(2,tech,permute(mean(duration,4),[2,1,3])); % 20 subjects in
rows * 5variables in column(lacc,aacc,ext,flex,time) * 4 techniques

% Friedman's test
for v=1:5

[F_t(v),~,stats(v)]=friedman([tech(:,v,1),tech(:,v,2),tech(:,v,3),tech(:,v,4)]
);
    d(:,v)=multcompare(stats(v));

end

figure()

b1=barwitherr([permute(std(tech(:,1,:),0,1),[3,2,1]),permute(std(tech(:,2,:),0
,1)/100,[3,2,1]),...

permute(std(tech(:,3,:),0,1),[3,2,1]),permute(std(tech(:,4,:),0,1),[3,2,1]),pe
rmute(std(tech(:,5,:),0,1),[3,2,1])/10],...

[permute(mean(tech(:,1,:),[3,2,1]),permute(mean(tech(:,2,:))/100,[3,2,1]),...
    permute(mean(tech(:,3,:),[3,2,1]),permute(-
mean(tech(:,4,:),[3,2,1]),permute(mean(tech(:,5,:),[3,2,1])/10)]);
    xticks([1,2,3,4]), xticklabels({'O-soto-gari','O-uchi-gari','Ippon-
seoi-nage','Tai-otoshi'})
    title('Variables comparison - NOT-AGONISTS')
    legend(b1,{'|a|_H_E_A_D (g)', '|d\omega/dt|_H_E_A_D / 100
(rad/s^2)', 'ext-angle (degree)', 'flex-angle (degree)', 'duration / 10 (ms)'}))

figure()
s=permute(std(tech(:, :, :),0,1),[2,3,1]);
m=permute(mean(tech(:, :, :)),[2,3,1]);
subplot(2,3,1)
barwitherr(s(1,:),m(1,:));
xticklabels({'T1','T2','T3','T4'})
title('Head acceleration module (g)'),
subplot(2,3,2)
barwitherr(s(2,:),m(2,:));
xticklabels({'T1','T2','T3','T4'})
title('Head angular acceleration module (rad/s^2)')
subplot(2,3,4)
barwitherr(s(3,:),m(3,:));
xticklabels({'T1','T2','T3','T4'})
title('Neck extension angle (degree)'),ylim([0,60])
subplot(2,3,5)
barwitherr(s(4,:),-m(4,:));
xticklabels({'T1','T2','T3','T4'})
title('Neck flexion angle (degree)')
subplot(2,3,[3,6])
barwitherr(s(5,:),m(5,:));
xticklabels({'T1','T2','T3','T4'})
title('Impact duration (ms)')
annotation('textbox', [0 0 1 1], 'String', 'TECHNIQUES COMPARISON -
NOT-AGONISTS', 'FontSize', 14, 'FontWeight', 'bold', 'EdgeColor', 'none',
'HorizontalAlignment', 'center')

% Controlling for not-normally distributed data (Kolmogorov-Smirnov
test)
for v=1:5
    for t=1:4
        KS(v,t,1)=kstest(tech(:,v,t));
        KS(v,t,2)=kstest(reshape(M3r(:,v,1,NAex,t),length(NAex),1));
        KS(v,t,3)=kstest(reshape(M3r(:,v,1,NAn,t),length(NAn),1));
        KS(v,t,4)=kstest(reshape(m3r(:,v,1,NAex,t),length(NAex),1));
        KS(v,t,5)=kstest(reshape(m3r(:,v,1,NAn,t),length(NAn),1));
    end
end

```

```
        KS(v,t,6)=kstest(reshape(M3r(:,v,2,NAex,t),length(NAex),1));
        KS(v,t,7)=kstest(reshape(M3r(:,v,2,NAn,t),length(NAn),1));
    KS(v,t,8)=kstest(reshape(mean(duration(:,NAex,t,:),4),length(NAex),1));
    KS(v,t,9)=kstest(reshape(mean(duration(:,NAn,t,:),4),length(NAn),1));
    KS(v,t,10)=kstest(permute(subjects_mean(431,14,1,NAex,t),[4,3,2,1]));
    KS(v,t,11)=kstest(permute(subjects_mean(431,14,1,NAn,t),[4,3,2,1]));
        end
    end
end
end
```


Acknowledgements

Firstly, I would like to offer my gratitude to my Supervisor, Professor Laura Gastaldi, who allowed me to work on a theme rarely analyzed in Engineer faculties: without her endorsing and her support, probably I would not be able to scientifically study a piece of myself, Judo. Moreover, I would like also to thank for her constant support in the whole development of this study.

Secondly, I would like to express my very great appreciation to PhD Valeria Rosso, who gave me in a rapid, schematic and complete way fundamental information about Statistics, which our courses unfortunately did not provide.

Then, I would like to thank all people from DLF Judo Alessandria that were involved in this study starting from all children, and all their parents that permitted me to exploit their young during the study, whose support was the biggest token of appreciation I have ever had. A particular thank goes to Mattia, the little thrower who accepted to enroll this study without any kind of doubt and participated always with a big smile on his face. Furthermore, I am obliged to the Agonists group of the Team for letting them to be heavily thrown by the coach; especially, I am in debt with "The Coach" Alessio who, even if busy and swamped by works and trainings, found always time to devote to me and to my project.

However, the greatest thank goes to the whole Judo family, in particular to the parents of this family, Maestro Italo, Maestra Silvia and Enzo, who introduced me to this Sport and taught me all their knowledge and experience about it.

Then, I would like to express my sincerest gratitude to everyone who helped me in this project, even not physically: at first, my girlfriend Agnese who guided cables all time during the tests, but specially she bore me in the darkest moments of the project, and even when I found myself irritating, she encouraged me with sweet words; my grandparents who supported and encouraged me in my whole university education, saying to me that it was too much; then, my cousins Elisa and Matteo, who helped me not just during the project but since I was a child, and my uncles, in particular Zio Sante who every day asked me how the thesis had been gone and talked to me with the appellative "Dottore" making me feeling real important and grown up; my friend Stefano, in which I found a role model, an objective to reach and more than a simple university classmate, and the "Biomechanical ladies" (I'm sorry I stole your words, Stefano) Clelia and Manuela who supported me during our whole period at the Politecnico with smiles and particular words of comfort and inspiration.

For the sake of brevity, I cannot cite all the members of my family and all my friends, but you know that I am proud of the constant support that each of you rendered to me every day.

Last but not least, I would like to thank my parents Graziella and Massimo for having given me the possibility of succeeding in this course. Thank you, Mum, for always supporting me, also in more challenging evenings and days, with sweet talks and encouragements (and special meals). Thank you, Dad, for the sustenance during all the way from the preliminary tests to the final data analysis, and for the great help during the roughest weeks, whenever things went wrong you did not doubt on aiding me all night long.

The thesis I wrote is even all your doing, thank you.

Ringraziamenti

In primo luogo, vorrei ringraziare la mia Relatrice, la professoressa Laura Gastaldi, la quale mi ha permesso di lavorare su un tema raramente analizzato nelle facoltà di Ingegneria: senza la sua approvazione e il suo sostegno, probabilmente non sarei stato in grado di studiare scientificamente una parte di me stesso, il Judo. Inoltre, vorrei ringraziarla anche per il suo costante sostegno durante tutto lo sviluppo di questo studio.

In secondo luogo, vorrei esprimere il mio apprezzamento alla Dottoranda Valeria Rosso, che mi ha dato in modo rapido, schematico e completo informazioni fondamentali per la tesi riguardo le parti di statistica, un argomento purtroppo non trattato dal nostro corso di Laurea.

Vorrei quindi ringraziare tutte le persone del DLF Judo Alessandria che sono state coinvolte in questo studio a partire da tutti i bambini, e tutti i loro genitori che mi hanno permesso di "sfruttare" i loro piccoli durante lo studio, il cui sostegno è stato il più grande segno di riconoscimento e fiducia che abbia mai avuto. Un ringraziamento particolare va a Mattia, il piccolo judoka che ha accettato di partecipare a questo studio in maniera continuativa senza alcun tipo di esitazione e ogni giorno si presentava sul tatami pronto a proiettare i compagni con un grande sorriso sul volto. Inoltre, sono in debito con il gruppo degli agonisti per essersi offerti e non aver avuto alcun timore a essere duramente proiettati dal Coach; in particolare, sono riconoscente a Coach Alessio che, anche se occupato e sommerso da lavori e allenamenti, ha trovato sempre tempo da dedicare a me e al mio progetto.

Tuttavia, il più grande ringraziamento va a tutta la famiglia del Judo, in particolare ai genitori di questa famiglia, il Maestro Italo, la Maestra Silvia e Enzo, che mi hanno introdotto a questo Sport e mi hanno insegnato tutta la loro conoscenza ed esperienza a riguardo.

Poi, vorrei esprimere la mia più sincera gratitudine a tutti coloro che mi hanno aiutato durante questo percorso, anche se non in termini concreti: per prima, la mia fidanzata Agnese che durante tutti i test ha manovrato i cavi per la buona riuscita delle acquisizioni, ma soprattutto mi ha sopportato nei momenti più bui del progetto e anche quando io stesso mi sentivo scontroso e arrogante, lei mi era pronta ad incoraggiarmi con parole dolci; i miei nonni che mi hanno incoraggiato e supportato durante tutto il mio percorso universitario, dicendo che l'impegno che ci stavo mettendo era troppo; i miei cugini Elisa e Matteo, che mi hanno aiutato non solo durante la tesi, ma fin da quando ero bambino, e i miei zii, in particolare lo Zio Sante che ogni giorno mi chiedeva notizie sulla tesi e parlava con me chiamandomi "Dottore", facendomi sentire importante per lui ed ormai grande; il mio amico Stefano, in cui ho trovato un modello da seguire, un obiettivo da raggiungere e molto più che un semplice compagno di università, e le "Biomechanical ladies" (scusa Stefano se ho rubato le tue parole) Clelia e Manuela che mi hanno sempre sostenuto durante il nostro percorso di studi al Politecnico con sorrisi e parole di conforto.

Per brevità, non posso citare tutti i membri della mia famiglia e tutti i miei amici, ma voi sapete che sono orgoglioso del costante sostegno che ognuno di voi mi ha reso ogni giorno.

Ultimi ma assolutamente non meno importanti, vorrei ringraziare i miei genitori Graziella e Massimo per avermi dato la possibilità di intraprendere e completare questo percorso. Grazie, Mamma, per avermi sempre sostenuto, anche nei pomeriggi e nelle giornate più impegnative con parole dolci e incoraggiamenti (e anche pasti deliziosi). Grazie, Papà, per il costante aiuto dai test preliminari fino all'analisi finale dei dati, e per il grande aiuto durante le settimane più difficili, ogni volta che le cose andavano male tu eri pronto ad aiutarmi tutta la notte.

Questa tesi è anche merito di Voi tutti, grazie.

